

ISSN 2587-6066



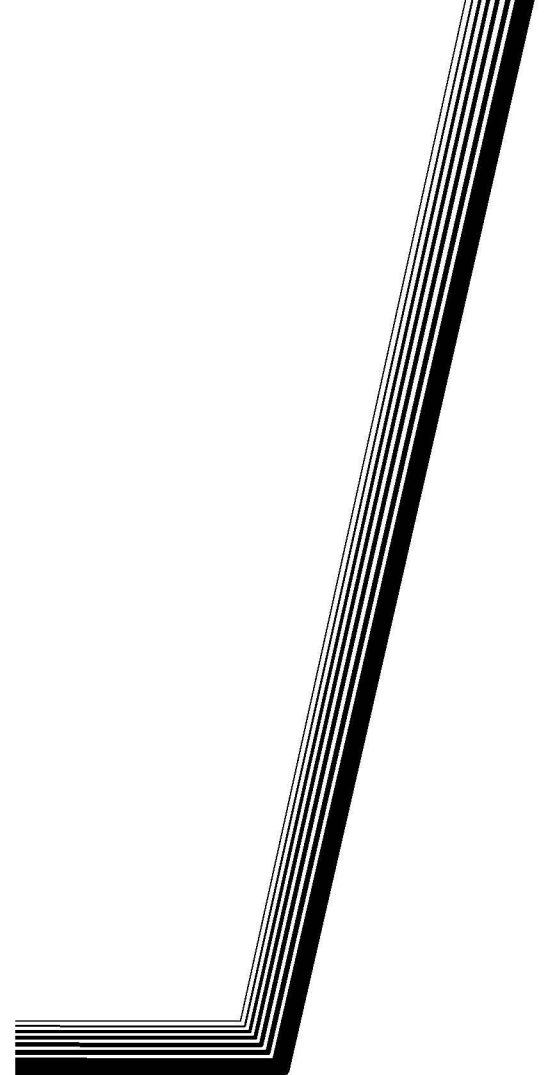
СИБИРСКИЙ ЖУРНАЛ НАУКИ И ТЕХНОЛОГИЙ

SIBERIAN JOURNAL OF SCIENCE AND TECHNOLOGY

**Том
Vol. 21, № 1**

КРАСНОЯРСК 2020

СИБИРСКИЙ ЖУРНАЛ НАУКИ И ТЕХНОЛОГИЙ



Том 21, № 1

Красноярск 2020

СИБИРСКИЙ ЖУРНАЛ НАУКИ И ТЕХНОЛОГИЙ

Том 21, № 1

Главный редактор

Сенашов Сергей Иванович, доктор физико-математических наук, профессор (СибГУ им. М. Ф. Решетнева)

Заместители главного редактора

Логинов Юрий Юрьевич, доктор физико-математических наук, профессор (СибГУ им. М. Ф. Решетнева)

Мурыгин Александр Владимирович, доктор технических наук, профессор, ответственный за подготовку выпусков журнала, содержащих секретные сведения (СибГУ им. М. Ф. Решетнева)

РЕДАКЦИОННАЯ КОЛЛЕГИЯ

Аплеснин С. С., доктор физико-математических наук, профессор (СибГУ им. М. Ф. Решетнева)

Галеев Р. Г., доктор технических наук (АО «НПП «Радиосвязь»)

Головенкин Е. Н., доктор технических наук, профессор (АО «ИСС»)

Левко В. А., доктор технических наук, доцент (СибГУ им. М. Ф. Решетнева)

Лившиц А. В., доктор технических наук, доцент (ИрГУПС)

Максимов И. А., доктор технических наук (АО «ИСС»)

Медведев А. В., доктор технических наук, профессор (СибГУ им. М. Ф. Решетнева)

Михеев А. Е., доктор технических наук, профессор (СибГУ им. М. Ф. Решетнева)

Москвичев В. В., доктор технических наук, профессор (СКТБ «Наука» ИВТ СО РАН)

Садовский В. М., доктор физико-математических наук, профессор (ИВМ СО РАН)

Сафонов К. В., доктор физико-математических наук, доцент (СибГУ им. М. Ф. Решетнева)

Сильченко П. Н., доктор технических наук, профессор (СФУ)

Смирнов Н. А., доктор технических наук, профессор (СибГУ им. М. Ф. Решетнева)

Терсков В. А., доктор технических наук, профессор (КРИЖТ ИрГУПС)

Чеботарев В. Е., доктор технических наук, доцент (АО «ИСС»)

Шайдуров В. В., доктор физико-математических наук, профессор (ИВМ СО РАН)

РЕДАКЦИОННЫЙ СОВЕТ

Васильев С. Н., академик РАН, доктор физико-математических наук, профессор (Москва)

Дегерменджи А. Г., академик РАН, доктор физико-математических наук, профессор (Красноярск)

Дегтерев А. С., доктор технических наук, профессор (Красноярск)

Калвода Л., кандидат наук, доцент (Прага, Чехия)

Колмыков В. А., кандидат технических наук, профессор (Химки)

Краточвилова И., доктор, доцент (Прага, Чехия)

Краус И., профессор (Прага, Чехия)

Лопатин А. В., доктор технических наук, профессор (Красноярск)

Лю Т., профессор (Пекин, Китай)

Минкер В., доктор, профессор (Ульм, Германия)

Миронов В. Л., член-корреспондент РАН, доктор физико-математических наук, профессор (Красноярск)

Павера Р., доцент (Братислава, Словакия)

Семенкин Е. С., доктор технических наук, профессор (Красноярск)

Тестоедов Н. А., член-корреспондент РАН, доктор технических наук, профессор (Железногорск)

Фошнер М., доктор, доцент (Марибор, Словения)

Чжанг Ш., доктор (Тяньцзинь, Китай)

Шабанов В. Ф., академик РАН, доктор физико-математических наук, профессор (Красноярск)

Швиденко А., доктор инженерных наук, профессор (Лаксенбург, Австрия)

Эйя Х., доктор инженерных наук, профессор (Тронхейм, Норвегия)

SIBERIAN JOURNAL OF SCIENCE AND TECHNOLOGY

Vol. 21, No 1

Chief Editor:

Senashov S. I., Dr.Sc., Professor (Reshetnev University)

Deputy Chief Editors

Loginov Y. Y., Dr.Sc., Professor (Reshetnev University)

Murygin A. V., Dr.Sc., Professor (Reshetnev University)

EDITORIAL BOARD

Aplesnin S. S., Dr.Sc., Professor
(Reshetnev University)

Galeev R. G., Dr.Sc.
(JSC "NPP "Radiosvyaz")

Golovenkin E. N., Dr.Sc., Professor
(ISS-Reshetnev Company)

Levko V. A., Dr.Sc., Professor
(Reshetnev University)

Livshits A. V., Dr.Sc., Professor
(Irkutsk State Transport University)

Maksimov I. A., Dr.Sc.
(ISS-Reshetnev Company)

Medvedev A. V., Dr.Sc., Professor
(Reshetnev University)

Mikheev A. E., Dr.Sc., Professor
(Reshetnev University)

Moskvichev V. V., Dr.Sc., Professor
(SDTB Nauka KSC SB RAS)

Sadovsky V. M., Dr.Sc., Professor
(ICM SB RAS)

Safonov K. V., Dr.Sc., Professor
(Reshetnev University)

Silchenko P. N., Doctor of Technical
Sciences, Professor (SibFU)

Smirnov N. A., Dr.Sc., Professor
(Reshetnev University)

Terskov V. A., Dr.Sc., Professor
(Irkutsk State Transport University)

Chebotarev V. Y., Dr.Sc., Professor
(ISS-Reshetnev Company)

Shaidurov V. V., Dr.Sc., Professor
(ICM SB RAS)

EDITORIAL COUNCIL

Vasiliev S. N., Academician of the Russian Academy
of Sciences, Dr.Sc., Professor (Moscow)

Degermendzhi A. G., Academician of the Russian
Academy of Sciences, Dr.Sc., Professor (Krasnoyarsk)

Degterev A. S., Dr.Sc., Professor (Krasnoyarsk)

Kalvoda L., Cand.Sc.-Ing., Associate Professor
(Prague, Czech Republic)

Kolmykov V. A., Cand.Sc., Professor (Khimki)

Kratochvilova I., Dr.-Ing., Associate Professor
(Prague, Czech Republic)

Kraus I., Sc.D., Professor (Prague, Czech Republic)

Lopatin A. V., Dr.Sc., Professor (Krasnoyarsk)

Liu T., Ph.D., Professor (Beijing, China)

Minker W., Dr.-Ing., Professor (Ulm, Germany)

Mironov V. L., Corresponding Member
of the Russian Academy of Sciences, Dr.Sc.,
Professor (Krasnoyarsk)

Pawera R., Associate Professor (Bratislava, Slovakia)

Semenkin E. S., Dr.Sc., Professor (Krasnoyarsk)

Testoedov N. A., Corresponding Member
of the Russian Academy of Sciences, Dr.Sc.,
Professor (Zheleznogorsk)

Fošner M., Ph.D. Associate Professor (Maribor, Slovenia)

Zhang S., Ph.D. (Tianjin, China)

Shabanov V. F., Academician of the Russian Academy
of Sciences, Dr.Sc., Professor (Krasnoyarsk)

Shvidenko A., Dr.-Ing., Professor (Laxenburg, Austria)

Oye H., Dr.-Ing., Professor (Trondheim, Norway)

К СВЕДЕНИЮ ЧИТАТЕЛЕЙ

«Сибирский журнал науки и технологий» является научным, производственно-практическим рецензируемым изданием. Свидетельство о регистрации средства массовой информации ПИ № ФС 77-70577 от 03.08.2017 г. выдано Федеральной службой по надзору в сфере связи, информационных технологий и массовых коммуникаций (Роскомнадзор).

ISSN 2587-6066.

Подписной индекс в каталоге «Пресса России» – 39263.

Зарегистрирован в Российском индексе научного цитирования (РИНЦ).

Включен в базу данных Ulrich's Periodicals Directory американского издательства Bowker.

Входит в перечень журналов ВАК по следующим научным специальностям:

05.07.02 Проектирование конструкция и производство летательных аппаратов (технические);

05.07.05 Тепловые электроракетные двигатели и энергоустановки летательных аппаратов (технические);

05.07.07 Контроль и испытание летательных аппаратов и их систем (технические);

05.13.01 Системный анализ, управление и обработка информации (по отраслям) (технические);

05.13.11 Математическое и программное обеспечение вычислительных машин, комплексов и компьютерных сетей (технические).

Выпускается с 2000 года. До 2002 года журнал носил название «Вестник Сибирской аэрокосмической академии имени академика М. Ф. Решетнева» («Вестник САА»), до мая 2017 года – «Вестник Сибирского государственного аэрокосмического университета имени академика М. Ф. Решетнева».

Каждый выпуск журнала включает три раздела:

1 раздел. Информатика, вычислительная техника и управление.

2 раздел. Авиационная и ракетно-космическая техника.

3 раздел. Технологические процессы и материалы.

Статьи публикуются бесплатно после обязательного рецензирования и при оформлении их в соответствии с требованиями редакции (www.vestnik.sibsau.ru). Журнал выходит 4 раза в год.

Электронная версия журнала представлена на сайте Научной электронной библиотеки (<http://www.elibrary.ru>) и сайте журнала (www.vestnik.sibsau.ru)

При перепечатке или цитировании материалов из журнала «Сибирский журнал науки и технологий» ссылка обязательна.

Учредитель и издатель

ФГБОУ ВО «Сибирский государственный университет науки и технологий имени академика М. Ф. Решетнева» (СибГУ им. М. Ф. Решетнева)

АДРЕС РЕДАКЦИИ, УЧРЕДИТЕЛЯ И ИЗДАТЕЛЯ:

Сибирский государственный университет науки и технологий имени академика М. Ф. Решетнева, Российская Федерация, 660037, г. Красноярск, проспект имени газеты «Красноярский рабочий», 31, П-416. Тел./ факс (391)291-90-19

E-mail: vestnik@sibsau.ru

Редактор Н. Н. ГОЛОСКОКОВА

Ответственный редактор английского текста
М. В. САВЕЛЬЕВА

Оригинал-макет и верстка М. А. СВЕТЛАКОВОЙ

Подписано в печать 25.03.2020. Формат 70×108/16.

Бумага офсетная. Печать плоская. Усл. печ. л. 16,5.

Уч.-изд. л. 21,1. Тираж 1000 экз. Заказ 2940. С 69/20.

Редакционно-издательский отдел СибГУ им. М.Ф. Решетнева.

Отпечатано в редакционно-издательском центре
СибГУ им. М. Ф. Решетнева.

Российская Федерация, 660037, г. Красноярск,
просп. им. газ. «Красноярский рабочий», 31.

Дата выхода в свет: 14.04.2020. Свободная цена

INFORMATION FOR AUTHORS AND SUBSCRIBERS

Siberian Journal of Science and Technology is a research, production and practical peer-reviewed journal. Included by the Higher Attestation Commission of the Russian Federation in the Index of Leading Russian Peer-Reviewed Journals and Periodicals, in which significant scientific dissertation results should be published when applying for a Dr.Sc. degree.

The journal is the official periodical of Reshetnev Siberian State University of Science and Technology.

Certificate of Registration as a Mass Media Resource. Certificate: PI No. FC 77-50577, dated 03 August 2017, given by Federal Supervision Agency for Information Technology, Communications and Mass Media.

The Journal is included in the following subscription catalogue 39263 – Pressa Rossii.

The journal is registered in the Russian Science Citation Index (RSCI). The journal is indexed in the database of Ulrich's Periodicals Directory.

The journal was first published in 2000. Prior to 2002 it had the title *Vestnik Sibirskoi aerokosmicheskoi akademii imeni akademika M. F. Reshetneva* (*Vestnik SAA*), prior to may 2017 it had the title *Vestnik Sibirskogo gosudarstvennogo aerokosmicheskogo universiteta imeni akademika M. F. Reshetneva* (*Vestnik SibGAU*).

The Journal is recommended for publishing the main results of research when applying for Cand. Sc. degree and Dr. Sc. degree upon the following specialties:

05.07.02 Engineering, Design and Manufacturing of Aircraft (Engineering);

05.07.05 Thermal Electric Jet Engines and Power Facilities of Aircraft (Engineering);

05.07.07 Control and Testing of Aircraft and its Systems (Engineering);

05.13.01 System Analysis, Management and Information Processing (branch-wise) (Engineering);

05.13.11 Mathematical Support and Software for Computers, Computer Systems and Computer Networks (Engineering).

Each issue consists of three parts:

Part 1. Informatics, computer technology and management.

Part 2. Aviation and Spacecraft Engineering.

Part 3. Technological Processes and Material Science.

Papers prepared in accordance with the editorial guidelines (www.vestnik.sibsau.ru) are published free of charge after being peer reviewed.

The journal is published four times a year.

An online version can be viewed at <http://www.elibrary.ru>

Siberian Journal of Science and Technology should be cited when reprinting or citing materials from the journal.

CONTACTS. Website: www.vestnik.sibsau.ru

Address: Reshetnev Siberian State University of Science and Technology.

31, Krasnoyarsky Rabochy Av., Krasnoyarsk, 660037, Russian Federation.

Tel./ fax (391)291-90-19; e-mail: vestnik@sibsau.ru

Editor N. N. GOLOSKOKOVA

Executive editor (English Language) M. V. SAVELYEVA
Layout original M. A. SVETLAKOVA

Signed (for printing): 25.03.2020. Format 70×108/16.

Offset Paper. Print flat. 16.5. Published sheets 21,1.

1000 copies. Order 2940. С 69/20.

Printing and Publication Department
Reshetnev University.

Printed in the Department of copying and duplicating
equipment Reshetnev University.

31, Krasnoyarsky Rabochy Av., Krasnoyarsk,
660037, Russian Federation.

Date of publication: 14.04.2020. Free price

СОДЕРЖАНИЕ

РАЗДЕЛ 1. ИНФОРМАТИКА, ВЫЧИСЛИТЕЛЬНАЯ ТЕХНИКА И УПРАВЛЕНИЕ

Иванов В. А., Еркаев Н. В. Полуаналитический метод расчета упруго-гидродинамического контакта	8
Львова А. П. Разработка способа повышения чувствительности в беспроводных оптических каналах передачи данных в видимом диапазоне световых волн	15
Раскина А. В., Виденин С. А., Чжан Е. А., Юсупова Р. Р. Особенности организации программной архитектуры адаптивных систем обработки информации, моделирования и управления	21
Романова Д. С. Исследование вариантов перехода от неограниченного параллелизма к ограниченному на примере умножения матриц	28
Ширяева Т. А., Хлупичев В. А., Шлепкин А. К., Мельникова О. Л. Метод обратного преобразования для анализа временных рядов	34
Ширяева Т. А., Шлепкин А. К., Филиппов К. А., Колмакова З. А. О функции распределения времени безотказной работы сложной вычислительной системы	41
Ярещенко Д. И. О непараметрической идентификации частично-параметризованного дискретно-непрерывного процесса	47

РАЗДЕЛ 2. АВИАЦИОННАЯ И РАКЕТНО-КОСМИЧЕСКАЯ ТЕХНИКА

Акзигитов А. Р., Акзигитов Р. А., Огородникова Ю. В., Дмитриев Д. В., Андронов А. С. Исследование системы мониторинга воздушного пространства ADS-B	56
Бегишев А. М., Журавлев В. Ю., Торгашин А. С. Особенности и возможный путь модернизации силоизмерительных устройств испытательных стендов жидкостных ракетных двигателей	62
Ключников А. В. Разработка и тестирование алгоритма обеспечения минимального угла отклонения главной центральной оси инерции в процессе балансировки летающей модели в одной плоскости коррекции	70
Комлев Г. В., Митрофанова А. С. К вопросу прогнозирования технического состояния жидкостных ракетных двигателей малой тяги	78
Непомнящий О. В., Краснобаев Ю. В., Яблонский А. П., Солопко И. В., Личаргин Д. В. Обеспечение экстремального регулирования мощности первичных источников энергии при их совместной работе на общую нагрузку	85
Филонова М. М. Перспективы в области разработки высоковольтных систем электропитания космического аппарата с модулем зарядно-разрядного устройства	96

РАЗДЕЛ 3. ТЕХНОЛОГИЧЕСКИЕ ПРОЦЕССЫ И МАТЕРИАЛЫ

Коновалов С. О., Бегешева О. Б., Хишем Абдельбаки, Рыбина У. И., Юхно М. Ю. Исследование электрических свойств сульфидов марганца допированных ионами тулия и иттербия	108
Михеев А. Е., Гирн А. В., Раводина Д. В., Елизарьева И. Г. Влияние предварительной подготовки поверхности титановых сплавов на характеристики МДО покрытий	115
Титенков С. В., Журавлев В. Ю. Особенности технологического совершенствования и оптимизации затрат производства 3D-конфигурации труб	125
Шестаков И. Я., Хилюк А. В. Влияние постоянного электрического поля на адсорбционную очистку воды от ионов железа	136

CONTENTS

PART 1. INFORMATICS, COMPUTER TECHNOLOGY AND MANAGEMENT

Ivanov V. A., Erkaev N. V. Semi-analytical method for calculating elastic-hydrodynamic contact	8
Lvova A. P. Development of method for increasing sensitivity in wireless optical data transmission channels in visible wavelength range	15
Raskina A. V., Videnin S. A., Chzhan E. A., Yusupova R. R. Peculiarities of design software architecture of adaptive information processing, modeling and control systems	21
Romanova D. S. Research of options of transition from unlimited to limited parallelism on the example of matrix multiplication	28
Shiryaeva T. A., Khlupichev V. A., Shlepkina A. K., Melnikova O. L. The use of the inverse transformation method for time series analysis	34
Shiryaeva T. A., Shlepkina A. K., Philippov K. A., Kolmakova Z. A. On the function of time distribution of a complex computing system uptime	41
Yareshchenko D. I. About non-parametric identification of partial-parametred discrete-continuous process	47

PART 2. AVIATION AND SPACECRAFT ENGINEERING

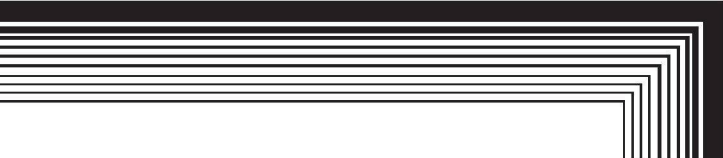
Akzigitov A. R., Akzigitov R. A., Ogorodnikova U. V., Dmitriev D. V., Andronov A. S. Analysis of the ADS-B airspace monitoring system	56
Begishev A. M., Zhuravlev V. Y., Torgashin A. S. Features and modernization methods of thrust measurement devices for liquid rocket engine test stands	62
Klyuchnikov A. V. Elaboration and testing of the algorithm which ensures an achievement of minimal deviation angle of flying model's main centroidal axis of inertia during her counterbalancing in a sole correction flatness	70
Komlev G. V., Mitrofanova A. S. To the question of forecasting the technical condition of low-thrust liquid rocket engines	78
Nepomnyashchiy O. V., Krasnobaev Y. V., Yablonsky A. P., Solopko I. V., Lichargin D. V. Ensuring extreme regulation of power of primary energy sources at their joint operation for total load	85
Filonova M. M. Prospects for the development of high-voltage power supply systems of spacecraft with a charge-discharge regulator	96

PART 3. TECHNOLOGICAL PROCESSES AND MATERIAL SCIENCE

Konovalov S. O., Begisheva O. B., Hichem Abdelbaki, Rybina U. I., Yuxhno M. Yu. Research on electrical properties of manganese sulphides doped by thulium and ytterbium ions	108
Mikheev A. E., Girn A. V., Ravodina D. V., Elizar'eva I. G. The influence of prefinishing operations at titanium alloys on the characteristics of mao coatings	115
Titenkov S. V., Zhuravlev V. Yu. Peculiar properties of technological improvement and optimization of production costs of 3D-configuration pipes	125
Shestakov I. Y., Khilyuk A. V. Influence of a constant electric field on the adsorption purification of water from iron ions	136



РАЗДЕЛ
PART
1



ИНФОРМАТИКА,
ВЫЧИСЛИТЕЛЬНАЯ
ТЕХНИКА И УПРАВЛЕНИЕ

INFORMATICS,
COMPUTER TECHNOLOGY
AND MANAGEMENT



UDC 517.958:531.32

Doi: 10.31772/2587-6066-2020-21-1-8-14

For citation: Ivanov V. A., Erkaev N. V. Semi-analytical method for calculating elastic-hydrodynamic contact. *Siberian Journal of Science and Technology*. 2020, Vol. 21, No. 1, P. 8–14. Doi: 10.31772/2587-6066-2020-21-1-8-14

Для цитирования: Иванов В. А., Еркаев Н. В. Полуаналитический метод расчета упруго-гидродинамического контакта // Сибирский журнал науки и технологий. 2020. Т. 21, № 1. С. 8–14. Doi: 10.31772/2587-6066-2020-21-1-8-14

SEMI-ANALYTICAL METHOD FOR CALCULATING ELASTIC-HYDRODYNAMIC CONTACT

V. A. Ivanov^{1,3*}, N. V. Erkaev^{2,3}

¹ Institute of Computational Technologies SB RAS
6, Akademika Lavrentyeva St., Novosibirsk, 630090, Russian Federation

² Institute of Computational Modeling SB RAS
50/44, Akademgorodok, Krasnoyarsk, 660036, Russian Federation

³ Siberian Federal University, Polytechnic Institute
26, Akademika Kirenskogo St., Krasnoyarsk, 660074, Russian Federation

*E-mail: VinTextrim@yandex.ru

A semi-analytical method for calculating elastic-hydrodynamic contact based on the partial use of Computer Aided Design / Computer Aided Engineering (CAD / CAE) packages and solutions of the integral equation of functional relationship between pressure and deformation have been described. The pressure in the lubricating layer is described by solving the modernized Reynolds equation taking into account the factors such as elastic deformation of surfaces in the contact zone, cavitation effect in the low-pressure region, and variable viscosity of the lubricant layer, which depends on thermodynamic parameters. Based on the stationary solution, a tensor damping coefficient has been obtained, with the help of which calculations of transient non-stationary modes that occur in cases of a sharp change in the external load have been further performed. A comparison of the results of modeling a plain bearing obtained by using the proposed semi-analytical method has been made and the full calculation performed using CAD / CAE programs such as ANSYS and COMSOL Multiphysics. The comparison showed good convergence of all numerical methods. At the same time, the “hybrid” method showed a number of advantages over direct calculations in CAD / CAE packages, such as: faster calculation speed, low requirements for computing resources and accounting for the cavitation effect. The described semi-analytical method allows to create digital twins of bearing units, centrifugal pumps and hydraulic supports used in satellite cooling systems and in rotary mechanisms of ground-based satellite dishes.

Keyword: hybrid modeling, digital twins, elastic-hydrodynamic contact.

ПОЛУАНАЛИТИЧЕСКИЙ МЕТОД РАСЧЕТА УПРУГО-ГИДРОДИНАМИЧЕСКОГО КОНТАКТА

В. А. Иванов^{1,3*}, Н. В. Еркаев^{2,3}

¹ Институт вычислительных технологий СО РАН
Российская федерация, 630090, г. Новосибирск, просп. Академика Лаврентьева, 6

² Институт вычислительного моделирования СО РАН
Российская федерация, г. Красноярск, Академгородок, 55, стр. 44

³ Сибирский федеральный университет, Политехнический институт
Российская Федерация, 660074, г. Красноярск, ул. Академика Киренского, 26

*E-mail: VinTextrim@yandex.ru

Описан полуаналитический метод расчета упруго-гидродинамического контакта, основанный на частичном использовании Computer Aided Design / Computer Aided Engineering (CAD/CAE) пакетов и решения интегрального уравнения функциональной связи между давлением и деформацией. Давление в смазочном слое описывается решением модернизированного уравнения Рейнольдса с учетом таких факторов, как упругая деформация поверхностей в зоне контакта, эффект кавитации в области низкого давления, переменная вязкость смазочного слоя, зависящая от термодинамических параметров. На основе стационарного решения получен тензорный коэффициент демпфирования, с помощью которого далее выполняются расчеты переходных нестационарных режимов, возникающих в случаях резкого изменения внешней нагрузки. Проведено сравнение результатов моделирования подшипника скольжения, полученных с помощью предложенного полуаналитического метода и полного расчета, выполненного с помощью CAD/CAE программ, таких как ANSYS и COMSOL

Multiphysics. Сравнение показало хорошую сходимость всех численных методов. При этом «гибридный» метод показал ряд преимуществ по сравнению с прямыми расчетами в CAD/CAE пакетах, таких как более быстрая скорость расчета, невысокие требования к вычислительным ресурсам и учет кавитационного эффекта. Описанный полуаналитический метод позволяет создавать цифровые двойники подшипниковых узлов, центробежных насосов и гидропор, использующихся в спутниковых системах охлаждения и поворотных механизмах наземных спутниковых антенн.

Ключевые слова: гибридное моделирование, цифровые двойники, упруго-гидродинамический контакт.

Introduction. In today's world, practically any engineer designing a moving mechanical system faces contact tasks in friction units. Modern trends in the design of aircraft friction units set severe constraints: maximum weight reduction with full durability retention. One of the most difficult things is contact problems of elastic-hydrodynamic interaction between two bodies, as it requires simultaneous consideration of many factors, such as elastic surfaces deformation, pressure and temperature dependent viscosity of the liquid layer and lubricant foaming in low pressure zones. The most challenging problem is deformation of the elastic surface, as under high loads it significantly affects the value of the geometric clearance in the liquid layer. There is a number of approximate analytical solutions to such problems [1–6], obtained within the framework of simplifying assumptions, which do not allow to solve the contact problem with high accuracy. Various multidisciplinary CAD/CAE software applications are now widely available (CAD – Computer Aided Design, CAE – Computer Aided Engineering) Complexes (ANSYS, SolidWorks, COMSOL Multiphysics, etc.). However, the use of such complexes for calculating non-stationary elastic-hydrodynamic tasks faces considerable difficulties due to the presence of very thin layers, huge pressure drops and rigidity of non-stationary tasks, which require very short steps in time and space. All these lead to sufficient computational and

time costs. In this case, it makes sense to combine analytical methods with limited numerical modeling to solve specific engineering problems. Such an approach of “hybrid” modeling allows to build a complete digital dynamic model of a projected or real unit, and to study its operability when various external factors change. This is particularly true for hard to access or completely unserviceable units, such as centrifugal pumps used for spacecraft cooling systems [7]. As an example, we will use the plain bearing schematically shown in fig. 1.

Here, ω is the angular speed of shaft rotation, φ is the azimuthal angle counted clockwise from the maximum clearance point, η and R_0 are eccentricity and radius of the cylindrical shaft, R_1 is the inner radius of the liner, R_2 and R_3 are the inner and outer radii of the cylindrical case, L is the bearing length. In calculations we use zero boundary conditions for deformations at the specified external boundary of the bearing case. A thin layer of liquid lubricant, called a lubricating layer, is disposed between the shaft and the liner. We also set zero boundary conditions for pressure at the bearing ends.

Separation of elastic and hydrodynamic tasks. One promising way of simplifying a general elastic-hydrodynamic problem is to divide it into sequentially solved simpler tasks: a hydrodynamic task related to pressure determination in liquid layer, and a contact task based on the determination of elastic deformation.

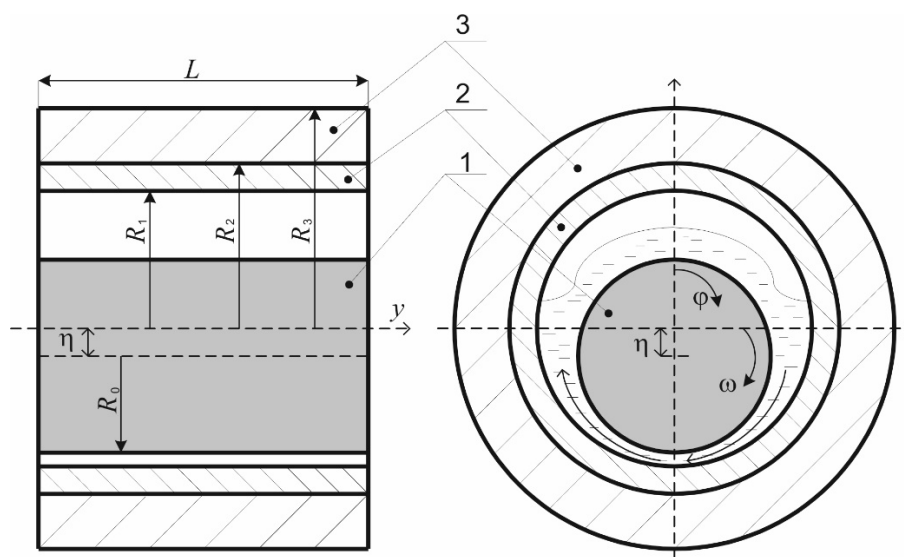


Fig. 1. Geometric diagram of a plain bearing:
1 – shaft; 2 – bronze liner; 3 – case

Рис. 1. Геометрическая схема подшипника скольжения:
1 – вал; 2 – бронзовый вкладыш; 3 – корпус

The relationship between elastic strain and pressure can generally be represented as follows:

$$\delta(x) = \int_{\Omega} P(x') K(x - x') d\Omega, \quad (1)$$

where δ and P are surface deflection and corresponding pressure, Ω is a contact pad. Function $K(x - x')$, which is a kernel of linear functional will be called flexibility function.

Flexibility function of $K(x - x')$ is a key element in the method of elastic and hydrodynamic task solutions. It is important to note that this function can be defined independently of the hydrodynamic problem solution. Thus, by setting some pressure distribution at the boundary of the bodies, it is possible to define appropriate deflection function δ as a result of the solution to the elastic problem for contact bodies.

Further, under the known functions δ and P , equation (1) can be considered as an integral equation with reference to function $K(x - x')$ which can be solved by decomposition on some orthogonal basis:

$$K(x - x') = \sum_{k=0}^n [M_k \Phi_k(x - x') + N_k \Psi_k(x - x')], \quad (2)$$

where M_k and N_k are orthogonal decomposition coefficients. In most cases, Ω zone can be considered rectangular and select trigonometric functions as basic functions for which the following equations are true:

$$\begin{aligned} \Phi_k(x - x') &= \Phi_k(x) \Psi_k(x') - \Psi_k(x) \Phi_k(x'), \\ \Psi_k(x - x') &= \Psi_k(x) \Psi_k(x') + \Phi_k(x) \Phi_k(x'). \end{aligned} \quad (3)$$

Adding (3) to (1), the following quotation system is obtained

$$\begin{aligned} \|\Phi_k\|^2 [M_k(P \cdot \Phi_k) + N_k(P \cdot \Psi_k)] &= (\delta \cdot \Phi_k), \\ \|\Psi_k\|^2 [M_k(P \cdot \Psi_k) - N_k(P \cdot \Phi_k)] &= (\delta \cdot \Psi_k). \end{aligned} \quad (4)$$

where

$$\|\Phi_k\|^2 = \|\Psi_k\|^2 = (\Phi_k \cdot \Phi_k) = (\Psi_k \cdot \Psi_k). \quad (5)$$

As a result of the system solution (4), the orthogonal decomposition coefficients M_k and N_k are calculated, thereby flexibility function is determined (2). It is important to note that restoring the flexibility function is an "incorrect task" [8] in which small-scale errors in the input data cause significant deviations in the outcome results. Therefore, to smooth the flexibility function, it is necessary to apply regularization [9].

Calculation of pressure. Pressure distribution P in the lubricating layer is determined from Reynolds equation [10]

$$\operatorname{div} \left[\frac{h^3}{12\mu} \nabla P \right] = \frac{1}{2} \nabla (\vec{V} h) + \frac{\partial h}{\partial t}, \quad (6)$$

where h – liquid layer thickness, V – sum of body velocities in the contact point

$$\vec{V} = \vec{V}_1 + \vec{V}_2.$$

At the same time thickness of the liquid layer h considers both the geometrical clearance between the contacting h_g bodies and the deformation of elastic δ of the surface caused by excessive pressure in the layer

$$\begin{aligned} h &= 1 + \eta \cos(\varphi) + \int_0^{2\pi} P(\varphi') K(\varphi - \varphi') d\varphi, \quad P > 0; \\ \vec{V} \nabla h &= 0, \quad P \leq 0, \end{aligned} \quad (7)$$

Where $K(\varphi - \varphi')$ is a flexibility function independent of the pressure distribution in the layer, but taking into account the geometric and elastic properties of the contacting materials [11].

It should be noted that equation (7) takes into account the cavitation effect (foaming) under negative pressure.

Importantly, viscosity of the lubricant layer μ strongly depends on the temperature T and pressure P . There is a set of empirical models of liquid layer viscosity change [12; 13], however the most accurate of which is Petrusevich's formula which approximates dependence of viscosity on temperature and pressure in an exponential view:

$$\mu(P, T) = \mu_0 \exp(\alpha P - \Omega_0 T), \quad (8)$$

where α is piezoelectric coefficient characterizing the change in viscosity depending on pressure, μ_0 is dynamic viscosity at $P = 0$, Ω_0 is a so-called viscosity slope coefficient.

Thermal calculation. Calculation of heat generating power Q for the plain bearing operating in hydrodynamic mode is defined by

$$Q = \frac{h^3}{12\mu} \left[\left(\frac{\partial P}{\partial y} \right)^2 + \frac{1}{R_1^2} \left(\frac{\partial P}{\partial \varphi} \right)^2 \right] + \frac{\mu}{h} V^2. \quad (9)$$

Let's write down the thermal conductivity equation in cylindrical coordinates:

$$\frac{1}{r} \frac{\partial}{\partial r} \left(r \frac{\partial T}{\partial r} \right) + \frac{1}{r^2} \frac{\partial^2 T}{\partial \varphi^2} = 0. \quad (10)$$

Solution to equation (10) can be represented as Fourier decomposition:

$$T = a_0 + \sum_{k=1}^{\infty} [a_k \cos(k\varphi) + b_k \sin(k\varphi)] + T_0. \quad (11)$$

At the inner boundary under $r = R_1$ we have a boundary condition for heat flow from the lubricating layer:

$$Q = -\chi \frac{\partial T}{\partial r}, \quad (12)$$

where Q is the heat generating power in the lubricating layer, defined by formula (9). The heat emission power function is also Fourier decomposed by harmonics:

$$Q = \Theta_0 + \sum_{k=1}^{\infty} [\Theta_k \cos(k\varphi) + \Theta_k \sin(k\varphi)], \quad (13)$$

$$\Theta_k = \frac{1}{\pi} \int_0^{2\pi} Q(\varphi) \cos(k\varphi) d\varphi,$$

$$\Theta_k^* = \frac{1}{\pi} \int_0^{2\pi} Q(\varphi) \sin(k\varphi) d\varphi, \quad (k = 1, 2, 3 \dots);$$

$$\Theta_0 = \frac{1}{2\pi} \int_0^{2\pi} Q(\varphi) d\varphi.$$

At the outer boundary we set the ambient temperature T_0 :

$$T(R_3) = T_0. \quad (14)$$

Applying Fourier decomposition to formula (12), we obtain the equations

$$-\chi \frac{\partial a_k}{\partial r} = \Theta_k, \quad -\chi \frac{\partial b_k}{\partial r} = \Theta_k^*. \quad (15)$$

Here, the factors a_k, b_k satisfy the differential equations:

$$\begin{aligned} \frac{1}{r} \frac{\partial}{\partial r} \left(r \frac{\partial a_k}{\partial r} \right) - \frac{k^2}{r^2} a_k &= 0, \\ \frac{1}{r} \frac{\partial}{\partial r} \left(r \frac{\partial b_k}{\partial r} \right) - \frac{k^2}{r^2} b_k &= 0, \\ \frac{1}{r} \frac{\partial}{\partial r} \left(r \frac{\partial a_0}{\partial r} \right) &= 0. \end{aligned} \quad (16)$$

While solving equations (16), we define coefficients a_k and b_k :

$$a_{k,j} = \Theta_{k,j} \tilde{a}_k, \quad b_{k,j} = \Theta_{k,j}^* \tilde{a}_k, \quad (17)$$

$$\begin{aligned} \tilde{a}_k &= -\frac{R_3}{k} \frac{1}{\chi \left[\left(\frac{R_1}{R_3} \right)^{k-1} + \left(\frac{R_3}{R_1} \right)^{k+1} \right]} \left[\left(\frac{R_1}{R_3} \right)^k - \left(\frac{R_3}{R_1} \right)^k \right], \\ \tilde{a}_0 &= \frac{R_1}{\chi} \ln \frac{R_3}{R_1}. \end{aligned}$$

Non-stationary loading. In case of sharp changes of external load F , disturbances in center-of-mass velocity occur, causing non-stationary shifts of liquid layer thickness and pressure distribution in contact zone, which leads to the change in the force reaction of the liquid layer against the external load associated with the pressure by the equation

$$\vec{W} = \int P \vec{N} dx'. \quad (18)$$

Under minor center-of-mass velocity disturbances, equation (18) can be represented as decomposition

$$\vec{W} = \vec{W}_0(\vec{x}_c) - \tilde{\lambda} \dot{\vec{x}}_c. \quad (19)$$

Here, the left part of the equation takes into account stationary bearing capacity of W_0 , while the right part – velocity disturbance in the center-of-mass, the tensor coefficient λ is a layer damping coefficients matrix. These coefficients determine pressure relaxation in the lubricating layer during non-stationary transient processes. The found functions of stationary carrying capacity and damping coefficients allow to write equation of body dynamics in the following form:

$$M \ddot{\vec{x}}_c + \tilde{\lambda} \dot{\vec{x}}_c - \vec{W}_0(\vec{x}_c) = -F. \quad (20)$$

The above method allows to find a self-consistent non-stationary solution to the problem of elastic-hydrodynamic interaction of bodies with any geometric parameters, with respect to their deformation. Based on this method a program has been written (in more detail [14]), which allows to efficiently calculate the self-consistent pressure distribution in the lubricating layer of the plain bearing. However, by changing clearance equation in the lubricating layer for another type of contact, the program becomes universal.

Comparison of proposed calculation method with CAD/CAE programs. Calculation of plain bearing lubricating layer (fig. 1) applying the above method is compared with the same calculation using ANSYS software complex based on finite element method. The calculation flowchart for both methods is shown in fig. 2.

Let's consider fig. 2 in more detail. In the first step of the “hybrid” method, we model the elastic deflection of the plain bearing in the ANSYS program (any other calculation program can be used, this is not fundamental) and set the load as an arbitrary distribution of pressure along the surface. As a result of calculation, elastic deflection of the liner is determined, which finishes the complex CAD/CAE programs use.

Further, knowing the pressure distribution in the lubricating layer and the corresponding elastic deformations, we restore the flexibility function according to the method described above. Then we shift to iterative calculation of lubricating layer [14], which takes into account variable viscosity of lubricant, cavitation effect, temperature change inside the layer and deformation of elastic surface. It is important to note that this algorithm is easily implemented in almost any software environment and makes calculations quickly and accurately for any load or eccentricity values.

When performing a full calculation in an ANSYS package, it is initially necessary to simulate the lubricating layer in ANSYS Fluid Flow, which at first glance should not cause any problems. However, at values of relative eccentricity of bearing more than 0.8 there are difficulties in modeling as the value of lubricating layer thickness becomes less than permissible (10^{-7} m). With these values, most CAD/CAE programs issue a simulation error and build a surface rather than a solid. In addition, CAD/CAE packages cannot take the cavitation effect into account, which affects the maximum pressure. Considering these limitations, we model a lubricating layer and determine the pressure generated by it, as well as calculate the heat generating power and temperature in the lubricating layer.

Next step is to simulate the bearing case, performing the same actions as in modeling deformation of the elastic layer in the “hybrid” method. The only difference is that the pressure distribution across the elastic layer is imported from the previously calculated lubricating layer. In order to shift to a non-stationary calculation, it is necessary to perform calculations for at least three different lubricating layers, that is, for three different values of relative eccentricity. The results are imported into ANSYS Twin Builder. Based on the previously obtained data, this package builds a lower-order plain bearing model by numerical approximation of the results, which

allows to determine in real time how the liner deflection and pressure change in the lubricating layer at a smooth change of load.

Let's compare the results of the solutions (fig. 3) obtained by "hybrid" modeling and modeling in ANSYS and SOMSOL Multiphysics packages [15]. Calculation was carried out for the following parameters: $L = 0.125$ m, $R_1 = 0.25$ m, $\mu = 0.19$ Pa·c, relative eccentricity $\eta = 0.5$, shaft rotation speed of 1000 rpm.

From fig. 3, calculations performed in ANSYS (curve 4) and COMSOL Multiphysics (curve 3) show the same results (difference not exceeding 1 %). Both calculations do not take into account the cavitation effect, which leads to a 15 % reduction in the maximum pressure compared to the "hybrid" method of calculation, taking into account the cavitation effect and excluding occurrence of negative pressure regions (curve 1). The results of the calculation using the "hybrid" method without cavitation are well

consistent with the calculations in CAD/CAE packages where the difference of maximum pressures in the layer does not exceed 6 %.

Comparative analysis of the above described results suggests that the semi-analytical "hybrid" calculation method shows good calculation accuracy provided its cost effectiveness. Herein, it has a number of advantages over numerical calculations in CAD/CAE programs. The first and rather significant advantage is the "cost of calculation" CAD/CAE packages that allow a number of calculations described above and have the required functionality have a very high cost, while any package that can perform static calculations (for example, ANSYS Student package) will be suitable for "hybrid" modeling. The second advantage of "hybrid" modeling is low computing resource requirements, while calculations in CAD/CAE packages require powerful computers that are also expensive.

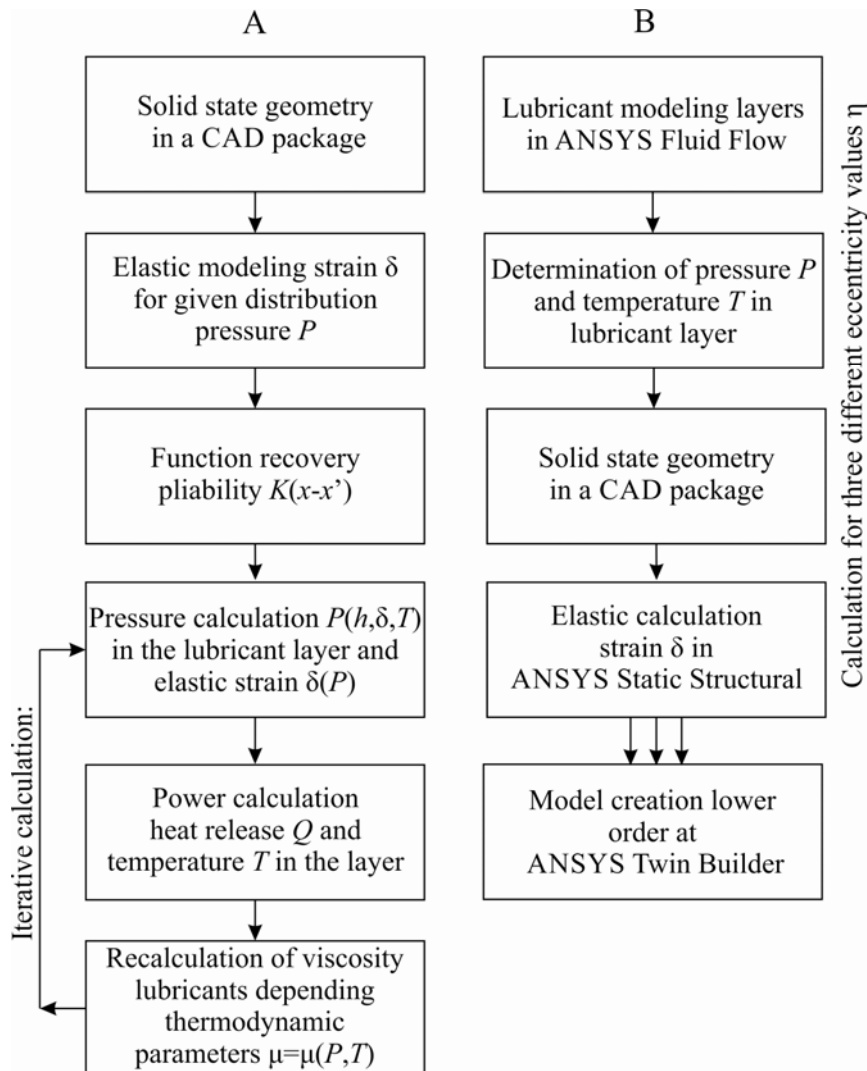


Fig. 2. Flowchart of methods for plain bearing calculation:
A – proposed "hybrid method"; B – calculation method using ANSYS

Рис. 2. Блок-схема методов расчета подшипника скольжения:
A – предлагаемый «гибридный метод»; B – методика расчета в ANSYS

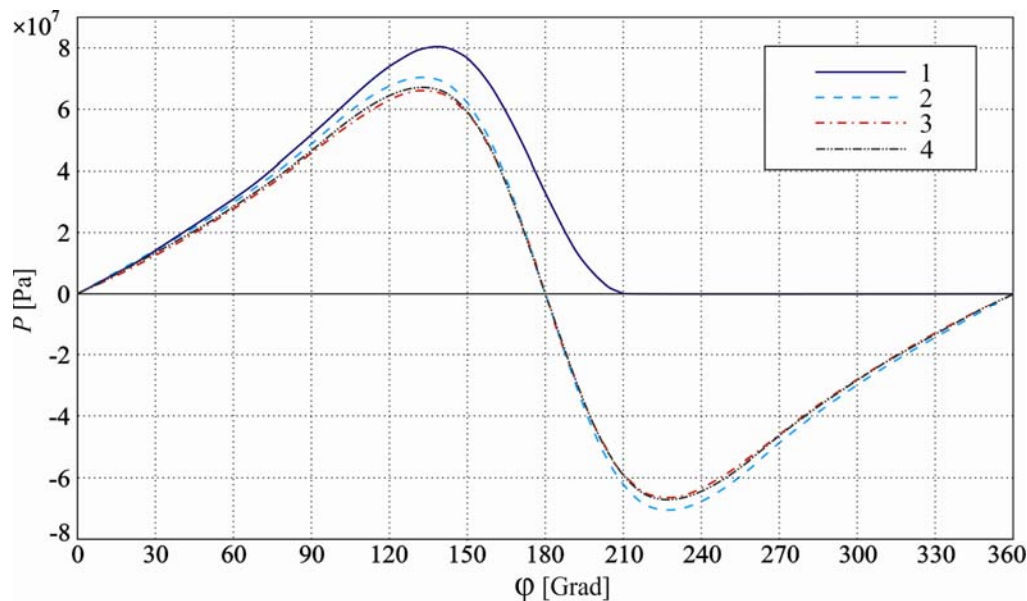


Fig. 3. Pressure in the lubricating layer of the plain bearing:
1 – semi-analytical solution that takes into account the cavitation effect; 2 – semi-analytical solution without taking into account the cavitation effect; 3 – modeling in COMSOL Multiphysics; 4 – modeling in ANSYS

Рис. 3. Давление в смазочном слое подшипника скольжения:

1 – полуаналитическое решение, учитывающее кавитационный эффект; 2 – полуаналитическое решение без учета кавитационного эффекта; 3 – моделирование в COMSOL Multiphysics; 4 – моделирование в ANSYS

The calculated and most important advantage of the “hybrid” simulation is the possibility of non-stationary calculation of the heavily loaded operation of the plain bearing or other type of contact interaction (the calculation technique will differ only by the clearance equation for a particular type of contact).

First, in a “hybrid” simulation, it is possible to set any size of the minimum clearance without restrictions for super-heavy loads. At the same time, modeling in CAD/CAE packages has a limit for minimum clearance values.

Second, “hybrid” modeling allows to take into account additional important physical factors that greatly complicate calculation: cavitation effect, which significantly affects pressure peak, variable viscosity of the lubricating layer, dependence on thermodynamic parameters, as well as sharp increase of pressure peak in the layer at sharp load jump. In CAD/CAE packages, this jump is not taken into account and the pressure rise occurs smoothly from the initial value to a new one with reference to the changed load.

Conclusion. The proposed method of “hybrid” simulation allows to calculate non-stationary elastic-hydrodynamic contact with minimal cost analysis, design and calculation resources taking into account such factors as elastic surface deformation, variable viscosity of lubricating layer and cavitation effect. This calculation method can be used in various engineering or technological departments to pre-evaluate a design unit, to optimize the existing one, as well as to create a digital twin of the friction unit in operation and to determine conditions of its normal performance in particular circumstances.

References

1. Williams J. A. Engineering tribology. New York, Oxford University Press Inc., 1994, 242 p.
2. Hamrock B. J., Schmid S. R., Jacobson B. O. Fundamentals of fluid film lubrication. New York, Marcel Dekker, Inc., 2004, 703 p.
3. Bair S. High-Pressure Rheology for quantitative elastohydrodynamics. *Tribology and Interface Engineering Series*. Elsevier, 2007, 54 p.
4. Szeri A. Z. Fluid film lubrication. Cambridge, Cambridge University Press, 2011, 273 p.
5. Lugt P. M., Morales-Espejel G. T. A Review of elasto-hydrodynamic lubrication theory. *Tribology Transactions*. 2011, Vol. 54, P. 470–496.
6. Galakhov M. A., Usov P. P. *Differentsial'nye i integral'nye uravneniya matematicheskoy teorii treniya* [Differential and integral equations of the mathematical theory of friction]. Moscow, Nauka Publ., 1990, 280 p.
7. Borovin G. K., Protopopov A. A. [Calculation of the optimal axial clearance of the semi-open impeller of the low-flow centrifugal pump of the spacecraft thermal control system]. *Preprinty IPM im. M.V. Keldysa*. 2013, No. 86, 16 p. (In Russ.).
8. Tikhonov A. N., Arsenin V. Ya. *Metody resheniya nekorrektnykh zadach* [Methods for solving incorrect tasks]. Moscow, Nauka Publ., 1979, 288 p.
9. Ivanov V. A., Erkaev N. V. [Nostedy oscillations of the roller contacting with riding surface with lubrication layer]. *Vestnik SibGAU*. 2017, Vol. 18, No. 1, P. 50–57 (In Russ.).
10. Terentev V. F., Erkaev N. V., Dokshanin S. G. *Tribonadejnost podshipnikovix uzlov v prisutstvii modifi-*

cirovanix smazochnix kompozicii [Tribo-durability of bearing units in a presence of modified lubricant compositions]. Novosibirsk, Nauka Publ., 2003, 142 p.

11. Ivanov V. A., Erkaev N. V. [Iterative calculation of trubo-contact between a roller and plate]. *Vestnik SibGAU*. 2014, No. 4(56), P. 48–54 (In Russ.).

12. Besportochnyy A. I., Galakhov M. A. *Matematicheskoe modelirovanie v tribotekhnike*. [Mathematical modeling in tribology]. Moscow, MFTI Publ., 1991, 88 p.

13. Galin L. A. *Kontaktnye zadachi teorii uprugosti i vyazkouprugosti* [Contact problems of the theory of elasticity and viscoelasticity]. Moscow, Fizmatlit Publ., 1980, 304 p.

14. Ivanov V. A. [Program complex of pressure calculation in lubricated slide bearing layer]. *Siberian Journal of Science and Technology*. 2018. Vol. 19, No. 3, P. 540–549 (In Russ.).

15. Ravindra M., Sandeep S. Analysis of hydrodynamic plain journal bearing. Excerpt from the Proceedings COMSOL Conference in Bangalore. 2013.

Библиографические ссылки

1. Williams J. A. Engineering tribology. N.-Y. : Oxford University Press Inc., 1994. 242 p.

2. Hamrock B. J., Schmid S. R., Jacobson B. O. Fundamentals of fluid film lubrication. N.-Y. : Marcel Dekker, Inc., 2004. 703 p.

3. Bair S. High-Pressure Rheology for quantitative elastohydrodynamics // *Tribology and Interface Engineering Series*. Elsevier, 2007. 54 p.

4. Szeri A. Z. Fluid film lubrication. Cambridge : Cambridge University Press, 2011. 273 p.

5. Lugt P. M., Morales-Espejel G. T. A Review of elasto-hydrodynamic lubrication theory // *Tribology Transactions*. 2011. Vol. 54. P. 470–496.

6. Галахов М. А., Усов П. П. Дифференциальные и интегральные уравнения математической теории трения. М. : Наука, 1990. 280 с.

7. Боровин Г. К., Протопопов А. А. Расчет оптимального осевого зазора полуоткрытого рабочего колеса центробежного малорасходного насоса системы терморегулирования космического аппарата // Препринты ИПМ им. М. В. Келдыша. 2013. № 86. 16 с.

8. Тихонов А. Н., Арсенин В. Я. Методы решения некорректных задач. М. : Наука, 1979. 288 с.

9. Иванов В. А. Еркаев Н. В. Нестационарные колебания ролика, контактирующего с твердой поверхностью, при наличии смазочного слоя // Вестник СибГАУ. 2017. Том 18, № 1. С. 50–57.

10. Терентьев В. Ф., Еркаев Н. В., Докшанин С. Г. Трибонадежность подшипниковых узлов в присутствии модифицированных смазочных композиций. Новосибирск : Наука, 2003. 142 с.

11. Иванов В. А., Еркаев Н. В. Итерационный расчет трибоконтакта ролика с пластиной // Вестник СибГАУ. 2014. № 4 (56). С. 48–54.

12. Беспорточный А. И., Галахов М. А. Математическое моделирование в триботехнике. М. : МФТИ, 1991. 88 с.

13. Галин Л. А. Контактные задачи теории упругости и вязкоупругости. М. : Физматлит., 1980. 304 с.

14. Иванов В. А. Программный комплекс расчета давления в смазочном слое подшипника скольжения // Сибирский журнал науки и технологий. 2018. Т. 19, № 3. С. 540–549.

15. Ravindra M., Sandeep S. Analysis of hydrodynamic plain journal bearing // Excerpt from the Proceedings COMSOL Conference in Bangalore. 2013.

© Ivanov V. A., Erkaev N. V., 2020

Ivanov Viktor Andreevich – Cand. Sc., researcher, laboratory of digital twins and big data analysis, Institute of Computational Technologies SB RAS; assistant of Applied mechanics department, Siberian Federal University, Polytechnic Institute. E-mail: Vintextrim@yandex.ru.

Erkaev Nikolai Vasilievich – Dr. Sc., professor, principle research scientist, Institute of Computational Modelling SB RAS; Professor of Applied mechanics department, Siberian Federal University, Polytechnic Institute. E-mail: nerkaev@gmail.com.

Иванов Виктор Андреевич – кандидат технических наук, научный сотрудник лаборатории цифровых двойников и анализа больших данных, Институт вычислительных технологий СО РАН; ассистент кафедры прикладной механики, Сибирский федеральный университет, Политехнический институт. E-mail: Vintextrim@yandex.ru.

Еркаев Николай Васильевич – доктор физико-математических наук, профессор, главный научный сотрудник, Институт вычислительного моделирования СО РАН; профессор кафедры прикладной механики, Сибирский федеральный университет, Политехнический институт. E-mail: nerkaev@gmail.com.

UDC 004.772

Doi: 10.31772/2587-6066-2020-21-1-15-20

For citation: Lvova A. P. Development of method for increasing sensitivity in wireless optical data transmission channels in visible wavelength range. *Siberian Journal of Science and Technology*. 2020, Vol. 21, No. 1, P. 15–20. Doi: 10.31772/2587-6066-2020-21-1-15-20

Для цитирования: Львова А. П. Разработка способа повышения чувствительности в беспроводных оптических каналах передачи данных в видимом диапазоне световых волн // Сибирский журнал науки и технологий. 2020. Т. 21, № 1. С. 15–20. Doi: 10.31772/2587-6066-2020-21-1-15-20

DEVELOPMENT OF METHOD FOR INCREASING SENSITIVITY IN WIRELESS OPTICAL DATA TRANSMISSION CHANNELS IN VISIBLE WAVELENGTH RANGE

A. P. Lvova

North-Caucasus Federal University
2, Kulakova Av., Stavropol, 355029, Russian Federation
E-mail: lvova.ap@gmail.com

The original method for encoding binary data streams based on QPSK quadrature phase shift keying in a wireless optical communication channel in the visible range is suggested. The algorithm for analyzing signals in the receiving tract is presented. It allows to analyze the presence of two or three pulses of different colors at the input, which will signal the presence of interference or the occurrence of "illumination". In addition, the algorithm provides a possibility of dynamic compensation of external "illumination" by changing the gain of the photodetectors and adjusting the brightness of emitting LEDs. The functional scheme of the device for realization of the offered coding method in the wireless channel on the basis of optical radiation has been developed. Given that most photodiodes are sufficiently wide-band in the visible range of light waves, to increase sensitivity of each color channel and selectivity of the receiving tract it is necessary to apply optical filters for each color channel. The most effective are interference filters made of optically transparent materials with different physical characteristics. The approach for calculating optical filters has been presented.

Keywords: wireless data transmission, optical data transmission channel in the visible wavelength range, encoding based on quadrature phase shift keying, color channel, Li-Fi.

РАЗРАБОТКА СПОСОБА ПОВЫШЕНИЯ ЧУВСТВИТЕЛЬНОСТИ В БЕСПРОВОДНЫХ ОПТИЧЕСКИХ КАНАЛАХ ПЕРЕДАЧИ ДАННЫХ В ВИДИМОМ ДИАПАЗОНЕ СВЕТОВЫХ ВОЛН

А. П. Львова

Северо-Кавказский федеральный университет
Российская Федерация, 355029, г. Ставрополь, просп. Кулакова, 2
E-mail: lvova.ap@gmail.com

Предложен способ кодирования двоичного потока данных на основе квадратурной фазовой манипуляции QPSK, обладающий высокой скоростью и контролем наличия ошибок в канале передачи данных. Представлен алгоритм анализа сигналов в приемном тракте, позволяющий анализировать присутствие двух или трех импульсов разных цветов на входе, что сигнализирует о наличии помехи или возникновении «засветки». Кроме того, алгоритм обеспечивает возможность динамической компенсации внешней «засветки» путем изменения коэффициента усиления фотоприемников и регулировки яркости излучающих светодиодов. Разработана функциональная схема устройства для реализации предлагаемого способа кодирования в беспроводном канале на основе оптического излучения. Учитывая, что большинство фотодиодов являются достаточно широкополосными в видимом диапазоне световых волн, для повышения чувствительности каждого цветового канала и селективности приемного тракта, предложено использовать оптические фильтры для каждого цветового канала. Наиболее эффективными являются интерференционные фильтры из оптически прозрачных материалов с различными физическими характеристиками. Представлен подход для расчета оптических фильтров.

Ключевые слова: беспроводная передача данных, оптический канал передачи данных в видимом диапазоне длин волн, кодирование на основе квадратурных фазовых манипуляций, цветовой канал, Li-Fi.

Introduction. In order to organize safe data transmission, it is proposed to build a wireless optical channel based on three-component (RGB) LEDs for room lighting and information transmission.

It is known [1] that the human eye is unable to detect pulsations of light flux at a frequency above 100 Hz. Thus, the use of pulse modulation at frequencies from 100 kHz to 10 MHz will allow data transmission and

room lighting without harm to health. Additionally, transmission of information over the wireless optical channel allows to precisely determine the perimeter of the protected area to ensure confidentiality of data transmitted [2].

A phase keying-based encoding method. In order to perform secure data transmission over a wireless optical communication channel, a method of encoding information based on quadrature phase keying has been developed. The encoding process is shown in fig. 1. A serial stream of input data bits $I(t)$ is converted into a series of N bit blocks $b_N, b_{N-1}, \dots, b_1, b_0$, each encoded by an RGB pulse burst. The pulse burst is represented as a set of pulses on each of the color channels during the reference signal period. Coding occurs on the basis of quadrature phase manipulations to four possible conditions of a phase in reference to basic signal ($45^\circ, 135^\circ, 225^\circ, 315^\circ$) [3]. Thus, the number of color channels $CC=3$, the number of possible phase states $FC=4$, the total number of unique combinations according to the rules of combinatorics [4] $M = CC^{FC} = 3^4 = 81$ state.

As a further limitation, it is determined that in one period of reference signal each color channel generates not more than one pulse, and also that in single period there cannot be two or more pulses with the same phase. Thus, the number of unique phase states is defined as

$$M = \prod_{j=0}^{CC-1} (FC - j) = 4 \cdot 3 \cdot 2 = 24. \quad (1)$$

When encoding binary signals, the number of bits transmitted over the reference signal period is given by

$$M_2 = \text{div} \left[\log_2 \prod_{j=0}^{CC-1} (FC - j) \right] = 4. \quad (2)$$

According to (2), in the case of a binary input data flow $I(t)$, the number of bits in each transmission unit is 4.

The remaining 8 states can be used to transmit overhead messages such as start and end of transmission, error, and data flow control.

Fig. 2 shows the coding diagram of one of the possible states for each of the channels. The dashed line diagram shows the possibility of pulse width modulation (PWM) of luminous flux intensity, which allows to adjust luminance of lighting devices to create comfortable operating conditions or to make adaptive adjustment of luminous flux level from the light source taking into account the change of illumination in the room. Similar technology is offered in [5].

Radiation power control when using LED lighting sources as transmitters has its limitations related to creation of required illumination or compensation of external illumination [6; 7]. Automatic adjustment of the photo-detectors sensitivity takes precedence over the power of light sources adjustment, as it allows to adjust it independently to the value of total illumination, and compensate for the constant component from additional light sources.

$b_3 b_2 = "00"$ $\varphi_R = 45^\circ$	$\text{for } b_1 = "0"$ $f_1 = \varphi_G(\varphi_R) = 90 - \varphi_R$	$\text{for } b_0 = "0"$ $f_3 = f_1 - 90$	F_1
		$\text{for } b_0 = "1"$ $f_3 = f_1 + 90$	
	$\text{for } b_1 = "1"$ $f_2 = \varphi_G(\varphi_R) = 180 - \varphi_R$	$\text{for } b_0 = "0"$ $f_3 = f_2 - 180$	
		$\text{for } b_0 = "1"$ $f_3 = f_2 - 90$	
$b_3 b_2 = "01"$ $\varphi_R = 135^\circ$	f_1	$\text{for } b_0 = "0"$ $f_3 = f_1 + 90$	F_2
		$\text{for } b_0 = "1"$ $f_3 = f_1 - 90$	
	f_2	$\text{for } b_0 = "0"$ $f_3 = f_2 + 180$	
		$\text{for } b_0 = "1"$ $f_3 = f_2 - 90$	
$b_3 b_2 = "10"$ $\varphi_R = 225^\circ$	f_1	F_1	
	f_2		
$b_3 b_2 = "11"$ $\varphi_R = 315^\circ$	f_1	F_2	
	f_2		

Fig. 1. The table of phase states of information encoding based on phase manipulations in a channel with spectral division

Рис. 1. Таблица фазовых состояний кодирования информации на основе фазовых манипуляций в канале со спектральным разделением

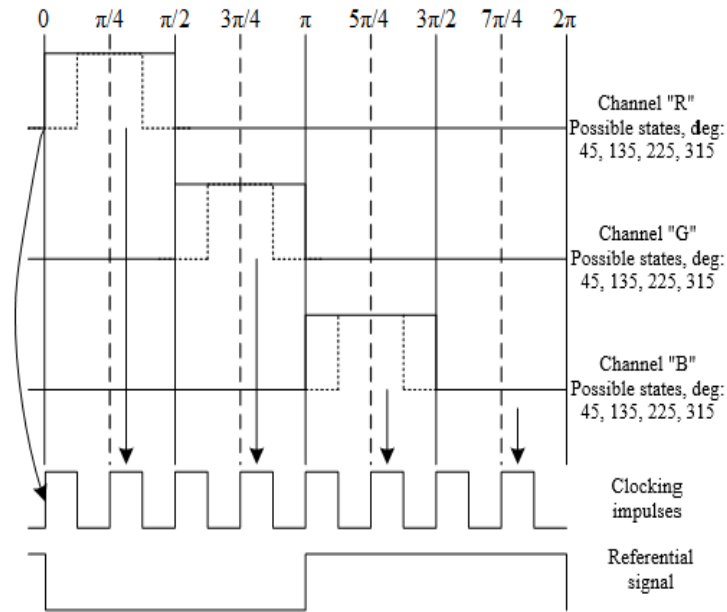


Fig. 2. The diagram of information encoding based on phase manipulations in a channel with spectral division

Рис. 2. Диаграмма кодирования информации на основе фазовых манипуляций в канале со спектральным разделением

Monitoring data link errors. The encoding method assumes that in one reference signal period, each color channel will generate one pulse of equal duration and all three color components will have different phases. Simultaneous presence of two or three pulses of different colors at the input will signal the presence of interference or occurrence of “illumination” – change of intensity of additional natural or artificial lighting [8]. Here, it is necessary to distinguish short-term pulses $\tau \sim 10^{-8} \div 10^{-6}$ c ($\tau \sim 10^{-8} \div 10^{-6}$ c) in three color channels, which are recognized as an error in the active phase of data transmission, or are used for synchronization of receiver and transmitter between data packages, and slowly variable signal ($\tau \sim 10^{-3} \div 10^1$ c) at the receiver input, which is a characteristic of illumination with natural or artificial light [9; 10]. When generating sync pulses, simultaneous pulses are proposed on all color channels for phase state $\varphi = 45^\circ$. Fig. 3 shows the flow chart of signal analysis in the receiving tract.

Such method ensures control and possibility of dynamic compensation of external “illumination” by changing the gain of photo-detectors and adjusting the brightness of emitting LEDs.

Functional diagram of fixed and mobile transceiver device. Fig. 4 is a functional diagram of an apparatus for implementing a wireless channel coding method according to the invention based on optical radiation. Input data stream of binary sequence $I(t)$ is supplied to input of digital data processing unit (DDP) [11]. The functions of the DDP unit are to generate a sequence of rectangular pulses for synchronization with the data source, to buffer the input data and control the flow, as well as to convert the sequence of bits into a sequence of four-bit units. The

synchronization signal is input to the clock to provide phase locked loop (PLL) [12; 13], and the output data stream enters the input of the serial encoding device (SED). SED operation algorithm implements the table of phase states shown in fig. 1.

Output signals from SED are transmitted to light intensity control units based on PWM, then to current keys of LED control. Receiving side consists of photo-detectors (photodiodes) with corresponding optical color filters, signal from which is supplied to input of operational amplifiers (OA) with adjustable gain factor, followed by a signal transmitted to the input of data processing device. The main functions of the DP unit are to generate a rectangular sequence of pulses for synchronizing the receiver and transmitter, as well as to analyze the state of signals of each of the color components (determine an error or “illumination”). Simultaneously, signals from outputs of OA of each color channel are supplied to the input of serial decoding device (SDD) which implements algorithm, reverse to initial one. Output stream of binary sequence data is generated at output of SDD.

Calculation of optical transmission filters. Given that most photodiodes are sufficiently wideband in the visible range of light waves, optical filters for each color channel need to be used to increase sensitivity of each color channel and selectivity of the receiving tract. Interference filters of optically transparent materials with different physical characteristics are considered to be the most effective [14].

Sufficient transmission functions can be obtained using just two different dielectric materials, with refractive indices n_L and n_H . Supposing you want to create a filter that passes the center wavelength λ_0 , a general scheme

for constructing such filters is to use alternating layers of high and low refractive index dielectric having a thickness of $1/4$ or $1/2$ wavelength λ_0 . The quarter-wave dielectric plate with refractive index n_L should have thickness of $\lambda_0/4n_L$. Since these thicknesses are very small at optical wavelengths, 'thin film' is more commonly used term instead of the term 'plate'. Dielectric thin films half wavelength thick λ_0 are called filter bands. The thin film filter structure used consists of several bands separated by several quarter-wave films. If H and L denote quarter-wave

films (for wavelength λ_0) of high and low refractive index dielectrics, respectively, then we can imagine a design of any filter using an HL sequence. Two characters H or L in a row denote a half-wave film. For example, if the slightly hatched dielectric has a low refractive index and the highly hatched dielectric has a high refractive index, the filter consisting of a number of dielectric films may be represented by the sequence $HLHLHLHL$. If the surrounding dielectrics are indicated by a symbol G (glass), the complete structure can be represented by the sequence $GHLHLHLHLG$.

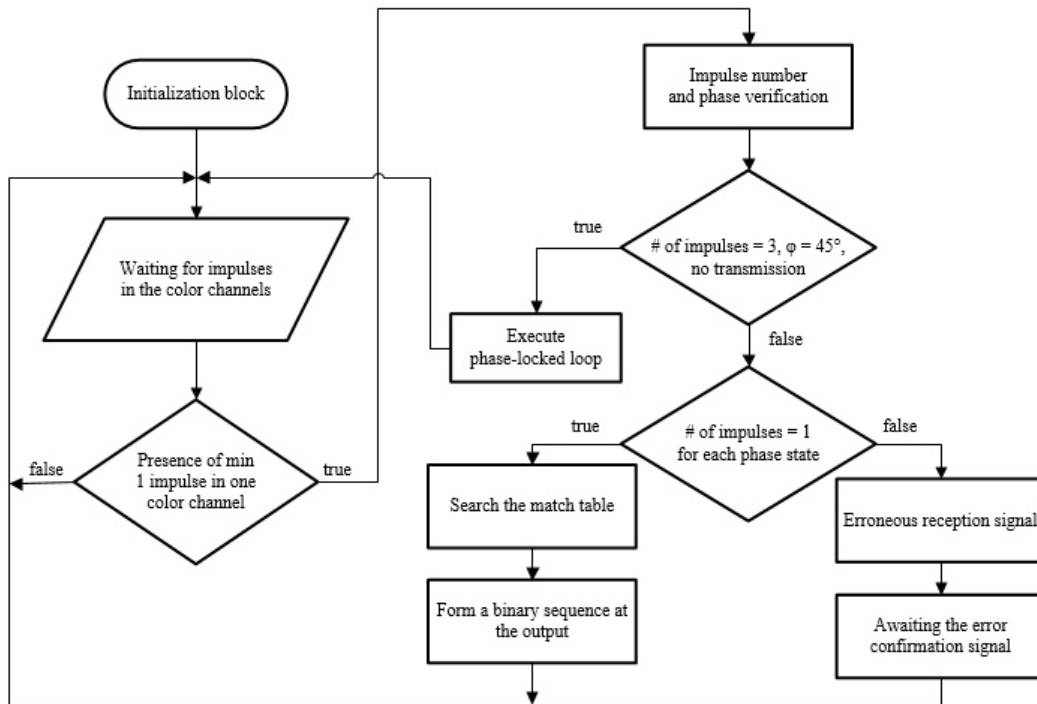


Fig. 3. The algorithm of signal analysis in the receiving tract

Рис. 3. Алгоритм анализа сигналов в приемном тракте

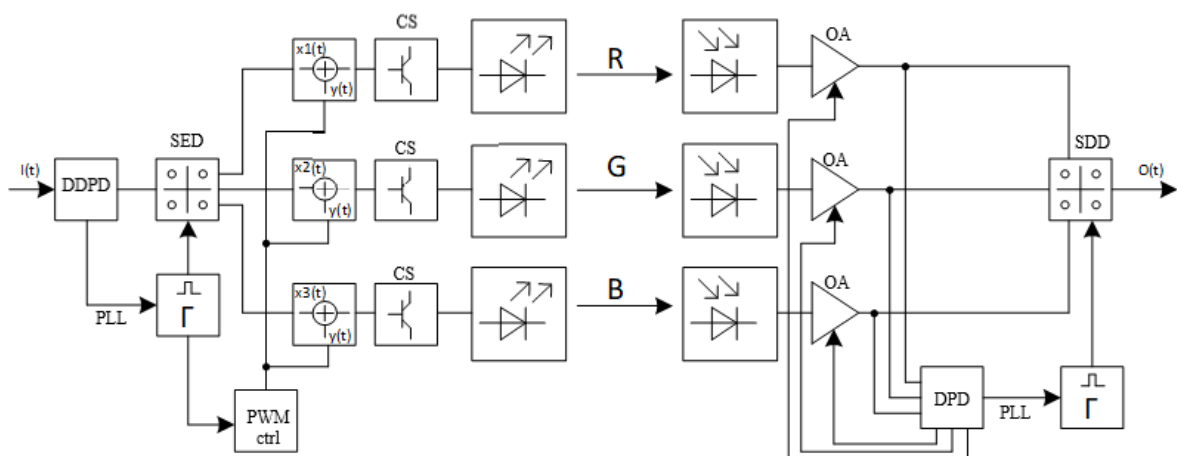


Fig. 4. The functional scheme of the device required to implement the suggested encoding method

Рис. 4. Функциональная схема устройства для реализации предлагаемого способа кодирования

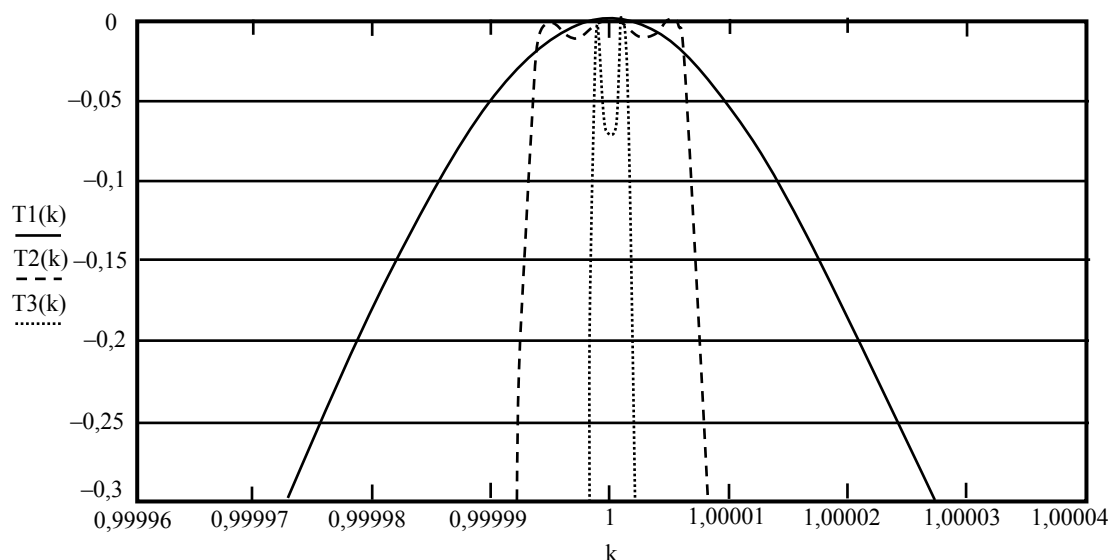


Fig. 5. Comparison of one-, two- and threeband filters

Рис. 5. Сравнение одно-, двух- и трехполостного фильтров

A narrower region of transmission and a stronger suppression of lateral wavelengths can be achieved by using more than three quarter-wave films [15]. As an example, the filter described by a sequence $G(HL)^9 HLL(HL)^9 HG$ is suggested. Marking $(HL)^k$ corresponds to a sequence $HLHL \dots HL$ (k times).

The use of multiple bands results in a flatter bandwidth and a sharp drop at the edges. Both effects are shown in fig. 5, in which the transmission function close to the center wavelength λ_0 is depicted for a one-, two-, and three-band dielectric thin film filter.

One-band filter is similar to the one described above. Two-band filter is described as a sequence

$$G(HL)^{12} HLL(HL)^{24} HLL(HL)^{12} HG.$$

Three-band filter is described as a sequence

$$G(HL)^{10} HLL(HL)^{21} HLL(HL)^{21} HLL(HL)^{10} HG.$$

Conclusion. Among the advantages of the proposed approach are: increase of information transfer speed in wireless channels based on VLC technology; improvement of noise immunity due to the applied coding technology and compensation algorithm of external light source luminance flux change (“illumination”); high channel security against unauthorized access to information implemented by means of distributed spectral coding; and possibility of more efficient filtering of light flux from VLC transmitter in red and blue color bands.

Thus, a method of encoding data in wireless optical communication channels having high noise immunity has been developed.

In order to increase sensitivity of each color channel and selectivity of the receiving tract, it is proposed to use optical filters for each color channel. Interference filters of optically transparent materials with different physical characteristics are the most effective.

References

1. Nikiforov S. D. [Physical Aspects of Semiconductor Light Perception by the Human Eye]. *Komponenty i tekhnologii*. 2008, No. 89, P. 84–94. (In Russ.).
2. Zaocheng Wang, Qi Wang, Wei Huang, Zhengyang. Visible Light Communications: Modulation and Signal Processing. 2017, Wiley-IEEE Press, 368 p.
3. Elgala H., Mesleh R., Haas H., Pricope B. OFDM visible light wireless communication based on white LEDs. *In IEEE 65th Vehicular Technology Conference*. Dublin, Ireland, 22–25 April 2007, VTC2007-Spring, P. 2185–2189.
4. Korn G. Korn T. *Spravochnik po matematike*. [Handbook of mathematics]. 1974, Moscow, Nauka Pub., 831 p.
5. Zhao S., Xu J., Trescases O. A dimmable LED driver for visible light communication (VLC) based on LLC resonant dc-dc converter operating in burst mode. *IEEE Applied Power Electronics Conference (APEC)*, Long Beach, USA, March 2013, P. 2144–2150.
6. Aliaberi A., Sofotasios P., Muhaidat S. Modulation Schemes for Visible Light Communications. *COMMNET* 1–10, 2019.
7. Dmitrov S., Haas H. Principles of LED Light Communications: Towards Networked Li-Fi. 2015, United Kingdom, Cambridge: Cambridge University Press, 207 p.
8. Malsugenov O., Chipiga A., Lvova A. Improving the Efficiency of Wireless Optical Transmission Channel in the Visible Wavelength Range. *Proceedings of the 7th Scientific Conference on Information Technologies for Intelligent decision making Support (ITIDS 2019) – advances in Intelligent Systems Research*. 2019, Vol. 166, P. 246–250.
9. Jamieson I. Visible Light Communication (VLC) Systems. July 14, 2010. Available at: <http://www.bemri.org/component/content/article/3-home/18-visible-light-communication-vlc-systems.html> (accessed 20.12.2019).

10. O'Brien, D., Kang, T.-G., and Matsumura, T. Visible Light Communication: Tutorial. 2010. Available at: http://www.ieee802.org/802_tutorials/2008-03/15-08-0114-02-0000-LC_Tutorial_MCSamsung-VLCC-Oxford_2008-03-17.pdf. In IEEE 802.15-08/0114-02 (accessed 20.12.2019).
11. Gauer J. *Opticheskie sistemy svyazi* [Optical communication systems]. 1989, Moscow, Radio i svyaz Publ., 504 p.
12. Sklyar B. *Cifrovaya svyaz. Teoreticheskie osnovy i prakticheskoe primeneniye* [Digital communication. Theoretical foundations and practical application]. 2007, Moscow, Williams Publ., 1104 p.
13. Sultanov A. H., Usmanov R. G., Sharifgaleev I. A., Vinogradova I. L. *Volonno-opticheskie sistemy peredachi: voprosy ocenki rabotosposobnosti* [Fiber-optic transmission systems: performance assessment issues]. 2005, Moscow, Radio i svyaz Publ., 373 p.
14. Varjel S. V. *Volonnyye breggovskie reshetki* [Fiber Bragg gratings]. 2015, St. Petersburg, Universitet ITMO Publ., 65 p.
15. Nureev I. I. [Modeling of spectral characteristics of phased fiber Bragg gratings as sensors of sensor systems]. *Sovremennye problemy nauki i obrazovaniya*. 2015, No. 1-1, P. 350–350 (In Russ.).
- IEEE Applied Power Electronics Conference (APEC), Long Beach, USA, March 2013. P. 2144–2150.
6. Aliaberi A., Sofotasios P., Muhaidat S. Modulation Schemes for Visible Light Communications. COMMNET 1-10, 2019.
7. Dmitrov S., Haas H. Principles of LED Light Communications: Towards Networked Li-Fi. 2015, United Kingdom, Cambridge: Cambridge University Press, 207 p.
8. Malsugenov O., Chipiga A., Lvova A. Improving the Efficiency of Wireless Optical Transmission Channel in the Visible Wavelength Range // Proceedings of the 7th Scientific Conference on Information Technologies for Intelligent decision making Support (ITIDS 2019) – advances in Intelligent Systems Research. 2019. Vol. 166. P. 246–250.
9. Jamieson I. Visible Light Communication (VLC) Systems. July 14, 2010 [Электронный ресурс]. URL: <http://www.bemri.org/component/content/article/3-home/18-visible-light-communication-vlc-systems.html> (accessed 20.12.2019).
10. O'Brien D., Kang T.-G., Matsumura T. Visible Light Communication: Tutorial. 2010. [Электронный ресурс]. URL: http://www.ieee802.org/802_tutorials/2008-03/15-08-0114-02-0000-LC_Tutorial_MCSamsung-VLCC-Oxford_2008-03-17.pdf. In IEEE 802.15-08/0114-02 (accessed 20.12.2019).
11. Гауэр Дж. Оптические системы связи : пер. с англ. М. : Радио и связь, 1989. 504 с.
12. Скляр Б. Цифровая связь. Теоретические основы и практическое применение. М. : Вильямс, 2007. С. 1104.
13. Волоконно-оптические системы передачи: вопросы оценки работоспособности / А. Х. Султанов, Р. Г. Усманов, И. А. Шарифгалиев, И. Л. Виноградова. М. : Радио и связь, 2005. 373 с.
14. Варжель С. В. Волоконные брегговские решетки. СПб. : Университет ИТМО, 2015. 65 с.
15. Нуреев И. И. Моделирование спектральных характеристик фазированных волоконных решеток Брэгга как датчиков сенсорных систем // Современные проблемы науки и образования. 2015. № 1-1. С. 350–350.

© Lvova A. P., 2020

Lvova Anna Pavlovna – PhD student, assistant lecturer, department of information security of automated systems, North-Caucasus Federal University, Institute of information technologies and telecommunications, E-mail: lvova.ap@gmail.com.

Львова Анна Павловна – аспирант, ассистент кафедры информационной безопасности автоматизированных систем; Северо-Кавказский федеральный университет, Институт информационных технологий и телекоммуникаций. E-mail: lvova.ap@gmail.com.

UDC 519.87

Doi: 10.31772/2587-6066-2020-21-1-21-27

For citation: Raskina A. V., Videnin S. A., Chzhan E. A., Yusupova R. R. Peculiarities of design software architecture of adaptive information processing, modeling and control systems. *Siberian Journal of Science and Technology*. 2020, Vol. 21, No. 1, P. 21–27. Doi: 10.31772/2587-6066-2020-21-1-21-27

Для цитирования: Раскина А. В., Виденин С. А., Чжан Е. А., Юсупова Р. Р. Особенности организации программной архитектуры адаптивных систем обработки информации, моделирования и управления // Сибирский журнал науки и технологий. 2020. Т. 21, № 1. С. 21–27. Doi: 10.31772/2587-6066-2020-21-1-21-27

PECULIARITIES OF DESIGN SOFTWARE ARCHITECTURE OF ADAPTIVE INFORMATION PROCESSING, MODELING AND CONTROL SYSTEMS

A. V. Raskina, S. A. Videnin, E. A. Chzhan, R. R. Yusupova

Siberian Federal University
79, Svobodnyy Av., Krasnoyarsk, 660041, Russian Federation
E-mail: raskina.1012@gmail.com

The article proposes an approach to developing the architecture of a service-oriented information processing system, modeling and process control. The system, which is being developed, is a tool for identifying, predicting and controlling discrete-continuous processes. Its mathematical apparatus is based on nonparametric algorithms of identification and control. The software architecture includes the following main modules: the module for processing data, modeling and forecasting output process variables and the process control module. The first module includes data preprocessing algorithms: normalization, centering and analysis of outliers and omissions. The modeling module is an algorithm for research and recovery dependencies between process variables, process identification using nonparametric estimation of the regression function from observations. The last module is an implementation of nonparametric dual control algorithms. Control devices built on the basis of these algorithms perform functions of both object control and its study.

The article discusses the application of architectural solutions based on two proven approaches in the field of software development: the composite approach and the service-oriented approach.. The main principles of composite architecture as a set of software systems with many characteristics that perform a specific task and service-oriented architecture as a modular approach to software development are described. The advantages of the applied composite service-oriented architecture over other variants of software architecture for control systems are shown, in particular, monolithic software architecture is compared with composite service-oriented architecture. This means that a researcher can use a single operation, which is a logically isolated, repeated task related to the production process of the enterprise. At the same time, it is necessary to ensure positive results when integrating with existing software products of enterprises which greatly complicates and requires the development of new components, as well as support for the "inherited" parts of the system.

Keywords: service-oriented architecture, software development, design of process control systems.

ОСОБЕННОСТИ ОРГАНИЗАЦИИ ПРОГРАММНОЙ АРХИТЕКТУРЫ АДАПТИВНЫХ СИСТЕМ ОБРАБОТКИ ИНФОРМАЦИИ, МОДЕЛИРОВАНИЯ И УПРАВЛЕНИЯ

А. В. Раскина, С. А. Виденин, Е. А. Чжан, Р. Р. Юсупова

Сибирский федеральный университет
Российская Федерация, 660041, г. Красноярск, просп. Свободный, 79
E-mail: raskina.1012@gmail.com

В статье предложен подход к разработке архитектуры сервис-ориентированной системы обработки информации, моделирования и управления технологическими процессами. Разрабатываемая система представляет собой инструментарий для идентификации, прогнозирования и управления дискретно-непрерывными процессами, математический аппарат которой основан на непараметрических алгоритмах идентификации и управления. Программная архитектура состоит из нескольких основных модулей: модуль обработки данных, моделирования и прогноза выходных переменных процесса, модуль управления технологическим процессом. Первый модуль включает в себя алгоритмы предобработки данных: нормализация, центрирование и анализ выбросов и пропусков. Модуль моделирования представлен алгоритмическим функционалом для исследования

и восстановления зависимостей между переменными процесса, идентификации процесса с использованием непараметрической оценки функции регрессии по наблюдениям. Последний модуль – это реализация непараметрических алгоритмов дуального управления. Управляющие устройства, построенные на основании данных алгоритмов, выполняют функции как управления объектом, так и его изучения.

В статье обсуждаются вопросы применения архитектурных решений, основанных на двух зарекомендовавших себя в области разработки программного обеспечения подходах – композитном и сервис-ориентированном. Описываются основные принципы композитной архитектуры как набора программных систем с множеством характеристик, которые выполняют определенную задачу, и сервис-ориентированной архитектуры как модульного подхода к разработке программного обеспечения. Показаны преимущества примененной композитной сервис-ориентированной архитектуры перед другими вариантами архитектур программного обеспечения для систем управления, в частности, в работе сравнивается монолитная программная архитектура с композитной сервис-ориентированной архитектурой. Выбранное архитектурное решение предоставляет возможность выстроить систему из набора независимых модулей, каждый из которых реализует отдельную операцию, которая является логически обособленной, повторяющейся задачей, являющейся составной частью производственного процесса предприятия. Использование описанного в работе подхода позволило достичь положительных результатов при интеграции с существующими программными продуктами предприятий, значительно сократить сложность и стоимость разработки новых компонентов, а также поддержки «унаследованных» частей системы.

Ключевые слова: сервис-ориентированная архитектура, разработка программного обеспечения, проектирование систем управления технологическими процессами.

Introduction. Today, to solve a complex of tasks related to the management and modeling of complex technological processes in various industries, the aerospace industry in particular, software and algorithmic tools are used to provide identification and process control functions. One example of this type of tool is adaptive process control systems, the operation of which is carried out using nonparametric theory [1–5]. The use of nonparametric identification and control algorithms allows modeling, forecasting, and process maintaining within the framework of technological regulations in conditions of priori information lack, when the parametric structure of the model of the process under study remains unknown from priori information [6–9]. This situation is quite common in the development of computer control systems, since in most cases a researcher has to work with poorly studied processes for which it is not possible to reasonably choose the parametric structure of the model. At the same time a number of requirements are imposed on the developed control system, which include: data synchronization from various control points; the ability to work with heterogeneous data (the system independently converts the data into a single format); the possibility of both autonomous operation of the control system and correction of the control actions of the system by an expert technologist; security by encrypting and backing up data. Thus, the main task of this study is to develop and design the architecture for software and algorithmic support that allows optimal operation of the system.

Functional diagram of the system. The information processing, modeling and control system is a set of subsystems which includes the following modules shown in fig. 1.

Process variables are monitored over a time interval Δt . The input and output of the process are represented by measurements forming a sample of the $\{u_i, x_i\}, i = \overline{1, s}$ form, where s is the sample size, u_i, x_i are the measurements of the object input and output at a time t_i . This sample is contained in the “Enterprise database” block.

The data processing module imports data of various formats, converts data into a single format with which the system works. Also, this module implements data preprocessing algorithms: normalization, centering, analysis of omissions in the observation sample. The result of the module operation is an internal database of the system, which contains the converted data in a single format.

The process identification module implements the following nonparametric identification algorithms [10].

In this paper, we consider the classes of control processes that can be described by equations of the form:

$$x_t = F(x_{t-1}, \dots, x_{t-k}, u_t, \xi_t). \quad (1)$$

Here F – unknown functional; k – order of the difference equation that is bounded $k \leq k_{\max}$; u_t – input variable of the object; x_t – output variable of the object; index t – discrete time; $\xi(t)$ – vector accidental hindrance.

Let us introduce the following designations:

$$z_t = (z_1, \dots, z_{k+1}) = (x_{t-1}, \dots, x_{t-k}, u_t), \quad (2)$$

then

$$x_t = F(z_t). \quad (3)$$

Taking into account redesignations (2), the model of the technological process under consideration can be reduced to the model of the dynamic system in discrete time, when not only variables u_t enter the input of the latter but also $x_{t-1}, x_{t-2}, \dots, x_{t-k}$ and so on.

Under these conditions the following nonparametric estimation of the regression function based on observational data $\{x_i, u_i, i = \overline{1, s}\}$ [11] can be used as a nonparametric model of the object:

$$x_s^t = \frac{\sum_{i=1}^s x_i \cdot \Phi\left(\frac{u_s - u_i}{c_s^u}\right) \prod_{j=1}^k \Phi\left(\frac{x_{s-j} - x_{i-j}}{c_s^{x[j]}}\right)}{\sum_{i=1}^s \Phi\left(\frac{u_s - u_i}{c_s^u}\right) \prod_{j=1}^k \Phi\left(\frac{x_{s-j} - x_{i-j}}{c_s^{x[j]}}\right)}, \quad (4)$$

where $\Phi(\cdot)$ – bell-shaped function, $c_s^u, c_s^{x[j]}$ – core blur coefficients that are found in the presence of a training sample from the task of minimizing the object output and model output correspondence index based on the sliding exam method, when the nonparametric model (4) excludes the q -e observation of the variable presented for the exam by index i :

$$R(c_s^u, c_s^{x[1]}, \dots, c_s^{x[k]}) = \sum_{q=1}^s \left(x_q(u_q, x_{q-1}, \dots, x_{q-k}) - x_q \right)^2 = \min_{c_s^u, c_s^{x[1]}, \dots, c_s^{x[k]}} \sum_{q \neq i}^s \dots \quad (5)$$

where the index i appears in the nonparametric model (4). The non – gradient method of multidimensional optimization, the Nelder-Mead method, is implemented as an optimization algorithm, since this method is effective at a low calculation speed of the minimized function. To select the initial vertices of the deformable polyhedron, a range of possible values of the nuclear function blur coefficients $c_s \in [0.01, 4]$ was specified, from which an $n + k + 1$ point was arbitrarily selected, where n is the number of input variables, k is the order of the difference equation, which form a simplex of $n + k$ -dimensional space.

The process control module implements the following control scheme (fig. 2).

The nonparametric dual control algorithm has the form [12]:

$$u_{s+1} = u_s^* + \Delta u_{s+1}, \quad (6)$$

where u_s^* – component that accumulates information about the object of research, and $\Delta u_{s+1} = \varepsilon(x_{s+1}^* - x_s)$ – “learning” search steps.

The dualism of algorithm (6) is as follows. At the first control steps the main role in the formation of control actions is played by the summand Δu_{s+1} from formula (6).

But during the accumulation of information about the object the role of the summand u_s^* increases.

In this case, the following expression can be taken as a summand u_s^* from equation (6):

$$u_s^* = \frac{\sum_{i=1}^s u_i \cdot \Phi\left(\frac{x_{s+1}^* - x_i}{c_s}\right) \prod_{j=1}^k \Phi\left(\frac{x_{s-j} - x_{i-j}}{c_s}\right)}{\sum_{i=1}^s \Phi\left(\frac{x_{s+1}^* - x_i}{c_s}\right) \prod_{j=1}^k \Phi\left(\frac{x_{s-j} - x_{i-j}}{c_s}\right)}. \quad (7)$$

The process control algorithm is constructed as follows.

Based on the rule for selecting significant variables, the order of the differential equation of the dynamic process model k is determined, which is later used for calculating control actions in (7) where only those variables that were selected by the algorithm are present.

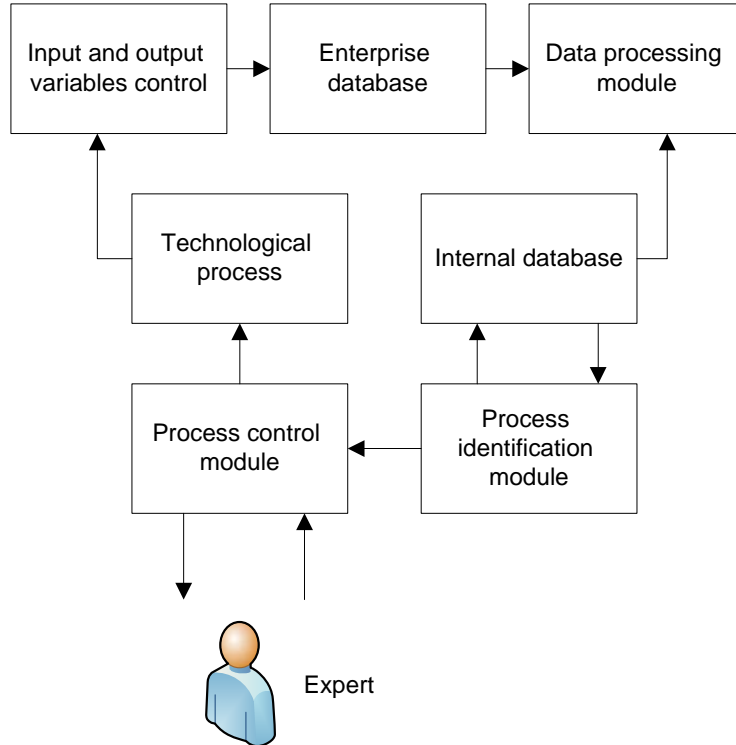


Fig. 1. Functional scheme of the developed adaptive information system for data processing, modeling and control

Рис. 1. Функциональная схема работы разрабатываемой адаптивной системы обработки информации, моделирования и управления

The quality of control is assessed by two characteristics:

1. Control time t_p – the time from the start of control to the moment when the output value differs from the task no more than a certain set value α . Usually: $\alpha = 0,05 y_{\text{cm}}$.

2. A relative control error W_p equal to the total deviation of the actual output of the process from the setting effect during the entire time of regulation in relation to the setting effect, expressed in relative values, in %

$$W_p = \frac{\frac{1}{s} \sum_{i=1}^s |x_i - x_i^*|}{x^*}.$$

The calculated values of control actions u_{s+1} are available for correction by an expert technologist. Thus, the developed system is a tool that includes the following main modules: the data processing module, modeling and forecasting of output process variables, and the process control module.

Software architecture of the system. When designing the software architecture, we took into account the fact that each of the modules can be easily replaced with a new implementation in case of changes in the technological process, as well as be supplemented with new ones when expanding the system's functionality.

Fig. 3 shows an example of the same system built on two different architectures. The classic version of the system is a single monolithic application within which you can identify a number of closely related subsystems built around specific large business processes. Although the architecture of such system is a three-layer architecture, its high connectivity significantly complicates the maintenance and implementation of new functionality in such system. In addition, the implementation of a new business process leads to the development of a new subsystem, most of the source code duplicates the code of existing subsystems.

The selection of basic elements from the system as well as the division of business processes into atomic operations and their transfer to a set of services that are independent of the implementation of other components of the system, allow us to build a more flexible system based on composite architecture. At the same time, the access to data is carried out through a single interface, and any subsystem can easily access services. Moreover, such separation of the system allows to divide the system into several parts with less effort: a data server, a service server, client applications.

Our architectural solution is based on two proven architectural approaches in the field of software development: composite and service-oriented. Composite architecture is a set of software systems with multiple characteristics that perform a specific task developed in the established order and based on a common set of basic tools. At the same time, integration and testing operations replace design and coding operations.

Service-oriented architecture is a modular approach to software development based on the use of distributed, loosely coupled interchangeable components equipped with standardized interfaces for interaction over standardized protocols.

The main difference and advantage of composite architecture over SOA is that the composite architecture provides flexibility on all layers (levels) of the application, while SOA provides flexibility only on one layer – the application layer (business logic) [13]. Since the composite architecture is essentially a further development of the service-oriented architecture and, accordingly, has all the advantages of the service-oriented approach in the software development. Composite applications are usually a further development of an already developed group of individual applications, from which basic sets of components and containers are allocated for their further integration with each other.

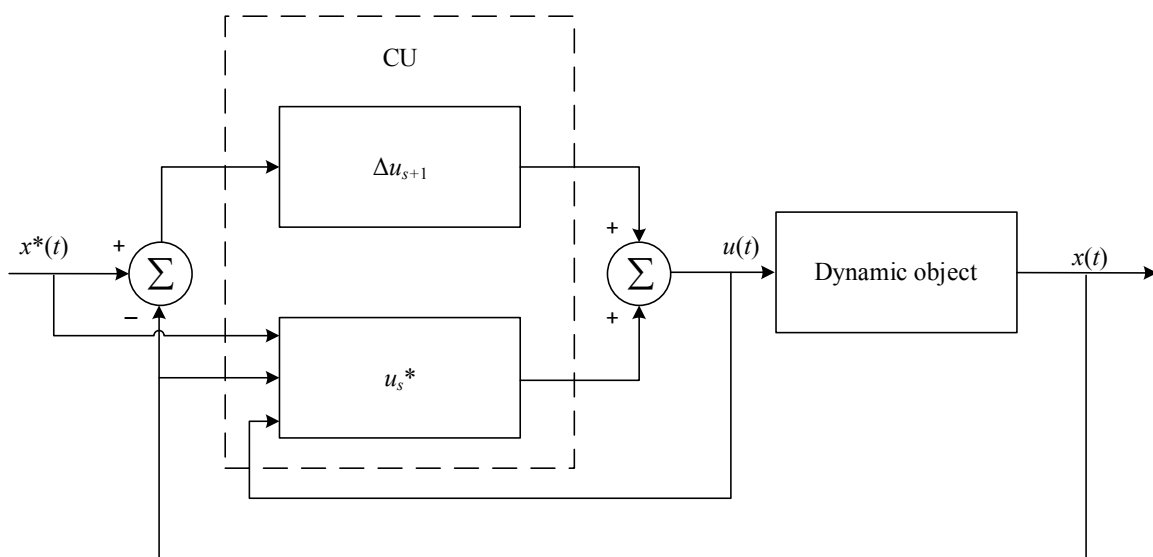


Fig. 2. Scheme of dual control of a dynamic object

Рис. 2. Схема дуального управления динамическим объектом

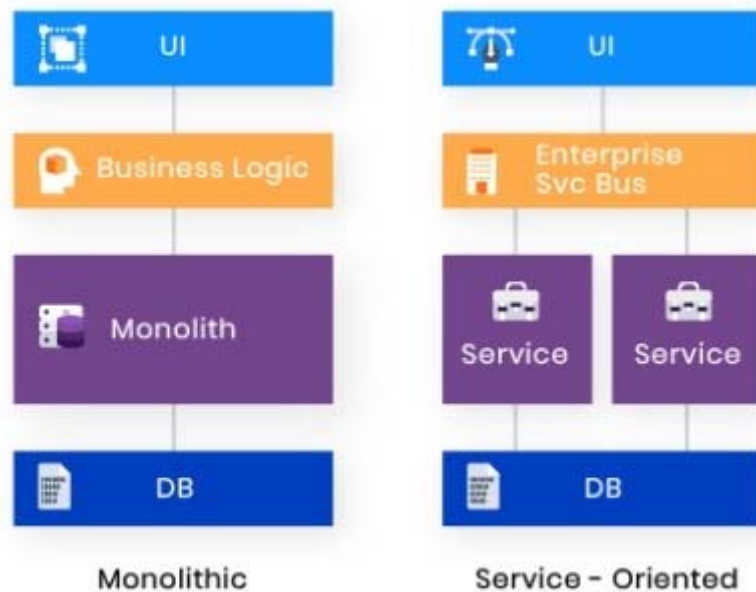


Fig. 3. Architecture Comparison

Рис. 3. Сравнение архитектур

Currently, the idea of building service-oriented applications based on composite architecture is widely used in various areas of software development and is the subject of study in many research centers. One of the largest organizations is Software Engineering Institute (SEI) [14].

At the moment, the Institute is a recognized international leader in the study of building composite service-oriented applications. Composite service-oriented architecture is an approach to designing software systems to organize existing software products so that disparate sets of complex, distributed systems and applications can be turned into a network of integrated, simple, and flexible resources.

Based on SEI's methodological recommendations, we designed and applied a hybrid architectural approach and thus obtained a composite service-oriented software system, which is a set of services, service components, and data access components that can be designed and deployed in a single application [15]. Interaction between services and various components is carried out by exchanging messages.

In our service-oriented composite architecture service components, which are the building blocks of our software system modules, play an important role. Each component is placed in a specific service container. Messages are sent to service containers and then redirected to the corresponding service components within them. In addition, service containers can interact with each other. For example, a message intended for a process is first sent to the container of that process, and then the service container processes the received information and redirects the messages to the corresponding service components within itself. Service components in the developed hybrid architecture solve the following tasks:

- describe and implement domain operations;
- define the rules of operations;
- transmit messages between system components.

The services themselves provide interaction between the composite application and its consumers. Communication with the service is performed using the specified protocols (for example, SOAP/HTTP). Data access components are used to retrieve and modify data based on messages sent from service components. The links describe how information is exchanged between services and service components, between different service components, or between service components and data access components.

The applied composite service-oriented architecture makes it possible to build a system from a set of independent modules, each of which implements a separate operation, which is a logically separate, repetitive task that is an integral part of the enterprise's production process. Moreover, services can be implemented independently of programming languages and other technical features of the implementation, which makes it possible to use different technologies.

Also, services can be written independently of other services in the system, you only need to know the interface of the services used, that is, the services will be loosely connected. The use of the architectural approach described in this paper also allowed us to achieve positive results when integrating with existing enterprise software products, significantly reducing the complexity and cost of developing new components, as well as supporting "inherited" parts of the system.

Conclusion. The work is devoted to the integrated development of the system designed for data preprocessing, modeling and control of multidimensional discrete-continuous processes. The core of the system is nonpara-

metric algorithms. Two basic algorithms are presented for modeling the process of unknown structure and control under conditions of incomplete data about the object. The developed system architecture is flexible – the replacement of key modules does not have irreversible consequences during the functioning of the system as a whole.

References

1. Levine W. S. et al. Control system advanced methods. – Boca Raton, FL : CRC press, 2011, 50 p.
2. Hovakimyan N., Cao C. Adaptive Control Theory: Guaranteed Robustness with Fast Adaptation. Society for Industrial and Applied Mathematics, 2010.
3. Jianling Q., Guang M. Design of glass furnace control system based on model-free adaptive controller. *Second International Conference on Computer Modeling and Simulation*. IEEE, 2010, Vol. 4, P. 130–133.
4. Eren-Oruklu M. et al. Adaptive system identification for estimating future glucose concentrations and hypoglycemia alarms. *Automatica*. 2012, Vol. 48, No. 8, P. 1892–1897.
5. Wu L., Qiu X., Guo Y. A simplified adaptive feedback active noise control system. *Applied Acoustics*. 2014, Vol. 81, P. 40–46.
6. Medvedev A. V. *Osnovy teorii adaptivnykh sistem* [Basic theory of adaptive systems]. Krasnoyarsk, SibGAU Publ., 2015, 525 p.
7. Medvedev A. V. [The theory of nonparametric systems. Simulation]. *Vestnik SibGAU*. 2010, Vol. 4 (30), P. 4–9 (In Russ.).
8. Raskina A. V. [Determination of the structure of a linear dynamic object in nonparametric identification problems]. *Vestnik SibGAU*. 2016, Vol. 4, P. 891–896 (In Russ.).
9. Bannikova A. V. Medvedev A. V. [On objects with memory management in a non-parametric uncertainty]. *Vestnik SibGAU*. 2014, Vol. 5(57), P. 26–37 (In Russ.).
10. Raskina A. V. *Neparametricheskie algoritmy identifikatsii i dual'nogo upravleniya dinamicheskimi ob'ektami*. *Dokt. Diss.* [Nonparametric algorithms of identification and dual control of dynamic objects. *Doct. Diss.*]. Krasnoyarsk, 2018, 122 p.
11. Nadaraya Je. A. *Neparametricheskie ocenki plotnosti veroyatnosti i krivoj regressii* [Nonparametric estimation of probability density and the regression curve]. Tbilisi, 1983, 194 p.
12. Fel'dbaum A. A. *Osnovy teorii optimal'nykh avtomaticheskikh sistem* [Fundamentals of the theory of optimal automatic systems]. Moscow, Fizmatgiz Publ., 1963, 552 p.
13. SOA in the Real World. Available at: <http://www.microsoft.com/en-us/download/details.aspx?id=16187> (accessed 20.12.2019).
14. Northrop L. *Software Product Lines Essentials*. L. Northrop. Pittsburg: SEI Carnegie Mellon University. 2008. 85 p.
15. Виденин С. А., Костюк А. В., Васильев Э. В. Сервис-ориентированная архитектура в современных информационных системах // *Современные научные исследования и инновации*. 2016. № 7. С. 121–123.

Библиографические ссылки

1. Control system advanced methods / Levine W. S. et al. Boca Raton, FL : CRC press, 2011. 50 p.
2. Hovakimyan N., Cao C. Adaptive Control Theory: Guaranteed Robustness with Fast Adaptation. Society for Industrial and Applied Mathematics, 2010.
3. Jianling Q., Guang M. Design of glass furnace control system based on model-free adaptive controller // *Second International Conference on Computer Modeling and Simulation*. IEEE. 2010. Vol. 4. P. 130–133.
4. Adaptive system identification for estimating future glucose concentrations and hypoglycemia alarms / Eren-Oruklu M. et al. // *Automatica*. 2012. Vol. 48, no. 8. P. 1892–1897.
5. Wu L., Qiu X., Guo Y. A simplified adaptive feedback active noise control system // *Applied Acoustics*. 2014. Vol. 81. P. 40–46.
6. Медведев А. В. Основы теории адаптивных систем / СибГАУ. Красноярск, 2015. 525 с.
7. Медведев А. В. Теория непараметрических систем моделирование // *Вестник СибГАУ*. 2010. № 4 (30). С. 4–9.
8. Раскина А. В. Определение структуры линейного динамического объекта в задачах непараметрической идентификации // *Вестник СибГАУ*. 2016. № 4. С. 891–896.
9. Банникова А. В. Медведев А. В. Об управлении объектами с памятью в условиях непараметрической неопределенности // *Вестник СибГАУ*. 2014. № 5(57). С. 26–37.
10. Раскина А. В. Непараметрические алгоритмы идентификации и дуального управления динамическими объектами : дисс. ... канд. техн. наук. Красноярск, 2018. 122 с.
11. Надарая Э. А. Непараметрические оценки плотности вероятности и кривой регрессии. Тбилиси : Изд. Тбил. у-та, 1983. 194 с.
12. Фельдбаум А. А. Основы теории оптимальных автоматических систем. М. : Физматгиз, 1963. 552 с.
13. SOA in the Real World [Электронный ресурс]. URL: <http://www.microsoft.com/en-us/download/details.aspx?id=16187> (дата обращения: 20.12.2019).
14. Northrop L. *Software Product Lines Essentials*. L. Northrop. Pittsburg: SEI Carnegie Mellon University. 2008. 85 p.
15. Виденин С. А., Костюк А. В., Васильев Э. В. Сервис-ориентированная архитектура в современных информационных системах // *Современные научные исследования и инновации*. 2016. № 7. С. 121–123.

© Raskina A. V., Videnin S. A., Chzhan E. A., Yusupova R. R., 2020

Raskina Anastasia Vladimirovna – Cand. Sc., associate professor of Department of Information Systems, Siberian Federal University, School of Space and Information Technology. E-mail: raskina.1012@yandex.ru.

Videnin Sergey Aleksandrovich – Cand. Sc., associate professor of Department of Information Systems, Siberian Federal University, School of Space and Information Technology. E-mail: videninserg@mail.ru.

Chzhan Ekaterina Anatolyevna – Cand. Sc., associate professor of Department of Intelligent Control Systems, Siberian Federal University, School of Space and Information Technology. E-mail: ekach@list.ru.

Yusupova Ramilya Ramilevna – student, Siberian Federal University, School of Space and Information Technology. E-mail: sr.eagleowl@gmail.com.

Раскина Анастасия Владимировна – кандидат технических наук, доцент кафедры информационных систем, Сибирский федеральный университет, Институт космических и информационных технологий. E-mail: raskina.1012@yandex.ru.

Виденин Сергей Александрович – кандидат педагогических наук, доцент кафедры информационных систем, Сибирский федеральный университет, Институт космических и информационных технологий. E-mail: videninserg@mail.ru.

Чжан Екатерина Анатольевна – кандидат технических наук, доцент кафедры интеллектуальных систем управления, Сибирский федеральный университет, Институт космических и информационных технологий. E-mail: ekach@list.ru.

Юсупова Рамиля Рамилевна – студент, Сибирский федеральный университет, Институт космических и информационных технологий. E-mail: sr.eagleowl@gmail.com.

UDC 004.021

Doi: 10.31772/2587-6066-2020-21-1-28-33

For citation: Romanova D. S. Research of options of transition from unlimited to limited parallelism on the example of matrix multiplication. *Siberian Journal of Science and Technology*. 2020, Vol. 21, No. 1, P. 28–33. Doi: 10.31772/2587-6066-2020-21-1-28-33

Для цитирования: Романова Д. С. Исследование вариантов перехода от неограниченного параллелизма к ограниченному на примере умножения матриц // Сибирский журнал науки и технологий. 2020. Т. 21, № 1. С. 28–33. Doi: 10.31772/2587-6066-2020-21-1-28-33

RESEARCH OF OPTIONS OF TRANSITION FROM UNLIMITED TO LIMITED PARALLELISM ON THE EXAMPLE OF MATRIX MULTIPLICATION

D. S. Romanova

Siberian Federal University
79, Svobodnyy Av., Krasnoyarsk, 660041, Russian Federation
E-mail: daryaooo@mail.ru

Today, there are many approaches to developing parallel programs. It is considered that it is more efficient to write such programs for a particular computing system. The article proposes to ignore the features of a particular computing system and outline plans for the development of a certain automated system that allows trying to improve code efficiency by developing programs with unlimited parallelism, as well as explore the possibility of developing more efficient programs using the restrictions imposed on maximum parallelism. This approach was demonstrated on the example of the analysis of various matrix multiplication algorithms. As a mathematical apparatus, the study considered various approaches to the description of algorithms to increase their implementation, including an approach based on unlimited parallelism and, also, an approach based on various restrictions on parallelism is proposed. In the course of the work, sequential and parallel methods of matrix multiplication were studied in detail, including tape and block algorithms. As a result of the study, various matrix multiplication methods (sequential, with left and right recursion, parallel methods) were studied and more effective ones were found in terms of the resources used and the restrictions imposed on parallelism. A sequential method and a cascade summation scheme were analyzed and proposed as possible ways of convolving the results of solving the problem obtained after the decomposition stage. Also, a number of programs with different levels of parallelism were developed and implemented in the functional-stream parallel programming language. In the future, such transformations can be carried out formally, relying on a knowledge base and a language that allows equivalent transformations of the original program in accordance with the axioms and algebra of transformations laid down in it, as well as replacing functions that are equivalent in results and have different levels of parallelization. These studies can be used to increase the efficiency of developed programs in terms of resource use in many branches of science, including in the field of software development for the needs of astronomy and rocket science.

Keywords: *unlimited parallelism, matrix multiplication, parallel programming.*

ИССЛЕДОВАНИЕ ВАРИАНТОВ ПЕРЕХОДА ОТ НЕОГРАНИЧЕННОГО ПАРАЛЛЕЛИЗМА К ОГРАНИЧЕННОМУ НА ПРИМЕРЕ УМНОЖЕНИЯ МАТРИЦ

Д. С. Романова

Сибирский федеральный университет
Российская Федерация, 660041, г. Красноярск, просп. Свободный, 79
E-mail: daryaooo@mail.ru

Сегодня существует много подходов к разработке параллельных программ. Считается более эффективным написание таких программ под определенную вычислительную систему (ВС). В статье предлагается абстрагироваться от особенностей той или иной ВС и наметить планы по разработке некой автоматизированной системы, позволяющей стремиться к повышению эффективности кода за счет создания программ с неограниченным параллелизмом, а также исследовать возможность разработки более эффективных программ с помощью ограничений, накладываемых на максимальный параллелизм. В качестве примера приводится анализ различных алгоритмов умножения матриц. В качестве математического аппарата в исследовании рассматривались различные подходы к описанию алгоритмов, в том числе, подход, основанный на неограниченном параллелизме. Предлагается подход, в основе которого лежат различные ограничения, накладываемые на параллелизм. В ходе работы подробно изучались последовательные и параллельные методы умножения матриц, в том числе, ленточные и блочные алгоритмы. В результате проведенного исследования были изучены различные методы умножения матриц (последовательные, с левой и правой рекурсией, параллельные) и найде-

ны более эффективные из них с точки зрения используемых ресурсов и ограничений, накладываемых на параллелизм. Были проанализированы и предложены последовательный метод и каскадная схема суммирования как возможные способы свертки результатов решения задачи, полученных после этапа декомпозиции. Также был разработан и реализован ряд программ с различным уровнем параллелизма на функционально-потокном языке параллельного программирования. В перспективе подобные преобразования можно проводить формально, опираясь на базу знаний и язык, допускающий эквивалентные преобразования исходной программы в соответствии с заложенными в него аксиомами и алгеброй преобразований, а также заменой эквивалентных по результатам функций, обладающих разным уровнем распараллеливания. Данные исследования можно применять для повышения эффективности разрабатываемых программ с точки зрения использования ресурсов во многих отраслях науки, в том числе, и в сфере разработки ПО для нужд астрономии и ракетостроения.

Ключевые слова: неограниченный параллелизм, матричное умножение, параллельное программирование.

Introduction. There are many different approaches for developing parallel programs. In parallel programming, special programming techniques are often used. And in most cases it is considered more efficient to write program code for a specific calculated system. Since the development of computer technology is proceeding at a rapid pace today, programmers have to rewrite code for a newly developed system. The main problem of the transition from traditional to parallel programming is that it is simply impossible to develop a universal executor with which it would be possible to achieve the same effective way of writing parallel programs [1–3]. In addition to the style of writing programs in a particular system, it is also necessary to take into account the amount of resources used and their computing power. Therefore, to implement effective parallel computing, you have to constantly rebuild the structure of the program.

The issue of creating tools to ensure portability of parallel programs has been studied for a long time. And all attempts to develop such systems were associated with writing programs for a generalized architecture [4].

It is proposed to focus not on the features of a particular computing system, but to use some kind of abstract system that allows trying to improve the efficiency of the code by developing programs with unlimited parallelism. Increasing the level of abstraction, it is possible to build various combinations, compressing parallelism, and therefore, the transition from unlimited parallelism to limited.

As a mathematical apparatus, the research considered various approaches to the description of algorithms to increase their implementation, including an approach based on unlimited parallelism. Also, the approach based on various restrictions on parallelism is proposed. In the course of the work, sequential and parallel methods of matrix multiplication were studied in detail, including band and block algorithms. After decomposition in the framework of solving the matrix multiplication problem,

various options were proposed for the subsequent summation of the obtained results of solving subproblems in order to increase the efficiency of resource use in a consistent way and in a cascading manner.

These studies can be applied in various fields of science, including the development of software in rocket science, which will further improve the missile control system.

Main part. Algorithm for solving the problem.

Statement of the problem. In fact, the statement of the problem is as follows. Two matrices are multiplied: $A [M] [L] \cdot B [L] [N] \Rightarrow C [M] [N]$, where the number of row multiplications by columns is $S = M \cdot N$.

In each combination of row multiplication by column, L pairs of elements are involved.

Therefore, the total number of simultaneously possible multiplications $P = M \cdot N \cdot L$, that is, it is set by the corresponding parallelepiped [5; 6].

Next, the multiplied elements for each combination of rows and columns begin to add up. In this case, it is possible to use the usual sequential addition method or in a cascade scheme.

Matrix multiplication. Matrix operations are quite time-consuming to implement, so they represent a classic area of application for parallel computing.

Sequential Matrix Multiplication Algorithm

If there are two square matrices A and B , then $C = A \cdot B$ is the result of their multiplication,

$$C_{ij} = \sum_{k=1}^n a_{ik} \cdot b_{kj}, \quad (1)$$

where $i = 1, \dots, n, j = 1, \dots, m$.

This algorithm for multiplying two matrices A and B is iterative and is oriented towards sequential calculation of rows of matrix C (fig. 1).

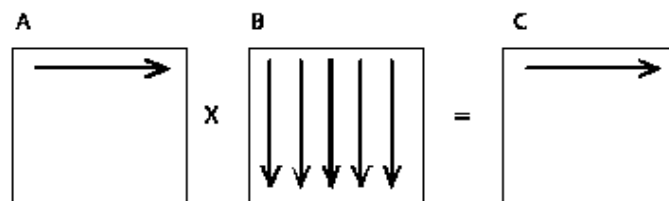


Fig. 1. First iteration of matrix multiplication in a sequential approach

Рис. 1. Первая итерация умножения матриц при последовательном подходе

When performing one iteration of the outer loop, one row of the resulting matrix is calculated [7].

In the sequential matrix multiplication algorithm, element-wise multiplication of all elements of the matrix occurs. The information graph in this case will be quite voluminous and therefore its analysis is difficult. In addition, this method of multiplication becomes ineffective if the size of the matrix exceeds the size of the processor cache. A search is needed for more efficient algorithms for solving this problem [8; 9].

From formula (1) it is clear that the calculation of each C_{ij} is independent and simultaneously, and it can be performed in parallel. This algorithm is with mass parallelism, since it contains a huge number of operations that can be performed simultaneously and independently of each other [9].

The choice of matrix separation method leads to the determination of a specific parallel computing method; the existence of different data distribution schemes generates a number of parallel matrix computing algorithms.

If we ignore the use of specific resources to solve the problem, then we can achieve increased program efficiency, gradually compressing initially unlimited parallelism.

The process of multiplication in this case will begin with the decomposition of the task into subtasks. That is, to solve problem (1), we consider the main combinations of multipliable matrix elements in i, j, k .

Variants are possible when the resulting rows, columns or groups of matrix columns are computed in parallel. For example, if you execute the loop body in i for each counter value in parallel, then the rows of the matrix product will be counted in parallel. If we interchange the cycles in i and j (which is quite possible due to the independence of the operations of nested cycles in i and j) and execute the body of the cycle in parallel for each counter value, we get a version of the program that contains columns in parallel. In addition, each element of the resulting matrix can also be counted in parallel [9].

Reduction steps when multiplying matrices and moving to parallel algorithms. As noted above, from the definition of the operation of multiplying the matrices A and B it follows that the elements of the resulting matrix C can be found independently of each other. The product of matrices can be considered as n^2 independent scalar products, or as n independent products of a matrix by a vector. In both cases, different algorithms are used [10].

In the first approach, for organizing parallel computations, the main subtask uses the procedure of determining one element of the resulting matrix C, and for all necessary calculations, each task must contain at least one row of matrix A and a column of matrix B. The total number of subtasks here is n^2 . In the second approach, to perform all the necessary calculations for the base subtask, one of the rows of matrix A and all columns of matrix B must be available. The number of subtasks is n [11].

To increase the efficiency of the matrix multiplication algorithm, it is logical to assume that if matrix multiplication is not performed element-wise, but line by line, this will make the algorithm more efficient in terms of parallelism. In this case, the general problem of matrix multiplication will be reduced to dividing it into subtasks. Fur-

ther, these subtasks will be combined to obtain a common necessary solution to the original problem.

Taking into account the foregoing, this algorithm can be considered as a process of solving independent subproblems of multiplying matrix A by columns of matrix B. At the same time, the information graph is simplified, in contrast to the case with a sequential multiplication algorithm. It all comes down to building a matrix multiplication graph. The introduction of macro operations is carried out in stages with a return level of detail of the operations or decomposition used [12].

Band algorithm. Consider band algorithms in which the matrices A and B are divided into continuous sequences of rows or columns (fig. 2). To carry out this procedure, each subtask contains row A of the matrix and access to columns B. One processor is allocated a number of rows and columns. A simple solution to this problem is to duplicate matrix B in all subtasks. Here the following way of organizing parallel computations for 3-3 matrices is possible [13]:

Such fine-grained tasks can be enlarged if the matrix size is greater than the number of computing elements or processors. In this case, the original matrix A and the resulting matrix C are divided into horizontal stripes. In this case, the size of such bands should be chosen equal to $k = n/p$ (if n is a multiple of p), which allows us to ensure distribution of the computational load across the computational elements uniformly [13].

The selected basic subtasks are characterized by an equal amount of transmitted data and the same computational complexity. In the case when the size of the matrices is greater than the number of computational elements (processors and/or cores) p , the basic subproblems can be enlarged by combining several adjacent rows of the matrix within one subproblem. In this case, the resulting matrix C and the original matrix A are divided into a series of horizontal stripes [13].

This band algorithm has good localization, and in addition, there is no interaction between data streams. But it should be noted that if we enlarge the subtasks, then we can move on to other matrix-multiplication algorithms that are more efficient in terms of parallelism – to block algorithms.

Transition to block algorithms. In such algorithms, the original matrices A, B and the resulting matrix C are represented as sets of blocks.

In this case, not only the resulting matrix, but also the matrix-arguments of matrix multiplication are divided between the threads of the parallel program into some rectangular blocks. This approach allows achieving good data localization and increased cache utilization.

Also there are well known parallel matrix multiplication algorithms based on block data division, oriented to multiprocessor computing systems with distributed memory. When developing algorithms focused on the use of parallel computing systems with distributed memory, it is necessary to take into account that placing all the required data in each subtask (in this case, placing the required sets of columns of matrix B and rows of matrix A in subtasks) will inevitably lead to duplication and significant growth of amount of memory used. As a result, some restrictions are imposed on the system, that is, the calculations must

be organized in such a way that at each current point in time the subtasks contain only part of the data necessary for the calculations, and access to the rest of the data is ensured by sending messages. Algorithms that implement the described approach include the Fox algorithm and the Cannon algorithm [14] (fig. 3).

The difference between these algorithms is the sequence of transfer of matrix blocks between the processors of any computing system.

It should be noted that after the decomposition step with the allocation of subtasks and the search for an effective parallel algorithm, it is necessary to summarize the obtained solutions from the subtasks to get the general result of solving the matrix multiplication problem.

From the point of view of parallelism, one can apply in this case not only sequential summation, but also more efficient parallel methods, for example, addition according to a cascade scheme (fig. 4).

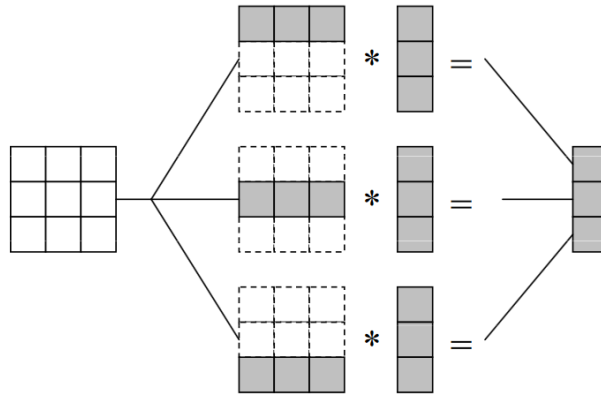


Fig. 2. The example of the organization of calculations in a matrix multiplication algorithm based on dividing matrices into rows

Рис. 2. Пример организации вычислений в алгоритме матричного умножения, основанного на разделении матриц на строки

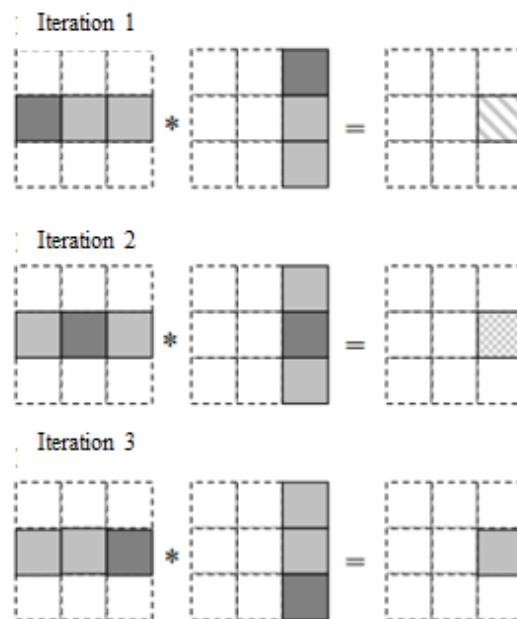


Fig. 3. Block matrix organization scheme

Рис. 3. Схема организации блочного умножения полос матрицы

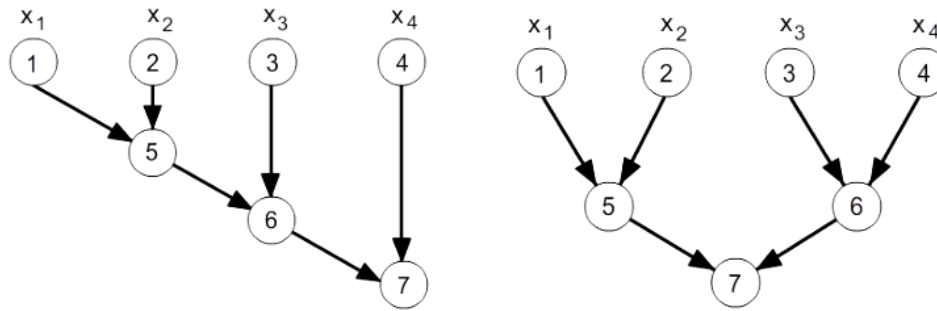


Fig. 4. Graphs of sequential (left) and cascade summation algorithms (right) [15]

Рис. 4. Графы алгоритмов последовательного (слева) и каскадного суммирования (справа) [15]

Conclusion. After the analysis of the above algorithms, it is planned to use the results to find the capabilities of equivalent transformations of various algorithms and to develop an automated system that allows its user to choose one or another algorithm to solve their problem in order to achieve the fastest and most effective solution with point of view of resources use.

Using algorithms that describe the maximum parallelism of the problem being solved, the developer offers additional methods for analyzing and deriving various algorithms with limited parallelism, which can be considered as use cases.

Consideration of all the algorithms studied in this paper, as well as their implementation in a functional data-flow parallel language that allows performing operations with maximum parallelism, opens up prospects for the further development and improvement of methods and approaches to enhance program efficiency.

Acknowledgments. This work was supported by the financial support of the Russian Fund of Federal Property in the framework of the scientific project No. 17-07-00288 A.

Благодарности. Исследование было выполнено при финансовой поддержке РФФИ в рамках научного проекта № 17-07-00288 A.

References

1. Legalov A. I. *Sovremennye problem informatiki i vychislitel'noi tekhniki* [Modern problems of computer science and computer technology: a training manual]. Tomsk, Publishing House SPB Graphics, 2012, 216 p. (In Russ.).
2. Legalov A. I. [Sorting methods obtained from the analysis of the maximum parallel program. Distributed and cluster computing]. *Izbrannye materialy 3 chkoli seminar. Institut komp'uternogo modelirovaniya SO RAN*. Krasnoyarsk, 2004, P. 119–134.
3. Legalov A. I. [On the management of computing in parallel systems and programming language]. *Naychnii vestnik NSTU*. 2004, No. 3 (18), P. 63–72 (In Russ.).
4. Voevodin V. V., Voevodin V. I. *Parallelnye vychisleniya* [Parallel computing]. SPb., BHV Petersburg Publ., 2002, 608 p.
5. Solomonik E., Demmel J. . Communication-optimal parallel 2.5D matrix multiplication and LU factorization algorithms. Department, University of California, Berkeley (February 2011), Available at: <http://www.eecs.berkeley.edu/Pubs/TechRpts/2011/EECS-2011-10.html> (accessed 01.12.2019).
6. Dongarra J. J., Duff L. S., Sorensen D. C., Vorst H. A. V. *Numerical Linear Algebra for High Performance Computers (Software, Environments, Tools)*. Soc for Industrial & Applied Math.P, 1999, P. 120–128.
7. Gergel V. P., Fursov V. A. *Lektsii po parallel'nim vychisleniyam* [Lectures on parallel computing: textbook]. Allowance. Samara, Samar. State Aerospace. University Publ., 2009, 164 p.
8. Legalov A. I., Kazakov F. A., Kuzmin D. A., Privalikhin D. V. [The model of functional-stream parallel computing and the Pythagoras programming language. Distributed and cluster computing]. *Izbrannye materialy vtoroi chkoli seminar. Institut Komp'uternogo modelirovaniya SO RAN*. Krasnoyarsk, 2002, P. 101–120 (In Russ.).
9. Legalov A. I. [Sorting methods obtained from the analysis of the most parallel program. Distributed and cluster computing]. *Izbrannye materialy tret'ei chkoli seminar. Institut Komp'uternogo modelirovaniya SO RAN*. Krasnoyarsk, 2004, P. 119–134 (In Russ.).
10. Wirth N. *Algoritmi i struktury danih* [Algorithms and data structures]. Moscow, Mir Publ., 1989, 360 p.
11. Fedotov I. E. *Modeli parallel'nogo programmirovaniya* [Parallel Programming Models]. Moscow, Solon-Press Publ., 2012, 384 p.
12. Legalov A. I., Nepomnyaschy O. V., Matkovsky I. V., Kropacheva M. S. Tail Recursion Transformation in Functional Dataflow Parallel Programs. *Automatic Control and Computer Sciences*. 2013, Vol. 47, No. 7, P. 366–372.
13. Miller R., Boxer L. *Posledovatel'nie i parallel'nie algoritmi: obshii podhod* [Serial and parallel algorithms: General approach]. Moscow, BINOM. Laboratory of Knowledge Publ., 2006, 406 p.
14. Lupin S. A., Posypkin M. A. *Tekhnologii parallel'nogo programmirovaniya* [Parallel Programming Technologies]. Moscow, Forum, Infra-M Publ., 2008, 208 p.

15. Herlihy M. The Art of Multiprocessor Programming. Morgan Kaufmann Publishers Inc., San Francisco, CA, USA. 2008, 508 p.

Библиографические ссылки

1. Легалов А. И. Современные проблемы информатики и вычислительной техники: учебное пособие. Сибирский федеральный университет. Томск : СПб Графикс, 2012. 216 с.
2. Легалов А. И. Методы сортировки, полученные из анализа максимально параллельной программы. Распределенные и кластерные вычисления // Избр. мат. 3 шк.-семинара. Ин-т вычислит. моделир. СО РАН. Красноярск, 2004. С. 119–134.
3. Легалов А. И. Об управлении вычислениями в параллельных системах и языках программирования // Научный вестник НГТУ. 2004. № 3 (18). С. 63–72.
4. Воеводин В. В., Воеводин Вл. В. Параллельные вычисления. СПб. : БХВ Петербург, 2002. 608 с.
5. Solomonik E., Demmel J. Communication-optimal parallel 2.5D matrix multiplication and LU factorization algorithms. Department, University of California, Berkeley (February 2011) [Электронный ресурс]. URL: <http://www.eecs.berkeley.edu/Pubs/TechRpts/2011/EECS-2011-10.html> (дата обращения: 01.12.2019).
6. Dongarra J. J., Duff L. S., Sorensen D. C., Vorst H. A. V. Numerical Linear Algebra for High Performance Computers (Software, Environments, Tools). Soc for Industrial & Applied. 1999. P. 120–125.
7. Гергель В. П., Фурсов В. А. Лекции по параллельным вычислениям. Самара : Изд-во Самар. гос. аэрокосм. ун-та, 2009. 164 с.
8. Модель функционально-потокковых параллельных вычислений и язык программирования «Пифагор». Распределенные и кластерные вычисления / А. И. Легалов, Ф. А. Казаков, Д. А. Кузьмин, Д. В. Привалихин // Избранные материалы второй Школы-семинара. Институт вычислительного моделирования СО РАН. Красноярск, 2002. С. 101–120.
9. Легалов А. И. Методы сортировки, полученные из анализа максимально параллельной программы. Распределенные и кластерные вычисления. Избр. мат. 3 шк.-семинара. Ин-т вычислит. моделир. СО РАН. Красноярск, 2004. С. 119–134.
10. Вирт Н. Алгоритмы и структуры данных. М. : Мир, 1989. 360 с.
11. Федотов И. Е. Модели параллельного программирования. М. : СОЛОН-ПРЕСС. Москва, 2012. 384 с.
12. Legalov A. I., Nepomnyaschy O. V., Matkovsky I. V., Kropacheva M. S. Tail Recursion Transformation in Functional Dataflow Parallel Programs // Automatic Control and Computer Sciences. 2013. Vol. 47, No. 7. P. 366–372.
13. Миллер Р., Боксер Л. Последовательные и параллельные алгоритмы: Общий подход. М. : БИНОМ. Лаборатория знаний, 2006. 406 с.
14. Лупин С. А., Посыпкин М. А. Технологии параллельного программирования. Серия: Высшее образование. М. : Форум ; Инфра-М, 2008. 208 с.
15. Herlihy M. The Art of Multiprocessor Programming. Morgan Kaufmann Publishers Inc., San Francisco, CA, USA. 2008. 508 p.

© Romanova D. S., 2020

Romanova Darya Sergeevna – postgraduate student, Siberian Federal University. E-mail: daryaoooo@mail.ru.

Романова Дарья Сергеевна – аспирант, Сибирский федеральный университет. daryaoooo@mail.ru.

UDC 338.27

Doi: 10.31772/2587-6066-2020-21-1-34-40

For citation: Shiryayeva T. A., Khlupichev V. A., Shlepkin A. K., Melnikova O. L. The use of the inverse transformation method for time series analysis. *Siberian Journal of Science and Technology*. 2020, Vol. 21, No. 1, P. 34–40. Doi: 10.31772/2587-6066-2020-21-1-34-40

Для цитирования: Ширияева Т. А., Хлупичев В. А., Шлепкин А. К., Мельникова О. Л. Метод обратного преобразования для анализа временных рядов // Сибирский журнал науки и технологий. 2020. Т. 21, № 1. С. 34–40. Doi: 10.31772/2587-6066-2020-21-1-34-40

THE USE OF THE INVERSE TRANSFORMATION METHOD FOR TIME SERIES ANALYSIS

T. A. Shiryayeva¹, V. A. Khlupichev¹, A. K. Shlepkin^{1*}, O. L. Melnikova²

¹Krasnoyarsk State Agrarian University
90, Mira Av., Krasnoyarsk, 660001, Russian Federation

²Khakas State University
90, Lenin Av., Abakan, 655017, Russian Federation

*E-mail: ak_kgau@mail.ru

In modern conditions of technology development, signs of systemacity are manifested to one degree or another in all areas, so the use of system analysis is an urgent task. In this case, the main factors in this situation are data processing and prediction of the state of a system. Mathematical modeling is used as a prediction method for a given subject area. A mathematical model is a universal tool for describing complex systems representing the approximate description of the class of phenomena of the external world expressed by mathematical concepts and language. The mathematical model can be represented as a set of systematic components and a random component. In this article, the object of prediction is the irregular random component of a model, which reflects the impact of numerous random factors. The origin, nature and laws of variation of the random variable are known, therefore, to simulate its behavior or predict its future value, one needs high degree of certainty to establish the form of continuous distribution function of the random variable. The empirical distribution function is calculated using the sample of random variable values. This empirical function is close to the values of the desired unknown function of distribution. The resulting empirical function is discrete, therefore it is necessary to apply piecewise linear interpolation to obtain a continuous distribution function. The predicted random component of time series has been included in the initial regression model. In order to compare augmented and initial regression models, several values were excluded from the time series and new prediction was built. The value of the average approximation error for assessing the quality of the model is calculated. The augmented regression model proved to be more effective than the original one.

Keywords: forecasting, time series analysis, inverse transformation, system analysis.

МЕТОД ОБРАТНОГО ПРЕОБРАЗОВАНИЯ ДЛЯ АНАЛИЗА ВРЕМЕННЫХ РЯДОВ

Т. А. Ширияева¹, В. А. Хлупичев¹, А. К. Шлепкин^{1*}, О. Л. Мельникова²

¹Красноярский государственный аграрный университет
Российская Федерация, 660001, Красноярск, просп. Мира, 90

²Хакасский государственный университет имени М. Ф. Катанова
Российская Федерация, 655017, Абакан, просп. Ленина, 90

*E-mail: ak_kgau@mail.ru

В современных условиях развития технологий признаки системности проявляются в той или иной степени во всех областях, поэтому использование системного анализа является актуальной задачей. При этом главными факторами в данной ситуации являются обработка данных и прогнозирование состояния системы. Для заданного объекта в качестве способа прогнозирования в данной работе применяется моделирование, а точнее математическое моделирование. Математическая модель – это универсальное средство исследования сложных систем, представляющее собой приближенное описание какого-либо класса явлений внешнего мира, выраженное с помощью математической символики.

Математическую модель можно представить как совокупность систематических компонентов и случайной составляющей. В данной статье регрессионная модель уже определена, а в качестве объекта прогнозирования рассмотрена остаточная нерегулярная компонента модели, которая отражает воздействие многочисленных факторов случайного характера.

Происхождение, природа и законы изменения данной случайной величины нам неизвестны, поэтому для моделирования ее поведения или предсказания ее будущих значений, необходимо с высокой степенью достоверности установить вид непрерывной функции распределения данной случайной величины.

Для этого была рассчитана эмпирическая функция распределения с помощью выборки из значений случайной величины. Данная эмпирическая функция в определенной степени приближена к значениям искомой неизвестной функции распределения. Полученная эмпирическая функция носит дискретный характер, поэтому необходимо применить кусочно-линейную интерполяцию и, таким образом, получить непрерывную функцию распределения.

В исходную регрессионную модель была включена спрогнозированная случайная компонента временного ряда. Для того чтобы сравнить дополненную и исходную регрессионные модели, из динамического ряда были исключены несколько значений и построен новый прогноз. Рассчитано значение средней ошибки аппроксимации для оценки качества модели. Дополненная регрессионная модель показала себя эффективнее исходной.

Ключевые слова: прогнозирование, анализ временных рядов, обратное преобразование, системный анализ.

Introduction. For the specialists involved in data analysis, in most cases prediction may be said to be the main goal and task. Modern methods of statistical forecasting are often able to predict almost any possible indicators with high accuracy [1].

Forecasting is a system of scientifically based ideas about the possible conditions of an object in the future and alternative ways of its development [2]. There are no universal prediction methods for all occasions. Any practical forecasting problem can be satisfactorily solved only by a limited number of methods [3]. The choice of a forecasting method and its effectiveness depend on many conditions: the purpose of the forecast, the period of its lead prediction, the level of detailing and the availability of initial information [4]. The most commonly used forecasting method is mathematical modeling. A mathematical model is an approximate description of a specific process or phenomenon of the external world, expressed using a mathematical apparatus [5].

The components of the time series. Commonly, when studying a time (dynamic) series, it is depicted in the form of the following mathematical model:

$$Y_t = \hat{Y}_t + E_t$$

where Y_t – time series value; \hat{Y}_t – systematic (deterministic) component of the time series; E_t – random component of the time series [6].

The systematic component of the time series Y_t is a result of the influence of constantly acting factors on the process being analyzed. Two main systematic components of the time series can be distinguished:

1. The trend of the time series.
2. The cyclic oscillations of the time series.

A trend is a general pattern of change in the indicators of the time series, stable and observed over a long period of time. A trend is described using some function, usually monotonic. This function is called 'trend function', or simply "trend" [7].

Among the factors that form the cyclical oscillations of the series, in turn, two components can be distinguished:

- 1) seasonality;
- 2) cyclicity.

Seasonality is a result of the influence of factors acting at a predetermined periodicity. These are regular fluctuations that are periodic in nature ending within a year.

The cyclic component is a nonrandom function that describes long (more than a year) periods of rise and fall [8; 9]

The random component of the time series E_t is the component of the time series remaining after the allocation of systematic components. It reflects the effects of numerous random factors; it is a random, irregular component.

Random variables are diverse in nature and origin, although the distribution law can be written in a uniform universal form, namely, in the form of a distribution function that is equally suitable for discrete and continuous random variables [10].

Inverse Transformation Method. For forecasting purposes, as well as simulation, one may need a method for generating the random component of a time series. For this purpose, we use the inverse transformation method.

Let the random variable X have the distribution function $F(x)$. We assume that $F^{-1}(x)$ is the inverse function of $F(x)$. Then the algorithm for generating the random variable X with the distribution function $F(x)$ will be the following:

1. Generate the value U having the uniform distribution over the interval $(0;1)$;
2. Return $X = F^{-1}(U)$.

Fig. 2 depicts this algorithm graphically; the random variable corresponding to this distribution function can take either positive or negative values; it depends on the specific value of U . In Fig. 1, the random number U_1 gives the positive value of the random variable X_1 as a result, while the random number U_2 gives the negative value of the random variable X_2 as a result [11].

Estimating the distribution function of a random variable. Let us consider the time series as a sequence x_1, x_2, \dots, x_n of independent and equally distributed, according to a certain law, random variables; this sequence is called the sample of volume n . Each $x_i (i = 1, 2, \dots, n)$ is called variation. Having the sample, we do not have information about the form of the distribution function $F(x)$. It is required to construct an estimate (approximation) for this unknown function.

The most preferred estimate of the function $F(x)$ will be the empirical distribution function $F_n(x)$.

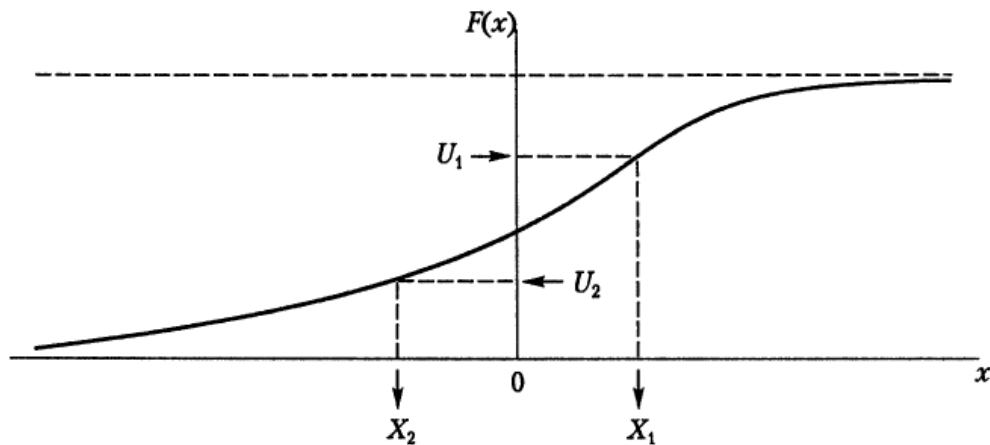


Fig. 1. Using the Inverse Transformation Method to generate a random variable

Рис. 1. Использование метода обратного преобразования для генерирования случайной величины

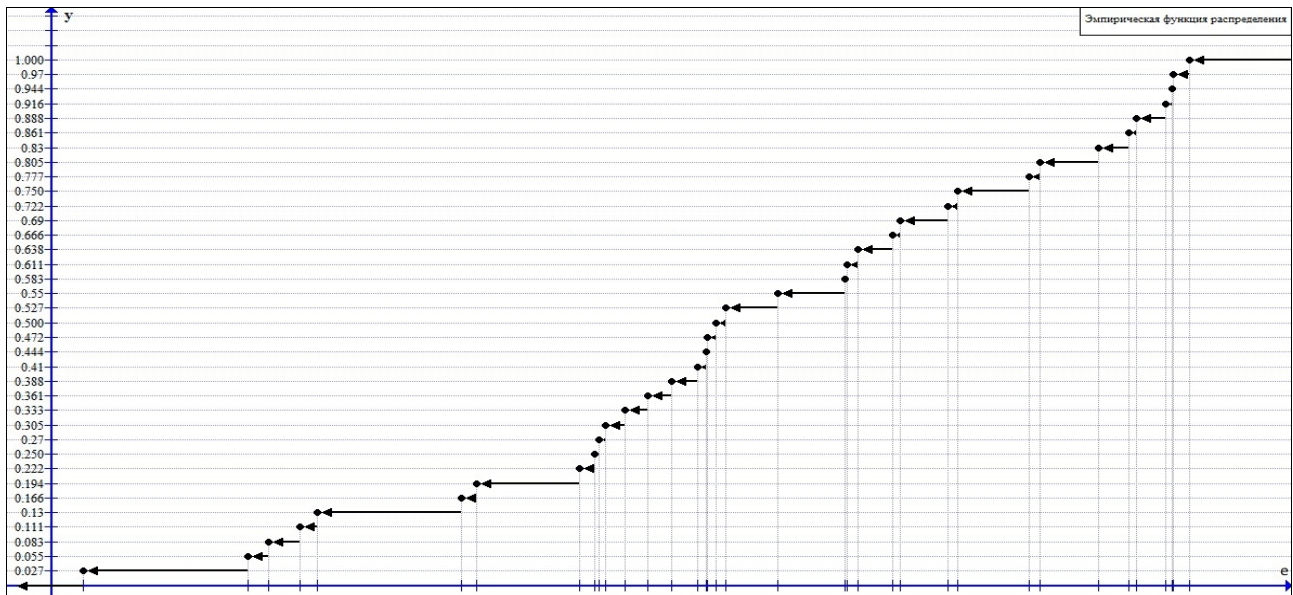
Fig. 2. Graph of the empirical distribution function $F_n(e)$

Рис. 2. График эмпирическая функция распределения $F_n(e)$

The empirical distribution function (sampling distribution function) is the function $F_n(x)$, which determines the relative frequency of the event $X < x$ for each x value, i. e.

$$F_n(x) = \frac{n_x}{n},$$

where n_x – the number of x_i values, less than x ; n – sample size.

With a sufficiently large sample size, the functions $F_n(x)$ and $F(x) = P(X < x)$ differ insignificantly from each other.

The difference between the empirical distribution function and the theoretical one is that the theoretical distribution function determines the probability of the event

$X < x$, and the empirical function determines the relative frequency of the same event [12].

The empirical distribution function has all the properties of the integral distribution function:

- 1) the values of the empirical distribution function belong to the interval $[0; 1]$;
- 2) $F_n(x)$ is non-decreasing function;
- 3) $F_n(x) = 0$ at $x \leq x_{\min}$, if x_{\min} is the smallest variation;

$F_n(x) = 1$ at $x > x_{\max}$, if x_{\max} is the largest variation [6].

However, to use the inverse transformation method, it is convenient to have a continuous distribution function; therefore, it is necessary to interpolate the obtained empirical function.

Building a predicted model. We give an example of using the inverse transformation method when constructing a predicted model. As the initial data, we use the average monthly indicators of power consumption in the Krasnoyarsk Territory for 3 years from January 2009 to December 2011 [13].

Using some regression model, the forecast values of the time series were calculated. Actual Y_t and predicted \hat{Y}_t values of the time series are presented in tab. 1

We build the empirical distribution function of the values of the deviations e_t of the predicted values \hat{Y}_t from the actual values Y_t of the time series $e_t = Y_t - \hat{Y}_t$. To do this, it is necessary to rank the sample $\{e_t\}$, thus obtaining the sample $\{e_{(t)} = \{e_{(1)} < e_{(2)} < \dots < e_{(n)}\}$ (tab. 2).

Since the frequency of each variation equals 1, the empirical function will have the following form:

$$F_n(e) = \begin{cases} 0, & e \in [-\infty, e_{(1)}); \\ \dots; \\ \frac{t}{n}, & e \in [e_{(t)}, e_{(t+1)}); \quad t = 0, 1, \dots, n; \\ \dots; \\ 1, & e \in [e_{(n)}, +\infty). \end{cases}$$

The graph of the function $F_n(e)$ is shown in fig. 2.

The obtained empirical function $F_n(e)$ has a discrete form. We use piecewise linear interpolation to obtain the continuous distribution function of the random variable $F_n^*(e)$. To do this, we use the equation of a straight line passing through two points:

$$y = (x - x_1) \times \left(\frac{y_2 - y_1}{x_2 - x_1} \right) + y_1.$$

The continuous distribution function of the random variable $F_n^*(e)$ will have the following form:

$$F_n(e) = \begin{cases} 0, & e \in (-\infty, e_{(1)}); \\ \dots; \\ (e' - e_{(t)}) \times \left(\frac{1/(n-1)}{e_{(t+1)} - e_{(t)}} \right) + \frac{t-1}{n-1}, & e \in [e_{(t)}, e_{(t+1)}); \quad t = 0, 1, \dots, n; \\ \dots; \\ 1, & e \in [e_{(n)}, +\infty). \end{cases}$$

Table 1

Actual Y_t and predicted \hat{Y}_t values of the time series

t	Y_t	\hat{Y}_t	t	Y_t	\hat{Y}_t	t	Y_t	\hat{Y}_t	t	Y_t	\hat{Y}_t
1	51.0123	53.09764	11	35.5809	43.42324	21	37.8690	44.58914	31	17.1468	15.15964
2	38.2345	38.37535	12	53.2584	54.26158	22	63.4957	57.61664	32	20.8548	21.45395
3	40.0023	35.24303	13	52.3887	52.69219	23	72.9843	72.28322	33	29.3791	31.55531
4	25.1288	32.13879	14	39.9125	41.30390	24	88.0214	83.09426	34	51.1710	44.09931
5	22.9338	27.08163	15	39.2113	32.14284	25	82.6095	79.01463	35	61.5869	59.79590
6	27.0146	20.64426	16	31.3420	24.38189	26	62.7282	63.15378	36	71.2594	73.02318
7	25.1154	17.77792	17	26.0102	19.52312	27	50.0250	48.20592			
8	16.6987	19.20278	18	20.5578	17.87433	28	29.6211	34.02474			
9	27.3114	23.86244	19	12.1214	22.62140	29	22.2954	22.75450			
10	29.2400	31.48983	20	24.9374	32.44863	30	17.8092	15.25792			

Table 2

Range of Values e_t and $e_{(t)}$

t	e_t	$e_{(t)}$	t	e_t	$e_{(t)}$	t	e_t	$e_{(t)}$	t	e_t	$e_{(t)}$
1	-2.085	-10.500	11	-7.842	-2.085	21	-6.720	1.791	31	1.987	6.370
2	-0.141	-7.842	12	-1.003	-1.764	22	5.879	1.819	32	-0.599	6.487
3	4.759	-7.511	13	-0.303	-1.391	23	0.701	1.987	33	-2.176	6.960
4	-7.010	-7.010	14	-1.391	-1.003	24	4.927	2.551	34	7.072	7.068
5	-4.148	-6.720	15	7.068	-0.599	25	3.595	2.683	35	1.791	7.072
6	6.370	-4.404	16	6.960	-0.459	26	-0.426	3.449	36	-1.764	7.337
7	7.337	-4.148	17	6.487	-0.426	27	1.819	3.595			
8	-2.504	-2.504	18	2.683	-0.303	28	-4.404	4.759			
9	3.449	-2.250	19	-10.500	-0.141	29	-0.459	4.927			
10	-2.250	-2.176	20	-7.511	0.701	30	2.551	5.879			

The graph of the function $F_{36}^*(e)$ is shown in fig. 3.

Evaluating the predicted model. For further analysis of this method, let us consider several forecast models [14]:

1. We take the value Y_t of the time series as a completely deterministic process, to carry out the forecast we use the values \hat{Y}_t calculated using the regression model;

2. The value Y_t of the time series will be taken as a random variable for which we construct the distribution function $F_n^*(e)$ and calculate the predicted values Y'_t ;

3. We will take the value Y_t of the time series as a set of values \hat{Y}_t calculated using the regression model and the random component e_t , for which we construct the distribution function $F_n^*(e)$ and calculate the predicted values e'_t .

Let us make the operational prediction of energy consumption levels. For this purpose, we exclude from consideration the last 5 observations from the sample and we calculate new estimates of the parameters of the

regression model, as well as the new distribution functions $F_{31}^*(x)$ and $F_{31}^*(e)$.

We apply the inverse transformation algorithm to the obtained functions $F_{31}^*(x)$ and $F_{31}^*(e)$. To this end, we generate the sample $\{u_t\}$ of random numbers having a uniform distribution in the interval $[0; 1]$, and return $Y't = F_{31}^{*-1}(u_t)$ and $e't = F_{31}^{*-1}(u_t)$. The calculation results are presented in tab. 3.

When considering the obtained results, it is clear that the sum $Y_t + e'_t$ is closer to the actual data than the predicted values calculated using the regression model. Thus, the predicted values smoothed out the predicted error to an extent (fig. 4).

As a criterion for assessing the quality of the model, we determine the value of the average approximation error, which is calculated using the formula [15]:

$$A = \frac{1}{n} \sum_{t=1}^n \left| \frac{Y_{act} - Y_{pr}}{Y_{act}} \right| \cdot 100 \%,$$

where Y_{pr} – predicted value of time series; Y_{act} – actual value of time series; n – size of time series [10].

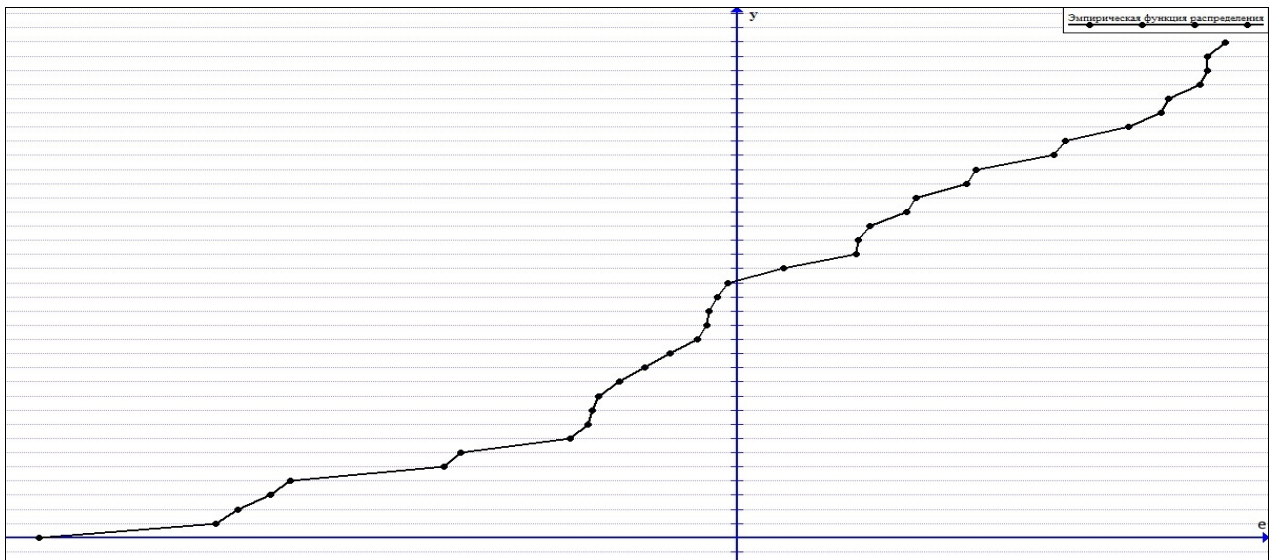


Fig. 3. Graph of the continuous distribution function $F_{36}^*(e)$

Рис. 3. График непрерывной функции распределения $F_{36}^*(e)$

Results of applying the inverse transformation algorithm

Table 3

№	t	\hat{Y}_t	u_t	e'_t	$Y_t + e'_t$	Y'_t
1	32	25.1456	0.0608	-7.1360	18.0096	6.9693
2	33	37.1619	0.6514	1.9654	39.1274	14.9283
3	34	52.0351	0.6577	2.1085	54.1436	15.2489
4	35	70.5459	0.0515	-7.1507	63.3952	6.8725
5	36	86.8325	0.5448	0.3808	87.2133	13.4902

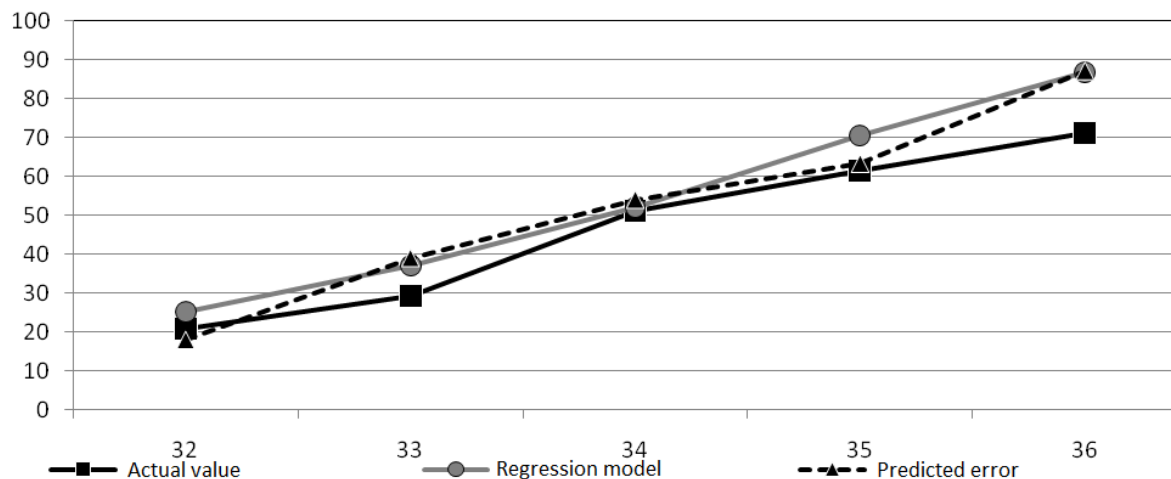


Fig. 4. Graph display of predicted results

Рис. 4. Графическое отображение результатов прогноза

The values of the average approximation error for \hat{Y}_t ,

Y'_t and $\hat{Y}_t + e'_t$ are the following:

- 1) $A(\hat{Y}_t) \approx 17,03\%$;
- 2) $A(Y'_t) \approx 71,18\%$;
- 3) $A(\hat{Y}_t + e'_t) \approx 15,59\%$.

The highest indicator of the average approximation error was obtained under the assumption that the time series Y_t is a random variable. The average approximation error for the regression model is 54.15 % less, which tells us that the time series is a determinate value. As a result of including values e'_t in regression, the average approximation error decreased by approximately 1.44 %.

Conclusion. The method presented above can be used to determine the continuous distribution function of a random variable and generate a random variable for predicting and simulation purposes.

References

1. Egorshin A. V. [Statement of the problem of forecasting the time series generated by a dynamic system]. Yoshkarala, Mary State. tech. un-t Publ., 2007, P. 136–140.
2. Urmaev A. S. *Osnovy modelirovaniya na EVM* [Computer modeling basics]. Moscow, Nauka Publ., 1978, 246 p.
3. Ezhova L. N. *Ekonometrika. Nachal'nyy kurs s osnovami teorii veroyatnostey i matematicheskoy statistiki*. [Econometrics. Initial course with the basics of probability theory and mathematical statistics. Textbook]. Irkutsk, Baykal'skiy gosudarstvenny universitet Publ., 2008, 287 p.
4. Anisimov A. S., Kononov V. T. [Structural identification of linear discrete dynamic system]. *Vestnik NSTU*, 2005, No. 1, P. 21–36 (In Russ.).
5. Khinchin A. Ya. *Raboty po matematicheskoy teorii massovogo obsluzhivaniya* [Works on the mathematical theory of queuing]. Moscow, Fizmatgiz Publ., 1963, 296 p.

6. Guiders M. A. *Obshchaya teoriya sistem* [General theory of systems]. Moscow, Globus-press Publ., 2005, 201 p.

7. Kondrashov D. V. [Forecasting time series based on the use of Chebyshev polynomials that are least deviated from zero]. *Bulletin of the Samara state. Those. University. Series: Engineering*, 2005, No. 32, P. 49–53 (In Russ.).

8. Pugachev V. S. *Teoriya veroyatnostey i matematicheskaya statistika* [Theory of Probability and Mathematical Statistics]. Moscow, Nauka Publ., 1979, 336 p.

9. Buslenko N. P. *Modelirovanie slozhnyh sistem* [Modeling complex systems]. Moscow, Nauka Publ., 1968, 230 p.

10. Pugachev V. S. *Teoriya sluchajnyh funktsiy i ee primeneniye k zadacham avtomaticheskogo upravleniya* [The theory of slash functions and its application to the problems of automatic control]. Moscow, Fizmatgiz Publ., 1960, 236 p.

11. Belgorodskiy E. A. [Some discussion problems of forecasting]. *Ural'skiy geologicheskij zhurnal*. 2000, No. 2, P. 25–32 (In Russ.).

12. Averill M. L., Kelton D. *Imitacionnoye modelirovanie* [Simulation modeling and analysis. Third edition]. SPb., Piter Publ., 2004, 505 p.

13. Dvoiris L. I. [Forecasting time series based on the analysis of the main components]. *Radiotekhnika*. 2007, No. 2, P. 68–71 (In Russ.).

14. Van der Waerden. *Matematicheskaya statistika* [Mathematical statistics]. Moscow, IL Publ., 1960, 436 p.

15. Grenander U. *Sluchajnye processy i statisticheskie vyvody* [Random processes and statistical inferences]. Moscow, IL Publ., 1961, 168 p. (In Russ.).

Библиографические ссылки

1. Егоршин А. В. Постановка задачи прогнозирования временного ряда порождаемого динамической системой. Йошкарала : Марийский гос. техн. ун-т. 2007. С. 136–140.

2. Урмаев А. С. Основы моделирования на ЭВМ. М. : Наука, 1978. 246 с.
 3. Ежова Л. Н. Эконометрика. Начальный курс с основами теории вероятностей и математической статистики. Иркутск : Байкальский гос. ун-т, 2008. 287с.
 4. Анисимов А. С., Кононов В. Т. Структурная идентификация линейных дискретных динамических систем // Вестник НГТУ. 2005. № 1. С. 21–36.
 5. Хинчин А. Я. Работы по математической теории массового обслуживания. М. : Физматгиз, 1963. 296 с.
 6. Гайдера М. А. Общая теория систем. М. : Глобус-пресс, 2005. 201 с.
 7. Кондрашов Д. В. Прогнозирование временных рядов на основе использования полиномов Чебышева, наименее уклоняющихся от нуля // Вестник Самарского гос. тех. ун-та. Серия: Технические науки. 2005. № 32. С. 49–53.
 8. Пугачев В. С. Теория вероятностей и математическая статистика. М. : Наука, 1979. 336 с.
 9. Бусленко Н. П. Моделирование сложных систем. М. : Наука, 1968. 230 с.
 10. Пугачев В. С. Теория случайных функций и ее применение к задачам автоматического управления. М. : Физматгиз, 1960. 236 с.
 11. Белгородский Е. А. О некоторых дискуссионных проблемах прогнозирования // Уральский геологический журнал. 2000. № 2. С. 25–32.
 12. Аверилл М. Л., Кельтон Д. Имитационное моделирование. СПб. : Питер, 2004. 505 с.
 13. Двойрис Л. И. Прогнозирование временных рядов на основе анализа главных компонент // Радиотехника. 2007. № 2. С. 68–71.
 14. Ван дер Варден. Математическая статистика. М. : ИЛ, 1960. 436 с.
 15. Гренандер У. Случайные процессы и статистические выводы. М. : ИЛ, 1961. 168 с.
- © Shiryaeva T. A., Khlupichev V. A.,
Shlepkin A. K., Melnikova O. L., 2020

Shiryaeva Tamara Alekseevna – Cand. Sc., Professor; Krasnoyarsk State Agrarian University. E-mail: info@kgau.ru.

Khlupichev Vladimir Aleksandrovich – Master's Student; Krasnoyarsk State Agrarian University. E-mail: vova.khlp@yandex.ru.

Shlepkin Anatoly Konstantinovich – Dr. Sc., Professor; Krasnoyarsk State Agrarian University. E-mail: ak_kgau@mail.ru.

Melnikova Olga Leonidovna – Cand. Sc., Professor; Khakas State University. E-mail: olga-l-melnikova@yandex.ru.

Ширяева Тамара Алексеевна – кандидат физико-математических наук, доцент, доцент кафедры информационных технологий и математического обеспечения информационных систем; Красноярский государственный аграрный университет. E-mail: info@kgau.ru.

Хлупичев Владимир Александрович – магистрант; Красноярский государственный аграрный университет. E-mail: vova.khlp@yandex.ru.

Шлепкин Анатолий Константинович – доктор физико-математических наук, профессор, профессор кафедры высшей математики и компьютерного моделирования; Красноярский государственный аграрный университет. E-mail: ak_kgau@mail.ru.

Мельникова Ольга Леонидовна – кандидат педагогических наук, доцент кафедры информационных технологий и систем; Хакасский государственный университет имени М. Ф. Катанова. E-mail: olga-l-melnikova@yandex.ru.

UDC 338.27

Doi: 10.31772/2587-6066-2020-21-1-41-46

For citation: Shiryayeva T. A., Shlepkin A. K., Philippov K. A., Kolmakova Z. A. On the function of time distribution of a complex computing system uptime. *Siberian Journal of Science and Technology*. 2020, Vol. 21, No. 1, P. 41–46. Doi: 10.31772/2587-6066-2020-21-1-41-46

Для цитирования: Ширяева Т. А., Шлепкин А. К., Филиппов К. А., Колмакова З. А. О функции распределения времени безотказной работы сложной вычислительной системы // Сибирский журнал науки и технологий. 2020. Т. 21, № 1. С. 41–46. Doi: 10.31772/2587-6066-2020-21-1-41-46

ON THE FUNCTION OF TIME DISTRIBUTION OF A COMPLEX COMPUTING SYSTEM UPTIME

T. A. Shiryayeva¹, A. K. Shlepkin^{1*}, K. A. Philippov¹, Z. A. Kolmakova²

¹Krasnoyarsk State Agrarian University
90, Mira Av., Krasnoyarsk, 660001, Russian Federation

²Khakas State University
90, Lenin Av., Abakan, 655017, Russian Federation

*E-mail: ak_kgau@mail.ru

Any space computing complex is a complicated system. A complicated system is understood as a set of functionally related heterogeneous devices designed to perform certain functions and solve problems facing the system. One of the important characteristics of a system is its uptime. This characteristic is often considered to be a random variable. However, such a mathematical model is quite limited, since the uptime depends on many characteristics (parameters) that describe a system. Therefore, the uptime can be assumed to be a continuous random field (that is, a random function of many variables). It is this approach that is used in this work. If there are certain restrictions on the uptime of a computing system, upper estimates are found for the distributions of a random number of system failures. Therefore, the problem of estimating Gaussian field distribution in Hilbert space arises.

Two theorems that allow calculating the probability of a Gaussian vector falling into a sphere of a given radius are proved in the paper.

The paper is devoted to the reliability of a computing system. The random number of a computing system failures $v(r)$ is a characteristic of its reliability. The $v(r)$ distribution is the distribution of the sum of a computing system random uptime. It is impossible to write down the distribution $v(r)$ explicitly. Therefore, one has to look for an estimate of these distributions from above. Assuming that the uptime of a computing system is the sum of many variables, the authors of the paper obtained the following results: it is shown that the problem of estimating the distributions of a random number of system failures can be considered as the problem of estimating the convergence rate in the central limit theorem in Banach spaces; if there are certain restrictions on the uptime of a computing system, upper estimates are found for the distributions of a random number of system failures. The estimates obtained can be used for further research in the theory of computing systems reliability. Knowing these upper estimates, it is possible to predict the level of average costs for computer systems restoration, as well as for the development of special mathematical and algorithmic support for analysis systems, for management, decision-making and information processing tasks.

Keywords: computing system, distribution function, systems analysis.

О ФУНКЦИИ РАСПРЕДЕЛЕНИЯ ВРЕМЕНИ БЕЗОТКАЗНОЙ РАБОТЫ СЛОЖНОЙ ВЫЧИСЛИТЕЛЬНОЙ СИСТЕМЫ

Т. А. Ширяева¹, А. К. Шлепкин^{1*}, К. А. Филиппов¹, З. А. Колмакова²

¹ Красноярский государственный аграрный университет
Российская Федерация, 660001, Красноярск, просп. Мира, 90

² Хакасский государственный университет имени М. Ф. Катанова
Российская Федерация, 655017, Абакан, просп. Ленина, 90

* E-mail: ak_kgau@mail.ru

Любой космический вычислительный комплекс представляет собой сложную систему. Под сложной системой понимают совокупность функционально связанных разнородных устройств, предназначенных для выполнения определенных функций и решения стоящих перед системой задач. Одной из важных характеристик работы системы является время ее безотказной работы. Часто эту характеристику считают случайной величиной. Но такая математическая модель является довольно ограниченной, так как время безотказной работы зависит от многих характеристик (параметров), описывающих систему. Поэтому можно предпо-

жить, что время безотказной работы есть непрерывное случайное поле (то есть случайная функция многих переменных). Именно такой подход применяется в данной работе. При наличии определенных ограничений на время безотказной работы вычислительной системы найдены верхние оценки для распределений случайного числа отказов системы. Поэтому возникает вопрос оценки распределения гауссовского поля в гильбертовом пространстве.

В работе доказаны две теоремы, которые позволяют вычислить вероятность попадания гауссовского вектора в шар заданного радиуса.

Данная работа посвящена надежности работы вычислительной системы. Одной из характеристик надежности вычислительной системы является случайное число ее отказов $v(r)$. Распределение $v(r)$ есть распределение суммы случайных времен безотказной работы вычислительной системы. Записать распределение $v(r)$ в явном виде невозможно. Поэтому приходится искать оценку этих распределений сверху. В предположении, что время безотказной работы вычислительной системы есть сумма многих переменных, в данной работе получены следующие результаты: показано, что задачу оценки распределений случайного числа отказов системы можно рассматривать как задачу оценки скорости сходимости в центральной предельной теореме в банаховых пространствах; при наличии определенных ограничений на время безотказной работы вычислительной системы найдены верхние оценки для распределений случайного числа отказов системы. Полученные оценки могут быть использованы для дальнейших исследований в теории надежности вычислительных систем. Зная эти верхние оценки, можно прогнозировать уровень средних затрат на восстановление вычислительных систем, а также для разработки специального математического и алгоритмического обеспечения систем анализа, для задач управления, принятия решений и обработки информации.

Ключевые слова: вычислительная система, функция распределения, системный анализ.

Introduction. Any space computing complex is a complicated system. A complicated system is understood as a set of functionally related heterogeneous devices designed to perform certain functions and solve problems facing the system. One of the important characteristics of a system is its uptime. This characteristic is often considered to be a random variable. However, such a mathematical model is quite limited, since the uptime depends on many characteristics (parameters) that describe a system.

Therefore, the uptime can be assumed to be a continuous random function of many variables. Such an assumption is used in the literature [1–15]. In this work we will also stick to it.

It is known that the characteristic functional of a random variable Y in the Hilbert space H is the functional

$$\varphi_Y(Z) = E \exp \{i(Z, Y)\},$$

where $z \in H$, (Z, Y) is the scalar product in H , $i = \sqrt{-1}$, E is the sign of mathematical expectation. Let R be the covariant vector of a random variable H , $EY = A$. If Y is a Gaussian vector in H , then its characteristic functional has the form:

$$\varphi_Y(Z) = \exp \{i(A, Z) - \frac{1}{2}(RZ, XZ)\}.$$

The converse is also true, that is, if Y has a characteristic functional that meets these requirements, then its distribution is Gaussian.

The covariant operator R of the Gaussian vector Y is a kernel and completely continuous one; therefore it has an orthonormal basis of eigenvectors e_k , $k = 1, 2, \dots$. Let us denote λ_k , that is, the eigenvalue of the operator R , corresponding to the eigenvector e_k . Let $\lambda_k > 0$ be random variables

$$\varepsilon_k = \frac{(Y - A, e_k)}{\sqrt{\lambda_k}}$$

which are independent, have a normal distribution and $E\varepsilon_k = 0$, $E\varepsilon_k^2 = 1$. Thus, the Gaussian vector Y can be written as

$$Y = A + \sum_{k=1}^{\infty} \sqrt{\lambda_k} \varepsilon_k e_k.$$

The representation of the Gaussian vector Y can be used in various calculations. In particular, if we denote $\alpha_k = (A, e_k)$, then the characteristic function for the real s of a random variable $|Y|_H^2$ has the form

$$\phi_{|Y|_H^2}(s) = E \exp \{is|A|_H^2\} \cdot \prod_{k=1}^{\infty} \frac{\exp \left\{ \frac{2\lambda_k \alpha_k^2 s^2}{\sqrt{1 - 2si\lambda_k}} \right\}}{\sqrt{1 - 2si\lambda_k}}.$$

It is known that the distribution $F(x)$ of a random variable is uniquely restored by the form of the characteristic function $\varphi(t)$:

$$F(y) - F(x) = \frac{1}{2\pi} \int_{-\infty}^{+\infty} \frac{e^{-itx} - e^{-ity}}{it} \varphi(t) dt,$$

then

$$\phi_{|Y|_H^2}(s) = \prod_{k=1}^{\infty} \frac{1}{\sqrt{1 - 2is\lambda_k}}.$$

Statement of the main results.

Theorem 1. Let λ_k be the eigenvalue of the covariant operator R of a Gaussian vector Y . Then the probability of Y falling into a sphere of radius r is

$$p(|Y|_H < r) = \frac{2}{\pi} \int_0^{+\infty} \frac{1}{t} \exp \left\{ -\frac{1}{4} \sum_{k=1}^{\infty} \ln \left(1 + (2t\lambda_k)^2 \right) \right\} \times \\ \times \cos \frac{tr^2 + \sum_{k=1}^{\infty} \arctg 2t\lambda_k + 2\pi k}{2} \sin \frac{tr^2}{2} dt.$$

Theorem 2. Let λ be the maximum eigenvalue of the covariant operator R of a Gaussian vector Y . Then the probability of Y falling into a sphere of radius r is equal to:

$$P(|Y|_H < r) \leq \frac{2}{\pi} \int_0^{\frac{2\pi}{r^2}} \frac{1}{t^4 \sqrt{1 + (2t\lambda)^2}} \sin \frac{tr^2}{2} dt.$$

The proof of Theorem 1. Since $P(Y_H < r) = P(Y_H^2 < r^2)$ then by the inversion formula:

$$\begin{aligned} P(|Y|_H^2 \leq r^2) &= F_{|Y|_H^2}(r^2) - F_{|Y|_H^2}(0) = \\ &= \frac{1}{2\pi} \int_{-\infty}^{+\infty} \frac{e^{-it0} - e^{-itr^2}}{it} \phi_{|Y|_H^2}(t) dt = \\ &= \frac{1}{2\pi} \int_{-\infty}^{+\infty} \frac{1 - e^{-itr^2}}{it} \prod_{k=1}^{\infty} \frac{1}{\sqrt{1 - 2it\lambda_k}} dt = \\ &= \frac{1}{2\pi} \int_{-\infty}^{+\infty} \frac{1 - e^{-itr^2}}{it} \frac{1}{\prod_{k=1}^{\infty} \sqrt{1 - 2it\lambda_k}} dt = \\ &= \frac{1}{2\pi} \int_{-\infty}^{+\infty} \frac{1 - (\cos tr^2 - i \sin tr^2)}{it} e^{-\ln \prod_{k=1}^{\infty} \sqrt{1 - 2it\lambda_k}} dt = \\ &= \frac{1}{2\pi} \int_{-\infty}^{+\infty} \frac{1 - (\cos tr^2 - i \sin tr^2)}{it} e^{-\frac{1}{2} \sum_{k=1}^{\infty} \ln(1 + 2it\lambda_k)} dt. \end{aligned}$$

Let us simplify the form of the function using the properties of the functions of the complex variable [4]:

$$\begin{aligned} \ln(1 - 2it\lambda_k) &= \ln|1 + 2it\lambda_k| + i(\arg(1 - 2it\lambda_k) + 2\pi k) \\ \arg(1 - 2it\lambda_k) &= \arctg 2t\lambda_k + 2\pi k. \end{aligned}$$

Substituting, we obtain

$$\begin{aligned} P(|Y|_H^2 \leq r^2) &= \frac{1}{2\pi} \int_{-\infty}^{+\infty} \frac{i \cos tr^2 + \sin tr^2 - i}{t} \times \\ &\times e^{\sum_{k=1}^{\infty} \ln(1 + (2t\lambda_k)^2)} e^{-\frac{1}{2} i \sum_{k=1}^{\infty} (\arctg 2t\lambda_k + 2\pi k)} dt. \end{aligned}$$

Let us use the properties of the functions of the complex variable again:

$$\begin{aligned} e^{-\frac{1}{2} i (\sum_{k=1}^{\infty} \arctg 2t\lambda_k + 2\pi k)} &= \\ = \cos \frac{\sum_{k=1}^{\infty} (\arctg 2t\lambda_k + 2\pi k)}{2} + i \sin \frac{\sum_{k=1}^{\infty} (\arctg 2t\lambda_k + 2\pi k)}{2}. \end{aligned}$$

In the future, for the convenience of calculations we introduce the following notation:

$$\begin{aligned} C &= \cos \frac{\sum_{k=1}^{\infty} (\arctg 2t\lambda_k + 2\pi k)}{2}, \\ S &= \sin \frac{\sum_{k=1}^{\infty} (\arctg 2t\lambda_k + 2\pi k)}{2}. \end{aligned}$$

Substituting the introduced notation in the formula, we obtain

$$\begin{aligned} P(|Y|_H^2 \leq r^2) &= \frac{1}{2\pi} \int_{-\infty}^{\infty} \frac{e^{-\frac{1}{4} \sum_{k=1}^{\infty} \ln(1 + (2t\lambda_k)^2)}}{t} dt = \\ &= C \sin tr^2 - iS \sin tr^2 + iC \cos tr^2 + S \cos tr^2 - iC - S) dt = \\ &= \frac{1}{2\pi} \int_{-\infty}^{\infty} \frac{e^{-\frac{1}{4} \sum_{k=1}^{\infty} \ln(1 + (2t\lambda_k)^2)}}{t} (C \sin tr^2 + S \cos tr^2 - S) dt + \\ &+ \frac{1}{2\pi} i \int_{-\infty}^{\infty} \frac{e^{-\frac{1}{4} \sum_{k=1}^{\infty} \ln(1 + (2t\lambda_k)^2)}}{t} (C \cos tr^2 - C - S \sin tr^2) dt. \end{aligned}$$

The imaginary part is 0, since the integrand is odd and is considered on the entire axis $(-\infty; +\infty)$. Then

$$\begin{aligned} P(|Y|_H^2 \leq r^2) &= \\ &= \frac{1}{2\pi} \int_{-\infty}^{\infty} \frac{e^{-\frac{1}{4} \sum_{k=1}^{\infty} \ln(1 + (2t\lambda_k)^2)}}{t} (C \sin tr^2 + S \cos tr^2 - S) dt. \end{aligned}$$

We take into account the following:

$$\begin{aligned} &\sin tr^2 \cos \frac{\sum_{k=1}^{\infty} \arctg 2t\lambda_k + 2\pi k}{2} + \\ &+ \cos tr^2 \sin \frac{\sum_{k=1}^{\infty} \arctg 2t\lambda_k + 2\pi k}{2} = \\ &= \cos \left(tr^2 + \frac{\sum_{k=1}^{\infty} \arctg 2t\lambda_k + 2\pi k}{2} \right) - \\ &- \sin \frac{\sum_{k=1}^{\infty} \arctg 2t\lambda_k + 2\pi k}{2} = \\ &= 2 \cos \frac{tr^2 + \sum_{k=1}^{\infty} \arctg 2t\lambda_k + 2\pi k}{2} \sin \frac{tr^2}{2}. \end{aligned}$$

As a result, the formula will take the form:

$$\begin{aligned} &\frac{1}{2\pi} \int_{-\infty}^{\infty} \frac{e^{-\frac{1}{4} \sum_{k=1}^{\infty} \ln(1 + (2t\lambda_k)^2)}}{t} (C \sin tr^2 + S \cos tr^2 - S) dt = \\ &= \frac{1}{2\pi} \int_{-\infty}^{\infty} \frac{e^{-\frac{1}{4} \sum_{k=1}^{\infty} \ln(1 + (2t\lambda_k)^2)}}{t} \times \\ &\times \left(2 \cos \frac{tr^2 + \sum_{k=1}^{\infty} \arctg 2t\lambda_k + 2\pi k}{2} \sin \frac{tr^2}{2} \right) dt = \end{aligned}$$

$$= \frac{1}{\pi} \int_{-\infty}^{\infty} \frac{e^{-\frac{1}{4} \ln(1+(2t\lambda_k)^2)}}{t} \times$$

$$\times \left(\cos \frac{tr^2 + \sum_{k=1}^{\infty} \arctg 2t\lambda_k + 2\pi k}{2} \sin \frac{tr^2}{2} \right) dt$$

Knowing that the function is symmetric with respect to the origin of coordinates, we can write

$$P(|Y|_H^2 \leq r^2) = \frac{2}{\pi} \int_{-\infty}^{\infty} \frac{e^{-\frac{1}{4} \ln(1+(2t\lambda_k)^2)}}{t} \times$$

$$\times \left(\cos \frac{tr^2 + \sum_{k=1}^{\infty} \arctg 2t\lambda_k + 2\pi k}{2} \sin \frac{tr^2}{2} \right) dt.$$

The theorem is proved.

The proof of Theorem 2. The practical use of Theorem 1 is difficult, since, firstly, the knowledge of all eigenvalues of λ_k is assumed, and secondly, the integral sign contains infinite sums. Therefore, one has to confine oneself to estimates from above the studied probability. It's obvious that

$$\exp \left\{ -\frac{1}{2} \sum_{k=1}^{\infty} \ln(1+(2t\lambda_k)^2) \right\} = \frac{1}{4} \cdot \frac{1}{\prod_{k=1}^{\infty} \sqrt[4]{1+(2t\lambda_k)^2}}.$$

Let $\lambda = \max_{k \geq 1} \lambda_k$, then

$$\frac{1}{t} \cdot \frac{1}{\prod_{k=1}^{\infty} \sqrt[4]{1+(2t\lambda_k)^2}} \leq \frac{1}{t} \cdot \frac{1}{\sqrt[4]{1+(2t\lambda_k)^2}}.$$

$$\frac{1}{t} \cdot \frac{1}{\prod_{k=1}^{\infty} \sqrt[4]{1+(2t\lambda_k)^2}} \leq \frac{1}{t} \cdot \frac{1}{\sqrt[4]{1+(2t\lambda_k)^2}}.$$

Consequently

$$P(|Y|_H < r) \leq \frac{2}{\pi} \int_0^{\infty} \frac{1}{t \sqrt[4]{1+4t^2\lambda^2}} \sin \frac{tr^2}{2} dt.$$

Let us consider the integrand

$$p(t) = \frac{1}{t \sqrt[4]{1+4t^2\lambda^2}} \sin \frac{tr^2}{2}.$$

It is obvious that $\lim_{t \rightarrow 0} p(t) \rightarrow \frac{r^2}{2}$, and it means the function $p(t)$ is a bounded one. $p(t) = 0$ at $t = \frac{2\pi k}{r^2}$. The function graph is a sinusoid $t \rightarrow \infty, p(t) \rightarrow 0$.

Hence

$$P(|Y|_H < r) \leq \frac{2}{\pi} \int_0^{\frac{2\pi}{r^2}} \frac{1}{t \sqrt[4]{1+(2t\lambda)^2}} \sin \frac{tr^2}{2} dt.$$

The theorem is proved.

Thus, one can find the numerical values of the upper probability estimates $P(|Y|_H < r)$ depending on the radius of the sphere r and the maximum eigenvalue λ of the covariant operator R . Table was compiled for some values of r and λ .

Upper numerical estimates in the case of Gaussian uptime of a computing system. Let

$$J(\lambda, r) = \frac{2}{\pi} \int_0^{\frac{2\pi}{r^2}} \frac{1}{t \sqrt[4]{1+4t^2\lambda^2}} \sin \frac{tr^2}{2} dt.$$

If the random uptime of the computing system is a normal random field, then its distribution determined by the norm of the space $C(K)$ can be estimated numerically from above. To do this, one only needs to know the value of the maximum eigenvalue λ of the covariance operator R . Then using the embedding inequality [5] we have:

$$P(|Y|_c < r) \leq P(a|Y|_h < r) = P\left(|Y|_h < \frac{r}{a}\right) \leq J\left(\lambda, \frac{r}{a}\right),$$

the constant a is equal to a fixed number, which is determined exactly depending on the number of variables d of the random field and the space H that is embedded in $C(K)$.

Conclusion. This paper is devoted to the reliability of the computing system. One of the characteristics of the computing system reliability is the random number of its failures $v(r)$. The distribution $v(r)$ is the distribution of the sum of random times $X_i(t)$ of the failure-free operation of the computing system, $i = 1, \dots, n$. It is impossible to write down the distribution $v(r)$ explicitly. Therefore, one has to look for an estimate of these distributions from above. Assuming that the uptime $X_i(t)$ of the computing system is the sum of many variables, the authors of the paper obtained following results:

– it is shown that the problem of estimating the distributions of a random number of system failures can be considered as the problem of estimating the rate of convergence in the central limit theorem in Banach spaces;

– if there are certain restrictions on the uptime $X(t)$ of the computing system, upper estimates are found for the distributions $F_n(r)$ of a random number of system failures. These estimates can be written as

$$F_n(r) \leq \left(\frac{r - Tn}{a\sqrt{n}} \right) + cn^{\beta} (\ln n)^{\gamma},$$

where $N(r)$ is the normal distribution, the constants a, c are determined earlier, the exponents β, γ are determined by the conditions on $X(t)$.

Numerical upper estimates of the form $N(r) \leq J(\lambda, r)$ are found for the normal distribution $N(r)$.

$$P(|Y|_H < r) \leq \frac{2}{\pi} \int_0^{\frac{2\pi}{r^2}} \frac{1}{t \sqrt[4]{1+(2t\lambda)^2}} \sin \frac{tr^2}{2} dt.$$

The estimates obtained can be used for further research in the theory of computing systems reliability.

Upper probabilities for $P(|Y|_C < r)$

r	$\lambda = 1$	$\lambda = 2$	$\lambda = 3$	r	$\lambda = 1$	$\lambda = 2$	$\lambda = 3$
0.1	0.0583	0.0415	0.0340	2.6	0.7586	0.6693	0.6034
0.2	0.1139	0.0817	0.0671	2.7	0.7659	0.6807	0.6161
0.3	0.1169	0.1200	0.0993	2.8	0.7724	0.6914	0.6282
0.4	0.2171	0.1580	0.1306	2.9	0.7783	0.7013	0.6397
0.5	0.2647	0.1941	0.1610	3.0	0.7836	0.7106	0.6506
0.6	0.3096	0.2289	0.1905	3.1	0.7884	0.7193	0.6610
0.7	0.3520	0.2624	0.2191	3.2	0.7926	0.7273	0.6708
0.8	0.3917	0.2945	0.2469	3.3	0.7965	0.7348	0.6801
0.9	0.4289	0.3253	0.2737	3.4	0.7999	0.7418	0.6893
1.0	0.4637	0.3549	0.2997	3.5	0.8029	0.7482	0.6972
1.1	0.4960	0.3831	0.3248	3.6	0.8057	0.7542	0.7051
1.2	0.5260	0.4101	0.3490	3.7	0.8082	0.7598	0.7125
1.3	0.5538	0.4358	0.3724	3.8	0.8104	0.7650	0.7195
1.4	0.5795	0.4603	0.3949	3.9	0.8124	0.7698	0.7261
1.5	0.6031	0.4836	0.4166	4.0	0.8142	0.7742	0.7323
1.6	0.6248	0.5057	0.4374	4.1	0.8159	0.7783	0.7382
1.7	0.6446	0.5266	0.4574	4.2	0.8173	0.7821	0.7437
1.8	0.6628	0.5465	0.4766	4.3	0.8187	0.7856	0.7489
1.9	0.6793	0.5653	0.4951	4.4	0.8199	0.7889	0.7538
2.0	0.6943	0.5830	0.5127	4.5	0.8210	0.7919	0.7584
2.1	0.7079	0.5997	0.5296	4.6	0.8219	0.7947	0.7627
2.2	0.7202	0.6154	0.5458	4.7	0.8228	0.7973	0.7668
2.3	0.7313	0.6302	0.5612	4.8	0.8224	0.7997	0.7706
2.4	0.7414	0.6441	0.5759	4.9	0.8237	0.8019	0.7742
2.5	0.7504	0.6571	0.5900	5.0	0.8251	0.8040	0.7776

The average number of system failures is $H(r) = \sum_{n=1}^{\infty} F_n(r)$, therefore, knowing the upper estimates for $F_n(r)$, one can obtain upper estimates for $H(r)$ and predict the level of average costs for the restoration of computing systems.

References

1. Barzilevich E. Yu., Belyaev Yu. K., Kashtanov V. A. et al. *Voprosy matematicheskoy teorii nadezhnosti* [Questions of the mathematical theory of reliability]. Moscow, Radio i svyaz Publ., 1983, 376 p.
2. Belyaev Yu. K., Dulina T. N., Chepurin E. V. [Calculation of the low probability of failure-free operation of complex systems. Part 1] *Izv. AN SSSR, Tekhnicheskaya kibernetika*. 1967, No. 2, P. 52–69 (In Russ.).
3. Belyaev Yu. K., Dulina T. N., Chepurin E. V. [Calculation of the lower limit of the probability of failure-free operation of complex systems. Part 2]. *Izv. AN SSSR, Tekhnicheskaya kibernetika*. 1967, No. 3, P. 63–78 (In Russ.).
4. Bentkus V. Yu., Rachkauskas A. Yu. [Estimates of the convergence rate of sums of independent random variables in a Banach space]. *Litovskiy mat. sb.* 1982, Vol. XXII, No. 4, P. 8–20 (In Russ.).
5. Bentkus V. Yu., Rachkauskas A. Yu. [Estimates of the convergence rate of sums of independent random variables in a Banach space]. *Litovskiy mat. sb.* 1982, Vol. XXII, No. 3, P. 12–18 (In Russ.).
6. Araujo de A., Gine E. The central limit theorem for the Real and Banach Valued Random Varicolles. New York: Yoth Willey and Sons, 1980.
7. Forter R., Mourier E. Les fonctions aleatoires dans les espaces de Banach. *Studia Math.* 1955, No. 15, P. 62–73.
8. Gine E. On the central limit theorem for sample continuous processes. *Annales of Profability.* 1974, P. 62–73.
9. Gine E., Marcus N.B. On the CLT in $C(K)$. *Leet Notes Math.* 1969, Vol. 89, P. 62–73.
10. Gotze F. On rate of convergence in central limit theorem in Banach spaces. *Annales of Profability.* 1976, Vol. XIV, No. 3, P. 852–859.
11. Hoffman-Yorgensen Y., Pisier G. The law of large members and the central limit theorem in Banach spaces. *Annales of Profability.* 1974, Vol. 4, P 587–599.
12. Le Cam L. Remarque sur le theoreme limite central dans les espaces localiment convexes. *Probab/ sur les Studia Aigebr. CNKS.* Paris, 1990, P. 233–245.
13. Levy P. Processus stochastiques et mouvement Brownian. Paris Gauthier-Villars, 1948.

14. Mourier E. Propriétés des caractéristiques d'un élément aléatoire dans un espace de Banach. *AkedSn Paris*. 1950, Vol. 231, P. 28–25.
15. Mourier E. Éléments aléatoires dans un espace de Banach. *Ann. Inst. H. Poincaré*. 1953, P. 161–244.

Библиографические ссылки

- Вопросы математической теории надежности / Е. Ю. Барзилович, Ю. К. Беляев, В. А. Каштанов и др. М.: Радио и связь, 1983. 376 с.
- Беляев Ю. К., Дулина Т. Н., Чепурин Е. В. Вычисление нижней доверительной границы для вероятности безотказной работы сложных систем. Ч. 1 // Изв. АН СССР. Серия: Техническая кибернетика. 1967. № 2. С. 52–69.
- Беляев Ю. К., Дулина Т. Н., Чепурин Е. В. Вычисление нижней доверительной границы для вероятности безотказной работы сложных систем. Ч. 2 // Изв. АН СССР. Серия: Техническая кибернетика. 1967. № 3. С. 63–78.
- Бенткус В. Ю., Рачкаускас А. Ю. Оценки скорости сближения сумм независимых случайных величин в банаховом пространстве // Литовский мат. сб. 1982. Т. XXII, № 4. С. 8–20.
- Бенткус В. Ю., Рачкаускас А. Ю. Оценки скорости сближения сумм независимых случайных величин в банаховом пространстве // Литовский мат. сб. 1982. Т. XXII, № 3. С. 12–18.
- Araujo de A., Gine E. The central limit theorem for the Real and Banach Valued Random Variables. New York: John Wiley and Sons, 1980.
- Forter R., Mourier E. Les fonctions aléatoires dans les espaces de Banach // *Studia Math.* 1955. No. 15. P. 62–73.
- Gine E. On the central limit theorem for sample continuous processes. *Annales of Probability*. 1974. P. 62–73.
- Gine E., Marcus N. B. On the CLT in $C(K)$ // *Leet Notes Math.* 1969. Vol. 89. P. 62–73.
- Gotze F. On rate of convergence in central limit theorem in Banach spaces // *Annales of Probability*. 1976. Vol. XIV, No. 3. P. 852–859.
- Hoffman-Yorgensen Y., Pisier G. The law of large numbers and the central limit theorem in Banach spaces // *Annales of Probability*. 1974. Vol. 4. P. 587–599.
- Le Cam L. Remarques sur le théorème limite central dans les espaces localement convexes. *Probab. sur les Structures Algébriques*. CNRS. Paris. 1990. P. 233–245.
- Levy P. *Processus stochastiques et mouvement Brownien*. Paris: Gauthier-Villars. 1948.
- Mourier E. Propriétés des caractéristiques d'un élément aléatoire dans un espace de Banach // *AkedSn Paris*. 1950. Vol. 231. P. 28–25.
- Mourier E. Éléments aléatoires dans un espace de Banach. *Ann. Inst. H. Poincaré* 1953. P. 161–244.

© Shiryaeva T. A., Shlepkin A. K., Philippov K. A., Kolmakova Z. A., 2020

Shiryaeva Tamara Alekseevna – Cand. Sc., Professor; Krasnoyarsk State Agrarian University. E-mail: info@kgau.ru.

Shlepkin Anatoly Konstantinovich – Dr. Sc., Professor; Krasnoyarsk State Agrarian University. E-mail: ak_kgau@mail.ru.

Filippov Konstantin Anatolyevich – Dr. Sc., Professor; Krasnoyarsk State Agrarian University. E-mail: info@kgau.ru.

Kolmakova Zlata Anatolyevna – Cand. Sc.; Khakas State University. E-mail: kolzlata@yandex.ru.

Ширяева Тамара Алексеевна – кандидат физико-математических наук, доцент, доцент кафедры информационных технологий и математическое обеспечение информационных систем; Красноярский государственный аграрный университет. E-mail: info@kgau.ru.

Шлепкин Анатолий Константинович – доктор физико-математических наук, профессор, профессор кафедры высшей математики и компьютерного моделирования; КрасГАУ, Красноярский государственный аграрный университет. E-mail: ak_kgau@mail.ru.

Филиппов Константин Анатольевич – доктор физико-математических наук, доцент, профессор кафедры информационных технологий и математического обеспечения информационных систем; Красноярский государственный аграрный университет. E-mail: info@kgau.ru.

Колмакова Злата Анатольевна – кандидат педагогических наук, заместитель директора по учебной работе Инженерно-технологического института; Хакасский государственный университет имени М. Ф. Катанова. E-mail: kolzlata@yandex.ru.

UDC 519.711.3

Doi: 10.31772/2587-6066-2020-21-1-47-53

For citation: Yareshchenko D. I. About non-parametric identification of partial-parametred discrete-continuous process. *Siberian Journal of Science and Technology*. 2020, Vol. 21, No. 1, P. 47–53. Doi: 10.31772/2587-6066-2020-21-1-47-53

Для цитирования: Ярещенко Д. И. О непараметрической идентификации частично-параметризованного дискретно-непрерывного процесса // Сибирский журнал науки и технологий. 2020. Т. 21, № 1. С. 47–53. Doi: 10.31772/2587-6066-2020-21-1-47-53

ABOUT NON-PARAMETRIC IDENTIFICATION OF PARTIAL-PARAMETRED DISCRETE-CONTINUOUS PROCESS

D. I. Yareshchenko

Siberian Federal University
26/1, Akademika Kirenskogo St., Krasnoyarsk, 660074, Russian Federation
E-mail: YareshchenkoDI@yandex.ru

The paper considers a new class of models under conditions of incomplete information. We are talking about multi-dimensional discrete-continuous processes for the case where the components of the vector of output variables are stochastically dependent. The nature of this dependence is a priori unknown, but for some channels the a priori information corresponds to both nonparametric and parametric type of the initial data in the process under study. Such a situation leads to a system of nonlinear equations, some of which will be unknown, while others are known accurate to the vector of parameters.

The main purpose of the model is to determine the forecast of output variables with known input, and for implicit nonlinear equations it is only known that one or another component of the output depends on other variables that determine the state of the object.

Thus, a rather nontrivial situation arises when solving a system of implicit nonlinear equations under conditions where in one channel of a multidimensional system equations themselves are not in the usual sense, while in others they are known up to parameters. Therefore, an object model cannot be constructed using the methods of the existing identification theory as a result of a lack of a priori information. If it was possible to parameterize the system of nonlinear equations, then with a known input this system should be solved, since it is known and the parameterization stage is over. However, in this case it is still necessary to evaluate parameters. The main content of this article is the solution of the identification problem in the presence of a partially-parameterized discrete-continuous process, despite the fact that the parameterization stage cannot be overcome without additional a priori information on the process under study.

In this regard, the scheme for solving the system of nonlinear equations can be represented as a certain sequential algorithmic chain. First, on the basis of the available training sample, including all components of the input and output variables observation, a residual vector is formed. After that, an estimate of the object output with known values of the input variables is constructed based on the estimates of Nadarai-Watson. Thus, for given values of the input variables of such a process, it is proposed to carry out a procedure for evaluating the forecast of output variables in accordance with the developed algorithmic chain.

Numerous computational experiments, studying the proposed models of partially-parameterized discrete-continuous processes have shown their rather high efficiency. The article presents the results of computational experiments illustrating the effectiveness of the proposed technology for predicting values of output variables from known input variables.

Keywords: *partially parameterized discrete-continuous process, identification, nonparametric estimates, KT-models.*

О НЕПАРАМЕТРИЧЕСКОЙ ИДЕНТИФИКАЦИИ ЧАСТИЧНО-ПАРАМЕТРИЗОВАННОГО ДИСКРЕТНО-НЕПРЕРЫВНОГО ПРОЦЕССА

Д. И. Ярещенко

Сибирский федеральный университет
Российская Федерация, 660074, ул. Академика Киренского, 26, корп. 1
E-mail: YareshchenkoDI@yandex.ru

В работе рассматривается новый класс моделей в условиях неполной информации. Речь идет о многомерных дискретно-непрерывных процессах для случая, когда компоненты вектора выходных переменных стохастически зависимы, причем характер этой зависимости априори неизвестен, но по некоторым каналам апри-

орная информация соответствует одновременно как непараметрическому, так и параметрическому типу исходных данных об исследуемом процессе. Подобная ситуация приводит к системе нелинейных уравнений, одни из которых будут неизвестны, а другие известны с точностью до вектора параметров.

Главное назначение модели состоит в определении прогноза выходных переменных при известных входных, причем для неявных нелинейных уравнений известно лишь то, что та или иная компонента выхода зависит от других переменных, определяющих состояние объекта.

Таким образом, возникает довольно нетривиальная ситуация решения системы неявных нелинейных уравнений в условиях, когда по одним каналам многомерной системы самих уравнений в обычном смысле нет, а по другим они известны с точностью до параметров. Следовательно, модель объекта не может быть построена с помощью методов существующей теории идентификации в результате недостатка априорной информации. Если бы можно было параметризовать систему нелинейных уравнений, то при известном входе следовало бы решить эту систему, поскольку она в данном случае известна, раз этап параметризации преодолен, правда, в этом случае необходимо еще выполнить оценку параметров. Основным содержанием настоящей статьи является решение задачи идентификации при наличии частично-параметризованного дискретно-непрерывного процесса, при этом этап параметризации не может быть преодолен без дополнительной априорной информации об исследуемом процессе.

В этой связи схема решения системы нелинейных уравнений может быть представлена в виде некоторой последовательной алгоритмической цепочки. Сначала на основании имеющейся обучающей выборки, включающей наблюдения всех компонент входных и выходных переменных, формируется вектор невязок. А уже после этого оценка выхода объекта при известных значениях входных переменных строится на основании оценок Надарая – Ватсона. Таким образом, при заданных значениях входных переменных такого процесса предлагается осуществить процедуру оценивания прогноза выходных переменных в соответствии с разработанной алгоритмической цепочкой.

Многочисленные вычислительные эксперименты по исследованию предлагаемых моделей частично-параметризованных дискретно-непрерывных процессов показали достаточно высокую их эффективность. В статье приводятся результаты вычислительных экспериментов, иллюстрирующих эффективность предлагаемой технологии прогноза значений выходных переменных по известным входным.

Ключевые слова: частично-параметризованный дискретно-непрерывный процесс, идентификация, непараметрические оценки, КТ-модели.

Introduction. In numerous occasions for many technological, manufacturing, and multidimensional processes of a discrete-continuous nature, researchers are put in conditions where it is necessary to build a model of the process under study. These processes are dynamic in nature, but controlled at discrete intervals, including different ones, which results in dynamic processes to be seen as inertia-free with a time delay. For example, when grinding any materials (clinker, coal), the time constant is 5–10 minutes, and the control of the output variable, such as the fineness of grinding, is measured every two hours. In this case, the investigated process can be presented as inertia-free with delay [1].

Similar processes are often found in mining or processing industries, such as metallurgy (steel smelting), power industry (coal burning), construction (cement production), oil refining (diesel purification) [2], and social sciences, including education (student learning) [3].

However, the most interesting and important thing is that while researching different processes there is a class of processes that is classified as T-processes [1]. Similar processes have stochastic dependence of output variables and require alternative methods of identification and control, slightly different from conventional ones. The main thing here is that identification of such objects should be carried out applying non-traditional for the existing theory of identification methods [4]. It is also interesting for the cases where a priori information corresponds to both non-parametric and parametric types of raw data on the process under investigation. Such processes are classified as KT processes [1].

A special feature of KT-processes is that equations of relations between input and output variables with accuracy to the vector of parameters are known for some channels of the multidimensional system, but are not known for the other channels, causing the fact that the mathematical description of the object is presented in the form of some analogue of the system with partially parameterized $F_j(u, x, \alpha) = 0$, $j = \overline{1, n}$ and unknown functions with the view $F_j(u, x) = 0$, $j = \overline{1, n}$. Thus, the problem of identification is reduced to the problem of solving the system of nonlinear equations of a partially-parameterized discrete-continuous process with respect to vector components, and known values of input variables u . Specific identification tasks will diverge by different amount of a priori information on different channels, and by the features of ongoing processes. What is important here is that we have to face a system of different equations in terms of mathematics, the solution of which will require development of special methods. In this case, it is advisable to use methods of non-parametric statistics [5; 6].

KT-processes. Currently, the role of inertia-free systems with delay identification is increasing [7; 8]. This is because some of the most important dynamic object output variables are measured at long intervals of time, far exceeding the time constant of the object.

Let's consider a general scheme of a discrete-continuous process that functions under conditions of diverse a priori information, including non-parametric uncertainty, which is consistent with identification theory in a broad sense.

Let's consider a general scheme of a discrete-continuous process that functions under conditions of diverse a priori information, including non-parametric uncertainty, which is consistent with identification theory in a broad sense.

A feature of multidimensional object identification is that the process being investigated is described by a system with implicit stochastic equations.

$$F_j(u(t-\tau), x(t), \xi(t))=0, \quad j=\overline{1, n}, \quad (1)$$

Where on some channels $F_j(\cdot)$ are unknown, and on other channels are known, τ – on different channels of multidimensional system [1]. Further, for simplicity τ will be omitted.

In general view, the investigated multidimensional system implementing the KT process can be shown in fig. 1.

In fig. 1 the following symbols are set: $u=(u_1, \dots, u_m)$ – m -dimensional vector of input variables, $x=(x_1, \dots, x_n)$ – n -dimensional vector of output variables, $\xi(t)$ – random interference influencing the process, vertical arrows indicate stochastic dependence of output variables, arc arrows show internal connection between variables, which is characteristic of a specific investigated process. Clearly, the nature of some relations remains unknown to the researcher.

Through various channels of the process under study, the dependence of the j component of vector \mathbf{x} may be represented as some dependence on certain components of vector \mathbf{u} : $x^{<j>} = f_j(u^{<j>})$, $j=\overline{1, n}$. Such functions are determined by the researcher on the basis of available a priori information and are called a composite vector. A composite vector is a vector composed of some components of the corresponding vector, $u^{<j>}=(x_2, x_5, x_7, x_8)$ in particular. It may also be any other set, for example, $u^{<5>}=(u_1, u_3, u_6)$ where $u^{<5>}$ is a composite vector, or $x^{<3>}=(u_1, u_3, x_2)$. In this case, the system of equations becomes:

$$\begin{cases} F_1(u^{<j>}, x^{<j>}, \alpha)=0, \\ F_2(u^{<j>}, x^{<j>}, \alpha)=0, \\ \dots \\ F_{n-1}(u^{<j>}, x^{<j>})=0, \\ F_n(u^{<j>}, x^{<j>})=0. \end{cases} \quad j=\overline{1, n}, \quad (2)$$

where $\hat{F}_j(\cdot)$ partially parameterized or unknown, α is a vector of parameters.

KT-models. Multidimensional processes which output variables acquire unknown stochastic relationships were called T-processes, so their models are respectively called T-models [1]. K-models are based on the use of diverse a priori information across different channels of a multidimensional object.

A KT model combines T-model elements with K-model elements and is a model in which there is a set of relationships between input and output variables, where dependences are known through some channels, for example, by focusing on the laws of physics, but unknown in other channels.

The main feature of modeling such a process in conditions of non-parametric uncertainty is the fact that the type of functions $F_j(u^{<j>}, x^{<j>})=0$, $j=\overline{1, n}$ is known for one certain channel and unknown for another. Naturally, the model system can be presented as follows:

$$\begin{cases} \hat{F}_1(u^{<j>}, x^{<j>}, \hat{\alpha})=0; \\ \hat{F}_2(u^{<j>}, x^{<j>}, \hat{\alpha})=0; \\ \dots \\ \hat{F}_{n-1}(u^{<j>}, x^{<j>}, \hat{\alpha})=0; \\ \hat{F}_n(u^{<j>}, x^{<j>}, \hat{\alpha})=0. \end{cases} \quad j=\overline{1, n}, \quad (3)$$

where \bar{x}_s, \bar{u}_s – time vectors (a data set, obtained by s-time point), in particular $\bar{x}_s=(x_1, \dots, x_s)= (x_{11}, x_{12}, \dots, x_{1s}, \dots, x_{21}, x_{22}, \dots, x_{2s}, \dots, x_{n1}, x_{n2}, \dots, x_{ns})$, but in this case some $\hat{F}_j(\cdot)$, $j=\overline{1, n}$ remain unknown. Therefore, let's consider the task of constructing KT models under non-parametric uncertainty that is under conditions where the system (3) is known for some channels and is not accurately known for others.

So let the input of the object receive input variable values, which are certainly measured. The presence of a learning sample x_i, u_i , $i=\overline{1, s}$ is necessary. In this case, estimation of the components of the output variable vector at known values, as already mentioned above, causes the need to solve the system of equations (3).

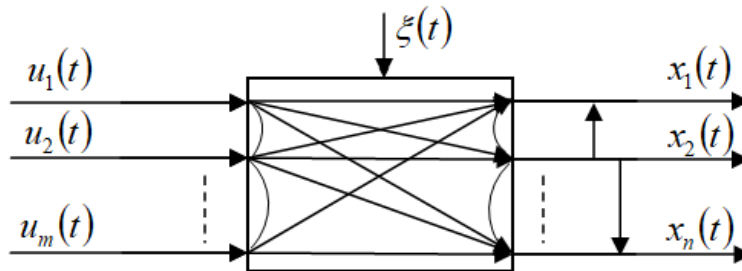


Fig. 1. Multidimensional system

Рис. 1. Многомерная система

In case the dependence of the output component on the component of the vector of input variables is not known, it is natural to use non-parametric estimation methods [9; 10].

The problem is that with a given value of the input variable vector $u = u'$, it is necessary to solve the system (3) with respect to the output variable vector x . For some channels of the multidimensional system, where equations accuracy within parameters is known, coefficients are found, for example, by the method of stochastic approximations [11]. For other channels where relations are unknown, the following algorithm chain [1] must be applied. First, inconsistencies are calculated by formula:

$$\varepsilon_{ij} = F_j(u^{<j>}, x^{<j>}(i), \bar{x}_s, \bar{u}_s), \quad j = \overline{1, n}, \quad (4)$$

where $F(u^{<j>}, x^{<j>}(i), \bar{x}_s, \bar{u}_s)$ is accepted as non-parametric estimates of Nadarai-Watson regression [12]:

$$\begin{aligned} \varepsilon_j(i) &= F_{ej}(u^{<j>}, x_j(i)) = \\ &= x_j(i) - \frac{\sum_{i=1}^s x_j[i] \prod_{k=1}^{<n>} \Phi\left(\frac{u'_k - u_k[i]}{c_{su_k}}\right)}{\sum_{i=1}^s \prod_{k=1}^{<n>} \Phi\left(\frac{u'_k - u_k[i]}{c_{su_k}}\right)}, \end{aligned} \quad (5)$$

where $j = \overline{1, n}$, $<m>$ – composite vector dimensions u_k . Bell curve function $\Phi\left(\frac{u'_k - u_k[i]}{c_{su_k}}\right)$ and blur parameter c_{su_k} comply with some convergence condition, so obtain the following:

$$\Phi(\cdot) < \infty; \quad c_s^{-1} \int_{\Omega(u)} \Phi(c_s^{-1}(u - u_i)) du = 1; \quad (6)$$

$$\begin{aligned} \lim_{s \rightarrow \infty} c_s^{-1} \Phi(c_s^{-1}(u - u_i)) &= \delta(u - u_i), \\ \lim_{s \rightarrow \infty} c_s &= 0, \quad \lim_{s \rightarrow \infty} s c_s = \infty. \end{aligned} \quad (7)$$

Next step is estimation of conditional mathematical expectation:

$$x_j = M\{x | u^{<j>}, \varepsilon = 0\}, \quad j = \overline{1, n}. \quad (8)$$

As estimate (8) we accept non-parametric estimate of Nadarai-Watson regression [12]:

$$\begin{aligned} \hat{x}_j &= \frac{\sum_{i=1}^s x_j[i] \cdot \prod_{k=1}^{<n>} \Phi\left(\frac{u_{k1} - u_{k1}[i]}{c_{su}}\right) \prod_{k_2=1}^{<m>} \Phi\left(\frac{\varepsilon_{k_2}[i]}{c_{se}}\right)}{\sum_{i=1}^s \prod_{k_1=1}^{<n>} \Phi\left(\frac{u_{k1} - u_{k1}[i]}{c_{su}}\right) \prod_{k_2=1}^{<m>} \Phi\left(\frac{\varepsilon_{k_2}[i]}{c_{se}}\right)}, \\ j &= \overline{1, n}, \end{aligned} \quad (9)$$

where bell curve $\Phi(\cdot)$ may be accepted in the form of triangular kernel (10) and (11), complying with the conditions (6), (7).

$$\Phi\left(\frac{u_{k1} - u_{k1}[i]}{c_{su}}\right) = \begin{cases} 1 - \frac{|u_{k1} - u_{k1}[i]|}{c_{su}}, & \frac{|u_{k1} - u_{k1}[i]|}{c_{su}} < 1, \\ 0, & \frac{|u_{k1} - u_{k1}[i]|}{c_{su}} \geq 1. \end{cases} \quad (10)$$

$$\Phi\left(\frac{\varepsilon_{k_2}[i]}{c_{se}}\right) = \begin{cases} 1 - \frac{|0 - \varepsilon_{k_2}[i]|}{c_{se}}, & \frac{|0 - \varepsilon_{k_2}[i]|}{c_{se}} < 1, \\ 0, & \frac{|0 - \varepsilon_{k_2}[i]|}{c_{se}} \geq 1. \end{cases} \quad (11)$$

Algorithms (5), (8) and (9) are an algorithm chain necessary to calculate the prediction of the components of the output vector under the known input components [1].

While carrying out this procedure, we obtain values of output variables x at input influences on the object $u = u'$, which is the main purpose of the desired model that can further be used in different control systems [9], including organizational systems [3].

The accuracy of the simulation is estimated by the following formula:

$$\delta = \frac{\sum_{i=1}^s |x_i - x_s(u_i)|}{\sum_{i=1}^s |x_i - \hat{x}|}, \quad (12)$$

where x_i – object observation, $x_s(u_i)$ – object output forecast, \hat{x} – average value for every vector component \bar{x} .

Computational experiment. An object with five input variables $u = (u_1, u_2, u_3, u_4, u_5)$, and three output variables $x = (x_1, x_2, x_3)$, was taken for the computational experiment. For this object, a sample of input and output variables was formed based on the system of equations of two parametric and one non-parametric channel. As a result, a learning sample was obtained \bar{u}_s, \bar{x}_s , where \bar{u}_s, \bar{x}_s are time vectors. If the task was to be solved for a real object, the learning sample would be formed as a result of measurements carried out by the available control means. In the case of stochastic dependence between output variables, it is natural to describe the process, for example, by the following system of equations:

$$\begin{cases} \hat{F}_{x1}(x_1, x_3, u_1, u_2, u_5) = 0; \\ \hat{F}_{x2}(x_1, x_2, u_4, u_5) = 0; \\ \hat{F}_{x3}(x_1, x_2, x_3, u_2, u_3, u_5) = 0. \end{cases} \quad (13)$$

Once a sample of observations has been obtained, it is possible to proceed with the task under study – to find the forecast of the values of the output variables x under the known input u . For the case where there was an equation dependency across the two channels, the coefficients were found applying the stochastic approximation method.

To begin with, the inconsistencies are calculated according to the procedure described above. Let us present the inconsistencies in the form of a system:

$$\begin{cases} \varepsilon_1(i) = \hat{F}_1(x_1^i, x_3^i, u_1^i, u_2^i, u_5^i); \\ \varepsilon_2(i) = \hat{F}_2(x_1^i, x_2^i, u_4^i, u_5^i); \\ \varepsilon_3(i) = \hat{F}_3(x_1^i, x_2^i, x_3^i, u_2^i, u_3^i, u_5^i). \end{cases} \quad (14)$$

where $\varepsilon_j, j=1,3$ – inconsistencies, for which corresponding components of the output vector cannot be obtained from parametrical equations.

Forecast for system (13) is performed according to formula (9) for each component of object output.

Input variables of newly generated input variables, i. e. not included in learning sample, are supplied to object input.

The tunable parameter will be the blur parameter, which in this case will be taken to be 0.4 (the value was

determined as a result of numerous experiments to reduce the quadratic error between the output of the model and the object) [13; 14], the blur parameter will be taken the same when counted in formulas (5) and (9), sample size $s = 2000$, interference $\xi = 0.07$. By component, we provide graphs for the object outputs x_1, x_2 and x_3 .

In fig. 2–4 ‘X’ shows the values of the variable output and the point of the model output. The figures demonstrate a comparison of the test sample output vector components true values and their predicted values obtained using algorithm (5)–(9). The figures show 20 sampling points due to the simplicity of results presentation, i. e. each one-hundred sampling point. The figures show that the model describes the object quite well at the interference of 7 % acting on the components of the output variables.

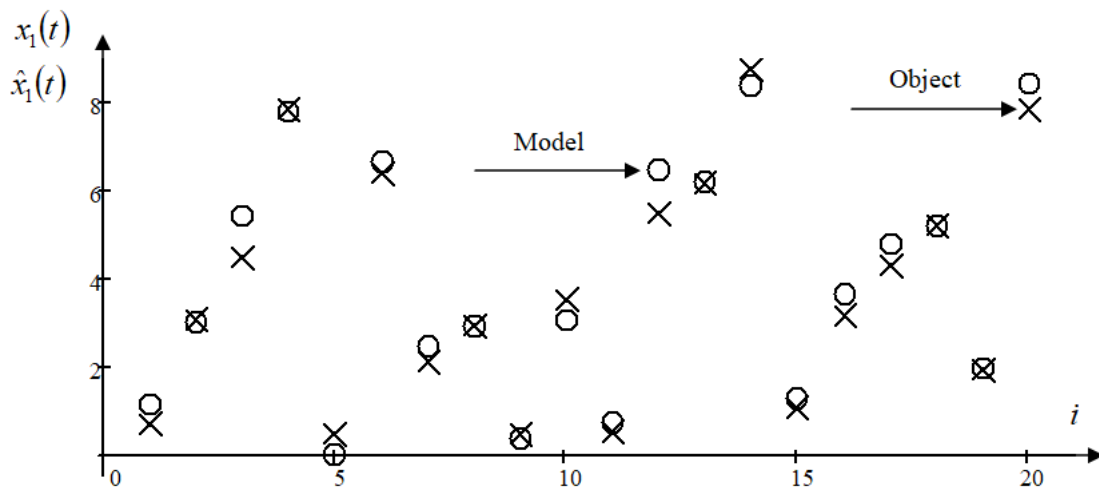


Fig. 2. Forecast values of the output variable x_1 with interference 7 %

Рис. 2. Прогнозные значения выходной переменной x_1 при помехе 7 %

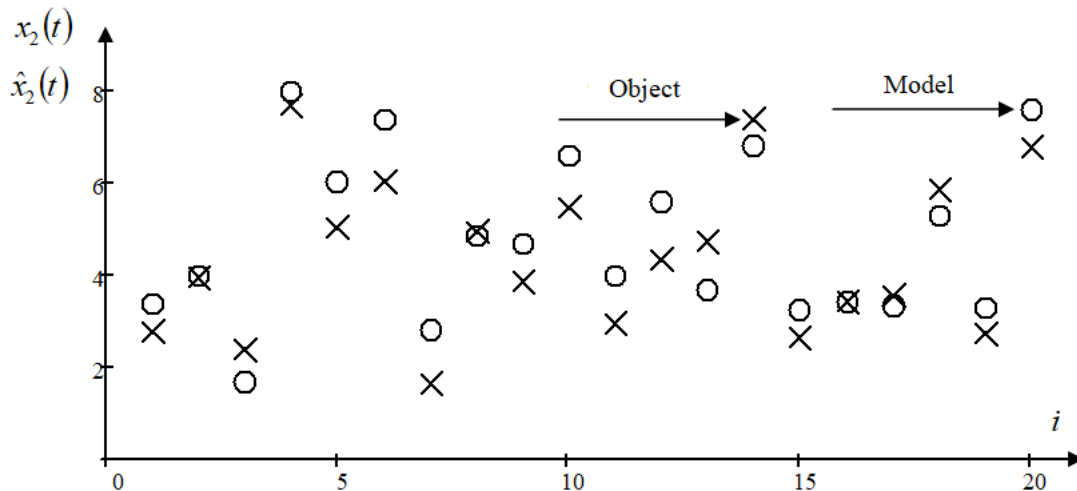
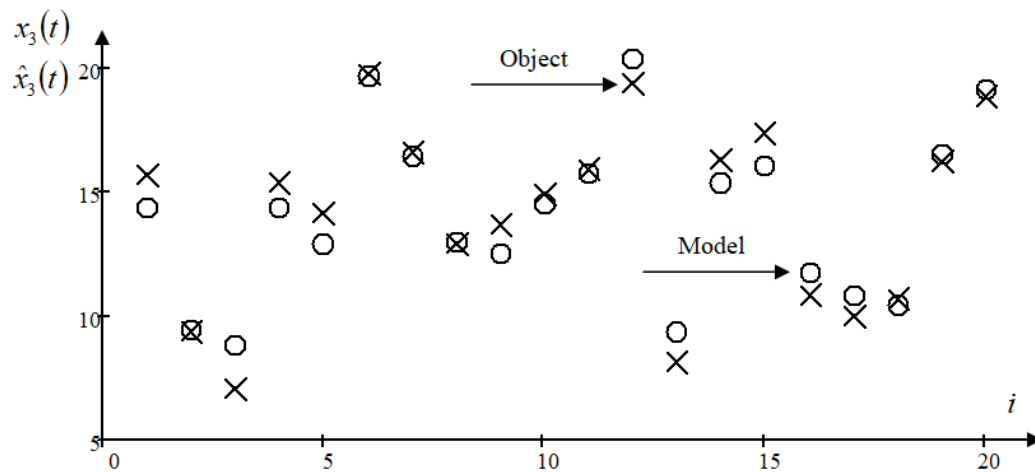


Fig. 3. Forecast values of the output variable x_2 with interference 7 %

Рис. 3. Прогнозные значения выходной переменной x_2 при помехе 7 %

Fig. 4. Forecast values of the output variable x_3 with interference 7 %Рис. 4. Прогнозные значения выходной переменной x_3 при помехе 7 %

In fig. 3, the prediction of the output variable is slightly worse than for the rest of the output variables, this may be affected by: the quality of the learning sample, the dependency of the variables, random interference, blur parameters, etc.

Conclusion. In the present work, the problem of identifying partially parameterized retarded multidimensional objects has been discussed. A number of features which appear include the fact that the identification task is considered in conditions of non-parametric uncertainty and, as a consequence, cannot be presented with precision to a set of parameters. Such processes can be well used in various control systems [15]. Based on the available a priori hypotheses, the system of equations describing the process is produced using composite vectors \mathbf{x} and \mathbf{u} . However, functions $F(\cdot)$ continue to be unknown for some channels. The article discusses the method of calculating output variables of an object with known input variables, which allows to use them in computer systems of various purposes.

It should also be noted that KT models have found their application in the actual catalytic hydrodeparaffinization process (or diesel purification process) and, as a result of computational experiments, have produced sufficiently satisfactory results [2].

Numerous computational experiments have shown quite satisfactory KT simulation results. Issues related to the introduction of different interferences, different volumes of learning samples were studied, as well as objects of different dimensions were investigated [4].

References

1. Medvedev A. V. *Osnovy teorii neparametricheskikh sistem. Identifikatsiya, upravlenie, prinyatie resheniy* [Fundamentals of the theory of nonparametric systems. Identification, management, decision making]. Krasnoyarsk, Reshetnev University Publ., 2018, 732 p.
2. Agafonov E. D., Medvedev A. V., Orlovskaya N. F., Sinyuta V. R., Yareshchenko D. I. *Prognoznaya model'*

prozessa kataliticheskoy gidrodeparafinizatsii v usloviyakh nedostatka apriornykh svedeniy [Predictive model of the process of catalytic hydrodewaxing in the absence of a priori information]. Tula, TulGU Publ., 2018, No. 9, P. 456–468 (In Russ.).

3. Medvedev A. V., Yareshchenko D. I. [About modeling of process of acquisition of knowledge by students at University]. *Vyshee obrazovanie segodnya*. 2017, No. 1, P. 7–10 (In Russ.).
4. Medvedev A. V., Yareshchenko D. I. [On non-parametric identification of T-processes]. *Siberian Journal of Science and Technology*. 2018, Vol. 19, No. 1, P. 37–44 (In Russ.).

5. Nadaraya E. A. *Neparametricheskoe ocenivanie plotnosti veroyatnostey i krivoy regressii* [Nonparametric estimation of probability density and regression curve]. Tbilisi, Tbilisskiy universitet Publ., 1983, 194 p.
6. Vasil'ev V. A., Dobrovidov A. V., Koshkin G. M. *Neparametricheskoe ocenivanie funktsionalov ot raspredeleniy stacionarnykh posledovatel'nostey* [Nonparametric estimation of functionals of stationary sequences distributions]. Moscow, Nauka Publ., 2004, 508 p.

7. Ehjkhoff P. *Osnovy identifikatsii sistem upravleniya* [Basics of identification of control systems]. Moscow, Mir Publ., 1975, 7 p.
8. Cypkin Ya. Z., *Osnovy informatsionnoy teorii identifikatsii* [Fundamentals of information theory of identification]. Moscow, Nauka Publ., 1984, 320 p.
9. Medvedev A. V. *Teoriya neparametricheskikh sistem. Upravlenie I* [The theory of non-parametric systems]. *Vestnik SibGAU*. 2010, No. 4 (30), P. 4–9 (In Russ.).

10. Medvedev A. V. *Neparametricheskie sistemy adaptatsii* [Nonparametric adaptation systems]. Novosibirsk, Nauka Publ., 1983, P. 173.
11. Cypkin Ya. Z. *Adaptatsiya i obuchenie v avtomaticheskikh sistemah* [Adaptation and training in automatic systems]. Moscow, Nauka Publ., 1968, 400 p.
12. Fel'dbaum A. A. *Osnovy teorii optimal'nykh avtomaticheskikh sistem* [Fundamentals of the theory of op-

timal automatic systems]. Moscow, Fizmatgiz Publ., 1963, P. 552.

13. Amosov N. M. *Modelirovanie slozhnyh system* [Modeling of complex systems]. Kiev, Naukova dumka Publ., 1968, 81 p.

14. Sovetov B. Ya., Yakovlev S. A. *Modelirovanie sistem: uchebnik dlya vuzov* [Modeling of systems]. Moscow, Vysshaya shkola, 2001, 343 p.

15. Antomonov Y. G., Harlamov V. I. *Kibernetika i zhizn'* [Cybernetics and life]. Moscow, Sov. Rossiya Publ., 1968, 327 p.

Библиографические ссылки

1. Медведев А. В. Основы теории непараметрических систем. Идентификация, управление, принятие решений : монография / СибГУ им. М. Ф. Решетнева. Красноярск, 2018. 732 с.

2. Прогнозная модель процесса каталитической гидродепарафинизации в условиях недостатка априорных сведений / Е. Д. Агафонов, А. В. Медведев, Н. Ф. Орловская и др. // Тула : ТулГУ, 2018. Вып. 9. С. 456–468.

3. Медведев А. В., Ярещенко Д. И. О моделировании процесса приобретения знаний студентами в университете // Высшее образование сегодня. 2017. Вып. 1. С. 7–10.

4. Медведев А. В., Ярещенко Д. И. О непараметрической идентификации Т-процессов // Сибирский журнал науки и технологий. 2018. Т. 19, № 1. С. 37–44.

5. Надарая Э. А. Непараметрическое оценивание плотности вероятностей и кривой регрессии. Тбилиси : Изд-во Тбилисского ун-та, 1983. 194 с.

6. Васильев В. А., Добровидов А. В., Кошкин Г. М. Непараметрическое оценивание функционалов от распределений стационарных последовательностей : отв. ред. Н. А. Кузнецов. М. : Наука, 2004. 508 с.

7. Эйкхофф П. Основы идентификации систем управления : пер. с англ. В. А. Лотоцкого, А. С. Манделя. М. : Мир, 1975. 7 с.

8. Цыпкин Я. З., Основы информационной теории идентификации. М. : Наука, 1984. 320 с.

9. Медведев А. В. Теория непараметрических систем. Управление 1 // Вестник СибГАУ. 2010. № 4 (30). С. 4–9.

10. Медведев А. В. Непараметрические системы адаптации. Новосибирск : Наука, 1983. 173 с.

11. Цыпкин Я. З. Адаптация и обучение в автоматических системах. М. : Наука, 1968. 400 с.

12. Фельдбаум А. А. Основы теории оптимальных автоматических систем. М. : Физматгиз, 1963. 552 с.

13. Амосов Н. М. Моделирование сложных систем. Киев : Наукова думка, 1968. 81 с.

14. Советов Б. Я., Яковлев С. А. Моделирование систем. М. : Высшая школа, 2001. 343 с.

15. Антомонов Ю. Г., Харламов В. И. Кибернетика и жизнь. М. : Сов. Россия, 1968. 327 с.


© Yareshchenko D. I., 2020

Yareshchenko Darya Igorevna – senior lecturer of the department Intelligent Control Systems, Siberian Federal University, Institute of Space and Information Technologies. E-mail: YareshchenkoDI@yandex.ru.

Ярещенко Дарья Игоревна – старший преподаватель кафедры интеллектуальных систем управления, Сибирский федеральный университет, Институт космических и информационных технологий. E-mail: YareshchenkoDI@yandex.ru.



РАЗДЕЛ
PART
2



АВИАЦИОННАЯ
И РАКЕТНО-
КОСМИЧЕСКАЯ ТЕХНИКА

AVIATION
AND SPACECRAFT
ENGINEERING



UDC 629.7.05

Doi: 10.31772/2587-6066-2020-21-1-56-61

For citation: Akzigitov A. R., Akzigitov R. A., Ogorodnikova U. V., Dmitriev D. V., Andronov A. S. Analysis of the ADS-B airspace monitoring system. *Siberian Journal of Science and Technology*. 2020, Vol. 21, No. 1, P. 56–61. Doi: 10.31772/2587-6066-2020-21-1-56-61

Для цитирования: Акзигитов А. Р., Акзигитов Р. А., Огородникова Ю. В., Дмитриев Д. В., Андронов А. С. Исследование системы мониторинга воздушного пространства ADS-B // Сибирский журнал науки и технологий. 2020. Т. 21, № 1. С. 56–61. Doi: 10.31772/2587-6066-2020-21-1-56-61

ANALYSIS OF THE ADS-B AIRSPACE MONITORING SYSTEM

A. R. Akzigitov, R. A. Akzigitov, U. V. Ogorodnikova, D. V. Dmitriev*, A. S. Andronov

Reshetnev Siberian State University of Science and Technology
31, Krasnoyarsky Rabochy Av., Krasnoyarsk, 660037, Russian Federation

*E-mail: gerundiy48@gmail.com

One of the most important aspects of flight safety is awareness of AC air position (AC is the short for aircraft). The leading method of stating AC airspace location is the use of radar systems – primary, secondary, combined primary – secondary surveillance radars-though radar systems have significant drawbacks. However, at present, more advanced technologies are also in use, for example, ADS-B and multilateration. This article is focused on ADS-B broadcasting. Global coverage, low cost, great amount of obtainable information makes Automatic Dependent Surveillance – Broadcast a highly efficient system. Application of the method for AC air positioning is equally effective for helicopters, especially for those operated by special emergency services. As for the infrastructure of air navigation, the research in this sphere is focused on surveillance systems necessary for reliable control of increasing air traffic. The problem of better awareness of AC air position is still acute and has always been the object of extensive research. At present, home-manufactured civil aviation helicopters are practically never equipped with ADS-B transponders, and hardly ever use the available resources of transceiver-based surveillance systems. The objective of the analysis presented is to demonstrate the applicability of Flightradar system options, as well as implementation of ADS – B transponders for helicopter fleet. Operating surveillance systems like Flightradar may considerably increase flight safety by improving the awareness of helicopters current air position.

Keywords: transponder, monitoring, aircraft (AC), aviation, flight safety, helicopter, airspace, control.

ИССЛЕДОВАНИЕ СИСТЕМЫ МОНИТОРИНГА ВОЗДУШНОГО ПРОСТРАНСТВА ADS-B

А. Р. Акзигитов, Р. А. Акзигитов, Ю. В. Огородникова, Д. В. Дмитриев*, А. С. Андронов

Сибирский государственный университет науки и технологий имени академика М. Ф. Решетнева
Российская Федерация, 660037, г. Красноярск, просп. им. газ. «Красноярский рабочий», 31

*E-mail: gerundiy48@gmail.com

Одним из важнейших аспектов в области безопасности полетов является осведомленность о местоположении воздушных судов (ВС). Основным методом определения местоположения ВС в пространстве является использование радарных систем: первичных, вторичных, совмещенных первично-вторичных обзорных радиолокаторов, но у радарных систем есть существенные недостатки. Однако сейчас используются и более современные технологии, например, такие как ADS-B и мультilaterация. В данной работе акцент будет нацелен на радиовещание ADS-B. Покрытие всей поверхности Земли, низкая стоимость, обширность предоставляемой информации делает автоматическое зависящее наблюдение – вещание крайне эффективной системой. Использование такого метода определения положения ВС является актуальным и для вертолетов, в особенности, состоящих в парке специальных служб. В области аэронавигационной инфраструктуры объектами исследования являются системы наблюдения, необходимые для безопасной организации растущих объемов воздушного движения. Проблема увеличения осведомленности местоположения ВС в пространстве является всегда актуальной и имеет обширное количество исследований в этой области. На данный момент отечественные вертолеты гражданской авиации практически не оснащаются ADS-B транспондерами, а также не используют доступные ресурсы следящей системы на базе этих приемопередатчиков. Целью исследования является обоснование применимости ресурсов системы Flightradar, а также оснащение парка вертолетов ADS-B транспондерами. Применение следящей системы, такой как Flightradar, позволит значительно увеличить безопасность полетов путем улучшения осведомленности о движении вертолетов в пространстве.

Ключевые слова: транспондер, мониторинг, ВС, авиация, безопасность полетов, вертолет, воздушное пространство, контроль.

Introduction. The awareness of AC air position is one of the most important aspects of flight safety. The leading method for AC air positioning is the use of radar systems: primary, secondary, combined primary – secondary surveillance radars, regardless of significant drawbacks of these systems [1; 2]:

- 1) No coverage of vast water areas and polar regions of the Earth.
- 2) No built-in mechanism for detecting invalid data in request or response signals.
- 3) The accuracy parameters are limited by the delay tolerance of the transponder, making the system unsuitable for aerodrome monitoring.
- 4) The high cost of radars hampers their promotion in hard-to-reach regions.

However, there are such advanced technologies as ADS-B and multilateration. In the article, the main object of analysis is ADS-B radio broadcasting. Its characteristics – coverage of the entire globe, low cost, the amount of provided information – make automatic dependent surveillance-broadcast a highly efficient system. This AC air positioning method is also applicable for helicopters, in particular, for emergency helicopter fleet. This allows effective monitoring of helicopters operated in hard-to-reach areas, as well as carrying out efficient rescue operations [3].

When used for air-to-ground surveillance, ADS-B offers significant advantages in the way of flight safety compared to procedural air traffic control without radar surveillance. ADS-B data can be used in application of such automatic safety tools as short-term conflict-warning signals, ATC instructions of keeping the cleared flight level, of keeping to the routing line, warnings of entering the danger area – all these increase the level of flight safety and airspace security. With the surveillance equipment, the air traffic controller has a much better picture of the environment [4; 5].

Mathematical method. Operation of Flightradar system is based on the map showing the planes that are currently airborne.

ADS-B functions demonstrate application of various methods and frequencies, in particular, the extended 1090 MHz squitter, as well as the universal access transceiver (UAT) (978 MHz) and a VHF digital link (VDL) of mode 4 (118–137 MHz).

Considering that ADS-B messages are radio-transmitted, they can be read and processed by any suitable receiver. Consequently, ADS-B is able to support both the ground function and the ASA function.

To receive and process ADS-B messages, ground surveillance stations are set up. In case of on-board versions, aircraft equipped with ADS-B receivers can process messages from other aircraft in order to determine their air position [6].

Attitude and speed data are transmitted twice per second. The aircraft identifying code is transmitted every five seconds. The ADS-B extended squitter (ES) transmission is integrated in many S-mode transponders, although that can also be performed by a transponder without the S mode. This analysis below concerns the introduction of certain technical solutions for the systems of AC monitoring in flight, with subsequent assessment of the performed modernization. The methods of carrying out AC modernization, the validity of decisions, the efficiency assessment are presented in the form of recommendations.

The radar refresh rate is one message in 4 s, the ADS-B rate – 0.5 s, and the RTK – 0.2 s. So, within the same time interval, more messages will be transmitted through the RTK than by means of the radar and the ADS-B, and radar messages will be least frequent [7; 8].

The data must be synchronized in order to obtain the accuracy of radar and ADS-B, and to compare the performance of radar and ADS-B. For this, the asynchronous multi-surveillance data must be extrapolated to keep pace with each other. The synchronization progress of ADS-B, radar and RTK is shown in fig. 1.

First, it should be noted that the time is just the same for the ADS-B data, the radar data, and the basic data.

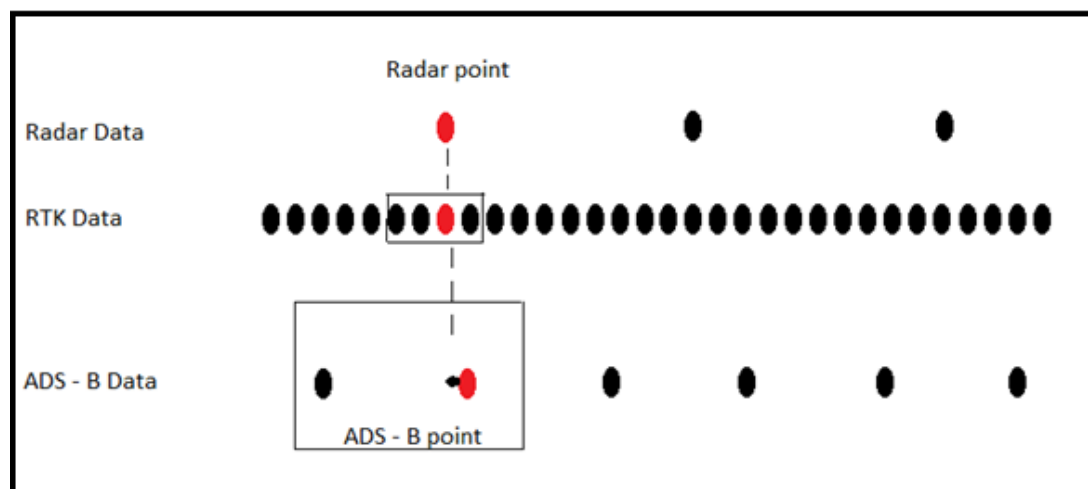


Fig. 1 The ADS-B, radar and RTK data synchronization progress

Рис. 1 Прогресс синхронизации ADS-B, РЛС и РТК

Then one can process the rest of the ADS-B data, the radar data and the basic data, so that they all are synchronized. Then, the following steps are performed [9]:

1) For the radar data, the reference time registered in the radar data is extracted, and the time T1 is marked.

2) The reference time registered in the initial data as the closest to T1 is extracted, and marked as T2.

3) Then, the location message (LA1, LO1), velocity message (V1) and heading message (H1) from T1-related radar data are received. The heading is determined as the angle between the AC flight direction and the true north heading, and H1 is taken from the radar messages of the radar station. This initially results from calculating the angle between the target and the antenna beam guidance.

4) This way, an extrapolated message of location (LA1E, LO1E) related to (LA1, LO1), V1 and H1 can be obtained.

The expressions are as follows:

$$\begin{cases} LA1E = LA1 + (T_2 - T_1)V_1 \cos H_1, \\ LO1E = LO1 + (T_2 - T_1)V_1 \sin H_1. \end{cases} \quad (1)$$

5) Further, the reference time registered in the ADS-B data as the closest to T2 is extracted, and marked as T3.

6) Then, the data on location (LA3, LO3), velocity (V3), and heading (H3) related to T3 are received from the ADS-B. H3 is taken from the ADS-B messages supplied by the station. Initially it was obtained from the navigation data source, and it is more accurate than the radar data.

7) An extrapolated message of location (LA3E, LO3E) related to (LA3, LO3), V3 and H3 can be obtained.

The expressions are as follows:

$$\begin{cases} LA3E = LA3 + (T_2 - T_3)V_3 \cos H_3, \\ LO3E = LO3 + (T_2 - T_3)V_3 \sin H_3. \end{cases} \quad (2)$$

In the radar data, the location message is expressed in polar coordinates, and the ADS-B data location message is expressed in WGS-84 coordinates. To compare the ADS-B data and the radar data, it is necessary to convert the polar coordinates to WGS-84 coordinates [10]. The conversion method presumes that, first, the oblique range, deviation angle and altitude are extracted from the radar data; next, the relative longitude and latitude of the radar station is calculated; finally, the sought longitude and latitude are obtained by adding relative longitude and latitude to the longitude and latitude of the radar station.

It is assumed that (φ, η) represent the longitude and latitude of the radar station, (latitude, longitude) are the latitude and longitude of the plane, (α, β) are the relative longitude and latitude of the radar station, h is the level of the plane, r is the oblique range, and θ is the deviation angle.

Transformation expression for latitude:

$$\begin{cases} \sqrt{r^2 - h^2} \cdot \cos \theta = R \cdot (\alpha \cdot \frac{\pi}{180}), \\ latitude = \alpha + \varphi. \end{cases} \quad (3)$$

Transformation expression for longitude:

$$\begin{cases} \sqrt{r^2 - h^2} \cdot \sin \theta = R \cdot \cos(latitude) \cdot (\beta \cdot \frac{\pi}{180}); \\ longitude = \beta + \eta. \end{cases} \quad (4)$$

It becomes obvious that the error between the position derived from the above expressions and the actual position is considerable, because the Earth is regarded as perfectly spherical, regardless of the problem of its eccentricity (the Earth is actually an ellipse). Hence, we improve the method [11; 12]:

1) The Earth coordinates issued by the radar station are converted to the Earth-centered and fixed (ECEF) coordinates;

2) The oblique range, deviation angle and altitude are extracted from the radar data in order to calculate the Cartesian coordinates of the plane;

3) the Cartesian coordinates of the plane are converted to ECEF coordinates;

4) the ECEF coordinates are converted to WGS-84 coordinates.

The expressions for making these conversions are as follows:

1) Expressions for converting the Earth coordinates to ECEF coordinates:

$$\begin{cases} x_r = (c + H_r) \cos L_r \cos \lambda_r; \\ y_r = (c + H_r) \cos L_r \sin \lambda_r; \\ z_r = (c(1 - e^2) + H_r) \sin L_r, \end{cases} \quad (5)$$

where (L_r, λ_r, H_r) – Earth coordinates of the station radar; (x_r, y_r, z_r) – ECEF coordinates; e – oblique range

$$c = \frac{E_q}{\sqrt{1 - e^2 \sin(2L)}} \quad (6)$$

where E_q – Earth radius.

2) Expressions for converting polar coordinates to Cartesian coordinates:

$$\begin{cases} x_n = r \cos \eta \cos \theta; \\ y_n = r \cos \eta \sin \theta; \\ z_n = r \cos \eta, \end{cases} \quad (7)$$

where (r, θ, η) – polar coordinates of the plane; (x_n, y_n, z_n) – Cartesian coordinates.

3) Expressions for converting Cartesian coordinates to ECEF coordinates:

$$\begin{cases} X_{rt}(k) = X_r + R X_{rl}(k); \\ R = \begin{bmatrix} -\sin \lambda_r & -\sin \lambda_r \cos L_r & \cos L_r \cos \lambda_r \\ \cos \lambda_r & -\sin L_r \sin \lambda_r & \cos L_r \sin \lambda_r \\ 0 & \cos L_r & \sin L_r \end{bmatrix}; \\ x_{rt}(k) = [x_{rt}(k) y_{rt}(k) z_{rt}(k)]^T; \\ x_r = [x_r y_r z_r]^T. \end{cases} \quad (8)$$

where $X_{rt}(k)$ – ECEF coordinates of the plane; $X_{rl}(k)$ – Cartesian coordinates of the plane; x_r – ECEF coordinates of the radar station; L_r, λ_r – longitude and latitude of the radar station.

4) Expressions of ECE coordinates through Earth coordinates:

$$\begin{cases} r = \sqrt{x^2 + y^2}; \\ a = (r^2 - A^2 e^4) / (1 - e^2); \\ b = (r^2 - A^2 e^4) / (1 - e^2); \\ q = 1 + 13.5z^2(a^2 - b^2) / (z^2 - b)^2; \\ p = \sqrt[3]{q + \sqrt{q^2 - 1}}; \\ t = (z^2 + b)(p + p^{-1}) / 12 - b / 6 + z^2 / 12; \\ L = \arctg \left\{ [z / 2 + \sqrt{t} + \sqrt{z^2 / 4 - b / 2 - t + az / (4\sqrt{t})}] / r \right\}; \\ \lambda = 2 \arctg[(\sqrt{x^2 + y^2} - x) / y], \end{cases} \quad (9)$$

where (x, y, z) – ECEF coordinates of the plane; (L, λ, H) – Earth coordinates of the plane; A – Earth semi-axis.

Accuracy assessment. To assess accuracy, taking the radar and the reference point data of the same time, we can obtain the distances between the synchronized ADS-B and the reference point data, and the distance between the synchronized radar and the reference point data. From the results of three flight tests performed, we can obtain the data presented in fig. 2.

The X coordinate is the error packet, and the Y coordinate is the percentage of the message. The ADS-B data are shown in blue and radar data – in red. Obviously, the ADS-B message volume is greater than that of the radar in a limited error packet, and it is less in a larger error packet, so we can conclude that the accuracy of the ADS-B data is higher than that of the radar data [13].

To present the ADS-B system in a more illustrative way, certain researches of Chinese scientists were taken

as the source of data. Observations were performed at Chengdu ground station.

Accumulation of ADS-B data reports from Chengdu ADS-B ground station for flight tests helps to determine the NUC distribution. As well, in case of collecting the ADS-B reports from Chengdu ADS-B ground station for about 40 days, we can determine the NUC distribution shown in fig. 3.

The number of reports received from Chengdu ADS-B ground station amounts to 41,776,974. The x-coordinate shows the value of NUC, and the y-coordinate – the percentage of the message. The red bar indicates a report that cannot meet the requirements of the radar service, and the green bar indicates a report that meets these requirements [14]. Chengdu ADS-B ground station data integrity assessment is presented in fig. 4. Most reports where NUC is larger than 4 comply with the requirements of the radar service, and most of the messages with NUC being 6 and 7 are of high quality.

Conclusion. For Russia, it is especially important to apply ADS-B for helicopters of the Ministry of Emergency Situations. This will improve the efficiency of rescue operations, awareness of the aircraft operation in remote areas. For example, in Canada and the United States, oil companies actively use ADS-B – equipped helicopters for flights to offshore oil rigs; the same is quite acceptable for Russian distant oil platforms [15].

The above-presented method meets most requirements. Using Flightradar surveillance system will increase flight safety. When the system employs ADS-B transmitters, the coverage area extension becomes incomparably cheaper than the cost of deploying radars. As the installation of transmitters in helicopters presents no difficulty, the improvement can be made without significant engineering changes.

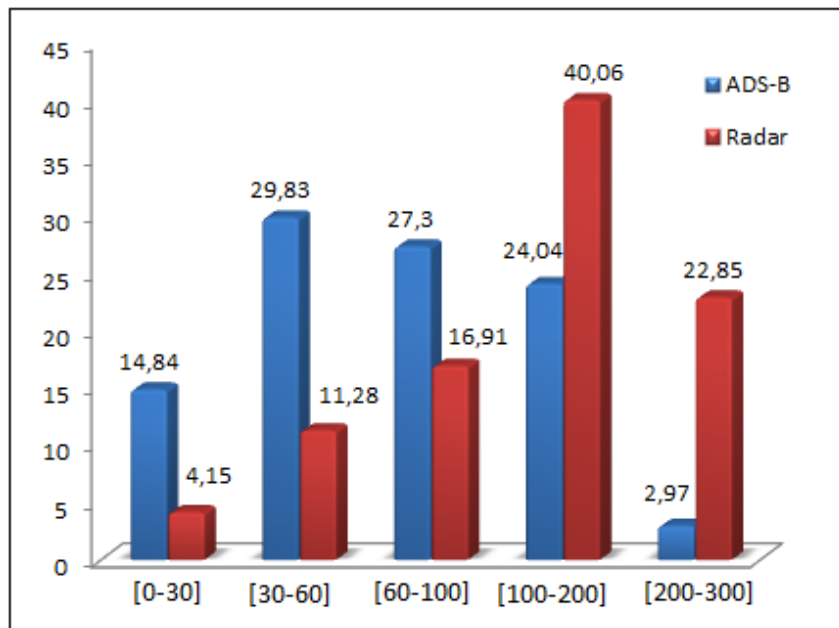


Fig. 2. The results of the accuracy evaluation of the ADS-B data in three flight tests

Рис. 2. Результаты оценки точности данных ADS-B в трех летных испытаниях

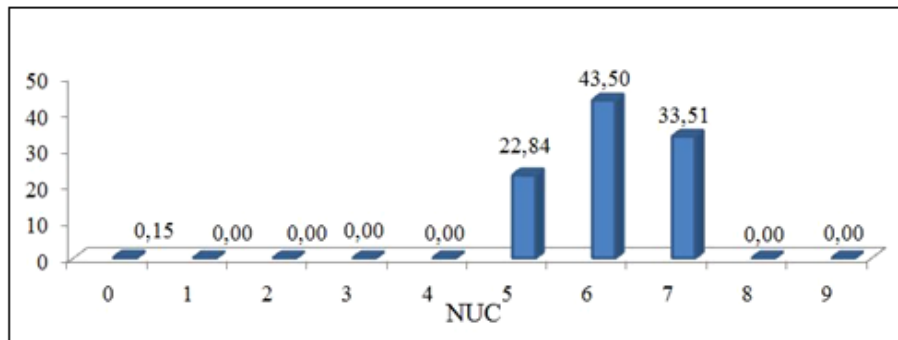


Fig. 3 Assessment of ADS-B data integrity

Рис. 3. Оценка целостности данных ADS-B

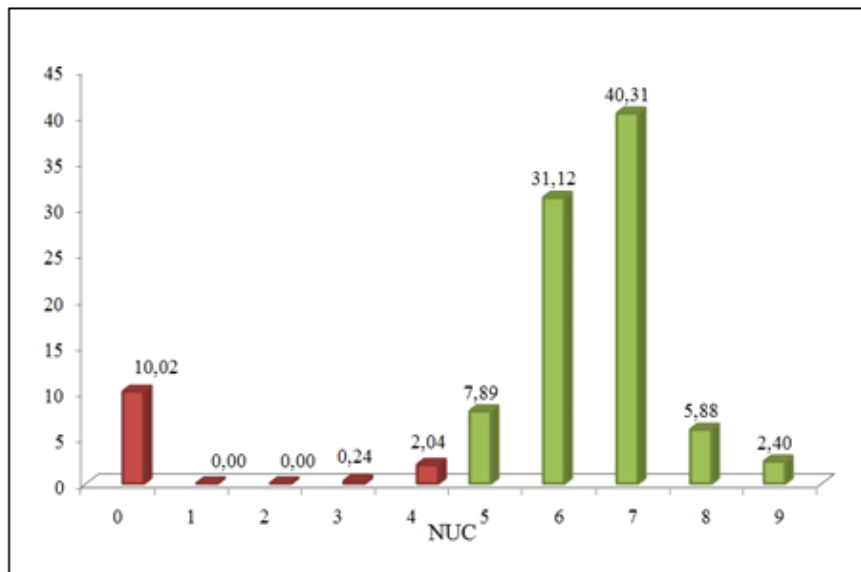


Fig. 4. Assessment of ADS-B data integrity (data of Chengdu ground station)

Рис. 4. Оценка целостности данных ADS-B наземной станции в Чэнду

The efficiency of the surveillance system is substantiated by the given comparative analysis. The general part is a review of the Flightradar system and the basic ADS-B transponder it employs; there is also a review of alternate data sources that can be processed by this surveillance system.

References

1. Lachapelle G. Navigation Accuracy for Absolute Positioning, AGARD Lecture Series 207. *System Implications and Innovative Applications of Satellite Navigation*. NATO, 1996, P. 4.1–4.10.
2. Kartsan I. N. [Method of positioning errors elimination along with operating navigation systems]. *Vestnik SibGAU*. 2008, No. 3 (20), P. 101–103 (In Russ.).
3. Weston J. L. Basic Principles of Strapdown Inertial Navigation Systems. Strapdown Inertial Navigation Technology. *Radar, sonar, navigation and avionics*. 2004. Ch. 3. P. 17–59.
4. Bochkarev V. V., Kryzhanovskiy G. A., Sukhikh N. N. *Avtomatizirovannoe upravlenie dvizheniem aviatsionnogo transporta* [Automated control of air traffic]. Moscow, Transport Publ., 1999, 319 p.
5. Tanjila F. Performance Analysis of Low Earth Orbit (LEO). Satellite Link in the presence of Elevation Angle, Fading, And Shadowing. Bangladesh, BRAC University Publ., 2009, 66 p.
6. Minimum operational performance standards for air traffic control radar beacon system/modeselect (atcrbs/mode S). *Airborne equipment*. 2008, Vol. 1.6, 534 p.
7. Mohammad A. Ayoubi, Aircraft ADS-B Data Integrity Check. *Conference paper*. 2004, P. 12.
8. Dunstone G. ADS-B Technology basics. *Surveillance Program Lead Airservices*. Australia, 2010, P. 33.
9. Sukkarieh S. Low Cost, High Integrity Aided Inertial Navigation Systems For Autonomous Land Vehicles. Ph. D. Thesis Univ. of Sydney. 2000, 136 p.
10. Jun Zh., Wei L. Study of ADS-B Data Evolution. *Chinese Journal of Aeronautics*. 2011, P. 6.

11. Jun Zh., Wei L., Yanbo Zh. *Chinese Journal of Aeronautics*. 2011, Vol. 24, Iss. 4, P. 461–466.
12. Orlando V. ADS-B 1090 MOPS. Revision A. 2002, 74 p.
13. Nesenjuk L. P., Fateev Yu. L., Barinov S. P. [Integrated inertial satellite system of orientation and navigation with spaced receiving antennae]. *Giroskopiya i navigatsiya*. 2000, No. 4 (31), P. 41–49 (In Russ.).
14. Tony Delovski. ADS-B over satellite. The World's first ADS-B receiver in space. *Conference paper*. May 2014, P. 17.
15. *Demodulyator signala ADS-B* [Demodulator of ADS-B signal]. Available at: <https://github.com/chenggiant/dump1090-matlab> (accessed: 10.11.2019).
- gle, Fading, And Shadowing. Bangladesh : BRAC University publ., 2009. 66 p.
6. Minimum operational performance standards for air traffic control radar beacon sestem/modeselect (atcrbs/mode S) // *Airborne equipment*. 2008. Vol. 1.6. P. 534.
7. Mohammad A. Ayoubi, Aircraft ADS-B Data Integrity Check // *Conference paper*. 2004. 12 p.
8. Dunstone G. ADS-B Technology basics. Surveillance Program Lead Airservices. Australia, 2010. P. 33.
9. Sukkarieh S. Low Cost, High Integrity Aided Inertial Navigation Systems For Autonomous Land Vehicles : Ph. D. Thesis Univ. of Sydney. 2000. P. 136.
10. Jun Zh., Wei L. Study of ADS-B Data Evulation // *Chinese Journal of Aeronautics*. 2011. Vol. ??? P. 6.
11. Jun Zh., Wei L., Yanbo Zh. **Название статьи?** // *Chinese Journal of Aeronautics*. 2011. Vol. 24, Iss. 4. P. 461–466.
12. Orlando V. ADS-B 1090 MOPS. Revision A. 2002. P. 74.
13. Интегрированная инерциальная спутниковая система ориентации и навигации с разнесенными приемными антеннами / Л. П. Несенюк [и др.] // *Гироскопия и навиагация*. 2000. № 4 (31). С. 41–49.
14. Tony Delovski ADS-B over satellite. The World's first ADS-B receiver in space // *Conferencepaper*. May 2014. P. 17.
15. Демодуляторсигнала ADS-B [Электронный ре-супс]. URL: <https://github.com/chenggiant/dump1090-matlab> (дата обращения: 10.11.2019).

Библиографические ссылки

1. Lachapelle G. Navigation Accuracy for Absolute Positioning, AGARD Lecture Series 207, *System Implications and Innovative Applications of Satellite Navigation*. NATO, 1996. P. 4.1–4.10.
2. Карцан И. Н. Метод исключения ошибок определения местоположения при одновременном использовании навигационных систем // *Вестник СибГАУ*. 2008. № 3 (20). С. 101–103.
3. Weston J. L. Basic Principles Lf Strapdown Inertial Navigation Systems. *Strapdown Inertial Navigation Technology*. 2nd ed. // Radar, sonar, navigation and avionics. 2004. Ch. 3. С. 17–59.
4. Бочкарев В. В., Крыжановский Г. А., Сухих Н. Н. Автоматизированное управление движением авиационного транспорта. М. : Транспорт, 1999. 319 с.
5. Tanjila F. Performance Analysis of Low Earth Orbit (LEO) *Satellite Link in the presence of Elevation An-*
- © Akzigitov A. R., Akzigitov R. A., Ogorodnikova U. V., Dmitriev D. V., Andronov A. S., 2020

Akzigitov Artur Revovich – senior professor, lecturer; Reshetnev Siberian State University of Science and Technology. E-mail: aakzigitov88@mail.ru.

Akzigitov Revo Avkhadiyevich – docent, acting director of the Institute of civil aviation and customs affair; Reshetnev Siberian State University of Science and Technology. E-mail: akzigitov-r@mail.ru.

Ogorodnikova Yulia Vladimirovna – student; Reshetnev Siberian State University of Science and Technology. E-mail: grand_espada24@mail.ru.

Dmitriev Danil Vadimovich – student; Reshetnev Siberian State University of Science and Technology. E-mail: gerundiy48@gmail.com.

Andronov Aleksandr Sergeyevich – postgraduate student; Reshetnev Siberian State University of Science and Technology. E-mail: pnk-sibsau@mail.ru.

Акзигитов Артур Ревович – старший преподаватель, преподаватель; Сибирский государственный университет науки и технологий имени академика М. Ф. Решетнева, кафедра ПНК. E-mail: aakzigitov88@mail.ru.

Акзигитов Рево Авхадиевич – доцент; и.о. директора ИГАиТД; Сибирский государственный университет науки и технологий имени академика М. Ф. Решетнева, кафедра ПНК. E-mail: akzigitov-r@mail.ru.

Огородникова Юлия Владимировна – студент; Сибирский государственный университет науки и технологий имени академика М. Ф. Решетнева, кафедра ТЭЛАД. E-mail: grand_espada24@mail.ru.

Дмитриев Данил Вадимович – студент; Сибирский государственный университет науки и технологий имени академика М. Ф. Решетнева, кафедра ПНК. Email: gerundiy48@gmail.com.

Андронов Александр Сергеевич – аспирант; Сибирский государственный университет науки и технологий имени академика М. Ф. Решетнева, кафедра ПНК. E-mail: pnk-sibsau@mail.ru.

UDC 621.45.018.2

Doi: 10.31772/2587-6066-2020-21-1-62-69

For citation: Begishev A. M., Zhuravlev V. Y., Torgashin A. S. Features and modernization methods of thrust measurement devices for liquid rocket engine test stands. *Siberian Journal of Science and Technology*. 2020, Vol. 21, No. 1, P. 62–69. Doi: 10.31772/2587-6066-2020-21-1-62-69

Для цитирования: Бегисhev А. М., Журавлев В. Ю., Торгашин А. С. Особенности и возможный путь модернизации силоизмерительных устройств испытательных стендов жидкостных ракетных двигателей // Сибирский журнал науки и технологий. 2020. Т. 21, № 1. С. 62–69. Doi: 10.31772/2587-6066-2020-21-1-62-69

FEATURES AND MODERNIZATION METHODS OF THRUST MEASUREMENT DEVICES FOR LIQUID ROCKET ENGINE TEST STANDS

A. M. Begishev*, V. Y. Zhuravlev, A. S. Torgashin

Reshetnev Siberian State University of Science and Technology
31, Krasnoyarsky Rabochny Av., Krasnoyarsk, 660037, Russian Federation

*E-mail alex-beg95@mail.ru

During the liquid rocket engines (LRE) testing, direct thrust measurement is carried out using thrust measurement devices. The aim of the work was, on the basis of existing data from the theory of tests and test stands devices, to highlight the design features of the thrust measurement devices and propose an option to improve the performance of this stand system. The work considers the basic circuit power schemes of thrust measurement devices by the example of power measuring systems of existing fire test stands and the features of work on preparing systems for testing. The types of calibration systems worked out in practice, their advantages and disadvantages, which constitute calibration errors, are considered. An option is proposed to modernize thrust measurement devices, in particular, through implementing of an electromechanical drive based on a planetary roller-screw mechanism as a force setting element into the calibration system. A possible general conceptual diagram of the power drive operation as a part of the calibration system of the thrust measurement devices is given. The advantages and disadvantages, the predicted effects of implementation are considered.

A more detailed analysis of this proposal may serve as an occasion for the modernization of the specific operational thrust measurement devices design at the fire test stand for LREs or may be a working option when designing a new thrust measurement device

Keywords: fire test stand, thrust measurement device, calibration system, electromechanical drive.

ОСОБЕННОСТИ И ВОЗМОЖНЫЙ ПУТЬ МОДЕРНИЗАЦИИ СИЛОИЗМЕРИТЕЛЬНЫХ УСТРОЙСТВ ИСПЫТАТЕЛЬНЫХ СТЕНДОВ ЖИДКОСТНЫХ РАКЕТНЫХ ДВИГАТЕЛЕЙ

А. М. Бегисhev*, В. Ю. Журавлев, А. С. Торгашин

Сибирский государственный университет науки и технологий имени академика М. Ф. Решетнева
Российская Федерация, 660037, г. Красноярск, просп. им. газ. «Красноярский рабочий», 31

*E-mail alex-beg95@mail.ru

В процессе испытания жидкостных ракетных двигателей (ЖРД) прямое измерение тяги осуществляется с помощью силоизмерительных устройств (СИУ). Целью работы было на основе существующих данных из теории огневых испытаний и устройств испытательных стендов выделить особенности конструкций СИУ и предложить вариант по улучшению работы данной стендовой системы. В работе рассмотрены основные принципиальные силовые схемы СИУ на примере силоизмерительных систем действующих огневых испытательных стендов ЖРД, а также рассмотрены особенности работ по подготовке системы силоизмерения к испытанию. Рассмотрены типы отработанных в практике градуировочных систем, их достоинства и недостатки, составляющие погрешности градуировки. Предложен вариант модернизации СИУ, в частности, внедрение в градуировочную систему в качестве силозадающего элемента электромеханического привода на базе планетарного роliko-винтового механизма (ПРВМ). Приведена возможная общая концептуальная схема работы силового привода в составе градуировочной системы СИУ. Рассмотрены достоинства и недостатки, прогнозируемые эффекты внедрения.

Более детальный анализ данного предложения может послужить поводом для модернизации конструкции того или иного конкретного действующего СИУ на огневом стенде испытания ЖРД или же явиться рабочим вариантом при проектировании нового СИУ.

Ключевые слова: испытательный стенд ЖРД, силоизмерительное устройство, градуировочная система, электромеханический привод.

Introduction. The rapid development of rocket and space technology entails the emergence of features that directly influence the reliability of the product at all stages of its life cycle. One of the most important final stages of serial or prototype production is the stage of rocket and space equipment ground testing. This stage of production makes it possible to determine the quantitative and (or) qualitative characteristics of a product, to assess the correctness of the adopted technical solutions in the design and manufacturing process, as well as to identify the type and the nature of product destruction in the event of an emergency test output.

The LREs and their units undergo ground testing at various stages of production but firing tests (i.e. the process of an engine comprehensive simulation) are the final and determining type of tests. The purpose of static firing tests is autonomous engine testing and in the case of flight firing tests all systems of the aircraft on which the engine is installed are checked [1].

The cost of the flight and static firing tests varies widely hence, flight tests are only the final stage of prototype development and the final conclusion on the compliance of this LRE construction with technical specifications and its suitability for serial production is given based on the test results [2]. The stage of firing tests represents a large amount of tests that the engine undergoes during the design and manufacturing process and therefore, the stage includes a whole range of questions: from the decision to adjust the design of the prototype engine during development tests to ensure output quality control of serial products.

Firing tests are carried out at the test complex using the specialized firing test stands equipped with the systems providing: simulation of object test conditions, test stands and product objects control, as well as testing results measurement and recording. During the test continuous registration of many physical parameters is carried out and all stand systems must be in well-functioning operation for its implementation. Stand systems are required to guarantee high reliability and measurement accuracy. No less important is the requirement for the technological effectiveness of stand systems which can include the quality and complexity of the preparatory work carried out before the test, as well as routine maintenance included in the scheduled outage.

Features of LRE thrust measurement. The thrust of a liquid rocket engine is one of the most important parameters to evaluate the engine characteristics. As is well known, the thrust of the engine chamber is the resultant of hydrogasdynamic forces acting on the inner surfaces of the chamber upon expiration of matter and environmental pressure forces acting on the chamber outer surfaces, with the exception of external aerodynamic drag forces [3]. This resulting force causes the movement of the apparatus, on which the engine is set. According to the definition, this kind of thrust force calculation is complicated and not quite accurate since it is necessary to know the law of pressure change along the entire length of the chamber which, especially on the tapering part of the nozzle (i.e. from the end of the combustion chamber to the critical section) is not always known. Hence, a reliable indicator of the engine thrust value can only be deter-

mined by directly measuring the engine thrust on a test stand. During the test high demands are made on the accuracy of its measurement: the permissible error in most cases should not exceed 0.3–0.5 % of the nominal value [4].

It is worth noticing that the focus of direct thrust measurement comes from both the type and class of the engine as well as the ability of the stand to create simulating conditions for the engine to work in the design mode. For powerful engine testing the stand design providing a vertical arrangement of the engine axis is the most appropriate. But the stand designs including thrust measurement systems for the horizontal location of tested engines are also known. For direct thrust measurement on the test stands a special force measurement system is used which includes specialized information transition channels and thrust measurement devices consisting of the following structural units: a machine, a calibration system and a measuring system (force transducers, displacement sensors).

Basic circuit power schemes of the thrust measurement devices. The design of the thrust measurement devices is a combination of the three above mentioned components but a fundamental difference is implied by the choice of the device circuit power scheme, i. e. a type of machine and a calibration system. The machine consists of two main elements: a stationary base and a frame to which the tested engine is mounted. Thus, the principle of interaction between the thrust measurement devices can be represented by the scheme shown in fig. 1. The frame which can be moveable or stationary perceives the thrust from the tested engine and transfers it to the measuring system and base. Depending on the design machines are divided into four groups: machines with elastic bonds between the stationary base and the moving frame, rigid machines, machines with minimal friction and special machines [5].

The calibration system with respect to the measuring system is intended for its verification and calibration. Choosing the type of calibration system as well as the hardware version depends on the machine design used for the thrust measurement devices. There are several calibration systems used at the test stands for powerful LREs: a hydraulic calibration system, a lever-operated calibrate system.

During the LRE tests the scheme of the thrust measurement devices for the machine with elastic bonds between the stationary base and the moving frame is mostly common since this scheme is easily integrated with all the main calibration systems. With this scheme the movable frame is usually hanged to the frame with strip suspension or flexible joints.

The first example of this circuit power scheme implementation is the thrust measurement devices of the stand № 1 manufactured by the "Testing and Refueling complex" (JSC Krasnash). The thrust measurement devices are a combination of the lever-operated calibrate system and the double-support machine with elastic bonds between the frame and the stationary base, the principle scheme is shown in fig. 2. According to this system design the stationary part is represented by two racks 1, mounted on the overlap between the fire compartment

(where the tested engine is installed) and the thrust measurement devices compartment where the measuring and calibration systems are located. 3-pin-springs 5 are used as elastic bonds, while the external petals of the springs are connected to the stationary part and the internal ones are linked to the movable part of the machine. The feed lines are taken and fixed to the stand frame. The product is mounted to the transition frame 4. If necessary, the movable part of the machine is locked relatively the stationary one using eighth locking screws 6. Force transducers 7 are installed on the adjusting inserts 8 between the stationary and movable parts of the machine and measure the impact force of the moving part. The signal generated by the force transducers is transmitted through special communication channels to the complex of measuring and computing and information-measuring systems. Two force transducers are installed on each machine support. In this case, each pair of force transducers is of the same type and duplicate.

The lever-operated calibration system consists of upper levers 11, 12 and lower levers 9, 10. The lower levers of the second kind, with a gear ratio of $i \approx 3.6$ are connected to the frame using rods 13 and to short arms of the upper levers using tenders 14. The upper levers of the first kind with a gear ratio of $i \approx 14$, rest upon fixed racks 15. Suspensions 16 are fixed on the long arms of the lower levers. Calibration loads are manually placed on the suspensions, which affects the complexity of the process. All connections of the levers with the other parts of the lever-operated calibration system are carried out using prisms and caps. Such a connection provides a constant gear ratio during an operation.

The accuracy of this calibration system depends on rigidity, accuracy of the operated levers gear ratio as well as on the condition of the knife-edge supports surfaces, since they have increased wear under vibration loads.

The second example of a power circuit scheme including the machine with elastic bonds between the base and the movable frame, but with a hydraulic calibration system according to operation [6] are the thrust measurement devices of the stand test manufactured by the JSC NPO

Energomash named after academician V. Glushko. The principle scheme is presented in fig. 3.

According to this thrust measurement system design, the fixed part is attached to the power ring 7 and includes: frames 4, 5; brackets 11, 12; a spacer 15; a hydraulic loader 13. The rest components form a movable part of the thrust measurement system. This movable part is connected to the base in transverse directions by means of tapes 18 and with the fixed part by means of springs 17. The springs have great stiffness in the plane perpendicular to the axis of the engine and soft one in the plane parallel to the axis of the engine. This permits free motion of the non-stationary part relative to the stationary one in the direction of the engine axis. During the test the traction force from the engine is sequentially transmitted through frames 1, 2, 3 to the force transducer 16 with the spacer 15. The spacer, in turn, presses on the frame 4. The frame 4 abuts against the frame clamps 5 and then against the power ring 7.

Calibration is carried out using a special power hydraulic loader 13, which lengthening abuts against the frame 5 and the force transducer 9. During loading the frame 3 is moved using the frame 6 and rods 10. With this "internal" loading the force ring 7 is not involved in the load perception.

The essence of creating the exact value of the calibration force, in this case, comes down to using an additional force transducer 9 and according to its testimony load and adjustment of the force developed by the hydraulic loading device is carried out. The hydraulic calibration system permits creating accurate force with remote control, which has a positive effect on the system technological effectiveness.

The group of rigid machines includes devices with a fixed frame. These machines are structurally the simplest and differ in minimum weight and overall dimension [5]. According to this scheme the force transducer is rigidly fixed to the supporting structure of the stand and the force is transmitted from the engine through a fixed frame i.e. a frame without any movable connection between the frame and the stationary base.

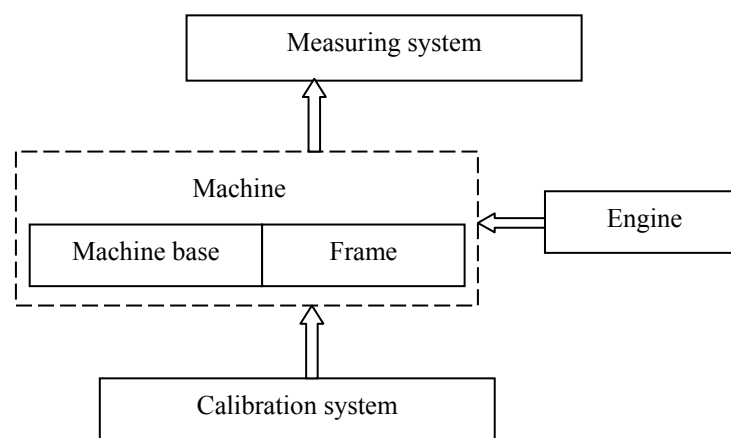


Fig. 1. Scheme of a test stand thrust measurement system for LREs

Рис. 1. Схема работы СИУ стенда испытаний ЖРД

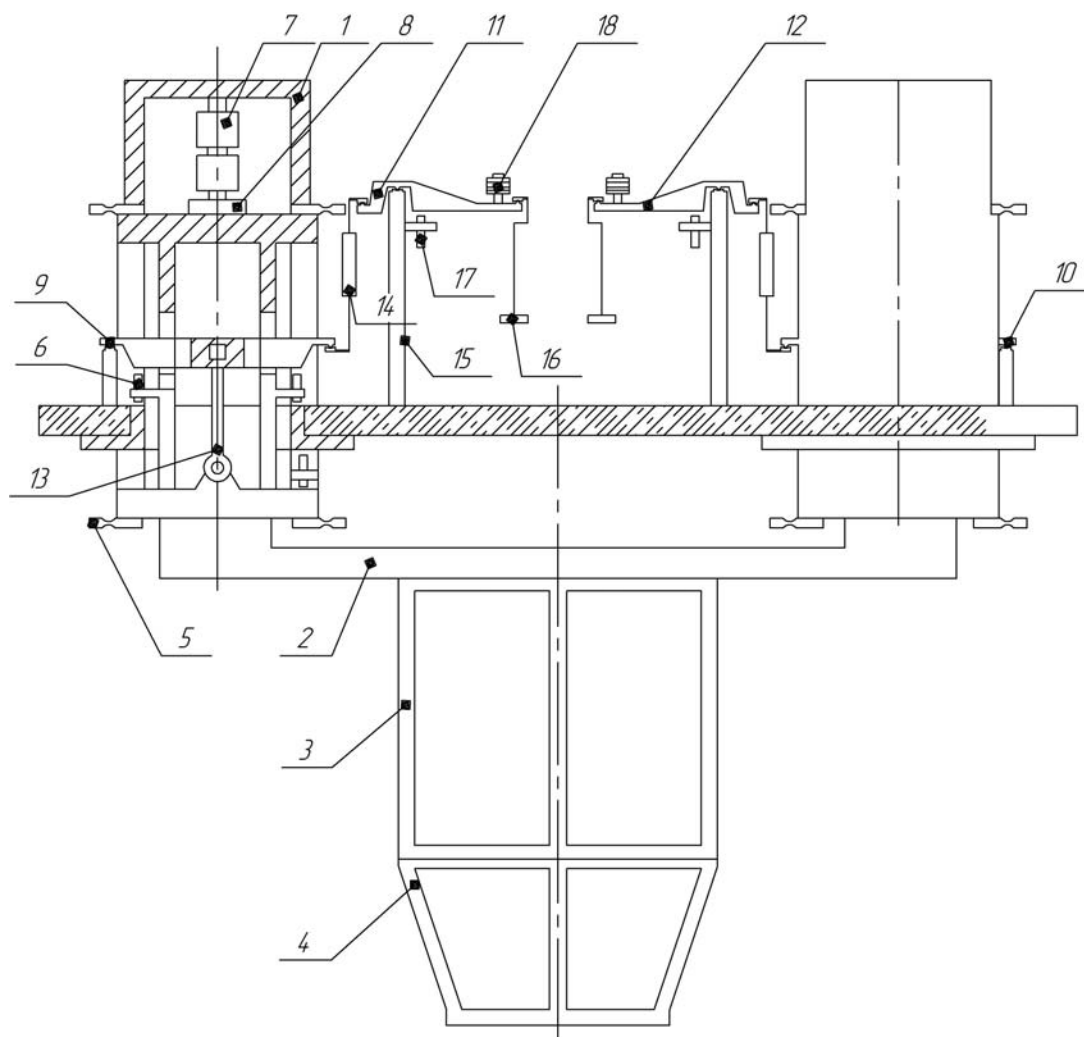


Fig. 2. Scheme of the thrust measurement system with a lever-operated calibrate system and the machine with elastic bonds between a frame and a stationary base:
 1 – rack; 2 – frame; 3 – stand frame; 4 – transition frame; 5 – 3-pin-springs; 6 – locking screw; 7 – force transducer;
 8 – adjusting insert; 9 – lever A1; 10 – lever A2; 11 – lever B1; 12 – lever B2; 13 – rod; 14 – tender; 15 – rack;
 16 – suspension; 17 – screw; 18 – balancing load

Рис. 2. Схема СИУ с РГУ и станком с упругими связями между рамой и станиной:
 1 – стойка; 2 – рама; 3 – рама стандовая; 4 – рама переходная; 5 – пружина Ш-образная; 6 – винт стопорный;
 7 – силоизмеритель; 8 – вкладыш регулировочный; 9 – рычаг А1; 10 – рычаг А2; 11 – рычаг В1; 12 – рычаг
 В2; 13 – тяга; 14 – тендер; 15 – стойка; 16 – подвеска; 17 – винт; 18 – груз балансировочный

In this case, the thrust measurement devices may not have a calibration system provided that the dismantled force transducer is periodically calibrated in the measuring laboratory and then installed at the workplace. The scheme is common for testing the small thrust LREs. The practical example of this thrust measurement system scheme is a test stand for the LREs with a thrust of up to 20 kN manufactured on the basis of the Aeronautics Institute of Technology in São José dos Campos, Brazil [7].

The group of machines with minimal friction includes machines in which the frame is moved with minimal friction, these are various kinds of rocking chairs, lunettes, trolleys. Currently, such machines are practically not used for the LRE testing. Whereas, when testing solid fuel rocket engines (SFRE) slipway equipment is widely used

to orient and mount the SFRE on a test stand in horizontal position [8]. Examples of this scheme practical application are sources [8; 9].

The fourth group of machines includes special devices that provide the ability to measure the LRE thrust whose structural features do not permit to test them on the above mentioned machines. For example, engines with nozzles located at an angle to the axis of the combustion chamber [5].

Revisiting the calibration of the trust measurement devices. Calibration is a technological operation which consists in obtaining a relationship between the values of the input measured parameter (in this case, the engine thrust force) and output informative parameter (depends on the type of sensor used). The calibration error, in turn, is the sum of systematic error of the means for setting the

force, the random component of the error during calibration and the error of the recording device [10]. The systematic component of the basic error depends on the type and specific design of the calibration system. The random component of the error during calibration depends on the following factors: instability of external indicators of the calibration process (indoor air temperature, the tempera-

ture of the thrust measurement devices), random collisions and vibration during calibration that cannot be eliminated, changes in the position of the force-setting elements.

Considering the main calibration systems and firing test stands used in the LRE thrust measurement system some of the features presented in table may be highlighted.

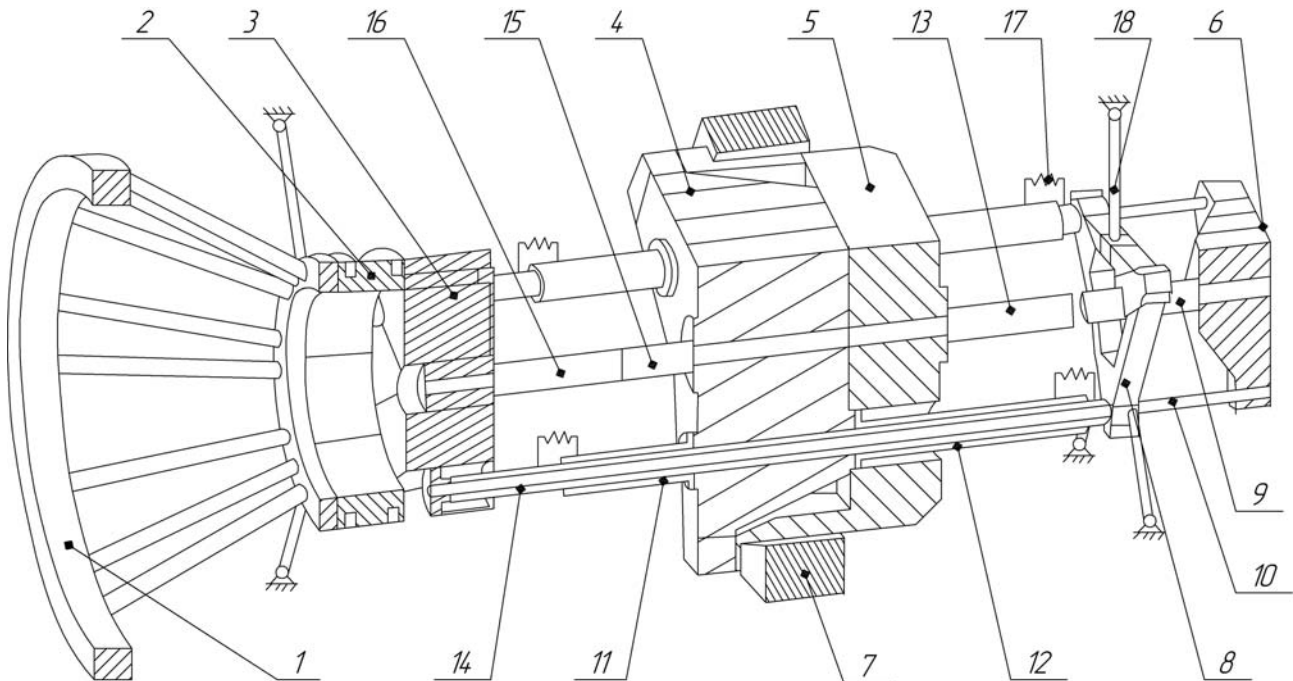


Fig. 3. Scheme of the thrust measurement system with a hydraulic calibration system and the machine with elastic bonds between the frame and the stationary base:

1–6 – power-absorbing frames; 7 – power ring; 8 – a triangle; 9 – force transducer; 10 – calibration bar; 11, 12 – bracket; 13 – hydraulic loader; 14 – movable bar; 15 – a spacer; 16 – force transducer; 17 – spring; 18 – tape (7 pieces)

Рис. 3. Схема СИУ с гидравлической градуировочной системой и станком с упругими связями между рамой и станиной:

1–6 – силовоспринимающие рамы; 7 – силовое кольцо; 8 – треугольник; 9 – силоизмеритель; 10 – градуировочная штанга; 11, 12 – кронштейн; 13 – гидронагружатель; 14 – подвижная штанга; 15 – проставка; 16 – силоизмеритель; 17 – пружина; 18 – лента (7 штук)

Comparison table of calibration systems

Feature	Lever-operated calibration system	Hydraulic calibration system
Calibration error	Depends on the accuracy and value of the levers gear ratio embedded in the design of a particular device (the accuracy of gear ratios can reach 0.01%), the accuracy of mounting prismatic supports, the accuracy of special loads	Depends on the measurement error of the reference force transducers (reaches about 0.1%), the accuracy of the force-setting equipment
Additional components	Special loads	Pumps, tanks, filters, valves, chokes, radiators etc.
Maintenance required	Periodic inspection and prophylactic replacement of prisms and caps, verification of the lever gear ratio, verification of the basic error when measuring force by repeated calibration	Checking and changing the oil, checking for leaks, replacing filters, servicing additional equipment, checking the basic error when measuring force by repeated calibration
Correction of the calibration step force value	Correction is not possible, the value of the calibration step is determined by the nominal mass of special loads	An additional reference force transducer is used and according to its testimony the load is made and the force is corrected
Remote effort creation	Unavailable when using loads	Available
Labor intensity	High	Low

To ensure more accurate thrust measurement readings the thrust measurement system calibration is carried out on the day of assigned test after the technological installation of the engine and connection of fuel lines and measuring pipelines, drain and purge lines, control and measurement systems cable trunks and all auxiliary fastening elements affecting the weight of the tested LRE. During the calibration process it is forbidden for workers to be in the stand or to perform work that may, in any way, affect the product.

A proposal for the thrust measurement systems modernization. The error of direct power LRE thrust measurement during the test consists of the measuring system (measuring components) error, calibration error, accuracy and completeness of various metrological characteristics when testing. These include several interference corrections: changes during the engine mass testing; changes in mass and temperature of the components; mismatch of the exemplary and measured effort points, the Bourdon effect and other phenomena affecting a particular thrust measurement system during the testing process [1]. With the development of computing technology one of the steps to modernize test systems was the implementation of new measurement and control systems on modern element bases to replace obsolete and worn-out ones [11].

As a result of this lever and hydraulic calibration systems may be replaced for electric ones as a form of the thrust measurement system design modernization. It is proposed to use a special electromechanical drive based on a planetary roller-screw mechanism as a power drive to create the calibration force.

The electromagnetic drive is an electric cylinder with the mechanism that converts electrical energy into mechanical. The planetary roller-screw mechanism is used at low feed speeds and high forces. In this mechanism the load from the lead screw is transferred to the nut through the rounded sides of the rollers (force transmission through the satellite rollers). The disassembled planetary roller-screw mechanism is shown in fig. 4.



Fig. 4. Disassembled planetary roller-screw mechanism [12]

Рис. 4. ПРВМ в разобранном виде [12]

Consider principles of its operation. In contrast with the planetary gear drive in which satellite axis move in a plane normal to the axis of central wheel rotation, in the mechanism under consideration threaded rollers as satellites execute three motions. The rollers rotate around their axes; rotate around the axis of the screw together with the separators; rolling around the thread of the nut rollers move along the axis of the nut together with the screw [13]. The advantages as the basis for considering the im-

plementation of this drive are the ability of the mechanism to work at high loads as well as the design simplicity and reliability which entails the simplification of the calibration device kinematic scheme. The electromechanical drive also allows remote control but unlike hydraulic systems it has a higher system response to the slightest changes and does not require the operation of additional equipment (as it is with hydraulic systems), only power and signal cables and a control unit are required for the electric cylinders operation. Electric cylinders are capable of operating at speeds of up to 1.5 m/s with forces of up to 400 kN, they have a stroke of up to 1.2 m with positioning accuracy of approximately 1 μm [14]. The use of electric cylinders as a force setting drive in the thrust measurement system is proposed to be carried out as it is shown in fig. 5.

Consider the case, when the maximum axial force created by the electromechanical drive is sufficient to calibrate the thrust measurement system. Depending on this system design the place of force application for measurement system calibration is determined. In the case of rigid machines or machines with elastic bonds between the frame and the stationary base the transmission of force set by the drive through the frame is meant. The system must include loading and control subsystems for functioning. Electric cylinders themselves are directly included in the loading subsystem and their number depends on the number of measurement branches and fixed supports of the thrust measurement machine. The control subsystem should include frequency and secondary converters, a strain gauge force transducer working on compression, power cables. To ensure operation the control subsystem should be integrated with the common stand control system. The value of the force created by the electric cylinder is entered in the PC software. And all the information about the amount of efforts is transmitted to the frequency converter through a processor module. The electric converter, in its turn, generates a supply voltage for the electric cylinder connected to it. The strain gauge force transducer is installed between the cylinder rod and the place of force application. Deformation of an elastic element causes imbalance of the strain gauge bridge. An electric unbalanced signal arrives at the secondary measurement converter for analog-to-digital conversion, and measured data processing and display [15]. Data on the actual force magnitude on the cylinder rod can ensure high accuracy of loading. The main error varies within errors of the primary and secondary transducers which can reach about 0.1 % in the case of using a strain gauge transducer. In the case when thrust measurement devices include stands for testing powerful ERLs which thrust reaches 1000 kN or more and when the electric cylinder maximum force is insufficient for calibration program a combination of the electromechanical drive and the lever-operated calibration system is proposed. The load from the electric cylinder is applied to a lever through which the increasing force is transmitted to the moving frame of the thrust measurement system.

As in the previous version, the work is carried out with electric voltage that is why this solution makes it possible to implement a stepless calibration method since the tasks of programming and force control are greatly simplified.

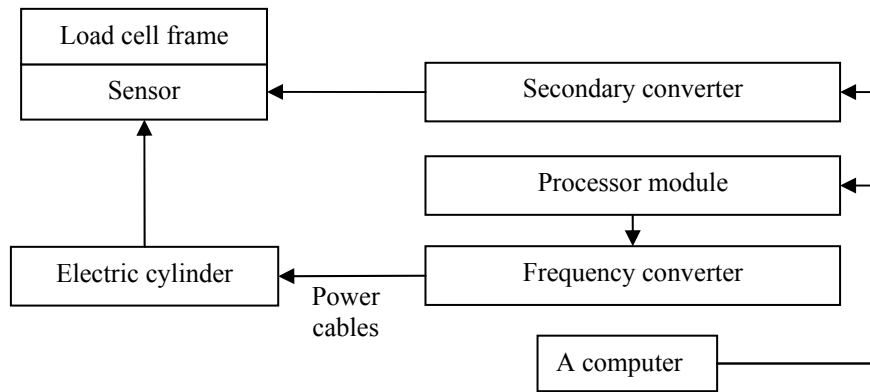


Fig. 5. Scheme of a calibration system based on an electromechanical drive

Рис. 5. Схема градуировочной системы на базе электромеханического привода

At the same time the remote control condition is fulfilled and this reduces the work complexity compared to standard calibration including the lever-operated calibration system. This scheme has inherent disadvantages of the lever calibration system in combination with advantages of the electric drive.

Electric cylinders have high efficiency (about 85 %) and the current consumption changes in proportion to the developed load. If it is necessary to minimize energy consumption the electric cylinders design permits graduated calibration since the electromagnetic brake is capable of holding the predetermined force. Whereas, the testing stand compartments have a category of increased fire hazard it is necessary to provide for explosion proof execution of operating elements to keep safe the electromechanical drive system.

Conclusion. Based on the theory of thrust measurement system design and practical use of thrust measurement devices on the LRE testing stands features, advantages and disadvantages of various principle thrust measurement system schemes were evaluated. A proposal is made for thrust measurement system modernization by implementing a calibration system based on the electromechanical drive. The general concept to use an electric cylinder as a calibration system loading device is presented. Disadvantages and prospects of implementing this drive into the calibration system of LRE firing test stands are estimated.

References

1. Yacunenkov V. G., Nazarov V. P., Kolomencev A. I. *Stendovye ispytaniya zhidkostnyh raketnyh dvigateley* [Bench tests of liquid rocket engines: a training manual]. Krasnoyarsk, 2016, 248 p.
2. Kolomencev A. I., Kraev M. V., Nazarov V. P. *Ispytanie i obespechenie nadezhnosti* [Testing and ensuring reliability]. Krasnoyarsk, 2006, 336 p.
3. Vasil'ev A. P., Kudryavcev V. M., Kuznecov V. A. *Osnovy teorii i rascheta zhidkostnyh raketnyh dvigateley* [Fundamentals of the theory and calculation of liquid rocket engines]. Moscow, Vyssh. Shkola Publ., 1983, 703 p.
4. Galeev A. G., Ivanov V. N., Katenin A. V. *Metodologiya ehkspperimental'noy otrabotki ZHRD i DU,*

osnovy provedeniya ispytaniy i ustrojstva ispytatel'nyh stendov [Methodology of experimental testing testing of LRE, the basics of testing and device test stand]. Kirov, MCNIP Publ., 2015, 436 p.

5. Zhukovskij A. E., Kondrusev V. S., Levin V. Ya. *Ispytanie zhidkostnyh raketnyh dvigateley* [Test of liquid rocket engines]. Moscow, Mashinostroenie Publ., 1981, 199 p.

6. Loshkarev A. N., Merzlyakov D. V., Milov A. E. [Calculated strength analysis of thrust-measuring device of stand for tests of rocket engines with a thrust of 1000 TF]. *Trudy NPO Energomash im. akademika V. P. Glushko*. 2012, No. 29. P. 311–327 (In Russ.).

7. Santos E. A., Alves W. F., Prado A. N. A. et al. Development of test stand for experimental investigation of chemical and physical phenomena in Liquid Rocket engine. *Journal of Aerospace Technology and Management*. 2011, P. 159–170. Doi: 10.5028/jatm.2011.03021111.

8. Vinickij A. M., Volkov V. T. *Konstrukciya i otrabotka RDTT* [Design and testing of solid propellant rocket motors]. Moscow, Mashinostroenie Publ., 1980, P. 98–106.

9. Bol'shakov A. N., Zaval'nyuk A. G. *Stend dlya izmereniya tyagi raketnogo dvigatelya* [Stand for measuring propulsion of a rocket engine]. Patent RF, F 02 K 9/96, 2004.

10. Etkin L. G. *Vibrochastotnye datchiki. Teoriya i praktika* [Vibration sensors. Theory and practice]. Moscow, Izd-vo MGTU im. N. E. Bauman Publ., 2004, 408 p.

11. Vinogradov V. A., Valov V. I. [Features of the preparation and conduct of fire and cold tests of liquid rocket engines at the Chemical Plant – a branch of OJSC “Krasnash”. *Reshetnevskie chteniya : materialy XIII Mezhdunar. nauch. konf. (10–12 noyabrya 2009, g. Krasnoyarsk) v 2 ch.* [International science and research conference (in memory of the Mikhail Fedorovich Redhetnev, general constructor of space vehicles and rocket systems)]. Krasnoyarsk, 2009, P. 102–103.

12. SKF compact inverted roller screw. Available at: https://www.skf.com/binary/77-68546/10592-EN_compact-inverted-roller-screw.pdf (accessed: 29.01.2020).

13. Ryakhovsky O. A., Vorobyov A. N., Marokhin A. S. [Planetary roller-screw mechanism for convert-

ing rotational motion into translational, made according to the “Inverted” scheme]. *News of higher educational institutions. Mechanical engineering*. 2013, No. 9, P. 44–48.

14. Nauchno-proizvodstvennoe predpriyatie MERA [Scientific-Production Enterprise MERA]. Available at: <http://nppmera.ru/npp-mera-peredovyye-resheniya-dlya-staticheskix-ispytaniy> (accessed: 29.01.2020).

15. Veselov A. V. [Modernization of the load-measuring device on the test benches of liquid rocket engines]. *Reshetnevskie chteniya : materialy XXII Mezhdunar. nauch. konf. (12–16 noyabrya 2018, g. Krasnoyarsk) v 2 ch.* [International science and research conference (in memory of the Mikhail Fedorovich Redhetnev, general constructor of space vehicles and rocket systems)]. Krasnoyarsk, 2018, P. 198–200.

Библиографические ссылки

1. Яцуненко В. Г., Назаров В. П., Коломенцев А. И. Стендовые испытания жидкостных ракетных двигателей / Сиб. гос. аэрокосмич. ун-т ; Моск. авиац. ин-т. Красноярск, 2016. 248 с.

2. Испытание и обеспечение надежности / А. И. Коломенцев, М. В. Краев, В. П. Назаров и др. ; Сиб. гос. аэрокосмич. ун-т ; Моск. авиац. ин-т. Красноярск, 2006. 336 с.

3. Основы теории и расчета жидкостных ракетных двигателей / А. П. Васильев, В. М. Кудрявцев, В. А. Кузнецов и др. М. : Высш. школа, 1983. 703 с.

4. Методология экспериментальной отработки ЖРД и ДУ, основы проведения испытаний и устройства испытательных стендов : монография / А. Г. Галеев, В. Н. Иванов, А. В. Катенин и др. Киров : МЦНИП, 2015. 436 с.

5. Испытание жидкостных ракетных двигателей / А. Е. Жуковский, В. С. Кондрусев, В. Я. Левин и др. М. : Машиностроение, 1981. 199 с.

6. Расчетный анализ прочности силоизмерительного устройства стенда для испытаний ЖРД с тягой 1000 тс / А. Н. Лошкарев, Д. В. Мерзляков, А. Е. Милов и др. // Труды НПО Энергомаш им. академика В. П. Глушко. 2012. № 29. С. 311–327.

7. Development of test stand for experimental investigation of chemical and physical phenomena in Liquid Rocket engine / E. A. Santos, W. F. Alves, A. N. A. Prado

et al. // *Journal of Aerospace Technology and Management*. 2011. P. 159–170. Doi: 10.5028/jatm.2011.03021111.

8. Конструкция и отработка РДТТ / А. М. Виноцкий, В. Т. Волков, И. Г. Волковицкий и др. М. : Машиностроение, 1980. С. 98–106.

9. Пат. 2225527 Российская федерация, F 02 K 9/96. Стенд для измерения тяги ракетного двигателя / Большаков А. Н., Завальнюк А. Г. № 2002114953/06 ; заявл. 05.06.2002 ; опубл. 10.03.2004.

10. Эткин Л. Г. Виброчастотные датчики. Теория и практика. М. : Изд-во МГТУ им. Н. Э. Баумана, 2004. 408 с.

11. Виноградов В. А., Валов В. И. Особенности подготовки и проведения огневых и холодных испытаний жидкостных ракетных двигателей на Химическом заводе – филиале ОАО «Красмаш» // Решетневские чтения : материалы XIII Междунар. науч. конф. (10–12 ноября 2009, г. Красноярск) : в 2 ч. / под общ. ред. Ю. Ю. Логинова ; Сиб. гос. аэрокосмич. ун-т. Красноярск, 2009. С. 102–103.

12. SKF compact inverted roller screw [Электронный ресурс]. URL: https://www.skf.com/binary/77-68546/10592-EN_compact-inverted-roller-screw.pdf (дата обращения: 29.01.2020).

13. Ряховский О. А., Воробьев А. Н., Марохин А. С. Планетарный ролик-винтовой механизм преобразования вращательного движения в поступательное, выполненный по «перевернутой» схеме // Известия высших учебных заведений. 2013. № 9. С. 44–48.

14. Научно-производственное предприятие «МЕРА» [Электронный ресурс]. URL: <http://nppmera.ru/npp-mera-peredovyye-resheniya-dlya-staticheskix-ispytaniy> (дата обращения: 29.01.2020).

15. Веселов А. В. Модернизация тягоизмерительного устройства на испытательных стендах жидкостных ракетных двигателей // Решетневские чтения : материалы XXII Междунар. науч. практ. конф. (12–16 ноября 2018, г. Красноярск) : в 2 ч. / под общ. ред. Ю. Ю. Логинова ; СибГУ им. М. Ф. Решетнева. Красноярск, 2018. С. 198–200.

© Begishev A. M., Zhuravlev V. Y., Torgashin A. S., 2020

Begishev Aleksey Mikhaylovich – graduate student; Reshetnev Siberian State University of Science and Technology. E-mail: alex-beg95@mail.ru.

Zhuravlev Viktor Yur'yevich – Cand. Sc., Professor; Reshetnev Siberian State University of Science and Technology. E-mail: vz@sibsau.ru.

Torgashin Anatoliy Sergeevich – graduate student; Reshetnev Siberian State University of Science and Technology. E-mail: ttorg23@gmail.com.

Бегишев Алексей Михайлович – аспирант; Сибирский государственный университет науки и технологий имени академика М. Ф. Решетнева. E-mail: alex-beg95@mail.ru.

Журавлев Виктор Юрьевич – кандидат технических наук, профессор кафедры двигателей летательных аппаратов; Сибирский государственный университет науки и технологий имени академика М. Ф. Решетнева. E-mail: vz@sibsau.ru.

Торгашин Анатолий Сергеевич – аспирант; Сибирский государственный университет науки и технологий имени академика М. Ф. Решетнева. E-mail: ttorg23@gmail.com.

UDC 681.828

Doi: 10.31772/2587-6066-2020-21-1-70-77

For citation: Klyuchnikov A. V. Elaboration and testing of the algorithm which ensures an achievement of minimal deviation angle of flying model's main centroidal axis of inertia during her counterbalancing in a sole correction flatness. *Siberian Journal of Science and Technology*. 2020, Vol. 21, No. 1, P. 70–77. Doi: 10.31772/2587-6066-2020-21-1-70-77

Для цитирования: Ключников А. В. Разработка и тестирование алгоритма обеспечения минимального угла отклонения главной центральной оси инерции в процессе балансировки летающей модели в одной плоскости коррекции // Сибирский журнал науки и технологий. 2020. Т. 21, № 1. С. 70–77. Doi: 10.31772/2587-6066-2020-21-1-70-77

ELABORATION AND TESTING OF THE ALGORITHM WHICH ENSURES AN ACHIEVEMENT OF MINIMAL DEVIATION ANGLE OF FLYING MODEL'S MAIN CENTROIDAL AXIS OF INERTIA DURING HER COUNTERBALANCING IN A SOLE CORRECTION FLATNESS

A. V. Klyuchnikov

Russian Federal Nuclear Centre – All-Russia Research Institute of Technical Physics
named after Academician E.I. Zababakhin
13, Vassilyeva St., Snezhinsk, 456770, Russian Federation
E-mail: a.klyuchnikov@bk.ru

High complexity and cost of developing flying models necessitate the use of such design and production techniques that would ensure the best flight technical and technological characteristics of the model also would raise of it operation effectiveness. These techniques include the experimental control method of flying model's mass-inertia asymmetry parameters during final assembly of the model. Solution of the problem of optimization the process of bringing parameters of mass-inertia asymmetry of the conical flying model to specified standards is considered in the article. The only correction plane is designed to be positioned close to cone face, away from the center mass of the flying model. The flying model as a component of prefabricated rotor is being balanced in dynamic mode on a low-frequency dynamic vertical stand, which based on gas bearings. Before balancing experiment the weigh, longitudinal center of mass and inertia moments of the flying model have to be controlled with use of another measurement equipment. As a criterion of optimization is sorted the reaching of minimum of the angle of deviation of principal longitudinal centroidal axis of inertia from geometrical axis of the flying model. But simultaneously the pre-set standard of center-mass shift from the geometrical axis must be ensured. Balancing algorithm, easy-to-realized by modern computers, is presented. Numerical illustration of balancing is given. The algorithm enables omitting intermediate steps of balancing, reducing them to one step (as a rule), and shortening the balancing time, as well. In one step of balancing the engineering model permits either bringing parameters of mass-inertia asymmetry of the flying model to specified standards, or diagnosing impossibility of attaining the specified standards with available design of flying model. The algorithm and balancing method are experimentally tested at newly-designed vertical dynamic stand on conical gas bearings. It's high precision and efficiency are corroborated.

Key words: mass-inertia asymmetry, balancing stand, axis of symmetry, axis of inertia, moment of inertia, correction plane, misbalance, algorithm.

РАЗРАБОТКА И ТЕСТИРОВАНИЕ АЛГОРИТМА ОБЕСПЕЧЕНИЯ МИНИМАЛЬНОГО УГЛА ОТКЛОНЕНИЯ ГЛАВНОЙ ЦЕНТРАЛЬНОЙ ОСИ ИНЕРЦИИ В ПРОЦЕССЕ БАЛАНСИРОВКИ ЛЕТАЮЩЕЙ МОДЕЛИ В ОДНОЙ ПЛОСКОСТИ КОРРЕКЦИИ

А. В. Ключников

Российский федеральный ядерный центр – Всероссийский научно-исследовательский институт
технической физики имени академика Е. И. Забабахина
Российская Федерация, г. Снежинск, ул. Васильева, 13
E-mail: a.klyuchnikov@bk.ru

Высокая стоимость, сложность разработки летающих моделей обуславливают необходимость применения методов проектирования и изготовления, которые позволили бы обеспечить наилучшие летно-технические и технологические характеристики модели и максимально повысить эффективность ее эксплуатации. К числу таких методов относится экспериментальный контроль параметров массо-инерционной асимметрии на заключительном этапе общей сборки летающей модели. В статье рассмотрено решение задачи оптимизации процесса приведения параметров массо-инерционной асимметрии летающей модели кона-

ской формы к заданным нормативам. Единственная плоскость коррекции конструктивно расположена вблизи торца конуса, на значительном расстоянии от центра масс летающей модели. Балансировка летающей модели проводится в динамическом режиме в составе сборного ротора на низкочастотном динамическом вертикальном балансировочном стенде с газовыми опорами. Перед балансировкой масса, продольное положение центра масс и моменты инерции летающей модели должны быть определены экспериментально с использованием другого измерительного оборудования. В качестве критерия оптимизации принято достижение минимального угла отклонения продольной главной центральной оси инерции относительно геометрической оси летающей модели при одновременном обеспечении заданного норматива по величине смещения центра масс с той же геометрической оси. В работе представлен алгоритм балансировки, легко реализуемый на современных компьютерах. Приведён числовой пример балансировки. Алгоритм позволяет исключить промежуточные шаги балансировки, сократив число шагов балансировки, как правило, до одного шага, а также сократив время проведения балансировочного эксперимента. За один шаг балансировки алгоритм позволяет либо привести параметры массо-инерционной асимметрии летающей модели к заданным нормативам, либо диагностировать невозможность для конкретной конструкции летающей модели обеспечить достижение заданных нормативов.

Ключевые слова: массо-инерционная асимметрия, балансировочный стенд, ось симметрии, ось инерции, момент инерции, центр масс, плоскость коррекции, дисбаланс, алгоритм.

Introduction. This article continues the work [1; 2], in which the problem of balancing in the dynamic mode with the minimum displacement of the center of mass from the geometric axis stabilized by rotation of the conical flying model (LM), the cone of which is characterized by a small half-angle of the solution, was considered. Balancing is performed at the final stage of the general assembly of the model. In accordance with the algorithm given in [1], the model is balanced as a part of a prefabricated rotor, on a low-frequency dynamic balancing stand with gas supports and a vertical axis of rotation [3; 4]. The balancing process involves the determination and subsequent reduction of the parameters of mass-inertial asymmetry of the model, which include the value of the transverse displacement of the center of mass from the geometric axis and the angle of deviation of the longitudinal main central axis of inertia (SCOI) relative to the same axis [5; 6], to the values not exceeding the maximum permissible values specified in the operational documentation for the model. The presence of a single correction plane does not allow to fully combine the longitudinal GCI with the geometric axis of the LM, which is usually chosen as the construction axis. A balancing option with optimization according to the criterion of achieving the minimum center of mass displacement for a particular LM design is usually chosen, given the significant effect of this parameter on the flight performance of the model [7].

Bringing the parameters to specified standards is carried out by adjusting the mass of the model. For these reasons a balancing weight is attached to the standard plane of the model correction, which is located, as a rule, at the end (or near the end) of the conical FM at a considerable distance from its center of mass. In this case, the mass and angular position of the balancing weight is calculated according to the results of measuring the imbalance vectors acting in two – in the upper (standard) and lower (hereinafter referred to as *B* and *H*, respectively) correction planes of the combined rotor, which includes a controlled model [8; 9]. As the lower correction plane, the lower end of the specialized technological adapter is used, inside of which the FM is vertically installed with droop in nose. Measuring the amplitudes and phases of the vi-

bration of the upper and lower supports, proportional to the values and angles of the imbalance vectors are carried out during spool down of the assembled rotor at a constant operating speed [10; 11]. Firstly, the methodology involves bringing the controlled FM to a state of quasistatic imbalance, and then modeling the state of momentary imbalance (excluding the transverse displacement of the center of mass) with the calculation of the assumed skew angle of the longitudinal MCAI relating to geometry axis *X* of the model. If this angle does not exceed the admissible limit value, then the parameters of the balancing weight are calculated and the mass of the FM is adjusted. And if it exceeds, then the estimated (at the same time as the minimum possible for this version of the model layout) transverse displacement of the center of mass is calculated, setting the value of the skew angle of the longitudinal center for equal to the admissible limit value. If at the same time, the estimated skew angle of the longitudinal MCAI does not exceed the specified admissible limit value, then the parameters of the balancing weight are calculated and the mass of the FM is adjusted. Otherwise, the balancing is stopped, and the FM is sent to the manufacturer for re-arrangement. The method is protected by patent of the Russian Federation under No. 2499985 [12].

However, there are flying models including that have a conical shape of the hull. To ensure dynamic stability and the operating efficiency it is more preferable to minimize the skew of the longitudinal MCAI relating to the geometric axis (while fulfilling the specified standard for the magnitude of the transverse displacement of the center of mass). This article proposes to consider a modification of the FM balancing algorithm [7; 12], which is aimed at solving the balancing problem by reducing the mass inertial asymmetry parameters to values not exceeding the specified admissible limit values of these parameters, but using the optimization according to the criterion of achieving the minimum possible for a controllable design of longitudinal MCAI in relation to the geometric axis of the model. A variant of the problem is considered when there is a priori information about the mass, the longitudinal position of the center of mass relating to both correction planes and the moments of inertia of the controlled model obtained using other equipment and meas-

uring instruments [8; 13; 14], as well as the balancing coefficients of the measuring system obtained when setting up the stand for the control object using test weights [15; 16].

Balancing algorithm. The proposed algorithm assumes that two initial starts of the assembled rotor are made with the FM rotated 180 degrees around the geometric axis inside the process adapter. Based on the results of measuring the vibrations of the supports, the parameters of initial imbalances \bar{D}_B^{NACH} and \bar{D}_H^{NACH} (acting in the correction planes) are calculated, as well as the initial parameters of the radius-vector $\bar{\rho}$ of the transverse displacement of the center of mass and the vector-angle of the longitudinal MCAI of the model $\bar{\alpha}_X$ relative to its geometric axis by formulas are also calculated [15]

$$\bar{\rho}^{NACH} = \frac{\bar{D}_B^{NACH} + \bar{D}_H^{NACH}}{M}; \quad (1)$$

$$\bar{\alpha}_X^{NACH} = \frac{1}{2} \arcsin \frac{2(\bar{D}_B^{NACH} x_B - \bar{D}_H^{NACH} x_H)}{\Delta I}, \quad (2)$$

where M – model mass, $\Delta I = I_e - I_a$ – difference between equatorial I_e and axial I_a moments of model inertia, x_B и x_H – the distance from the center of the model mass to the upper and lower correction plane, respectively. Then a balancing calculation is performed if the initial value of at least one of the parameters characterizing the asymmetry in the initial mass distribution of the FM exceeds the corresponding maximum permissible value ρ_{dop} or α_{Xdop} , specified in the operational documentation for the model. In the process of calculation, the effect of imbalances in the correction planes modeling the intermediate states of the unbalanced FM is simulated. The results of the calculation are: either the determination of the mass and angle of installation of the balancing weight (its attachment to the standard plane allows to correct the mass of the FM, ensuring that the values of the monitored parameters are adjusted to the specified standards with optimization according to the criterion of reaching the minimum possible angle of skew of the longitudinal MCAI relative to the geometric axis of the model), or evidence for being unable to provide simultaneously two controlled parameters of mass-inertial asymmetry for the given model layout according to the given standards [7].

At the first step of the algorithm of balancing calculation, it is assumed that the FM is put into a mode of quasi-static imbalance, that is when its geometric axis and longitudinal MCAI intersect, but not in the center of mass. This allows for further calculations to operate exclusively with collinear imbalance vectors acting in opposite correction planes. In order to put the FM into a quasi-static imbalance mode, the effect of the initial imbalance in the upper (regular) correction plane should be eliminated, specifying in it, as was shown in [2], compensating for an imbalance \bar{D}_B^{COMP} equal in value, but opposite in the direction of the initial imbalance \bar{D}_B^{NACH} . In this case, in the lower plane of the correction according to figure an addi-

tional imbalance will be formed, which is directed opposite to the imbalance \bar{D}_B^{COMP} value of which is determined by the following formula

$$D_H^{DPL1} = D_B^{COMP} \cdot K_{HB}, \quad (3)$$

where K_{HB} – influence coefficient of the upper plane of correction on the lower plane of correction in case of imbalance in the upper plane of correction, determined experimentally during the pre-adjustment of the stand [15–17]. Shift of balance \bar{D}_H^{DPL1} , in turn, create imbalances \bar{D}_H^{COMP} of equal geometrical sum of imbalances \bar{D}_H^{DPL1} и \bar{D}_H^{NACH} , instead of imbalance \bar{D}_H^{NACH} in the lower correction plane according to the following formulas

$$D_H^{COMP} = \sqrt{D_H^{NACH^2} + D_H^{DPL1^2} + 2D_H^{NACH} D_H^{DPL1} \times \cos(\beta_H^{NACH} - \beta_H^{DPL1})}; \quad (4)$$

$$\beta_H^{COMP} = \arctg \frac{\sin \beta_H^{NACH} + \sin \beta_H^{DPL1}}{\cos \beta_H^{NACH} + \cos \beta_H^{DPL1}}, \quad (5)$$

where β_H^{NACH} and β_H^{DPL1} – phase angles of imbalances \bar{D}_H^{NACH} и \bar{D}_H^{DPL1} respectively. In this case, since there will be no imbalance in the upper correction plane, the longitudinal MCAI will intersect with the geometric axis, and the transverse displacement of the center of mass of the FM will be characterized by the following value

$$\rho^{COMP} = \frac{D_H^{COMP}}{M}. \quad (6)$$

At the second step, the transfer of the FM to the regime of static unbalance should be simulated, that is when the longitudinal MCAI is parallel to the geometric axis and there is no skew between these axes. To do this, the corrective imbalance \bar{D}_B^{KORR} must be set in the standard correction plane, in accordance with fig., codirectional imbalance and defined by the following formula

$$D_B^{KORR} = \frac{D_H^{COMP}}{1 + K_{HB}}. \quad (7)$$

In this case, an additional imbalance will be formed in the lower plane of correction \bar{D}_H^{DPL2} , opposed to imbalance \bar{D}_B^{KORR} and defined by the following formula

$$D_H^{DPL2} = D_B^{KORR} K_{HB}. \quad (8)$$

This, in turn, will lead to the formation of an imbalance correction in the lower plane \bar{D}_H^{CORR} (instead of imbalance \bar{D}_H^{COMP}) of equal sum of the opposing imbalances \bar{D}_H^{COMP} and \bar{D}_H^{CORR} . Amount of unbalance D_H^{CORR} will be determined by the following formula

$$D_H^{CORR} = D_H^{COMP} - D_H^{DPL2}. \quad (9)$$

Equality of equipolence imbalances \bar{D}_B^{CORR} and \bar{D}_H^{CORR} provides the elimination of the skew of the longitudinal MCAI with respect to the geometric axis and the transfer of the FM to the mode of static imbalance.

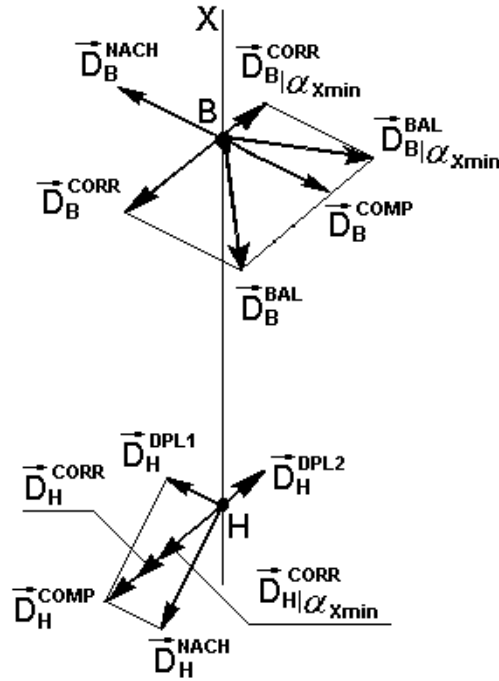


Diagram of counterbalancing calculation

Диаграмма балансировочного расчёта

In this case, the estimated value of the residual transverse displacement of the center of mass from the geometric axis of the FM, which will appear as a result of eliminating the transverse displacement of the center of mass, can be calculated by the following formula

$$\rho^{CORR} = \frac{2D_B^{CORR}}{M}, \quad (10)$$

If the condition $\rho^{CORR} \leq \rho_{dop}$ is met, the value D_B^{BAL} is defined and the angle position α_B^{BAL} balancing imbalance vectors \vec{D}_B^{BAL} , using the corresponding parameters of the unbalance vectors simulated in the regular correction plane B \vec{D}_B^{CORR} и \vec{D}_B^{COMP} .

Balancing vector parameters \vec{D}_B^{BAL} can be calculated using the following formulas in accordance with the figure representing the geometric sum of imbalances \vec{D}_B^{COMP} and \vec{D}_B^{CORR}

$$D_B^{BAL} = \sqrt{D_B^{COMP^2} + D_B^{CORR^2} + 2D_B^{COMP} D_B^{CORR} \cos(\alpha_B^{COMP} - \alpha_B^{CORR})}; \quad (11)$$

$$\alpha_B^{BAL} = \arctg \frac{\sin \alpha_B^{COMP} + \sin \alpha_B^{CORR}}{\cos \alpha_B^{COMP} + \cos \alpha_B^{CORR}}. \quad (12)$$

where α_B^{COMP} and α_B^{CORR} – unbalance phase angles \vec{D}_B^{COMP} and \vec{D}_B^{CORR} respectively. Then for the case $\alpha_X^{OST} = 0$, $\rho^{OST} = \rho^{CORR} \leq \rho_{dop}$ the mass of the balancing weight is calculated according to the formula

$$m^{BAL} = \frac{D_B^{BAL}}{r_B}, \quad (13)$$

herewith the installation angle of the balancing weight on the upper (standard) correction plane φ^{BAL} will match the phase angle α_B^{BAL} of imbalance \vec{D}_B^{BAL} .

Hereafter the FM mass is adjusted by attaching the balancing weight to the balancing plane B, thereby ensuring that both parameters of the mass-inertial asymmetry are brought to values not exceeding the maximum permissible values. In this case the skew of the longitudinal MCAI relative to the geometric axis is eliminated. However, in case the value ρ^{CORR} exceeds the maximum permissible value ρ_{dop} , it is necessary to calculate the estimated minimum possible deviation angle of the longitudinal MCAI relative to the geometric axis α_{Xmin} , which can be achieved by changing the imbalance in the correction plane B while reducing the transverse displacement of the center of mass of the FM to the admissible limit value ρ_{dop} according to the formula

$$\alpha_{Xmin} = \frac{1}{2} \arcsin 2 \times \left(\frac{\left(\frac{\rho_{dop} M - D_H^{COMP}}{1 - K_{HB}} \right) (x_B + K_{HB} x_H) - D_H^{COMP} x_H}{\Delta I} \right). \quad (14)$$

In case the reported value α_{Xmin} will exceed the specified admissible limit value, the balancing experiment

is terminated, and the FM will be rejected and sent to the manufacturer for rebuilding due to the calculation that there is no possibility of simultaneously bringing the magnitude of the displacement of the center of mass and the angle of deviation of the longitudinal MCAI relating to geometric axis to values not exceeding the specified maximum admissible limit value. Otherwise, if the inequality $|\alpha_{X \min}| \leq \alpha_{Xdop}$ is correct, the value of the imbalance vector $\vec{D}_{B|\alpha_{X \min}}^{CORR}$, ensuring the achievement of the minimum value $|\alpha_{X \min}|$ when setting the displacement of the center of mass equal to ρ_{dop} is determined by the formula

$$D_{B|\alpha_{X \min}}^{CORR} = \frac{\rho_{dop} M - D_H^{COMP}}{1 - K_{HB}}, \quad (15)$$

at the same time, a positive calculation result will mean that the directions of these imbalances $\vec{D}_{B|\alpha_{X \min}}^{CORR}$ and \vec{D}_B^{CORR} coincide, while a negative result, on the other hand, indicates that their directions are opposite. Due to the mutual influence of the correction planes, an imbalance $\vec{D}_{H|\alpha_{X \min}}^{CORR}$ will appear in the correction plane H, which is co-directed to the imbalance \vec{D}_H^{COMP} , the value of which is determined by the formula

$$\vec{D}_{H|\alpha_{X \min}}^{CORR} = \vec{D}_H^{COMP} + \vec{D}_H^{DPL3}, \quad (16)$$

where D_H^{DPL3} – is a value of additional imbalance \vec{D}_H^{DPL3} (not shown in fig. 1), appearing in the correction plane H as a result of the effect of an imbalance $\vec{D}_{B|\alpha_{X \min}}^{CORR}$ in the correction plane B and oppositely directed imbalance $\vec{D}_{B|\alpha_{X \min}}^{CORR}$. D_H^{DPL3} is determined by the formula

$$D_H^{DPL3} = D_{B|\alpha_{X \min}}^{CORR} K_{HB}. \quad (17)$$

Hereafter, the value $D_{B|\alpha_{X \min}}^{BAL}$ and the angular position $\alpha_{B|\alpha_{X \min}}^{BAL}$ of the vector of balancing imbalance $\vec{D}_{B|\alpha_{X \min}}^{BAL}$ are determined using the appropriate parameters of the imbalance vectors $\vec{D}_{B|\alpha_{X \min}}^{CORR}$ and \vec{D}_B^{COMP} modeled in the balancing plane of correction B. After that, the mass of the balancing weight $m_{\alpha_{X \min}}^{BAL}$ is determined, the which setting is carried out in the angular position corresponding to the angular position of the imbalance $\vec{D}_{B|\alpha_{X \min}}^{BAL}$.

To determine the value of the balancing imbalance, mass and setting angle of the balancing load, the following formulas are used:

$$D_{B|\alpha_{X \min}}^{BAL} = \sqrt{D_B^{COMP^2} + D_{B|\alpha_{X \min}}^{CORR^2} + 2D_B^{COMP} D_{B|\alpha_{X \min}}^{CORR} \times \cos(\alpha_B^{COMP} - \alpha_{B|\alpha_{X \min}}^{CORR})}, \quad (18)$$

where $\alpha_{B|\alpha_{X \min}}^{CORR}$ – unbalance angular position $\vec{D}_{B|\alpha_{X \min}}^{CORR}$;

$$\alpha_{B|\alpha_{X \min}}^{BAL} = \arctg \frac{\sin \alpha_B^{COMP} + \sin \alpha_{B|\alpha_{X \min}}^{CORR}}{\cos \alpha_B^{COMP} + \cos \alpha_{B|\alpha_{X \min}}^{CORR}}; \quad (19)$$

$$m_{B|\alpha_{X \min}}^{BAL} = \frac{D_{B|\alpha_{X \min}}^{BAL}}{r_B}. \quad (20)$$

After that, the mass of the FM is adjusted by attaching the balancing weight to the balancing plane B, ensuring that the setting angles of the balancing weight and the vector of the balancing unbalance coincide, and confidence firing of the assembled rotor is performed to confirm the correctness of the calculation. Based on the results of the confidence firing, the parameters of residual imbalances \vec{D}_B^{OST} and \vec{D}_H^{OST} operating in the corresponding correction planes after setting the balancing weight are determined, and the residual mass and inertial asymmetry parameters are calculated according to a formula (neglecting the mass of the balancing weight, as it is obviously practically insignificant compared to the mass of the controlled FM):

$$\bar{\rho}^{OST} = \frac{\vec{D}_B^{OST} + \vec{D}_H^{OST}}{M}; \quad (21)$$

$$\bar{\alpha}_X^{OST} = \frac{1}{2} \arcsin \frac{2(\vec{D}_B^{OST} x_B - \vec{D}_H^{OST} x_H)}{\Delta I}. \quad (22)$$

The performance of the considered algorithm can be estimated using a specific numerical example.

Example of calculating the balance weight. The balancing of the FM will be calculated with the following values of the task parameters:

- model mass $M = 100000$ g;
- distance from the center of mass of the FM to the upper correction plane $x_B = 570$ mm;
- radius of the upper correction plane $r_B = 200$ mm;
- distance from the center of mass to the lower plane of correction $x_H = 800$ mm;
- difference between the equatorial and axial moments of inertia $\Delta I = 8,5 \cdot 10^9$ g·mm²;
- admissible limit value of the transverse displacement of the center of mass $\rho_{dop} = 0,1$ mm;
- admissible limit value of cramp angle of MCAI $\alpha_{Xdop} = 10' \approx 0,166667^\circ$;
- influence coefficient of the upper correction plane on the lower correction plane in case of imbalance in the upper correction plane $K_{HB} = 0,3$;
- initial imbalance in the upper correction plane $D_B^{NACH} = 25000$ g·mm, phase angle $\alpha_B^{NACH} = 80^\circ$;
- initial imbalance in the lower correction plane $D_H^{NACH} = 10000$ g·mm, phase angle $\beta_H^{NACH} = 115^\circ$;
- whence the initial values of the asymmetry parameters of the masses of the FM in accordance with (1) и (2):

$$\rho^{NACH} = 0,34 \text{ mm};$$

$$\bar{\alpha}_X^{NACH} = 3,62'.$$

Since it was found that the initial values of the parameters of mass-inertial asymmetry exceed the

specified admissible limit value, we carry out a balancing calculation to achieve the conditions

$$\begin{cases} \alpha_X^{OST} = \alpha_{X \min} \leq \alpha_{Xdop}; \\ \rho^{OST} \leq \rho_{dop}. \end{cases} \quad (23)$$

We transfer the FM to the state of quasistatic imbalance, for which we introduce an imbalance \vec{D}_B^{COMP} with parameters $D_B^{COMP} = 25000$ g·mm, phase angle $\alpha_B^{COMP} = 260^\circ$, compensating for the effect of the initial imbalance \vec{D}_B^{NACH} in the upper correction plane. An additional imbalance \vec{D}_H^{DPL1} will appear in the lower correction plane, the value of which in accordance with (3) will be $D_H^{DPL1} = 7500$ g·mm, and the phase angle $\beta_H^{DPL1} = 80^\circ$. The imbalance \vec{D}_H^{DPL1} in total with the imbalance \vec{D}_H^{NACH} in accordance with (4) and (5) will form an imbalance \vec{D}_H^{COMP} in the lower correction plane with the parameters: $D_H^{COMP} = 16707$ g·mm, phase angle $\beta_H^{COMP} = 97.5^\circ$. Whence transverse displacement of the center of mass of the FM, in accordance with formula (6), total $\rho^{COMP} = 0.167$ mm, which exceeds the specified value despite the presence of a skew of the longitudinal MCAI.

Using (7) we calculate the parameters of the corrective imbalance \vec{D}_B^{CORR} , the action of which in the upper plane of the correction will eliminate the misalignment of the longitudinal MCAI relating to the geometric axis of the controlled flying model: $D_B^{CORR} = 12851.5$ g·mm, phase angle $\alpha_B^{CORR} = 97.5^\circ$. In this case, in accordance with (8) a new additional imbalance vector \vec{D}_H^{DPL2} will be formed in the lower correction plane due to the interaction of the correction planes with the parameters: $D_H^{DPL2} = 3855.5$ g·mm, phase angle $\beta_H^{DPL2} = 277.5^\circ$. This, in turn, in accordance with (9) will cause an imbalance \vec{D}_H^{CORR} in the lower plane of correction with the parameters: $D_H^{CORR} = 12851.5$ g·mm, phase angle $\beta_H^{CORR} = 97.5^\circ$.

To fulfill the condition $\alpha_X^{CORR} = 0$, arising from the equality of the values of the co-directed imbalance vectors \vec{D}_B^{CORR} и \vec{D}_H^{CORR} , the estimated transverse displacement of the center of mass from the geometric axis of the FM in accordance with expression (10) will be $\rho^{CORR} = 0.257$ mm, which exceeds the specified admissible limit value ρ_{dop} .

Using formula (14), we calculate the minimum skew angle of the longitudinal MCAI $\alpha_{X \min}$, not exceeding the value $\alpha_{\Gamma/\Delta_{don}}$ wherein it is possible to provide a value of the transverse displacement of the center of mass for this FM design equal to ρ_{dop} . As a result of the calculation, we shall obtain: $\alpha_{X \min} = -8.5'$, i. e. inequality

$|\alpha_{X \min}| \leq \alpha_{Xdop}$ will be correct. In this case, the minus sign indicates the inclination of the longitudinal MCAI with its upper end towards the geometric axis of the FM.

We shall define the value of the imbalance vector $\vec{D}_{B|\alpha_{X \min}}^{CORR}$ in the plane of correction B, ensuring the achievement of the value $|\alpha_{X \min}|$, according to the formula (15). We shall obtain: $D_{B|\alpha_{X \min}}^{CORR} = 9581.4$ g·mm, phase angle $\alpha_{B|\alpha_{X \min}}^{CORR} = 277.5^\circ$. The value of imbalance $\vec{D}_{H|\alpha_{X \min}}^{CORR}$ which is co-directional to imbalance \vec{D}_H^{KOMP} we shall define according to the formula (16): $D_{H|\alpha_{X \min}}^{CORR} = 19581.4$ g·mm, phase angle $\beta_{H|\alpha_{X \min}}^{CORR} = 97.5^\circ$. Moreover, the value of the additional imbalance \vec{D}_H^{DPL3} , oppositely directed to the imbalance $\vec{D}_{B|\alpha_{X \min}}^{CORR}$, will be defined as following (17): $D_H^{DPL3} = 2874.4$ g·mm, phase angle $\beta_H^{DPL3} = 97.5^\circ$.

Using the corresponding parameters of the simulated imbalance vectors $\vec{D}_{B|\alpha_{X \min}}^{CORR}$ and \vec{D}_B^{COMP} , we shall determine the value and the angular position of the vector of the balancing imbalance $\vec{D}_{B|\alpha_{X \min}}^{BAL}$ in the regular correction plane using formulas (18) and (19): $D_{B|\alpha_{X \min}}^{BAL} = 34259.3$ g·mm, phase angle $\alpha_{B|\alpha_{X \min}}^{BAL} = 268.75^\circ$.

In accordance with (20) the mass of the balancing weight will be $m_{B|\alpha_{X \min}}^{BAL} = 171.3$ g, and its setting angle $\varphi_{B|\alpha_{X \min}}^{BAL}$ in the correction plane B will coincide with the angle $\alpha_{B|\alpha_{X \min}}^{BAL}$, i. e. will be equal to 268.75° .

To assess the correct operation of the considered algorithm, we shall make sure that the estimated value of the displacement of the center of mass $\rho_{|\alpha_{X \min}}^{CALC}$ will be a value close to ρ_{dop} after attaching the weights to the FM.

Imbalance value $\vec{D}_{H|\alpha_{X \min}}^{BAL}$ (not shown on figure), oppositely directed to imbalance $\alpha_{B|\alpha_{X \min}}^{BAL}$, appearing in place of imbalances D_H^{DPL1} and D_H^{DPL3} in the plane of correction H as a result of the imbalance $D_{B|\alpha_{X \min}}^{BAL}$, can be determined by the formula

$$D_{H|\alpha_{X \min}}^{BAL} = D_{B|\alpha_{X \min}}^{BAL} K_{HB}. \quad (24)$$

Thus: $D_{H|\alpha_{X \min}}^{BAL} = 10498.8$ g·mm, phase angle $\beta_{H|\alpha_{X \min}}^{BAL} = 88.75^\circ$. The calculated value of the displacement of the center of mass of the FM, omitting the mass of the balancing weight (as insignificantly small), will be defined by the formula:

$$\rho_{|\alpha_{X \min}}^{CALC} = \frac{\vec{D}_B^{NACH} + \vec{D}_H^{NACH} + \vec{D}_{B|\alpha_{X \min}}^{BAL} + \vec{D}_{H|\alpha_{X \min}}^{BAL}}{M}. \quad (25)$$

We shall obtain: $\rho_{|\alpha_{X \min}}^{CALC} = 0.11$ mm, which practically corresponds to the set value ρ_{dop} .

Thus, as a result of the calculation carried out according to the proposed algorithm, the required parameters of the balancing weight were found, the installation of which ensures the fulfillment of condition (23) with a deviation of the longitudinal MCAI from its geometric axis as low as practicable for this FM. Good consistency of the calculated data is confirmed, which proves the correctness of the balancing calculation.

Conclusion. The considered balancing algorithm for a conical flying model in dynamic mode using a single correction plane structurally located at a considerable distance from the center of mass of the model, with optimization according to the criterion of achieving the minimum skew angle of the longitudinal main centroidal axis of inertia, complements the algorithm [1; 2; 12]. The algorithm has been pilot tested with getting positive results on a newly designed vertical dynamic balancing stand with gas supports and is protected by patent of the Russian Federation under No. 2694142 [18]. Work is being carried out to introduce the algorithm into the FM balancing method. The algorithm allows to reduce the number of balancing steps (as a rule, to one step), or by calculation to prove the impossibility of balancing the FM with the given parameters, and, accordingly, reduce the time of the balancing experiment.

References

1. Klyuchnikov A. V. [Development and improvement of the algorithm single-plane balancing in a dynamic mode of high-speed flying models]. *Vestnik SibGAU*. 2015. Vol. 16, No. 2, P. 411–416 (In Russ.).
2. Klyuchnikov A. V. [Numerical algorithm for the optimization of process trim tapered flying models on dynamic balancing stand]. *Vestnik SibGAU*. 2016, Vol. 17, No. 2, P. 309–317 (In Russ.).
3. Glazyrina L. M., Karpovitskiy M. S., Klyuchnikov A. V., Malgin A. I., Smirnov G. G., Fomin Yu. P. *Balansirovochnyy stend s vertikalnoy osyu vrashcheniya* [Balancing stand with vertical axis of gyration]. Patent RF, no. 2292533, 2007.
4. Glazyrina L. M., Karpovitskiy M. S., Klyuchnikov A. V., Malgin A. I., Smirnov G. G., Fomin Yu. P. *Sposob balansirovki rotora* [Rotor's counterbalancing method]. Patent RF, no. 2292534, 2007.
5. Dmitriyevskii A. A., Lysenko L. N., Bogodistov S. S. *Vneshnyaya ballistika* [External ballistics]. Moscow, Mashinostroenie Publ., 1991, 640 p.
6. Pravdin V. M., Shanin A. P. *Ballistics of uncontrollable flying machines* [Ballistika neupravlyaemih letatelnykh apparatov]. Snezhinsk, RFNC-VNIITF Publ., 1999, 496 p.
7. Klyuchnikov A. V. [The algorithm of single-plane dynamic balancing process of a conical flying prototype with optimization by criteria of achieve the minimum deviation of main centroidal axis of inertia]. *Materialy XXIII Mezhdunarodnoy nauchnoy konferentsii "Reshetnevskie chteniia"* [Proc. 23th Int. Technol. Conf. "Reshetnev reading"]. Krasnoyarsk, 2019, Part 1, P. 30–32 (In Russ.).
8. Ilinykh V. V., Klyuchnikov A. V., Mihailov E. F., Timoshchenko A. G. [Technological support of quality during the manufacture of hypersonic uncontrollable flying models]. *Vestnik SibGAU*. 2013, Vol. 49, No. 3, P. 191–196 (In Russ.).
9. Klyuchnikov A. V. [Method of eliminate a technological rig on measurement results during dynamic counterbalancing of flying vehicle]. *Materialy XIX Mezhdunarodnoy nauchnoy konferentsii "Reshetnevskie chteniia"* [Proc. 19th Int. Technol. Conf. "Reshetnev reading"]. Krasnoyarsk, 2015, Part 1, P. 21–23 (In Russ.).
10. Abyshev N. A., Klyuchnikov A. V., Mikhailov E. F., Chertkov M. S. [Stand for precise non-contactable counterbalancing in dynamic regimen of conical rotors]. *Trudy XIX Mezhdunarodnogo simpoziuma "Nadyozhnost i kachestvo"* [Proc. 19th Int. Technol. Symp. "Reliability & Quality"]. Penza, 2014, Vol. 2, P. 234–236 (In Russ.).
11. Klyuchnikov A. V. [Test equipment for diagnostics of a mass symmetry distribution of compound rotor's details]. *Trudy IX Mezhdunarodnoy nauchno-prakticheskoy konferentsii "Innovatsii na osnove informatsionnykh i kommunikatsionnykh tekhnologiy"* [Proc. 9th Int. Scientif. and Pract. Conf. "Innovations Based on Information and Communication Technologies"]. Moscow, 2012, Part 1, P. 21–23 (In Russ.).
12. Klyuchnikov A. V. *Sposob balansirovki rotora v odnoy ploskosti korrektsii* [Method of rotor's counterbalancing in singular place for correction]. Patent RF, no. 2499985, 2013.
13. Klyuchnikov A. V. [Precised mathematical model for valuing of mass-inertia asymmetry parameters of a lengthened rotor]. *Trudy XVII Mezhdunarodnogo simpoziuma "Nadyozhnost i kachestvo"* [Proc. 17th Int. Technol. Symp. "Reliability & Quality"]. Penza, 2013, Vol. 1, P. 224–227 (In Russ.).
14. Andreev S. V., Klyuchnikov A. V., Mihailov E. F. [Prospects of application of dynamic counterbalancing method for testing of flying machine's mass-inertia asymmetry parameters]. *Materialy XVIII Mezhdunarodnoy nauchnoy konferentsii "Reshetnevskie chteniia"* [Proc. 18th Int. Technol. Conf. "Reshetnev reading"]. Krasnoyarsk, 2014, Part 1, P. 8–10 (In Russ.).
15. Klyuchnikov A. V. *Sposob nastroyki balansirovochnogo stenda dlya opredeleniya parametrov masso-inertsionnoy asimetrii rotorov* [Method of adjusting a counterbalance machine for determination of rotors' mass-inertia parameters]. Patent RF, no. № 2453818, 2013.
16. Klyuchnikov A. V. [Methodical ensuring a process of individual adjusting the dynamic balancing machine in the controlled object]. *Trudy XIV Mezhdunarodnoy nauchno-prakticheskoy konferentsii "Innovatsii na osnove informatsionnykh i kommunikatsionnykh tekhnologiy"* [Proc. 14th Int. Scientif. and Pract. Conf. "Innovations Based on Information and Communication Technologies"]. Moscow, 2017, P. 382–386 (In Russ.).
17. Andreev S. V., Klyuchnikov A. V., Lysykh A. V., Mikhailov E. F. [Calibrate operations during detail's module counterbalancing on a non-adjusted dynamic counterbalance machine]. *Trudy XVIII Mezhdunarodnogo simpoziuma "Nadyozhnost i kachestvo"* [Proc. 18th Int. Technol. Symp. "Reliability & Quality"]. Penza, 2013, Vol. 2, P. 129–131 (In Russ.).
18. Klyuchnikov A. V. *Sposob balansirovki rotora v odnoy ploskosti korrektsii* [Method of rotor's counterbalancing in singular place for correction]. Patent RF, no. 2694142, 2019.

Библиографические ссылки

1. Ключников А. В. Развитие и совершенствование алгоритма одноплоскостной балансировки в динамическом режиме высокоскоростной летающей модели // Вестник СибГАУ. 2015. Т. 16, № 2. С. 411–416.
2. Ключников А. В. Численный алгоритм оптимизации процесса уравнивания конической летающей модели на динамическом балансировочном стенде // Вестник СибГАУ. 2016. Т. 17, № 2. С. 309–317.
3. Пат. 2292533 Российская Федерация, МПК G 01 М 1/02. Балансировочный стенд с вертикальной осью вращения / Л. М. Глазырина, М. С. Карповицкий, А. В. Ключников, А. И. Мальгин, Г. Г. Смирнов, Ю. П. Фомин. № 2004112999/28 ; заявл. 27.04.2004 ; опубл. 27.01.2007, Бюл. № 3. 8 с.
4. Пат. 2292534 Российская Федерация, МПК G 01 М 1/04. Способ балансировки ротора / Л. М. Глазырина, М. С. Карповицкий, А. В. Ключников, А. И. Мальгин, Г. Г. Смирнов, Ю. П. Фомин. № 2004112998/28 ; заявл. 27.04.2004 ; опубл. 27.01.2007, Бюл. № 3. 8 с.
5. Дмитриевский А. А., Лысенко Л. Н., Богодисов С. С. Внешняя баллистика. М. : Машиностроение, 1991. 640 с.
6. Правдин В. М., Шанин А. П. Баллистика неуправляемых летательных аппаратов. Снежинск : РФЯЦ-ВНИИТФ, 1999. 496 с.
7. Ключников А. В. Алгоритм одноплоскостной балансировки летающей модели конической формы с оптимизацией по критерию достижения минимального отклонения главной центральной оси инерции // Решетнёвские чтения : материалы XXIII Междунар. науч. конф. (11–15 ноября 2019, Красноярск) : в 2 ч. / под общ. ред. Ю. Ю. Логинова ; Сиб. гос. ун-т. Красноярск, 2019. Ч. 1. С. 30–32.
8. Технология обеспечения качества при изготовлении высокоскоростных неуправляемых летающих моделей / В. В. Ильиных, А. В. Ключников, А. В. Лысых и др. // Вестник СибГАУ. 2013. № 3 (49). С. 191–196.
9. Ключников А. В. Способ устранения влияния технологической оснастки на результаты измерений в процессе динамической балансировки летательного аппарата // Решетнёвские чтения : материалы XIX Междунар. науч. конф. (10–13 ноября 2019, г. Красноярск) : в 2 ч. / под общ. ред. Ю. Ю. Логинова ; Сиб. гос. аэрокосмич. ун-т. Красноярск, 2015. Ч. 1. С. 21–23.
10. Стенд для прецизионной бесконтактной балансировки конических роторов в динамическом режиме / Н. А. Абышев, А. В. Ключников, Е. Ф. Михайлов, М. С. Чертков // Надежность и качество : тр. 19 междунар. симп. (26 мая – 1 июня 2014, г. Пенза.) : в 2 т. / под ред. Н. К. Юркова ; Пенз. гос. ун-т. Пенза, 2014. Т. 2. С. 234–236.
11. Ключников А. В. Испытательное оборудование для диагностики симметричности распределения масс сложных роторных деталей // Инновации на основе информационных и коммуникационных технологий : тр. IX междунар. науч.-практ. конф. (1–10 октября 2012, г. Сочи.) / под ред. С. У. Увайсова ; МИЭМ НИУ ВШЭ. Москва, 2012. С. 362–364.
12. Пат. 2499985 Российская Федерация, МПК G 01 М 11/16. Способ балансировки ротора в одной плоскости коррекции / А. В. Ключников. № 2012114312/28 ; заявл. 11.04.2012 ; опубл. 27.11.2013, Бюл. № 33. 9 с.
13. Ключников А. В. Уточнённая математическая модель оценки и обеспечения параметров массо-инерционной асимметрии длинномерного роторного модуля // Надежность и качество : тр. междунар. симп. (26 мая – 1 июня 2014, г. Пенза.) : в 2 т. / под ред. Н. К. Юркова ; Пенз. гос. ун-т. Пенза, 2014. Т. 1. С. 224–227.
14. Андреев С. В., Ключников А. В., Михайлов Е. Ф. Перспективы применения метода динамической балансировки для определения параметров асимметрии масс летательного аппарата // Решетнёвские чтения : материалы XVIII Междунар. науч. конф. (11–14 ноября 2014, г. Красноярск) : в 3 ч. / под общ. ред. Ю. Ю. Логинова ; Сиб. гос. аэрокосмич. ун-т. Красноярск, 2014. Ч. 1. С. 8–10.
15. Пат. 2453818 Российская Федерация, МПК G 01 М 01/22. Способ настройки балансировочного стенда для определения параметров массо-инерционной асимметрии роторов / А. В. Ключников. № 2011100182/28 ; заявл. 11.01.2011 ; опубл. 27.11.2013, Бюл. № 17. 8 с.
16. Ключников А. В. Методическое обеспечение процесса индивидуальной настройки динамического балансировочного стенда на объект контроля // Инновационные, информационные и коммуникационные технологии : материалы XIV междунар. науч.-практ. конф. (1–10 октября 2017 г. Сочи.) / под ред. С. У. Увайсова ; Ассоциация выпускников и сотрудников ВВИА им. проф. Жуковского. Москва, 2017. С. 382–386.
17. Калибровочные операции в процессе модульной балансировки детали на ненастроенном динамическом балансировочном стенде / С. В. Андреев, А. В. Ключников, А. В. Лысых, Е. Ф. Михайлов // Надежность и качество : тр. XVIII междунар. симп. (27 мая – 3 июня 2013, г. Пенза) : в 2 т. / под ред. Н. К. Юркова ; Пенз. гос. ун-т. Пенза, 2013. Т. 2. С. 129–131.
18. Пат. 2694142 Российская Федерация, МПК G 01 М 11/16. Способ балансировки ротора в одной плоскости коррекции / А. В. Ключников. № 2018134252/28 ; заявл. 27.09.2018 ; опубл. 09.07.2019, Бюл. № 19. 9 с.

© Klyuchnikov A. V., 2020

Klyuchnikov Aleksandr Vassilyevich – Cand. Sc., head of the designer's department; Federal State Unitary Enterprise "RFNC-VNIITF named after Academician E. I. Zababakhin". E-mail: a.klyuchnikov@bk.ru.

Ключников Александр Васильевич – кандидат технических наук, начальник конструкторского отдела; ФГУП «РФЯЦ-ВНИИТФ имени академика Е. И. Забабахина». E-mail: a.klyuchnikov@bk.ru.

UDC 629.07.058

Doi: 10.31772/2587-6066-2020-21-1-78-84

For citation: Komlev G. V., Mitrofanova A. S. To the question of forecasting the technical condition of low-thrust liquid rocket engines. *Siberian Journal of Science and Technology*. 2020, Vol. 21, No. 1, P. 78–84. Doi: 10.31772/2587-6066-2020-21-1-78-84

Для цитирования: Комлев Г. В., Митрофанова А. С. К вопросу прогнозирования технического состояния жидкостных ракетных двигателей малой тяги // Сибирский журнал науки и технологий. 2020. Т. 21, № 1. С. 78–84. Doi: 10.31772/2587-6066-2020-21-1-78-84

TO THE QUESTION OF FORECASTING THE TECHNICAL CONDITION OF LOW-THRUST LIQUID ROCKET ENGINES

G. V. Komlev^{1,2*}, A. S. Mitrofanova^{1,3}

¹Reshetnev Siberian State University of Science and Technology
31, Krasnoyarsky Rabochy Av., Krasnoyarsk, 660037, Russian Federation

²JSC “Krasmach”

29, Krasnoyarsky Rabochy Av., Krasnoyarsk, 660123, Russian Federation

³JSC “Academician M. F. Reshetnev “Information Satellite Systems”

52, Lenin St., Zheleznogorsk, Krasnoyarsk region, 662972, Russian Federation

*E-mail: komlev_gv@mail.ru

In the rapidly developing space and rocket industry, spacecrafts are being equipped with low-thrust liquid rocket engines. High requirements are imposed on the reliability, efficiency and economy of fuel use for this type of rocket engine. To ensure monitoring of the characteristics of spacecrafts, a functional diagnostic system is used, which includes telemetry and analytical data processing. Telemetry performs the functions of receiving and transmitting information. Information processing is carried out in computer centers located on the spacecraft and the Earth. The most promising computing tool capable of predicting time series and classifying a large amount of interconnected data is considered an artificial neural network. In this regard, the subject of research in the work is data processing methods based on an artificial neural network. The purpose of the work is to develop a method for forecasting the technical condition of low-thrust liquid rocket engines using an artificial neural network.

The relevance of research on the use of a neural network in the system of functional diagnostics of low-thrust liquid rocket engines for spacecraft is explained in the introduction. In the main part, an analysis of many telemetric data of the rocket engine is carried out and their strength in the forecast of the main diagnostic parameters is determined. It is proposed to use traction, specific impulse, and temperature of the structure as diagnostic parameters. The prognostic capabilities of the neural network were investigated and a schematic diagram of a method for predicting the technical condition of a low-thrust liquid rocket engine was developed. In the developed method, at the first stage, the neural network performs the approximation of the function and extrapolates the time series of telemetric data; the second stage determines the probable class of the technical condition of the engine.

The conclusion outlines a plan for further experimental research in the study area and provides recommendations on the development and improvement of algorithms for functioning of artificial neural networks as part of the functional diagnostics system of the spacecraft. Due to the generalized nature of the methodological schemes, the results of the work can be applied to any type of rocket engines and used at all enterprises of the rocket and space industry of the corresponding profile.

Keywords: rocket engine, telemetry, neural network, diagnostic parameter, approximation, classification, forecasting.

К ВОПРОСУ ПРОГНОЗИРОВАНИЯ ТЕХНИЧЕСКОГО СОСТОЯНИЯ ЖИДКОСТНЫХ РАКЕТНЫХ ДВИГАТЕЛЕЙ МАЛОЙ ТЯГИ

Г. В. Комлев^{1,2*}, А. С. Митрофанова^{1,3}

¹Сибирский государственный университет науки и технологий имени академика М. Ф. Решетнева
Российская Федерация, 660037, г. Красноярск, просп. им. газ. «Красноярский рабочий», 31

²АО «Красмаш»

Российская Федерация, 660123, г. Красноярск, просп. им. газ. «Красноярский рабочий», 29

³АО «Информационные спутниковые системы» имени академика М. Ф. Решетнева»

Российская Федерация, 662972, г. Железногорск Красноярского края, ул. Ленина, 52

*E-mail: komlev_gv@mail.ru

В стремительно развивающейся ракетно-космической отрасли создаются космические аппараты, снабжённые жидкостными ракетными двигателями малых тяг. К данному типу ракетных двигателей предъявляются высокие требования по надёжности, эффективности и экономичности использования топлива. Для

обеспечения мониторинга характеристик космических аппаратов используют систему функциональной диагностики, в состав которой входят средства телеметрии и аналитической обработки данных. Телеметрия выполняет функции получения и передачи информации. Обработка информации выполняется в вычислительных центрах, находящихся на космическом аппарате и Земле. Наиболее перспективным вычислительным инструментом, способным проводить прогнозирование временных рядов и классифицировать большой объём взаимосвязанных данных, считают искусственную нейронную сеть. В связи с этим предметом исследований в работе являются способы обработки данных с применением искусственной нейронной сети. Цель работы заключается в разработке метода прогнозирования технического состояния жидкостных ракетных двигателей малых тяг с использованием искусственной нейронной сети.

Во введении обосновывается актуальность исследований по использованию нейросети в системе функциональной диагностики жидкостных ракетных двигателей малых тяг для космических аппаратов. В основной части проводится анализ множества телеметрических данных ракетного двигателя и определена их весомость при прогнозе основных диагностических параметров. В качестве диагностических параметров предложено использовать тягу, удельный импульс и температуру конструкции. Исследованы прогностические возможности нейросети и разработана принципиальная схема метода прогнозирования технического состояния жидкостного ракетного двигателя малой тяги. В разработанном методе на первом этапе нейросеть выполняет аппроксимацию функции и экстраполяцию временного ряда данных телеметрических данных, на втором – определяет вероятный класс технического состояния двигателя.

В выводах намечен план дальнейших экспериментальных исследований в данной области и даются рекомендации по разработке и совершенствованию алгоритмов функционирования искусственных нейронных сетей в составе системы функциональной диагностики космического аппарата. В силу обобщённого характера методических схем, результаты работы могут применяться к любому типу ракетных двигателей и использоваться на всех предприятиях ракетно-космической отрасли соответствующего профиля.

Ключевые слова: ракетный двигатель, телеметрия, нейросеть, диагностический параметр, аппроксимация, классификация, прогнозирование.

Introduction. In the rocket and space industry, in the development of spacecrafts (SC), a significant part of the project time is occupied by the development of low-thrust liquid rocket engines (ZhRDMT). With this type of propulsion systems, the spacecraft can perform complex maneuvers in space [1; 2].

The terminology in GOST 22396–77 “Low-thrust liquid engines” defines ZhRDMT as executive bodies of a spacecraft control system with a thrust from 0.01 to 1600 N. The low-thrust liquid engines can be combined into a low-thrust liquid engine module as an assembly unit consisting of several liquid-propellant engines and at least one common element (power frame, panel, fuel supply system, thermal insulation, etc.).

The purpose of the low-thrust liquid rocket engines and their operating conditions impose on them a whole series of specific requirements and the following in particular:

- multi-mode, due to continuous operation (duration up to $\tau_b > 10^3$ s) and in various pulse modes with a minimum on-time of 0.03 s or less and with various pauses – from 0.03 s to several days; the pulsed mode is divided into the mode of single short switching with long pauses between switching on, the pulsed mode, when short switching is alternating with pauses of various durations, and the mode of “connected” switching with very short pauses;
- a large resource for the total operating time – up to 50.000 s or more;
- a large resource for the total number of on-time periods – up to 10^6 ;
- the possibility of any combination of on-time and pauses;
- ensuring high efficiency, specific impulse (I_{sp}) of more than 2950 Ns/kg (300 s) for two-component low-

thrust liquid engines on a self-igniting pair of “nitrogen tetroxide (NT) and asymmetric dimethylhydrazine (ADMH)”;

- high reliability during operation – more than 10 years, which requires an acceptable thermal state, both during engine operation and during prolonged silence.

Low-thrust liquid rocket engines should have high reliability indicators, minimum weight and outer dimensions, increased resource, efficiency, stability, and minimal energy consumption. Ensuring a high level of these indicators at all stages of operation of a rocket engine requires accurate control of diagnostic parameters (DP) with subsequent prediction of the technical condition [3; 4]. For these purposes, the spacecraft is equipped with a functional diagnostic system (FDS), which allows to obtain diagnostic information about the low-thrust liquid rocket engine quickly, process data and issue a decision on the strategy for further operation.

Algorithms for monitoring DP and fault detection in FDS are based on mathematical models of work processes [5–8].

At present the development of rocket technology is impossible without telemetry on spacecraft engines. Telemetry tools collect and convert sensor signals, store and transmit information to the control center. The use of telemetry can increase the information content and completeness of tests of low-thrust liquid rocket engines, reduce the number of tests and streamline planning in the shortest possible time [9; 10].

The main tasks of diagnosing low-thrust liquid rocket engines using telemetry tools are as follows [11]:

- determination of the correct functioning of the engine at all possible operating modes;
- troubleshooting, indicating the location and possible cause of occurrence;

- assessment of reliability indicators;
- predicting the correct functioning of the engine during further operation.

Despite the great successes in the development of low-thrust liquid rocket engines and methods for diagnosing them, it is practically impossible to determine the whole set of defects, this is due to the fact that violations of the integrity of engine components and work processes can equally manifest themselves in diagnostic signs. In addition, the design and arrangement of the sensors are imperfect, as a result, when evaluating the DP there are limitations in the accuracy of the results [11], and in the case of a large set of diagnostic data, it is difficult to determine the degree of their interdependence and the degree of weight in determining the technical condition.

Nowadays these problematic issues are successfully solved by calculation methods using artificial neural networks (ANNs). This is due to the ability of ANNs to learn how to approximate functions and extrapolate, divide a lot of diagnostic data into classes and select the most informative features that carry the most complete information about the hidden laws of the state of the system. All of these operations ANN can perform in parallel with limited information [12–14].

In accordance with the abovementioned **the aim of the work** is to develop a method for predicting the technical condition of low-thrust liquid rocket engines using ANNs when processing telemetric data.

Selection of defining telemetry data for ANN. The spacecraft's active life in outer space is limited by the fuel reserves on board and can be increased by increasing the efficiency of its use. Depending on the tasks performed, the low-thrust liquid rocket engines should operate continuously and in pulse modes. When operating in the pulse mode, the low-thrust liquid rocket engine must have a minimum time to reach the steady state when the engine is turned on and a minimum thrust decay time when it is turned off. The number of engine starts during operation is hundreds of thousands; therefore, the impact of fuel economy is significant. It is of great importance for engines of the control system to ensure a minimum and stable momentum value of the engine afteraction pulse. The afteraction pulse is mainly a function of the valve response time, valve volumes and the number of unreacted fuel components.

A high level of dynamic and energy characteristics of the engine will depend to a large extent on the effective organization of the liquid-phase interaction of the fuel components, which will intensify the course of the conversion of fuel into high-temperature combustion products of the engine. On the other hand, to increase the reliability of low-thrust liquid rocket engines, it is necessary to reduce thermal loads on structural elements.

In the spectrum of thrust fluctuations, the frequency characteristics of the engine can be distinguished, the change of which can be used as a sign of a violation of normal functioning. Therefore, thrust is of independent importance and should be considered as a necessary DP in assessing the correct functioning of the engine [11].

Thus, the thrust (P), specific impulse of thrust (I_v) and the thermal state of the structure (T_{frame}) should be used as the DP for the low-thrust liquid rocket engine [15–17].

When determining these DPs, the general telemetric data are [15]:

m_f – mass fuel consumption, kg/s;

T_f – fuel temperature, K;

p_c – the pressure in the combustion chamber, Pa;

t_v – valve performance, s;

t_w – engine working time, s.

The selected factors are the most informative and carry all the information about the relationships among the DP. Therefore, the full range of telemetry tools for monitoring and transferring these characteristics to the ANN, as well as a special neural network algorithm, should be included in the FDS for the low-thrust liquid fuel engine.

Possibilities of ANN when processing telemetric data of a low-thrust liquid rocket engine. At present, more serious requirements are made to the information content of the telemetry information transmission channel from the spacecraft [18]. In modern FDS of rocket engines, DPs are divided into slowly and rapidly changing ones, the first include pressure, temperature, fuel consumption, position of the drives, the second include ripple of the propellant components, vibration and voltage of the body parts. Slowly changing diagnostic parameters are measured with a frequency from 0 to 100 Hz, rapidly changing ones are measured with a frequency from 100 to 30.000 Hz [11]. Telemetry sensors are installed based on the design features of the engine, and often they do not meet the requirements to ensure the necessary depth of diagnostics.

The transmission speed of 8 kbit/s in the telemetry channel of the spacecraft control system is considered unsatisfactory [19]. An increase in information content of the channel can be achieved by increasing the physical speed of telemetry and the frequency of the radio channel range and thus increasing high technical costs. Another solution is to compress the information before sending it to the channel.

An additional point is that there are errors in the orientation and stabilization of the spacecraft, which lead to fluctuations in the measured values, as a result the incoming telemetry information may contain lost portions of the communication session with the spacecraft.

When making diagnostic monitoring during the flight of the low-thrust liquid rocket engines, not only processed telemetry information with minimal data loss is important, but also its high-quality visualization and analysis. Decoding the recorded signal significantly reduces the control efficiency of the spacecraft; this operation takes from 15 to 20 minutes, which takes a quarter of the average orbital period of many small spacecrafts [20; 21].

The listed factors that inhibit the process of operational control of the spacecraft also include special software for processing telemetric information.

For this reason, in order to increase the speed and accuracy of real-time of telemetric data of low-thrust liquid rocket engines, it is advisable to use ANN. As already mentioned, the main advantage of ANNs over other artificial computing systems is the ability to learn, generalize and highlight hidden relationships between input and output data. ANNs make it possible to increase the reliability of the spacecraft operation due to the intelligent analysis

and prediction of possible deviations of the onboard subsystem parameters from the established standard values. In the space industry, ANNs are increasingly being used in solving management, control, and diagnostic tasks [22–24].

The main functional unit of the ANN is a neuron. The synapses receive data from the sensors of the FDS into the neurons. At the output the data is converted in accordance with the settings of the neurons using various functions (fig. 1). The input of one neuron may be the outputs of other neurons. The accuracy of solving problems is determined by the number of neurons, connections and their activation properties.

To solve forecasting problems using ANNs, the function approximation approach is used. In this case, the adjustable parameters of the neural network during training take the form corresponding to some function that describes the time series of telemetry data. It should be noted that forecasting makes sense only when a previous

change in diagnostic features predetermines the future value.

The forecasting process is reduced to the following sequence of stages [25–27]:

- preparation of initial telemetry data;
- training of the ANN;
- checking the adequacy of the ANN;
- description of the ANN using algebraic or logical functions with a purpose to use it further.

At the same time, the ANN can be used as a classifier of the state of a low-thrust liquid rocket engine (fig. 2). When solving the classification problem, the ANN breaks down the set of telemetry input signals, determines which class the input signal belongs to, and signals new states. It means that the neural network can identify previously unknown classes of the state of diagnosed systems, which is very important for developing new strategies for the further operation of the rocket engine.

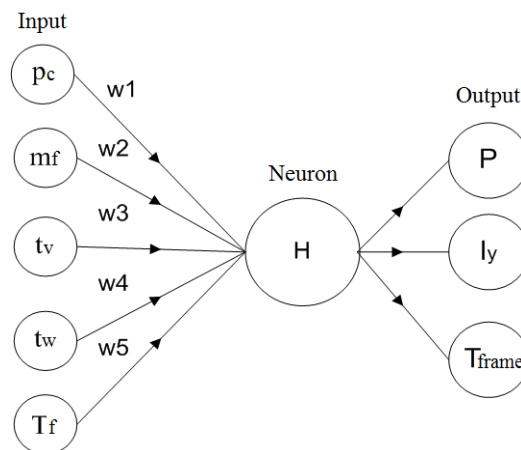


Fig. 1. ANN structure in FDS of rocket engines, where
 $H = p_k \cdot w_1 + m_f \cdot w_2 + t_v \cdot w_3 + t_w \cdot w_4 + T_f \cdot w_6$;
 w_i – coupling weight; $P, I_y, T_{frame} = f(H)$

Рис. 1. Структура ИНС в СФД ракетных двигателей, где
 $H = p_k \cdot w_1 + m_f \cdot w_2 + t_{кл} \cdot w_3 + t_{раб} \cdot w_4 + T_{топ} \cdot w_6$;
 w_i – весовой коэффициент связи; $P, I_y, T_{кон} = f(H)$

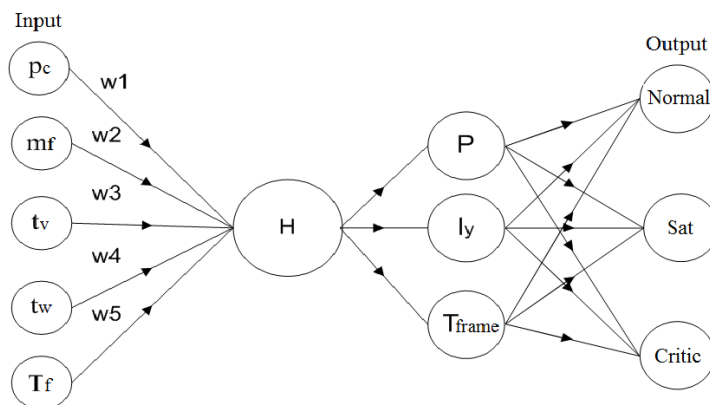


Fig. 2. Scheme of the neural network as a classifier of probabilistic states of a low-thrust liquid rocket engine

Рис. 2. Схема работы нейросети как классификатора вероятностных состояний ЖРДМТ

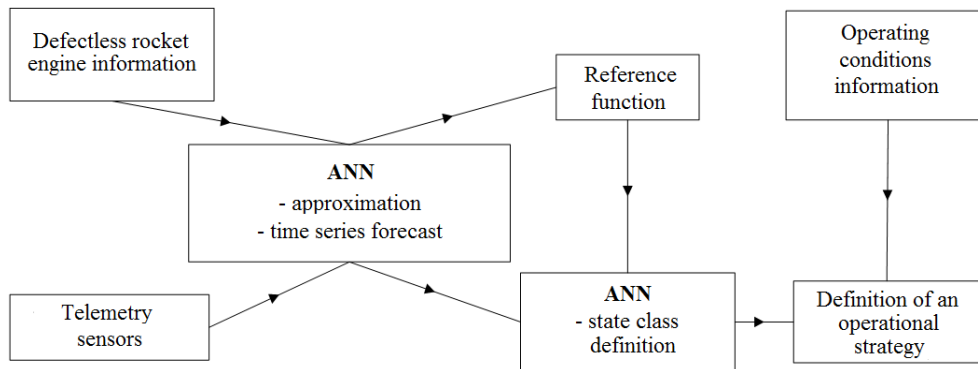


Fig. 3. Block diagram of a method for forecasting the technical condition of a rocket engine

Рис. 3. Блок-схема метода прогнозирования технического состояния ракетного двигателя

In this case, the ANN calculates the probability of the current state and assigns the state of the engine to one of the classes distinguished by the standards. Having processed the set of incoming data, the output neuron produces a signal corresponding to a certain class of technical condition (normal, satisfactory, critical).

Thus, the ANN can be used as a tool for calculating the value of the DP in a certain period of time and as a determinant of the current technical condition of a low-thrust liquid rocket engine.

A method for forecasting the technical condition of a low-thrust liquid rocket engine based on the ANN.

The general objective of the method for forecasting the technical condition of rocket engines, using the ANN as the analytical block of the FDS, is reduced to comparing the approximated function of the current value of the DP with its reference value in appropriate operating conditions. At the same time, the tasks of extrapolating the time series of telemetric data values for a given period of time and determining the class of the engine condition are solved (fig. 3). The proposed method consists of the following steps:

- telemetry of the functioning of the low-thrust liquid rocket engine;
- a control data set training of the ANN;
- extrapolation of the DP value for a given period of time in the ANN;
- defining the class of the current state in the ANN;
- formation of a further operational strategy.

Conclusion 1. In the case of a close interrelationship of the telemetric data of diagnostic features, it is difficult to determine the degree of their weight in determining the class of the current technical condition, as well as to forecast the further development of the functioning processes of the low-thrust liquid rocket engine.

2. The most informative features of the normal functioning of the low-thrust liquid rocket engine should include: mass fuel consumption, fuel temperature, pressure in the combustion chamber, valve performance and engine operating time. The selected features are necessary when regulating traction, specific impulse and temperature of structural elements.

3. The use of the ANN to forecast the technical condition of the low-thrust liquid rocket engine, under the conditions of a minimum amount of information coming

from the sensors of the FDS, makes it possible to extrapolate time series accurately and determine the current state of the system. But the use of the ANN involves training and retraining, which imposes significant restrictions on the efficiency of control of low-thrust liquid propellant rocket engines during the flight.

4. To verify the effectiveness of the developed method, first of all, it is required to develop a simulation model capable of generating a discrete data stream, which is telemetric information about the diagnostic features of low-thrust liquid rocket engines, and after that the ANN will be trained in forecasting and distinguishing technical condition classes. The final stage of verification should be carried out using real experimental data.

References

1. Ageenko Ju.I., Pegin I.V. [Confirmation of the energy efficiency of liquid propellant rocket engines with a deflector centrifugal mixture formation scheme]. *Vestnik Samarskogo gosudarstvennogo aerokosmicheskogo universiteta*. 2014, No. 5, Iss. 3, P. 46–54 (In Russ.).
2. Sirant A. L. *Issledovanie vliyaniya neideal'nostey rabocheho impul'sa zhidkostnykh raketnykh dvigateley maloy tyagi na dinamiku malogo kosmicheskogo apparata. Kand. Diss.* [Investigation of the effect of imperfect working impulse of liquid propulsion thruster on the dynamics of a small spacecraft. Cand. Diss.]. Samara, 2008, 153 p.
3. Hruckij O. V. *Prognozirovanie tehničeskogo sostojanija funkcional'no-samostojatel'nyh elementov sudovoy energeticheskoy ustanovki. Kand. Diss.* [Prediction of the technical condition of functionally independent elements of a ship power plant. Cand. Diss.]. SPb., 1996, 263 p.
4. Gerasimova D. S., Savina M. G., Gejman V. N. [Updating and extending aircraft technology resources]. *Aktual'nye problemy aviatsii i kosmonavtiki*. 2015, Vol. 1, P. 686–688 (In Russ.).
5. Martirosov D. S., Kolomencev A. I. [Functional diagnostics of LRE in real time]. *Aviatsionno-kosmicheskaya tekhnika i tekhnologiya*. 2012, No. 7, P. 197–201 (In Russ.).
6. Martirosov D. S., Sin'kov S. A. [A method for evaluating the maximum achievable accuracy of deter-

mining the parameters of the elements of rocket engines in their functional diagnostics]. *Tr. NPO Energomash im. akad. V. P. Glushko*. 2005, No. 23, P. 151–160 (In Russ.).

7. Kolbaja T. Ch., Pasmurnov S. M., Jakush D. Ju. [Development of technology for creating a system for diagnosing and emergency protection of liquid rocket engines]. *Inzhenernyy zhurnal: Nauka i innovatsii*. 2016, No. 8. Available at: <http://www.engjournal.ru/catalog/arise/teje/1524.html> (In Russ.).

8. Bondar' A. I., Pasmurnov S. M., Jakush D. Ju. [Software and software for the emergency protection and control system for rocket engines and the procedure for testing it]. *Nauka i tehnologii. Sb. nauch. tr. RAN*. 2015, Vol. 5, P. 137 (In Russ.).

9. Skovoroda-Luzin V. I. *Telemetriya. Glaza i ushi Glavnogo konstruktora* [Telemetry. Eyes and ears of the Chief Designer]. Moscow, Overley Publ., 2009, 320 p.

10. Polenov D. Ju. *Jevoljucija teletrii v raketnoj tehnike*. [The evolution of telemetry in rocket technology]. *Molodoy uchenyy*. 2014, No. 6, P. 216–218 (In Russ.).

11. Levochkin P. S., Martirosov D. S., Bukanov V. T. [Problems of functional diagnostics of liquid rocket engines]. *Vestnik MGTU im. N. Je. Bauman. Ser. "Mashinostroenie"*. 2013, No. 1, P. 72–88 (In Russ.).

12. Gorban' A. N., Rossiev D. A. *Neyronnye seti na personal'nom komp'yutere* [Neural networks on a personal computer]. Novosibirsk, Nauka Publ., 1996, 276 p.

13. Kruglov V. V., Borisov V. V. *Iskusstvennye neyronnye seti. Teoriya i praktika* [Artificial neural networks. Theory and practice]. Moscow, Goryachaya liniya Publ., 2002, 382 p.

14. Ljubimova T. V., Gorelova A. V. [The solution to the problem of forecasting using neural networks]. *Innovacionnaya nauka*. 2015, No. 4, P. 39–43 (In Russ.).

15. Kolomencev A. I., Hohlov A. N. [Optimal test planning of liquid propulsion rocket engines of small thrusts to determine their main parameters and characteristics]. *Vestnik PNPU. Aerokosmicheskaya tekhnika*. 2016, No. 47, P. 109–122 (In Russ.).

16. Dobrovolskiy M. V. *Zhidkostnye raketnye dvigateli. Osnovy proektirovaniya* [Liquid rocket engines. Design basics]. Moscow, Izd-vo MGTU im. N. Je. Bauman Publ., 2006, 488 p.

17. Druzhin A. N. *Teplovaya i energeticheskaya effektivnost' do i sverkhzvukovykh gazovykh zaves v raketnykh dvigatelyakh maloy tyagi. Kand. Diss.* [Thermal and energy efficiency before and supersonic gas curtains in small thrust rocket engines. Cand. Diss.]. Samara, 2002, 213 p.

18. Majorova V. I., Grishko D. A., Remen' B. A., Ambarcumov A. A., Kaldarov I. S. [Automation of receiving and processing backup telemetric information from space]. *Vestnik MGTU im. N. Je. Bauman*. 2013, No. 1 (90), P. 89–99 (In Russ.).

19. Lukin F. A., Shahmatov A. V., Mushovec K. V., Zelenkov P. V. [The mechanism of controlled telemetry of a spacecraft]. *Vestnik SibGAU*. 2012, No. 5 (45), P. 140–144 (In Russ.).

20. Il'in V. A. *Teleupravlenie i teleizmerenie* [Remote control and telemetry] Moscow, Jenergoizdat Publ., 1982, 560 p.

21. Milicin A. V., Samsonov V. N., Hodak V. A. et al. *Otobrazhenie informacii v Centre upravleniya kosmicheskimi poletami* [Display of information in the Space Flight Control Center]. Moscow, Radio i svyaz Publ., 1982, 192 p.

22. Emel'janova Ju. G., Talalaev A. A., Fralenko V. P., Hachumov V. M. [Neural network method for detecting malfunctions in space subsystems]. *Trudy mezhdunarodnoy konferencii "Programmnye sistemy: teoriya i prilozheniya"* [Proceedings of the international conference "Software systems: theory and applications"] (Pereslavl' Zaleskiy, Russia, may 2009). 2009, P. 133–143 (In Russ.).

23. Efimov V. V., Kozyrev G. I., Loskutov A. I. et al. *Neyrokomp'yutery v kosmicheskoy tekhnike* [Neurocomputers in space technology. Radio engineering]. Moscow, 2004, 317 p.

24. Efimov V. V. [Neurointellectualization of onboard control systems for spacecraft surveillance]. *Mehatronika, avtomatizacija, upravlenie*. 2006, No. 10, P. 2–15 (In Russ.).

25. Labinskij A. Ju., Utkin O. V. [To the question of approximation of a function by a neural network]. *Prirodnye i tehnogennye riski (fiziko matematicheskie i prikladnye aspekty)*. 2016, No. 1, P. 5–11 (In Russ.).

26. Rutkovskij L., Pilin'skiy M., Rutkovskaja D. *Neyronnye seti, geneticheskie algoritmy i nechetkie sistemy* [Neural networks, genetic algorithms and fuzzy systems]. Moscow, Telekom Publ., 2004, 385 p.

27. Tarhov D. A. *Neyronnye seti kak sredstvo matematicheskogo modelirovaniya* [Neural networks as a means of mathematical modeling]. Moscow, Radio-tehnika Publ., 2006, 48 p.

Библиографические ссылки

1. Агеенко Ю. И., Пегин И. В. Подтверждение энергетической эффективности ЖРДМТ с дефлекторно-центробежной схемой смесеобразования // *Вестник Самарского гос. аэрокосмич. ун-та*. 2014. № 5, ч. 3. С. 46–54.

2. Сирант А. Л. Исследование влияния неидеальностей рабочего импульса жидкостных ракетных двигателей малой тяги на динамику малого космического аппарата : дис. ... канд. техн. наук. Самара, 2008. 153 с.

3. Хруцкий О. В. Прогнозирование технического состояния функционально-самостоятельных элементов судовой энергетической установки : дис. ... канд. техн. наук. СПб., 1996. 263 с.

4. Герасимова Д. С., Савина М. Г., Гейман В. Н. Обновление и продление ресурсов авиационной техники // *Актуальные проблемы авиации и космонавтики*. 2015. Т. 1. С. 686–688.

5. Мартиросов Д. С., Коломенцев А. И. Функциональная диагностика ЖРД в режиме реального времени // *Авиационно-космическая техника и технология*. 2012. № 7. С. 197–201.

6. Мартиросов Д. С., Синьков С. А. Способ оценки предельно достигаемой точности определения параметров элементов ЖРД при их функциональной

диагностике // Тр. НПО Энергомаш им. акад. В. П. Глушко. 2005. № 23. С. 151–160.

7. Колбая Т. Ч., Пасмурнов С. М., Якуш Д. Ю. Разработка технологии создания системы диагностирования и аварийной защиты жидкостных ракетных двигателей // Инженерный журнал: Наука и инновации. 2016. Вып. 8 [Электронный ресурс]. URL: <http://www.engjournal.ru/catalog/arise/teje/1524.html>.

8. Бондарь А. И., Пасмурнов С. М., Якуш Д. Ю. Программно-математическое обеспечение системы аварийной защиты и управления ЖРД и процедура его тестирования // Наука и технологии : сб. науч. тр. РАН. 2015. Т. 5. С. 137.

9. Сковорода-Лузин В. И. Телеметрия. Глаза и уши главного конструктора. М. : ООО «Оверлей», 2009. 320 с.

10. Поленов Д. Ю. Эволюция телеметрии в ракетной технике // Молодой учёный. 2014. № 6. С. 216–218.

11. Левочкин П. С., Мартиросов Д. С., Буканов В. Т. Проблемы функциональной диагностики жидкостных ракетных двигателей // Вестник МГТУ им. Н. Э. Баумана. Сер. «Машиностроение». 2013. № 1. С. 72–88.

12. Горбань А. Н., Россиев Д. А. Нейронные сети на персональном компьютере. Новосибирск : Наука. 1996. 276 с.

13. Круглов В. В., Борисов В. В. Искусственные нейронные сети. Теория и практика. М. : Горячая линия. 2002. 382 с.

14. Любимова Т. В., Горелова А. В. Решение задачи прогнозирования с помощью нейронных сетей // Инновационная наука. 2015. № 4. С. 39–43.

15. Коломенцев А. И., Хохлов А. Н. Оптимальное планирование испытаний жидкостных ракетных двигателей малых тяг для определения их основных параметров и характеристик // Вестник ПНИПУ. Аэрокосмическая техника. 2016. № 47. С. 109–122.

16. Добровольский М. В. Жидкостные ракетные двигатели. Основы проектирования / под ред. Д. А. Ягодникова. М. : Изд-во МГТУ им. Н. Э. Баумана. 2006. 488 с.

17. Дружин А. Н. Тепловая и энергетическая эффективность до и сверхзвуковых газовых завес

в ракетных двигателях малой тяги : дис. ... канд. техн. наук. Самара. 2002. 213 с.

18. Автоматизация приема и обработки резервной телеметрической информации с космических / В. И. Майорова, Д. А. Гришко, Б. А. Ремень и др. // Вестник МГТУ им. Н. Э. Баумана. 2013. № 1 (90). С. 89–99.

19. Механизм управляемой телеметрии космического аппарата / Ф. А. Лукин, А. В. Шахматов, К. В. Мушовец, П. В. Зеленков // Вестник СибГАУ. 2012. № 5 (45). С. 140–144.

20. Ильин В. А. Телеуправление и телеизмерение. М. : Энергоиздат, 1982. 560 с.

21. Отображение информации в Центре управления космическими полетами / А. В. Милицин, В. Н. Самсонов, В. А. Ходак и др. М. : Радио и связь, 1982. 192 с.

22. Нейросетевой метод обнаружения неисправностей в космических подсистемах : тр. междунар. конф. «Программные системы: теория и приложения» / Ю. Г. Емельянова, А. А. Талалаев, В. П. Фраленко, В. М. Хачумов (г. Переславль-Залесский, Россия, май 2009). 2009. Т. 1. С. 133–143.

23. Нейрокомпьютеры в космической технике / В. В. Ефимов, Г. И. Козырев, А. И. Лоскутов и др. М. : Радиотехника, 2004. 317 с.

24. Ефимов В. В. Нейроинтеллектуализация бортовых комплексов управления космических аппаратов наблюдения // Мехатроника, автоматизация, управление. 2006. № 10. С. 2–15.

25. Лабинский А. Ю., Уткин О. В. К вопросу аппроксимации функции нейронной сетью // Природные и техногенные риски (физико-математические и прикладные аспекты). 2016. № 1. С. 5–11.

26. Рутковский Л., Пилинский М., Рутковская Д. Нейронные сети, генетические алгоритмы и нечеткие системы. М. : Телеком, 2004. 385 с.

27. Тархов Д. А. Нейронные сети как средство математического моделирования. М. : Радиотехника, 2006. 48 с.

© Komlev G. V., Mitrofanova A. S., 2020

Komlev Georgii Viktorovich – postgraduate student, Reshetnev Siberian State University of Science and Technology; master tester of measuring systems, JSC “Krasnash”. E-mail: komlev_gv@mail.ru.

Mitrofanova Anna Sergeevna – postgraduate student, Reshetnev Siberian State University of Science and Technology; software engineer, JSC “Information Satellite Systems” named after academician M. F. Reshetnev”. E-mail: jgotka@mail.ru.

Комлев Георгий Викторович – аспирант, Сибирский государственный университет науки и технологий имени академика М. Ф. Решетнева; мастер-испытатель измерительных систем, АО «Красмаш». E-mail: komlev_gv@mail.ru.

Митрофанова Анна Сергеевна – аспирант, Сибирский государственный университет науки и технологий имени академика М. Ф. Решетнева; инженер-программист, АО «Информационные спутниковые системы» имени академика М. Ф. Решетнёва». E-mail: jgotka@mail.ru.

UDC 621.31.629.78

Doi: 10.31772/2587-6066-2020-21-1-85-95

For citation: Nepomnyashchiy O. V., Krasnobaev Y. V., Yablonsky A. P., Solopko I. V., Lichargin D. V. Ensuring extreme regulation of power of primary energy sources at their joint operation for total load. *Siberian Journal of Science and Technology*. 2020, Vol. 21, No. 1, P. 85–95. Doi: 10.31772/2587-6066-2020-21-1-85-95

Для цитирования: Обеспечение экстремального регулирования мощности первичных источников энергии при их совместной работе на общую нагрузку / О. В. Непомнящий, Ю. В. Краснобаев, А. П. Яблонский и др. // Сибирский журнал науки и технологий. 2020. Т. 21, № 1. С. 85–95 Doi: 10.31772/2587-6066-2020-21-1-85-95

ENSURING EXTREME REGULATION OF POWER OF PRIMARY ENERGY SOURCES AT THEIR JOINT OPERATION FOR TOTAL LOAD

O. V. Nepomnyashchiy*, Y. V. Krasnobaev, A. P. Yablonsky, I. V. Solopko, D. V. Lichargin

Siberian Federal University, Space and Information Technology Institute

26b, Kirensky St., Krasnoyarsk, 660074, Russian Federation

*E-mail: 2955005@gmail.com

Heterogeneous energy sources and homogeneous energy sources with different characteristics are frequently used in autonomous power supply systems. Solar batteries are widely used as primary energy sources for on-board power supply systems of spacecrafts, unmanned and manned aircrafts. Renewable energy sources such as solar, wind, geothermal and hydro energy, serve as primary energy sources of terrestrial autonomous power supply systems.

Matching primary energy sources with different characteristics and operating conditions within a unified power supply system leads to problems connected with the power control of energy sources, which determines the relevance of the considered problems.

The main aim of the study is to develop a combination of primary energy sources and control techniques which allow using primary energy sources with different characteristics and operating conditions in unified autonomous power supply system.

The objectives of the study are to create the simulation model of a power supply system using MATLAB/Simulink software; to develop and test control algorithms for primary energy source controllers that would allow to maintain the needed battery charging current; to develop and test control algorithms for primary energy source controllers that would allow the primary energy sources to operate in the maximum power point tracking mode and to minimize the maximum power point search time.

Methods used in the study: the simulation of a power supply system using MATLAB 7.9 Simulink software.

Results: the simulation model of a power supply system including two primary energy sources with different characteristics is designed. In the case of excess power generating by the primary energy source, its controller operates in the battery charging mode. When the primary source power shortage occurs, its controller operates in the maximum power point tracking mode. The proposed power supply system structure allows controlling two energy sources independently, thus the primary energy source controllers can operate in different modes. This provides flexibility of the power supply system. The use of fuzzy logic control algorithm increases the accuracy and search speed of the maximum power point tracking algorithm. Simulation results confirmed the efficiency of the proposed solar controller operation algorithms in all modes stated above. The efficiency of controller operation modes selection algorithm was confirmed in different operating conditions. The proposed algorithms allow implementing the effective control of primary power sources depending on power supply system operating conditions.

Keywords: autonomous power supply system, solar cell, solar controller, simulation model, battery, maximum power point tracking.

ОБЕСПЕЧЕНИЕ ЭКСТРЕМАЛЬНОГО РЕГУЛИРОВАНИЯ МОЩНОСТИ ПЕРВИЧНЫХ ИСТОЧНИКОВ ЭНЕРГИИ ПРИ ИХ СОВМЕСТНОЙ РАБОТЕ НА ОБЩУЮ НАГРУЗКУ

О. В. Непомнящий*, Ю. В. Краснобаев, А. П. Яблонский, И. В. Солопко, Д. В. Личаргин

Сибирский федеральный университет, Институт космических и информационных технологий

Российская Федерация, 660074, г. Красноярск, ул. Академика Киренского, 26б

*E-mail: 2955005@gmail.com

В системах электропитания космических аппаратов, беспилотных и пилотируемых летательных аппаратов в качестве первичных источников энергии широко используются солнечные батареи. Для энергоснабжения наземных автономных объектов находят применение возобновляемые источники энергии различной природы, позволяющие использовать энергию Солнца, ветра, волн, рек, приливов и т. п.

Применение в составе автономной системы электропитания разнородных источников энергии позволяет осуществлять генерацию электрической энергии на интервалах времени, когда отсутствует поступление энергии от части используемых источников.

Согласование первичных источников энергии с различными характеристиками и условиями работы в рамках одной системы электропитания приводит к возникновению дополнительных сложностей, связанных с регулированием мощности источников, что и определяет актуальность рассматриваемых задач.

Цель исследования: разработка способов объединения первичных источников энергии с различными характеристиками и условиями работы в единую автономную систему электропитания и алгоритмов управления контроллерами этих источников.

Задачи: создание имитационной модели системы электропитания в среде MATLAB/Simulink; разработка и проверка алгоритма управления контроллерами первичных источников, обеспечивающего поддержание желаемого тока заряда аккумуляторной батареи системы электропитания; разработка и проверка алгоритмов управления контроллерами первичных источников, обеспечивающих отбор максимальной мощности от каждого из нескольких первичных источников, в том числе и с минимизацией времени поиска точки максимальной мощности.

Методы исследования: имитационное моделирование системы электропитания с использованием языка Simulink, входящего в состав программного пакета MATLAB 7.9.

Результаты: разработана имитационная модель системы электропитания, включающая два источника энергии с различными характеристиками. При избытке мощности, генерируемой первичным источником энергии, контроллер источника энергии находится в режиме заряда аккумуляторной батареи заданным фиксированным током. При дефиците мощности первичного источника контроллер функционирует в режиме поиска экстремальной мощности. Структура системы электропитания позволяет управлять двумя источниками энергии независимо друг от друга. Таким образом, контроллеры источников энергии могут находиться в различных режимах работы, обеспечивая повышенную гибкость системы электропитания. Использование алгоритма управления на нечеткой логике увеличивает скорость поиска точки максимальной мощности, а также повышает точность работы алгоритма. Проведенные с использованием разработанной модели испытания подтвердили работоспособность алгоритмов управления контроллеров солнечной батареи во всех режимах работы. Подтверждена работоспособность алгоритма выбора режима работы контроллеров в различных условиях. Предложенные алгоритмы позволяют осуществлять эффективное регулирование мощности первичных источников энергии в зависимости от различных условий работы автономной системы электропитания.

Ключевые слова: автономная система электропитания, солнечная батарея, контроллер солнечной батареи, имитационная модель, аккумуляторная батарея, экстремальное регулирование.

Introduction. In the autonomous power supply systems (PSS) wide used renewable energy sources. In PSS of spacecrafts and unmanned and manned aircrafts the solar panel are widely used as primary sources of energy [1–3]. Renewable energy sources, such as the sun, wind, waves, rivers, tides, etc., provide energy to ground-based autonomous objects [2–5].

Heterogeneous energy sources, and in some cases homogeneous energy sources with different characteristics are studied below. The use of various combinations of dissimilar energy sources allows reducing the consumer's dependence on changing external conditions that affect the output of the useful power of some autonomous power supply systems [3–7]. In space-based PSSs, the primary sources (PS) of energy are mainly solar panels (SP) [8–11].

Design features of the placement of several SPs on the spacecraft can lead to significantly diverse external characteristics of these SPs.

Coordination of primary energy sources with different characteristics and operating conditions within the unified PSS leads to additional difficulties in ensuring their joint work, in particular, with extreme power control of each PS.

Problem formulation. Autonomous power supply systems include directly primary energy sources, a storage

battery (SB), a cable network and PS controllers, made in the form of converters with control devices.

The article describes operating algorithms and structure of SP controllers is a part of an autonomous power supply system with solar panels as primary energy sources. The operating algorithm of the SP controller should provide a charge of the battery with a constant current of a given value, as well as charging battery with a decreasing current while maintaining a certain fixed voltage on the battery in the case when the current power of the battery exceeds the total power consumed by the load and the battery. In the case when the current SP power is less than the total power consumed by the load and the battery, the SP controller operates in the search mode for extreme power and provides the selection of maximum power from the SP.

PSSs of microsatellites and small spacecrafts usually include several sections of solar panels located on each side of the spacecraft [8–10]. Therefore, the SP sections of such a spacecraft are in various lighting conditions and make various contributions to the total power of the solar cells. Moreover, sections of the SP can have different characteristics, and the maximum power that each section of the SP can generate depends not only on the individual characteristics of the section, but also on the orientation of the section on the Sun.

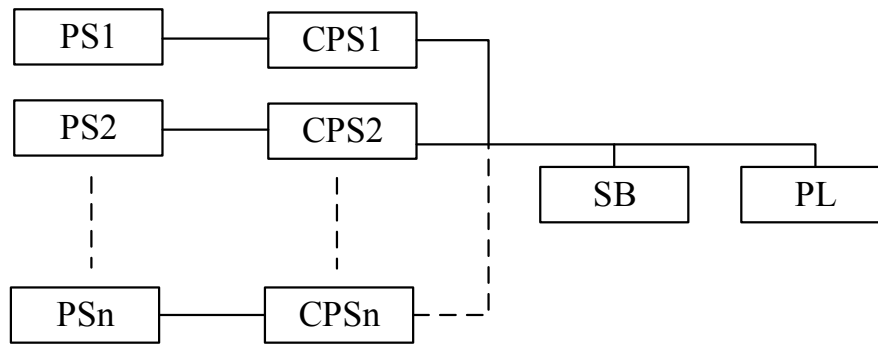


Fig. 1. Structural diagram of autonomous power supply system with several primary energy sources

Рис. 1. Структурная схема автономной системы энергоснабжения с несколькими первичными источниками энергии

When several SPs with different characteristics are connected to the total load in parallel using a common voltage converter [4; 8; 9], the position of the operating points on the power characteristic of each energy source cannot be individually controlled, since the SP controller in this case will provide control of the position of the operating point on the resulting power characteristic of parallel connected SP. In the extreme power selection mode, this leads to a decrease in the total power given by the SP to the load. Thus, it becomes necessary to use individual SP controllers, which can provide regulating the position of the operating points on the power characteristics for the SP independently.

The state-of-art of microcontroller technology allows reducing the size of the control device and implementing control of the SP controller based on the microcontroller [12]. At the same time, it becomes possible to implement not only a step-by-step algorithm for searching an extremum of SP power [13–15], but also more complex algorithms that speed up the searching process for an extremum and increase the power level generated by SP while reducing the amplitude of the operating point oscillations on the current-voltage characteristic of the SP in a neighborhood maximum power points [16; 17]. The acceleration of the extremum search process is especially important in the case of spacecraft rotation around its axis with a certain angular speed [9; 10]. Approaches to the implementation of a power supply system with several energy sources, as well as control algorithms for SP controllers, are considered in this paper.

Solutions. When solving the problem of regulating the power of each primary source individually, we use the structural diagram of an autonomous PSS, shown in fig. 1

In accordance with the structural diagram shown in fig. 1, energy sources PS1 and PSn are connected in series to the controllers PS (CPS1 and CPSn). Output terminals controllers CPS1-CPSn connected to the SB and the power load (PL). Thus, it becomes possible to implement independent control of energy sources and ensure the operation of the following controller operation modes:

- battery charge mode with direct current of the given fixed value;
- search mode for the extreme power of the solar battery.

When power of the source is available and the battery needs to be charged, the SP controller charges the battery with direct current of the given fixed value $I_{SB.set}$ subject to the limitation of the voltage U_{SB} on the battery. Fig. 2 shows a block diagram of an algorithm for charging a battery with a given fixed current.

According to the algorithm, the SP controller reads the voltage and current signals of the battery, after which the condition for the voltage on the battery managed to reach its maximum voltage value is checked. If this condition is met, then the SP controller disconnects the battery from the energy source. If the condition is not met, then the equality of the present current value and the set value of the optimal charge current is checked. If the present current value is in a certain predetermined range, then it is equal to the optimal charging current with some error, then the demanded cycle ratio remains constant. If the charge current is less than the specified one, taking into account the error, then the pulse duty ratio increases by a certain amount, otherwise it decreases. The magnitude of the change in the duty cycle of pulses in one step of the algorithm is set programmatically and does not change during the operation of the algorithm.

If the primary source of a power shortage is detected, the SP controller selects the extreme power of the solar battery operating in accordance with the developed extreme power search algorithm. In the extreme power search mode, the operating point on the SP power characteristic performs oscillations in the nearest of the maximum power point. In this case, part of the SP power exceeding the power consumed by the load, is supplied to the battery charge. Fig. 3 shows a block diagram of a step-by-step algorithm of the controller operates in the search mode for extreme power [16].

In the extreme power search mode, the controller reads the current and voltage signals of the SP, and then multiplies them. If the signals are measured for the first time, then the current power is defined as the power received from the SP in the previous step. Next, an increase in the fill factor of the control pulses by a certain value k is viewed, being determined by the controller based on fuzzy logic occurred, then the current power of the SP is again calculated. If the power has increased to the value compared to the value stored in the previous step, then a

further increase in the duty cycle is observed. In the case when the measured power decreases, the direction of movement of the operating point is changed according to the power characteristic of the SP, and, consequently, a decrease in the fill factor of the control pulses is viewed.

The value of step k in the extreme power search mode is calculated by the fuzzy logic control unit [18–20], the

input variables of which are the derivative of the power with respect to voltage dP / dV for one step of searching for extreme power, as well as the absolute change in power dP for this step.

Fuzzy terms of the values of step k depending on the values of the terms of the input variables of the controller are given in table.

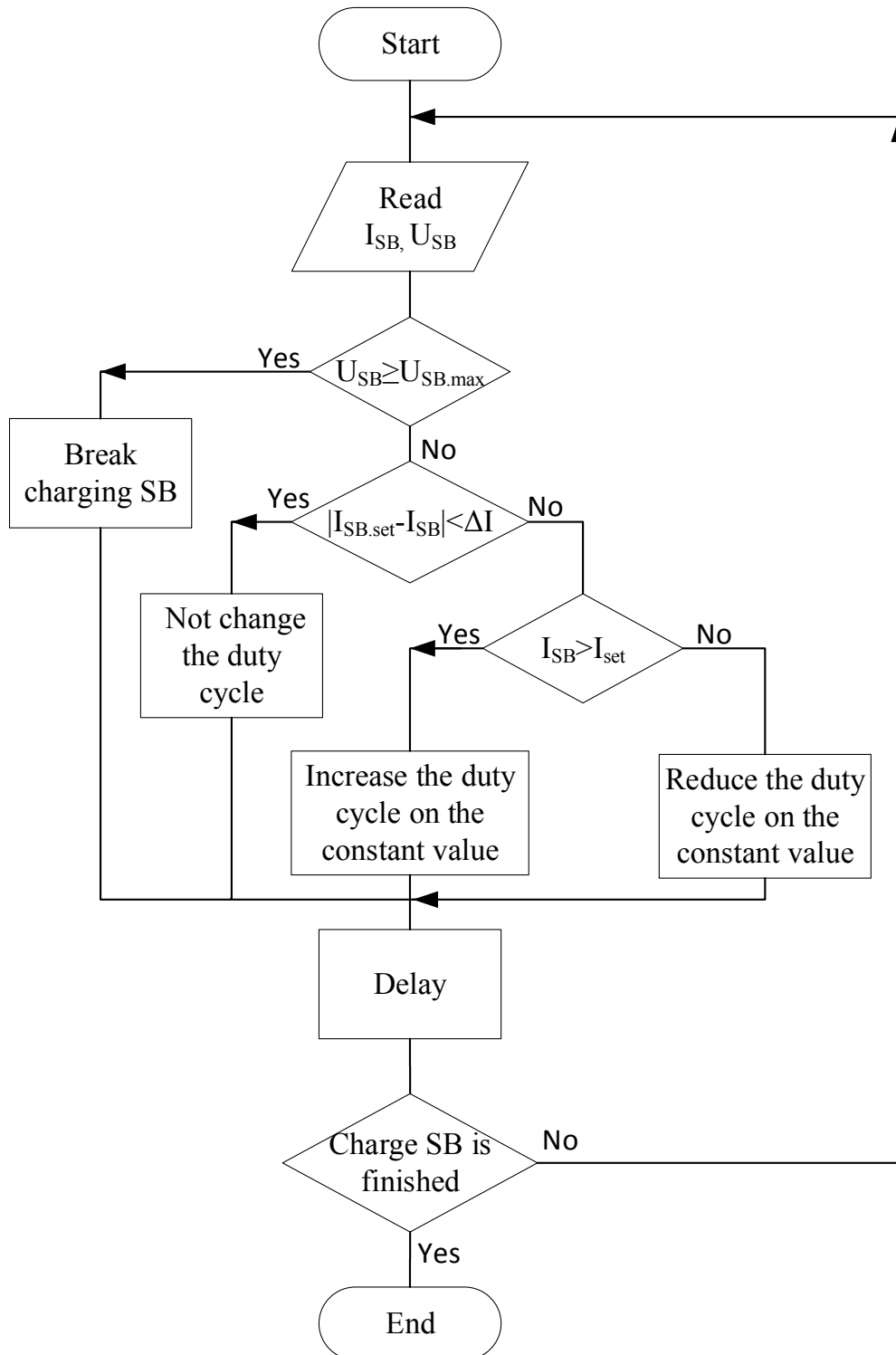


Fig. 2. Flowchart of the algorithm of specified fixed current battery charging mode

Рис. 2. Блок-схема алгоритма зарядки аккумулятора фиксированного тока

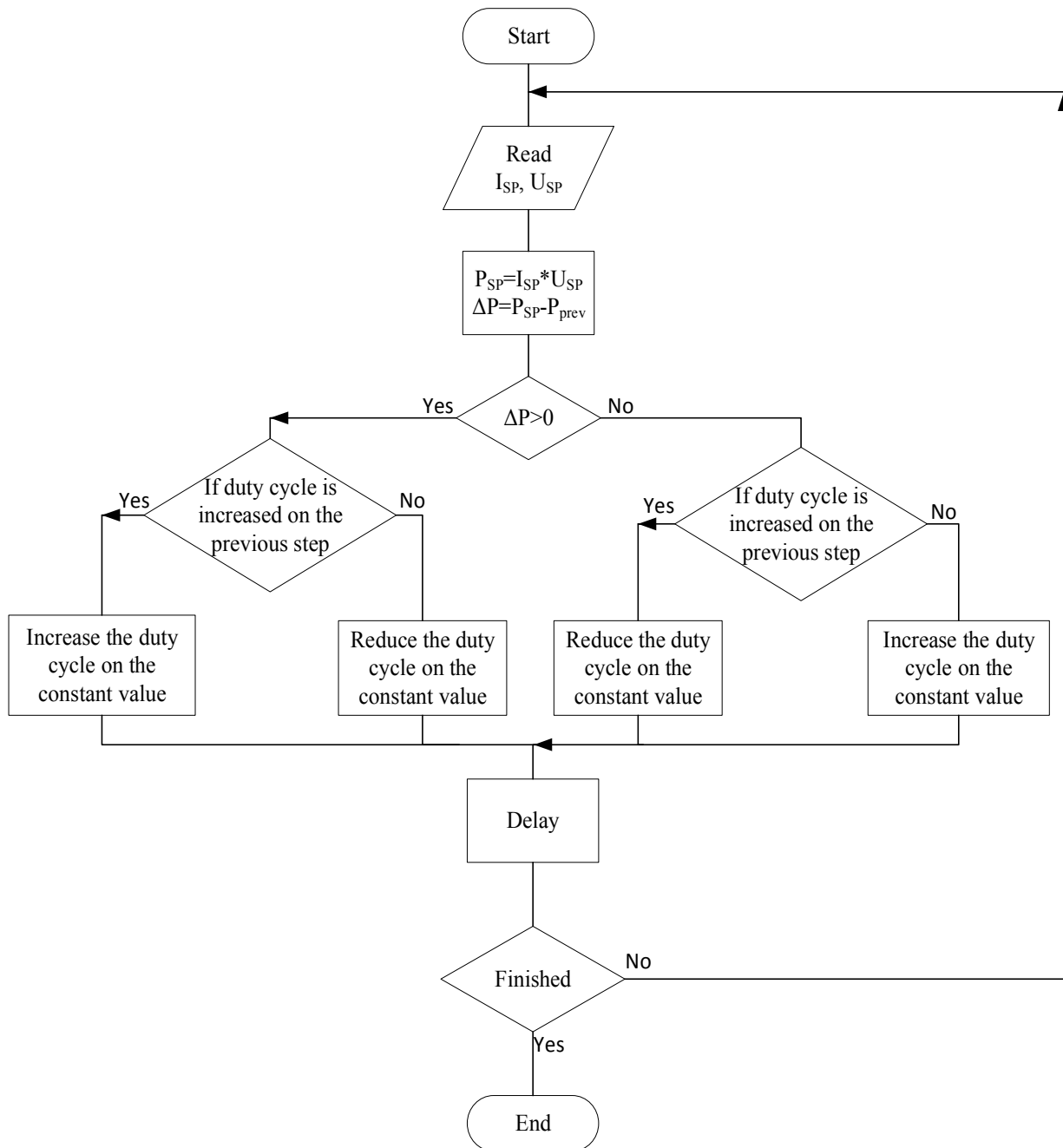


Fig. 3. Flowchart of maximum power point tracking algorithm

Рис. 3. Блок-схема алгоритма отслеживания точки максимальной мощности

Values of k step terms in the maximum power point tracking mode

$\frac{dP}{dV}$	NL (Negative large)	NS (Negative small)	NZ (Near zero)	PS (Positive small)	PL (Positive large)
NL (Negative large)	Highest	High	Middle	High	Highest
NM (Negative moderate)	High	Middle	Low	Mode Middle rate	High
NS (Negative small)	Middle	Low	Lowest	Low	Middle
NZ (Near zero)	Low	Lowest	Lowest	Lowest	Low
PS (Positive small)	Middle	Low	Lowest	Low	Middle
PM (Positive moderate)	High	Middle	Low	Middle	High
PL (Positive large)	Highest	High	Middle	High	Highest

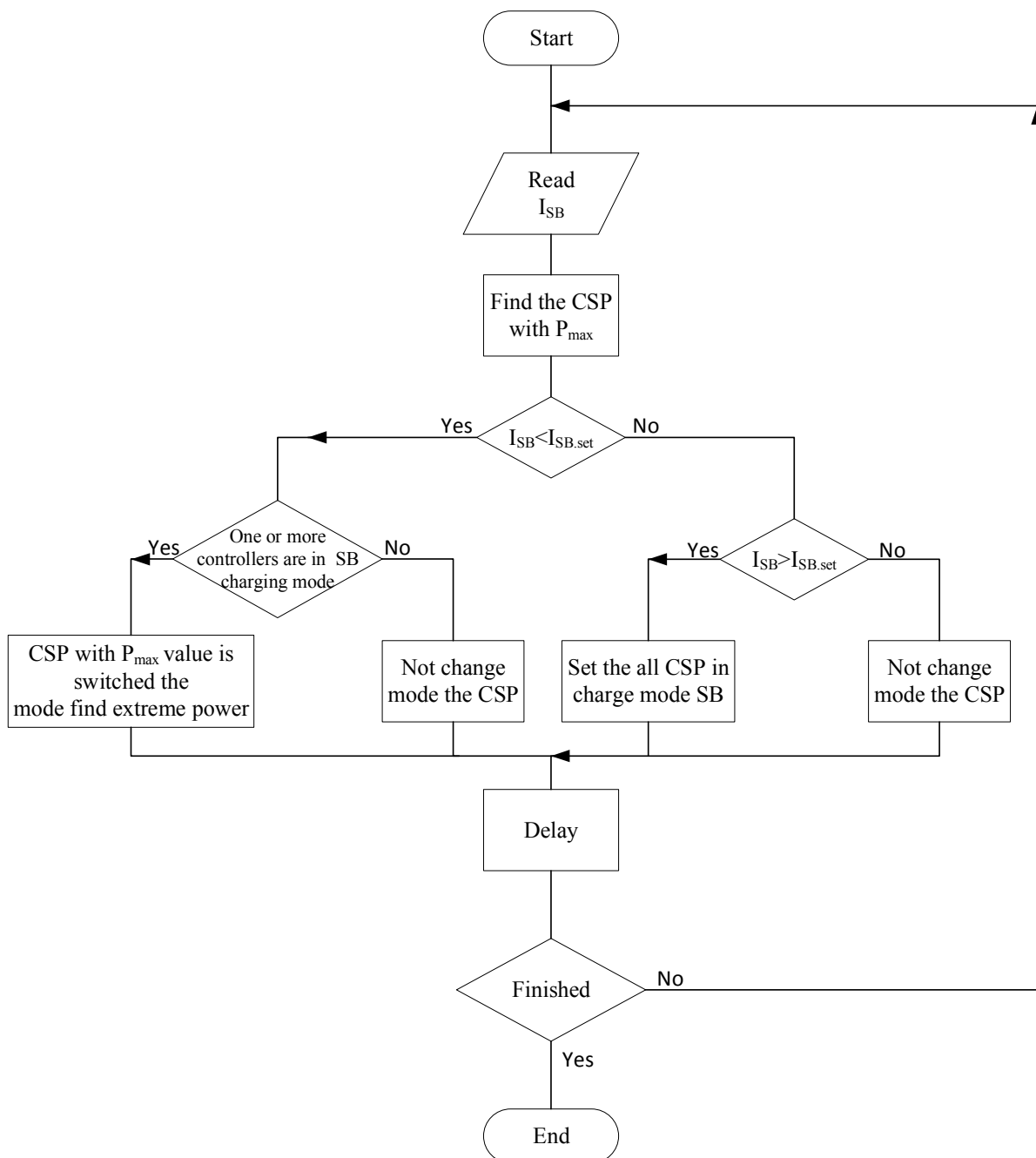


Fig. 4. Flowchart of solar controllers operation modes selection algorithm

Рис. 4. Блок-схема алгоритма выбора режима работы контроллеров солнечных батарей

The choice of the current operating modes of the SP controllers is determined by the unit selecting an operating mode (USOM). The flowchart of the operation algorithm USOM of the SP controllers is shown in fig. 4. The mode selection block at each step of operation determines the SP controller with the highest current power value. If the SP controller with the highest power value operates in the battery charge mode with a fixed current, and the current value of the charging current I_{SB} is less than the specified $I_{SB.set}$, this controller is put into the search mode for extreme power. The choice of the SP controller with the highest power value is due to the potentially largest increase in the current delivered to the load and to the

battery charge after switches it to the extreme power search mode.

This allows reducing the time for switching operating modes of other SP controllers in the case of transferring the switch of one controller to the extreme power search mode and achieves the set value of the charging current $I_{SB.set}$. If controllers operate in the extreme power search mode, and the charging current value I_{SB} is still less than the specified $I_{SB.set}$, the controller operating mode does not change, since in this case it is not possible to ensure a further increase in the power transmitted from the sources. In the case when the SP controllers operate in the search mode of extreme power, and the value of the

charging current I_{SB} exceeds the set value $I_{SB.set}$, all SP controllers are switched to the battery charge mode with a fixed current. Each cycle of the mode selection unit finishes with the time delay necessary to complete the transient processes after changing the operation mode of the SP controller.

To test the proposed control algorithms was developed of a simulation model the power supply system with two primary sources in the MATLAB / Simulink environment was developed, the module is shown in fig. 5.

The simulation model of the power supply system contains two primary sources of energy represented by the solar panels SP1 and SP2, which represent several series-connected solar cells from the library of components of Simscape [21]. SP1 and SP2 are connected to the controllers a CSP1 and CSP2 running on the total load PL in the form of resistors R2 and R3 and the battery – SB with an internal resistance R1. SP controllers consist of control units (CU1 and CU2) together with voltage converters CSP1 and CSP2 and represent functional blocks, the functioning algorithms of which accord with the control algorithms shown in fig. 2 and 3.

The converters CSP1 and CSP2, which are part of the controllers CSP1 and CSP2 accord with the scheme of a step-down voltage converter [4; 8; 13–16]. USOM is a functional block that contains the m-code as a built-in function for the Simulink environment [22]. The input of the mode selection block receives signals about the current operating mode of each controller, the current power values of each energy source, as well as the current value of the current I_{SB} of the battery. The USOM functioning algorithm is developed in accordance with the flowchart shown in fig. 4.

A comparative analysis of the operation of extreme power search algorithms with a fixed step and a variable step is shown in fig. 6.

The analysis of time diagrams of the extreme power search algorithm operating showed that the use of a variable step in the extreme power search algorithm based on fuzzy logic increases the search speed of the maximum power point by 50.8%. The searching algorithm for extreme power with a variable step, developed using fuzzy logic, also reduces the underutilization of the SP power caused by fluctuations in the operating point relative to the point of maximum power of the SP by 2.8 %.

In fig. 7 shows a time diagrams of the current battery I_{SB} , it explains the process of changing the operating modes of the SP controllers.

In the time interval from $t = 0$ to t_0 , the controllers of the power supply system do not change the fill factor of the control pulses of the converters and the current of the battery I_{SB} charge remains constant. At time t_0 , both power system controllers are put into battery charge mode with a given fixed current. At this time, a gradual increase in the fill factor of the control pulses occurs, which leads to an increase in current I_{SB} up to the value of the optimal charge current $I_{SB.set} = 10$ A. At the time t_1 , the process of increasing the fill factor of the pulses ends, since the value of the charging current I_{SB} becomes equal to $I_{SB.set}$ with some predetermined error. At the time t_2 , an additional load is connected, which leads to a stepwise increase in the load current and a decrease in the charging current I_{SB} , after which the controller starts the process of increasing the duty cycle of the pulses in order to achieve the specified optimal value $I_{SB.set}$ with the charging current.

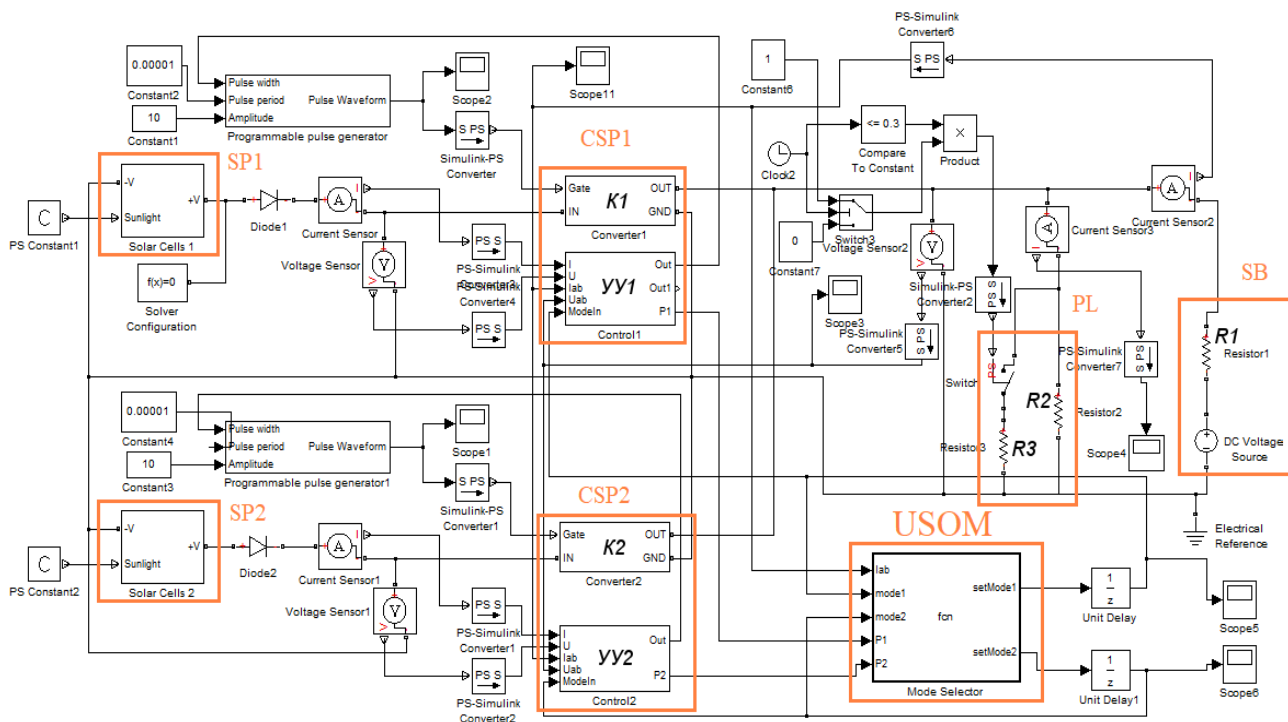


Fig. 5. Simulation model of the power supply system with two primary energy sources

Рис. 5. Имитационная модель системы электроснабжения с двумя первичными источниками энергии

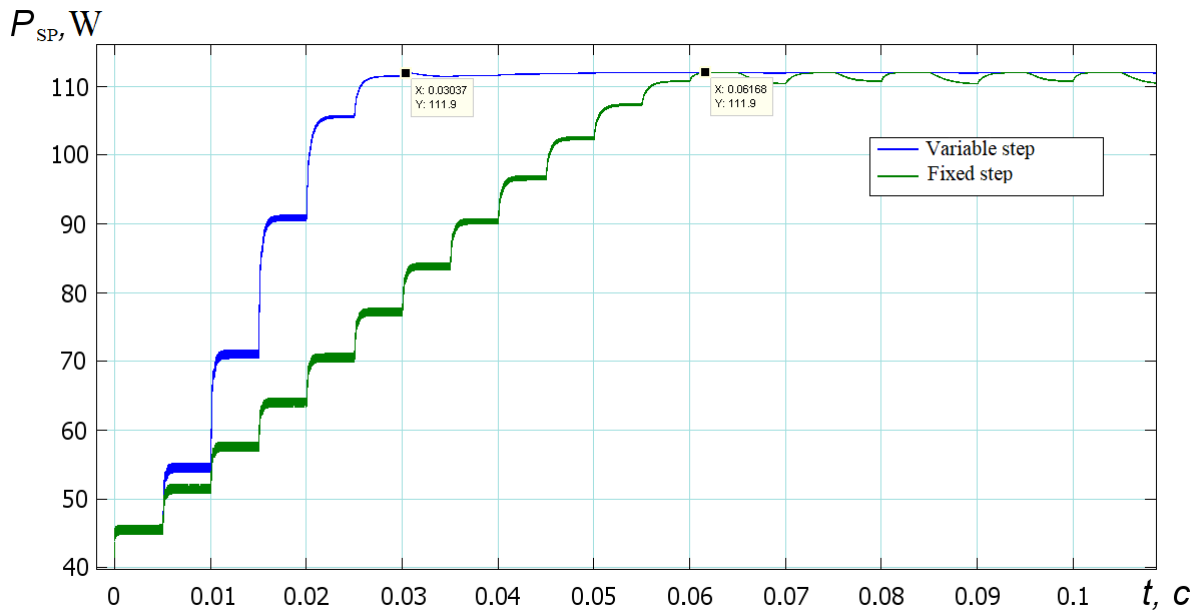


Fig. 6. Change in solar panel power in the maximum power point tracking mode

Рис. 6. Изменение мощности солнечной панели в режиме отслеживания точки максимальной мощности

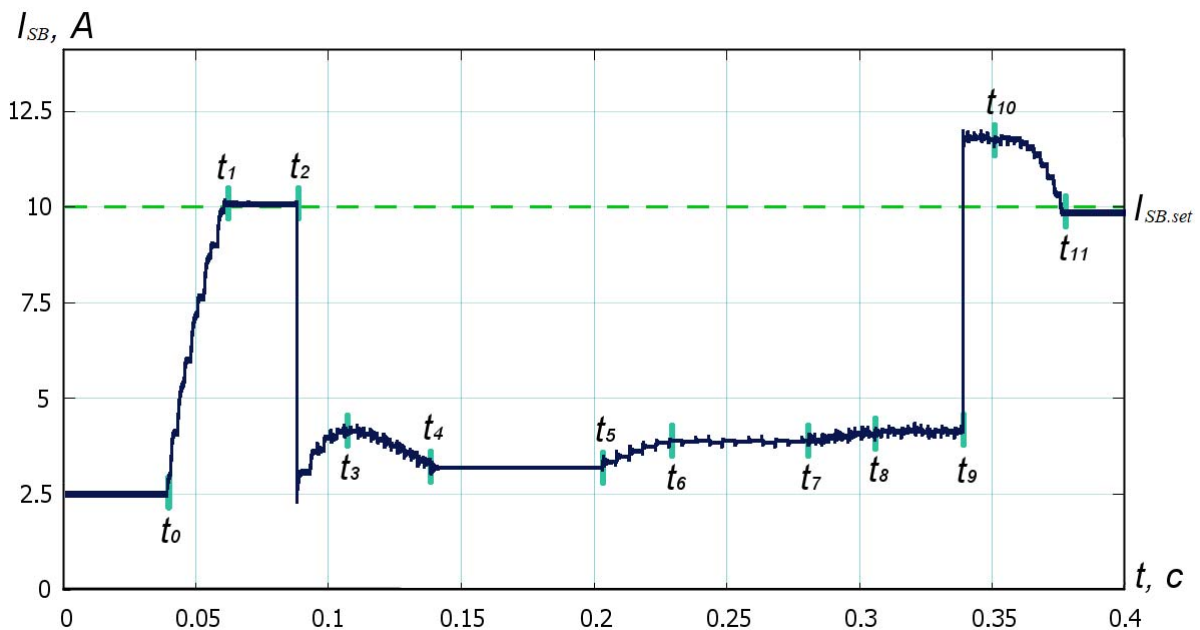


Fig 7. Change in battery current in the process of solar controllers modes switching

Рис 7. Изменение тока батареи в процессе переключения режимов работы солнечных контроллеров

At time t_3 , the operating points on the characteristics of the solar cells SP1 and SP2 are located in the vicinity of the maximum power point, but the controllers, in accordance with the control algorithm, continue the process of increasing the fill factor of the control pulses up to time t_4 , when the maximum value of the fill factor

is observed. Since the optimal value of the charging current $I_{SB.set} = 10$ A was not achieved during the operation of the SB charge mode algorithm, at the time t_5 , the SP controller with the highest current power value (in this case SP1) switches to the search for extreme power, and the operating point on the power characteristic SP1 starts

moving towards the point of maximum power of the solar battery. By the time t_6 , the operating point on the power characteristic SP1 reaches the vicinity of the maximum power point, which, however, does not lead to the achievement of the specified optimal value $I_{SB.set}$ by the charging current I_{SB} . Further, at the time t_7 , the SP controller with a lower value of the current power (SP2) switches to the extreme power search mode, and the operating point on the power characteristic SP2 starts moving towards the maximum power point. By the time t_8 , the operating point on the power characteristic SP2 reaches a neighborhood of the maximum power point. At the time t_9 , the additional load is switched off, which leads to a stepwise decrease in the load current and an increase in the charging current I_{SB} . At time t_{10} , the mode selection unit, in accordance with the operation algorithm, switches both controllers to the battery charge mode with a fixed current, after which the process of decreasing the duty cycle of the pulses begins in order to achieve the specified optimal value $I_{SB.set}$ by the charging current. By the time t_{11} , the charge current I_{SB} of the battery again reaches its optimum value $I_{SB.set} = 10$ A with some predetermined error.

Conclusion.

1. Operating several electric energy sources including energy stores within of unified autonomous power supply system erases the problem of their coordinated teamwork aimed at the effective utilization of their occur, in particular a problem of the maximal outfeed of energy from renewed energy sources.

2. The simulation model of the power supply system, including two energy sources with various characteristics has been developed. At surplus of the capacity generated by a primary energy source, the energy source controller operates in battery charging mode with a given fixed current. In the case of primary source power shortage the controller operates in a mode of search of extreme capacity. The structure of the power supply system allows operating two energy sources independently. Thus, energy source controllers can operate in various modes of operation, providing the raised flexibility of power supply system. The use of control algorithm on the base of fuzzy logic increases speed of search of a point of the maximal capacity, as well as increases accuracy of the implementation of the algorithm.

3. The experimental study of the developed model have confirmed working capacity of control algorithms of the solar battery controllers in all operation modes. The efficiency of the algorithm for choosing the controller operating modes in various conditions is confirmed. The introduced algorithms provides effective capacity regulation of primary energy sources depending on various operating conditions for autonomous power supply systems.

References

1. Wu B., Zhuo F., Long F., Gu W., Qing Y., Liu Y. A management strategy for solar panel – battery – super capacitor hybrid energy system in solar car. 8th International Conference on Power Electronics – ECCE Asia; 30 May–3 June 2011.
2. Zhu, X., Guo, Z., Hou, Z., Gao, X. and Zhang, J. Parameter's sensitivity analysis and design optimization of solar-powered airplanes. *Aircraft Engineering and Aerospace Technology*, 2016. Vol. 88 No. 4, pp. 550–560.
3. Lawhorn D., Rallabandi Vandana., Ionel D. Power Electronics Powertrain Architectures for Hybrid and Solar Electric Airplanes with Distributed Propulsion. 2018 AIAA/IEEE Electric Aircraft Technologies Symposium (EATS); 12–14 July 2018.
4. Dontsov O., Ivanchura V., Krasnobaev Y., Post. S. [Autonomous power supply system with extreme power control of primary energy sources]. *Izvestiya Tomskogo politekhnicheskogo universiteta. Inzhiniring georesurov*. 2016, Vol. 327, No. 12, P. 35–44 (In Russ.).
5. Trends 2013 in photovoltaic applications. Survey report of selected IEA countries between 1992 and 2012. Available at: http://helapco.gr/pdf/IEA_PVPS_Trends_Report_2013_v1_0_01.pdf (accessed 15.09.2019).
6. Lukutin B. *Decentralizovannye sistemy elektrosnabzheniya s vetrovymi i solnechnymi elektrostantsiyami* [Decentralized power supply systems with wind and solar power stations]. Tomsk, Tomsk Polytechnic University Publ., 2015, 100 p.
7. International Renewable Energy Agency: Vision and Mission. Available at: <http://www.irena.org/menu/index.aspx?mnu=cat&PriMenuID=13&CatID=9> (accessed 16.09.2019).
8. Soustin B. *Sistemy elektropitaniya kosmicheskikh apparatov* [Spacecraft power supply systems]. Novosibirsk, Nauka Publ., 1994, 318 p.
9. Fortescue P., Swinerd G., Stark J. (Eds.). (2011, August). *Spacecraft Systems Engineering*, (4th ed.). John Wiley & Sons, Ltd, 2011, 691 p.
10. Norton C., Pellegrino S., Johnson M. (2014, July) *Small Satellites: A Revolution in Space Science*. Available at: <http://www.kiss.caltech.edu/study/smallsat/KISS-SmallSat-FinalReport.pdf> (accessed 21.09.2019).
11. Makridenko L., Boyarchuk K. *Mikrospuntniki. Tendentsiya razvitiya. Osobennosti rynka i sotsialnoe znachenie* [Microsatellites. Development trend. Market characteristics and social impact]. Available at: <http://jurnal.vniem.ru/text/102/2.pdf> (accessed 24.09.2019).
12. The development of microprocessor technology. The structure and mode of modern microprocessors. Available at: http://life-prog.ru/view_articles.php?id=334 (accessed 24.09.2019).
13. Shinyakov Y., Otto A., Osipov A., Chernaya M. Autonomous power plant with extreme step regulator of solar battery power. *Alternative Energy and Ecology*. 2015, No. (8–9), P. 12–18.
14. Ivanchura V. I. [Solar cell controller with maximum power point tracking]. *Elektromekhanicheskie preobrazovateli energii. VI Mezhdunarodnaya nauchno-tekhnicheskaya konferentsiya* [Electromechanical energy converters. VI International research conference]. Tomsk, 9–11 October 2013. Vol. 6, P. 180–185 (In Russ.).
15. Post S., Dontsov O., Ivanchura V., Krasnobaev Yu. [A simulation model of the solar cell controller]. *Izvestiya Tomskogo politekhnicheskogo universiteta. Tekhnika i tekhnologiya v energetike*. 2014, Vol. 325, No. 4, P. 111–120 (In Russ.).

16. Dontsov O., Ivanchura V., Krasnobaev Y. (2015, Sep 9th). A Fuzzy Logic Solar Controller with Maximum Power Point Tracking. *Journal of Siberian Federal University. Engineering & Technologies*. 2015. Vol. 6, No. 8, P. 786–794.
 17. Liu C. An Asymmetrical Fuzzy-Logic-Control-Based MPPT Algorithm for Photovoltaic Systems. *Energies*. 2014, Vol. 7, P. 2178–2193.
 18. Asai K. *Prikladnye nechetkie sistemy* [Applied fuzzy systems]. Moscow, Mir Publ., 1993, 368 p.
 19. Leonenkov A. *Nechetkoe modelirovanie v srede MATLAB i fuzzyTECH* [Fuzzy systems simulation in MATLAB and fuzzyTECH software]. Saint-Petersburg, BKV-Petersburg Publ., 2005, 736 p.
 20. Shtovba S. *Vvedenie v teoriyu nechetkikh mnozhestv i nechetkuyu logiku* [An introduction to fuzzy set theory and fuzzy logic]. Available at: <http://matlab.exponenta.ru/fuzzylogic/book1/index.php> (accessed 3.10.2019).
 21. Ibbini M. Simscape solar cells model analysis and design. *Computer Applications in Environmental Sciences and Renewable Energy*. Kuala Lumpur, 2014, P. 97–103.
 22. Schematic simulation in the Simscape and SimElectronics software. Available at: http://www.kit-e.ru/articles/circuit/2014_4_174.php (accessed 3.10.2019).
- Библиографические ссылки**
1. Wu B., Zhuo F., Long F., Gu W., Qing Y., Liu Y. A management strategy for solar panel — battery — super capacitor hybrid energy system in solar car // 8th International Conference on Power Electronics – ECCE Asia. 30 May – 3 June 2011.
 2. Parameter's sensitivity analysis and design optimization of solar-powered airplanes / Zhu X., Z. Guo, Z. Hou, X. Gao, J. Zhang // *Aircraft Engineering and Aerospace Technology*. 2016. Vol. 88 No. 4. P. 550–560.
 3. Lawhorn D., Rallabandi V., Ionel D. Power Electronics Powertrain Architectures for Hybrid and Solar Electric Airplanes with Distributed Propulsion // 2018 AIAA/IEEE Electric Aircraft Technologies Symposium (EATS). 12–14 July 2018.
 4. Автономная система электропитания с экстремальным регулированием мощности первичных источников энергии / О. Донцов, В. Иванчура, Ю. Краснобаев, С. Пост // *Известия Томского политехнич. ун-та*. 2016. Т. 327, № 12. С. 35–44.
 5. Trends 2013 in photovoltaic applications. Survey report of selected IEA countries between 1992 and 2012 [Электронный ресурс]. URL: http://helapco.gr/pdf/IEA_PVPS_Trends_Report_2013_v1_0_01.pdf (дата обращения 15.09.2019).
 6. Лукутин Б., Муравлев И., Плотноков И. Децентрализованные системы электроснабжения с ветровыми и солнечными электростанциями. Томск : Изд-во Томского политехнич. ун-та, 2015. 100 с.
 7. International Renewable Energy Agency: Vision and Mission [Электронный ресурс]. URL: <http://www.irena.org/menu/index.aspx?mnu=cat&PriMenuID=13&CatID=9> (дата обращения 16.09.2019).
 8. Соустин Б. Системы электропитания космических аппаратов. Новосибирск : Наука ; Сибирская издательская фирма, 1994. 318 с.
 9. Fortescue P., Swinerd G., Stark J. (Eds.). (2011, August). *Spacecraft Systems Engineering*, (4th ed.). John Wiley & Sons, Ltd, 2011. 691 p.
 10. Norton C., Pellegrino S., Johnson M. (2014, July) Small Satellites: A Revolution in Space Science [Электронный ресурс]. URL: <http://www.kiss.caltech.edu/study/smallsat/KISS-SmallSat-FinalReport.pdf> (дата обращения 21.09.2019).
 11. Макриденко Л., Боярчук К. Микроspuntniki. Микроспутники. Тенденция развития. Особенности рынка и социальное значение [Электронный ресурс]. URL: <http://jurnal.vniim.ru/text/102/2.pdf> (дата обращения 24.09.2019).
 12. Развитие микропроцессорной техники. Структура и режимы современных микропроцессоров [Электронный ресурс]. URL: http://life-prog.ru/view_articles.php?id=334 (дата обращения 24.09.2019).
 13. Shinyakov Y., Otto A., Osipov A., Chernaya M. Autonomous power plant with extreme step regulator of solar battery power // *Alternative Energy and Ecology*. 2015. No. (8-9). P. 12–18.
 14. Иванчура В., Краснобаев Ю., Донцов О., Пост С. Контроллер солнечной батареи с экстремальным регулированием // *Электромеханические преобразователи энергии : VI Междунар. науч.-техн. конф. ЭПЭ–2013*. Томск, 2013. С. 180–185.
 15. Пост С., Донцов О., Иванчура В., Краснобаев Ю. Имитационная модель контроллера солнечной батареи // *Известия Томского политехнич. ун-та. Техника и технология в энергетике*. 2014. Т. 325, № 4. С. 114–120.
 16. Dontsov O., Ivanchura V., Krasnobaev Y. A Fuzzy Logic Solar Controller with Maximum Power Point Tracking // *Journal of Siberian Federal University. Engineering & Technologies*. 2015. Vol. 6, No. 8. P. 786–794.
 17. Liu C. An Asymmetrical Fuzzy-Logic-Control-Based MPPT Algorithm for Photovoltaic Systems // *Energies*. 2014. Vol. 7. P. 2178–2193.
 18. Асаи К., Ватада Д., Иваи С. Прикладные нечеткие системы / пер. с япон. ; под ред. Т. Тэрано, К. Асаи, М. Сугэно. М. : Мир, 1993. 368 с.
 19. Леоненков А. Нечеткое моделирование в среде MATLAB и fuzzyTECH. СПб. : БХВ-Петербург, 2005. 736 с.
 20. Штовба С. Введение в теорию нечетких множеств и нечеткую логику [Электронный ресурс]. URL: <http://matlab.exponenta.ru/fuzzylogic/book1/index.php> (дата обращения: 3.10.2019).
 21. Ibbini M. Simscape solar cells model analysis and design. *Computer Applications in Environmental Sciences and Renewable Energy*. Kuala Lumpur. 2014. P. 97–103.
 22. Schematic simulation in the Simscape and SimElectronics software [Электронный ресурс]. URL: http://www.kit-e.ru/articles/circuit/2014_4_174.php (дата обращения 3.10.2019).
- © Nepomnyashchiy O. V., Krasnobaev Y. V.,
Yablonsky A. P., Solopko I. V., Lichargin D. V., 2020

Oleg Vladimirovich Nepomnyashchiy – Cand. Sc., Professor, Head of the Department Computer Scienc; Siberian Federal University, Institute of Space and Information Technologies. E-mail: ONepomnuashy@sfu-kras.ru

Yuriy Vadimovich Krasnobaev – Dr. Sc., Professor Department of Automation Systems, Automated Control and Design; Siberian Federal University, Institute of Space and Information Technologies. E-mail: YKrasnobaev@sfu-kras.ru.

Aleksei Pavlovich Yablonsky – Postgraduate Student, Assistant Lecturer department of Computer Science; Siberian Federal University, Institute of Space and Information Technologies. E-mail: AYablonskiy@sfu-kras.ru.

Irina Vladimirovna Solopko – Senior Lecturer Department of Automation Systems, Automated Control and Design; Siberian Federal University, Institute of Space and Information Technologies. E-mail: ISolopko@sfu-kras.ru

Dmitrij Viktorovic Lichargin – Cand. Sc., Associate Professor Department of Foreign Languages; Siberian Federal University, Institute of Space and Information Technologies. E-mail: DLichargin@sfu-kras.ru.

Олег Владимирович Непомнящий – кандидат технических наук, профессор, заведующий кафедрой вычислительной техники; Сибирский федеральный университет, Институт космических и информационных технологий. E-mail: ONepomnuashy@sfu-kras.ru.

Юрий Вадимович Краснобаев – доктор технических наук, профессор кафедры систем автоматики, автоматизированного управления и проектирования; Сибирский федеральный университет, Институт космических и информационных технологий. E-mail: YKrasnobaev@sfu-kras.ru.

Алексей Павлович Яблонский – аспирант, ассистент кафедры вычислительной техники; Сибирский федеральный университет, Институт космических и информационных технологий. E-mail: AYablonskiy@sfu-kras.ru.

Ирина Владимировна Солопко – старший преподаватель кафедры систем автоматики, автоматизированного управления и проектирования; Сибирский федеральный университет, Институт космических и информационных технологий. E-mail: ISolopko@sfu-kras.ru.

Дмитрий Викторович Личаргин – кандидат технических наук, доцент кафедры разговорного иностранного языка; Сибирский федеральный университет, Институт космических и информационных технологий. E-mail: DLichargin@sfu-kras.ru.

UDC 621.31

Doi: 10.31772/2587-6066-2020-21-1-96-105

For citation: Filonova M. M. Prospects for the development of high-voltage power supply systems of spacecraft with a charge-discharge regulator. *Siberian Journal of Science and Technology*. 2020, Vol. 21, No. 1, P. 96–105. Doi: 10.31772/2587-6066-2020-21-1-96-105

Для цитирования: Филонова М. М. Перспективы в области разработки высоковольтных систем электропитания космического аппарата с модулем зарядно-разрядного устройства // Сибирский журнал науки и технологий. 2020. Т. 21, № 1. С. 96–105. Doi: 10.31772/2587-6066-2020-21-1-96-105

PROSPECTS FOR THE DEVELOPMENT OF HIGH-VOLTAGE POWER SUPPLY SYSTEMS OF SPACECRAFT WITH A CHARGE-DISCHARGE REGULATOR

M. M. Filonova

Tomsk State University of Control System and Radio Electronics
40, Lenina Av., Tomsk, 634050, Russian Federation
E-mail : cmm91@inbox.ru

Changing the low-voltage level of the output load power bus (27–28 V) in the power supply system (PSS) of the spacecraft (SC) to a high-voltage (100 V) allowed us to significantly reduce the SC mass in connection with the reduction in the mass of cables and energy converting equipment (ECE). However, a number of problems have arisen related to the difficulty of matching the increased voltage levels of energy sources and loads, taking into account the necessary level of reliability of the PSS. Therefore, the issues of choosing the PSS structure and methods for developing ECE are relevant and priority task facing their developers. To date, in the field of development and creation of high-voltage high-power PSS of SC, a promising direction is their design based on integrated ECE modules, in particular, on the basis of modules of charge-discharge regulators (CDR) of accumulator batteries (AB).

In the article, a calculation and comparative analysis of the SC PSS structures with the connection of the CDR module to the solar battery (SB) bus and with the connection of the CDR module to the output load power bus is performed. In the course of analysis of the results obtained, it was found that both options for the PSS implementation can be optimal depending on the given curve of the SC load and the requirements for the PSS for specific energy, weight-dimension and other characteristics. The final choice of the SC PSS structure should be made subject to the specific power of the ECE and the subsequent calculation of the weight-dimension characteristics of the alternative PSS. Simulation of two options for the implementation of the AB CDR module was carried out: a push-pull converter with one inductor and a Weinberg converter with a magnetically coupled inductor and an additional power diode. It is established that both investigated options can be used in the development and creation of the CDR module of the high-voltage PSS of spacecraft. However, the design of CDR module based on the Weinberg converter can significantly reduce the values of the used inductors and output capacitors subject to the required levels of output voltage ripple.

Keywords: spacecraft, power supply system, maximum power point tracking mode, battery charge-discharge regulator, Weinberg converter.

ПЕРСПЕКТИВЫ В ОБЛАСТИ РАЗРАБОТКИ ВЫСОКОВОЛЬТНЫХ СИСТЕМ ЭЛЕКТРОПИТАНИЯ КОСМИЧЕСКОГО АППАРАТА С МОДУЛЕМ ЗАРЯДНО-РАЗРЯДНОГО УСТРОЙСТВА

М. М. Филонова

Томский государственный университет систем управления и радиоэлектроники
Российская Федерация, 634050, г. Томск, просп. Ленина, 40
E-mail: cmm91@inbox.ru

Изменение низковольтного уровня напряжения выходной шины питания нагрузки (27–28 В) в системе электропитания (СЭП) космического аппарата (КА) на высоковольтный (100 В) позволило существенно уменьшить массу КА в связи со снижением массы кабелей и энергопреобразующей аппаратуры (ЭПА). Однако возник ряд проблем, связанных со сложностью согласования возросших уровней напряжений источников энергии и нагрузки с учетом обеспечения необходимого уровня надежности СЭП. Поэтому выбор структуры СЭП и способов схемотехнической реализации ЭПА является актуальной и первоочередной задачей, стоящей перед разработчиками. На сегодняшний день в области разработки и создания высоковольтных СЭП КА перспективным направлением считается их проектирование на основе объединённых модулей ЭПА, в частности, на основе модулей зарядно-разрядных устройств (ЗРУ) аккумуляторных батарей (АБ).

В статье проведен расчет и сопоставительный анализ структур СЭП КА с подключением модуля ЗРУ к шине солнечной батареи (БС) и выходной шине питания нагрузки. В ходе анализа полученных результатов установлено, что оба варианта реализации СЭП могут быть оптимальны в зависимости от заданной циклограммы нагрузки КА и предъявляемых к СЭП требованиям по удельным энергетическим, габаритно-массовым и иным характеристикам. Окончательный выбор структуры СЭП должен проводиться при условии учета удельной мощности ЭПА и последующего расчета габаритно-массовых характеристик альтернативных вариантов СЭП. Проведено имитационное моделирование двух вариантов реализации модуля ЗРУ АБ: двухтактного преобразователя с одним дросселем и преобразователя Вейнберга с магнитосвязанным дросселем и дополнительным силовым диодом. Установлено, что оба исследованных варианта могут быть использованы при разработке и создании модуля ЗРУ высоковольтной СЭП КА. Однако проектирование ЗРУ на основе преобразователя Вейнберга позволяет значительно уменьшить номиналы используемых дросселей и выходных конденсаторов при условии обеспечения требуемых уровней пульсаций выходных напряжений.

Ключевые слова: космический аппарат, система электропитания, энергопреобразующая аппаратура, модуль зарядно-разрядного устройства, преобразователь Вейнберга.

Introduction. For the purpose of high-quality and timely performance of tasks implemented by spacecraft, it is necessary to develop their reliable power supply systems (PSS) with the most improved specific energy and dimensional mass characteristics. One of the first and main tasks that arise during the development and creation of PSS SC is the choice of their structure. The PSS must implement a reasonable consumption of the capacity generated by solar and accumulator batteries (SB and AB) in order to provide consumers with the required types of electric energy with the specified quality indicators. The problem is solved by calculation and comparative analysis of options for the PSS structures, followed by selection of the most optimal one from the point of view of the accepted criteria for system efficiency (weight, dimensions, energy characteristics, etc.) [1].

Since the 70s of the 20th century, the development of PSS is based on structural schemes with serial or parallel voltage regulators (VR) of the SB [2; 3]. The output voltage of the stabilized load supply bus was mainly 27–28 V. The most widely used parallel-serial structure in Russia allows implementing the extreme power control mode of the SB and its maximum usage [4; 5]. Such PSS are implemented on SC developed by the leading companies of the Russian space Agency: JSC “Academician M. F. Reshetnev “Information Satellite Systems” (Zheleznogorsk), JSC “NPO n.a. S.A. Lavochkin” (Khimki), JSC “RCC “Progress” (Samara). They are widely used as at a low voltage output of the PSS the maximum value of open circuit voltage of SB at the moment of exit from the Earth shadow does not exceed 80 V. That allows to easily compiling a list of used power items and materials. However, the schemes designed by traditional methods and worked out over many years of operation do not allow obtaining the necessary high quality indicators, taking into account the constantly increasing requirements for improving the characteristics of the PSS.

The creation of a high-voltage (100 V) PSS for automated SC allows significant reducing of the mass of SC in connection with the reduction of the mass of cables and energy converting equipment (ECE). However, there is a number of issues appeared due to the rise of higher voltage power sources and their correlation with the necessary level of reliability of PSS SC. The main problem is an increase in the SB voltage when the SC leaves the Earth's shadow, which is unacceptable because of the possibility

of electrostatic discharges between the SB photodiode chains and current-collecting elements and the occurrence of an emergency mode of the PSS [6; 7]. To limit the voltage on the SB, it is necessary to use special devices or implement the modes of operation of the PSS that do not allow increasing the voltage on the SB more than 180V [8].

The developers of high-voltage PSS for large space platforms (up to 20 kW) for geostationary orbit solved the problem by selecting the optimal shunt structure at that time, in which the output voltage on the load is stabilized by limiting the voltage on the SB during the entire service life. Examples of such space platforms are Express-2000, Spacebus 4000, etc. [5]. The use of shunt PSS is optimal for achieving high energy characteristics in the case of geostationary orbits with constant illumination and a uniform cyclogram of the SC load. However, the calculation of the PSS is performed at the end of the service life under conditions of degradation of energy sources, which negatively affects its characteristics. Until the SB reaches the characteristics corresponding to the degradation state and the worst operating conditions in this structure, it will be significantly underutilized in capacity.

An urgent task for today, the solution of which will allow to achieve a significant improvement in the characteristics of high-voltage PSS of SC, taking into account the non-simultaneous processes of charge and discharge of AB, is the development of PSS with modules of battery charging and discharge devices [9].

Structures of a high-voltage PSS with a battery charge-discharge regulator. Fig. 1 shows the options for implementing the structures of high-voltage PSS with the CDR module of AB, where L is the load.

Tab. 1 shows the ratio for determining required levels of current values generated by the SB and AB capacities, taking into account the efficiency of PSS in accordance with the operation modes of the alternative variants of PSS and graphs of SC load.

Tab. 1 symbols: $P_{BC}(\tau)$ – current value of SB power BS, $P_H(\tau)$ – current value of load power, $P_{AB_ZY}(\tau)$ – current value of the AB power charge, $P_{AB_PY}(\tau)$ – current value of the AB discharge power, $\eta_{PH}(\tau)$ – the efficiency coefficient PH, $\eta_{ZY}(\tau)$ – efficiency coefficient of CDR module in AB charging process, $\eta_{PY}(\tau)$ is the efficiency coefficient of the CDR in the discharging of AB, $\eta_{AB}(\tau)$ – the rate of AB.

For arbitrarily composed abruptly variable cyclograms of the SC load and the graph of the generated SB power (fig. 2, 3) the processes of energy flows in the PSS and the calculation taken at the same values of the efficiency

of ECE (95 %) were investigated with objective of comparative analysis of alternative structures of PSS and determination its optimal structure, subject to minimizing the overall power of ECE [1].

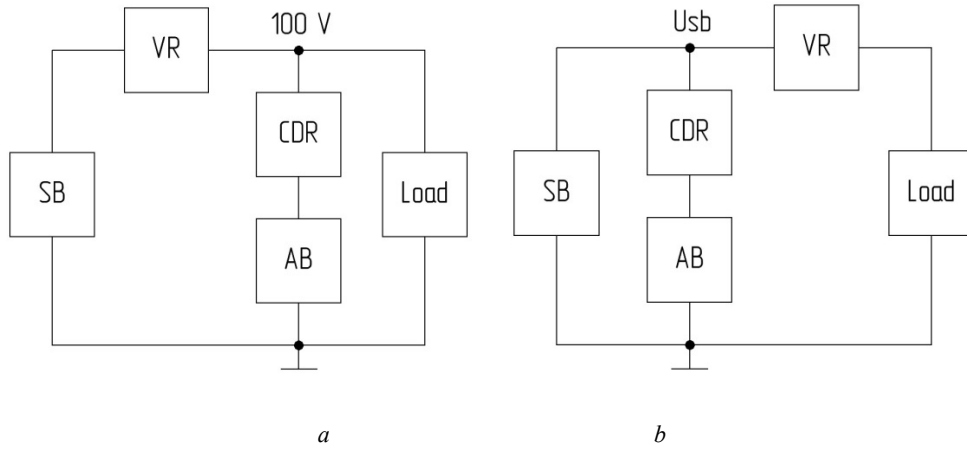


Fig. 1. The structure of the high voltage SC PSS with the connection of the battery charge-discharge regulator to the load output bus (a), to the solar battery bus (b)

Рис. 1. Структуры высоковольтных СЭП КА с подключением модуля ЗРУ к шине питания нагрузки (a) и шине солнечной батареи (б)

Table 1

Current values of SB, AB and load capacities in the PSS

Mode of energy supply loads:	PSS with connection of the CDR module to the load bus	PSS with connection of the CDR module to the SB bus
From SB	$P_H(\tau) = P_{BC}(\tau) \cdot \eta_{PH}(\tau)$	$P_H(\tau) = P_{BC}(\tau) \cdot \eta_{PH}(\tau)$
From SB and charge of AB	$P_{BC}(\tau) = \frac{P_H(\tau)}{\eta_{PH}(\tau)} + \frac{P_{AB_3Y}(\tau)}{\eta_{3Y}(\tau)}$	$P_{BC}(\tau) = \frac{P_H(\tau)}{\eta_{PH}(\tau)} + \frac{P_{AB_3Y}(\tau)}{\eta_{3Y}(\tau)}$
From SB and discharge AB	$P_H(\tau) = P_{BC}(\tau) \cdot \eta_{PH}(\tau) + P_{AB_PY}(\tau) \cdot \eta_{PY}(\tau) \cdot \eta_{AB}(\tau)$	$P_H(\tau) = P_{BC}(\tau) \cdot \eta_{PH}(\tau) + P_{AB_PY}(\tau) \cdot \eta_{PY}(\tau) \cdot \eta_{PH}(\tau) \cdot \eta_{AB}(\tau)$
From AB	$P_H(\tau) = P_{AB_PY}(\tau) \cdot \eta_{PY}(\tau) \cdot \eta_{AB}(\tau)$	$P_H(\tau) = P_{AB_PY}(\tau) \cdot \eta_{PY}(\tau) \cdot \eta_{PH}(\tau) \cdot \eta_{AB}(\tau)$

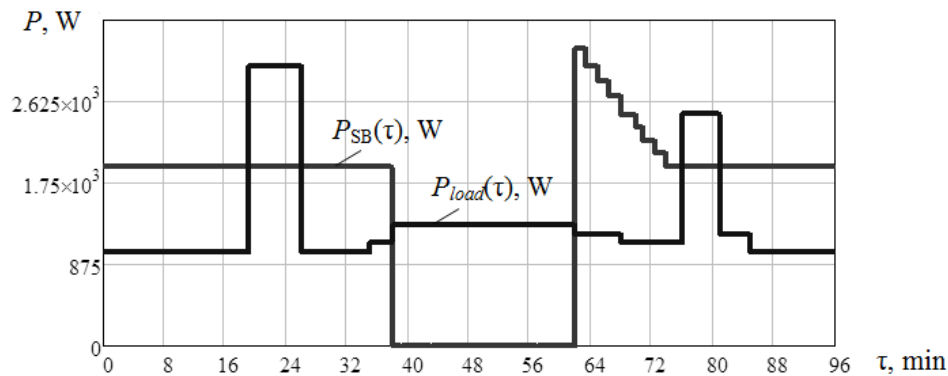


Fig. 2. Load cyclogram 1 and graph of the SB generated power in the PSS

Рис. 2. Циклограмма нагрузки 1 и график генерируемой БС мощности в СЭП

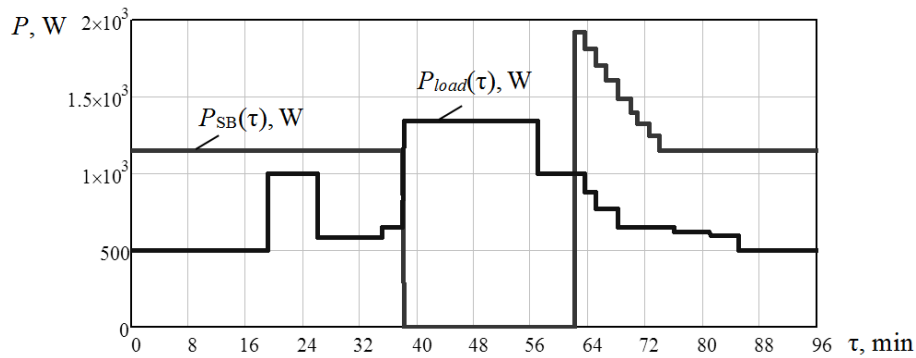


Fig. 3. Load cyclogram 2 and graph of the SB generated power in the PSS

Рис. 3. Циклограмма нагрузки 2 и график генерируемой БС мощности в СЭП

Table 2

Calculated values of the mass of energy sources and ECE capacities in the PSS

Parameter	PSS with connection of the CDR module to the load bus	PSS with connection of the CDR module to the SB bus
	Cyclogram load 1	
SB mass, kg	39.57	39.57
AB mass, kg	46.65	49.11
Maximum calculated capacity of CDR in CR mode, W	1835.4	1932.0
Maximum calculated capacity of CDR in DR mode, W	3157.9	3324.1
Maximum calculated capacity PH, W	3195.1	3157.9
Parameter	Cyclogram load 2	
SB mass, kg	23.78	23.78
AB mass, kg	36.32	38.23
Maximum calculated capacity of CDR in CR mode, W	848.8	893.4
Maximum calculated capacity of CDR in DR mode, W	1421.1	1495.8
Maximum calculated capacity PH, W	1920	1421.1

Tab. 2 shows the main design parameters for alternative versions of the EPA for different cyclograms of the SC load.

Within the cyclogram load 1 of the SC, the mass of the SB in the alternative versions of the PSS is the same. The mass of the AB in the PSS with the connection of the CDR module to the SB bus is greater by 2.46 kg. However, given that in practice the AB are selected with a certain margin, the mass of the AB for both versions of the PSS can be equal.

The maximum calculated power of the CDR in the CR mode and in the DR mode in the PSS with the connection of the CDR module to the SB bus is greater by 166 W and 97 W, respectively, compared to the maximum calculated power of the CDR of the alternative implementation of the PSS. However, in the PSS with the connection of CDR to SB bus maximum design capacity of WL is 37 W less because some part of SB generated power is consumed by CR to provide AB charging.

Within the cyclogram load 2 of the SC, the mass of the SB in the alternative versions of the PSS is the same. The mass of the AB in a PSS with the CDR module con-

nected to the SB bus is greater by 1.91 kg. However, as described above, in practice, the mass of the AB for both versions of the PSS may be equal.

The maximum calculated capacity of the CDR in the CR mode and in the DR mode in the PSS with the connection of CDR to the SB is 44.6 and 74.7 W more respectively, compared to maximum calculated capacity of CDR in alternative PSS. However, in a PSS with the CDR module connected to the SB bus, the maximum calculated power of the WL is less by 498.9 W.

In the course of studying the processes of distribution of energy flows in the PSS from tab. 2 it can be seen that the SC PSS with a sharply variable load cyclogram 1 is advisable to design according to the implementation option of the PSS with the connection of the CDR module to the output bus of the load power supply. However, when the load cyclogram is 2, it is advisable to design the SC PSS according to the implementation option of the PSS with the connection of the CDR module to the SB bus. The final choice of the PSS structure should be made subject to taking into account the specific power of the energy-generating equipment used and the subsequent

calculation of the dimensional and mass characteristics of alternative PSS options.

Simulation of CDR module of the accumulator battery. One of the options for the schematic implementation of the CDR module is its development based on a push-pull converter with a single inductor [10].

In the LTspice IV environment, simulation models of the CDR based on a push-pull converter with a single inductor for the charge and discharge modes of the AB were developed (fig. 4, 5). The parameters of the elements of the simulation model of CDR: accumulator battery voltage in the discharge mode U_{AB_PA3} is equal to 55 V; the voltage of the output power bus load U_H is 100 V; the

inductance of each winding of the transformer TV1.1 and TV1.2 is equal to 35 μ H; inductance of the inductor L4 is 9.4 μ H; frequency f is equal to 100 kHz for model transistor IRFP4668; diode model Mbr20200ct; the capacitor of 7.4 μ F and 32 μ F. It is accepted that the output voltage ripple should not exceed 1 %. Converter capacity in the discharge mode is equal to 1500 W at a voltage level of the output power bus load of 100 V. The converter capacity in the charge mode is 900 W at a voltage level of charging AB equal to 60 V.

Fig. 6, 7 show the waveforms of the voltages flowing in the converter in the discharge and charge mode of the AB.

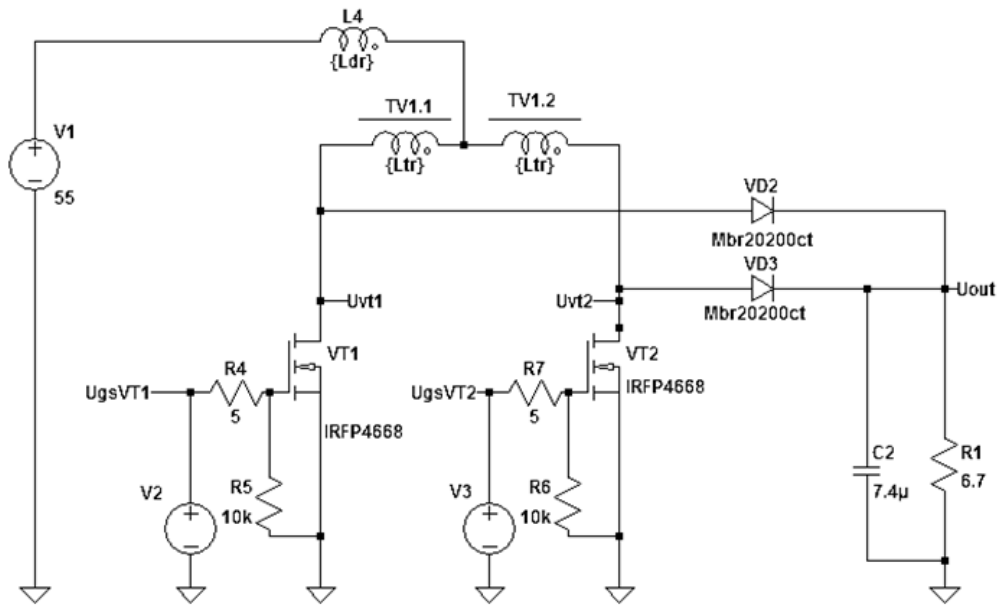


Fig. 4. Simulation model of CDR in AB discharge mode

Рис. 4. Имитационная модель ЗРУ в режиме разряда АБ

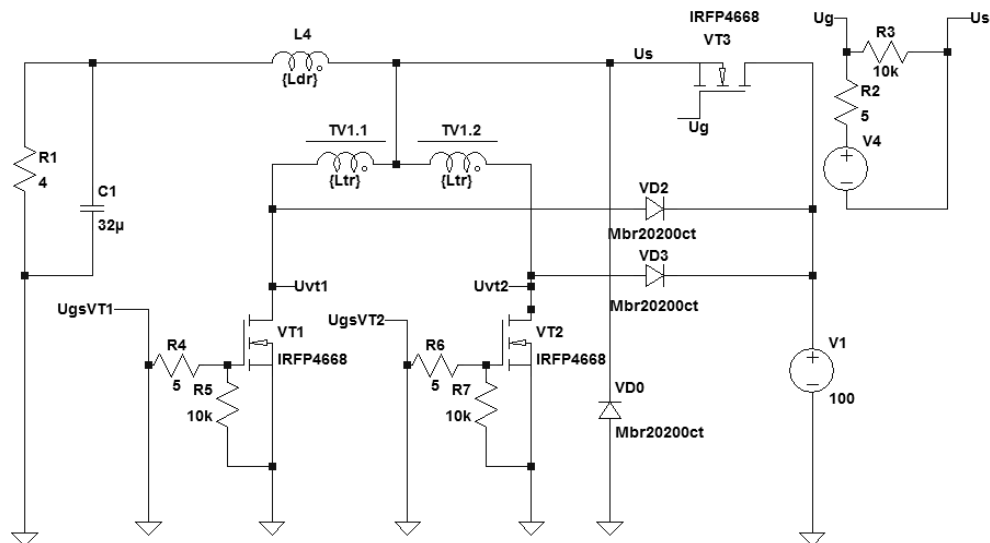


Fig. 5. Simulation model of CDR in AB charge mode

Рис. 5. Имитационная модель ЗРУ в режиме заряда АБ

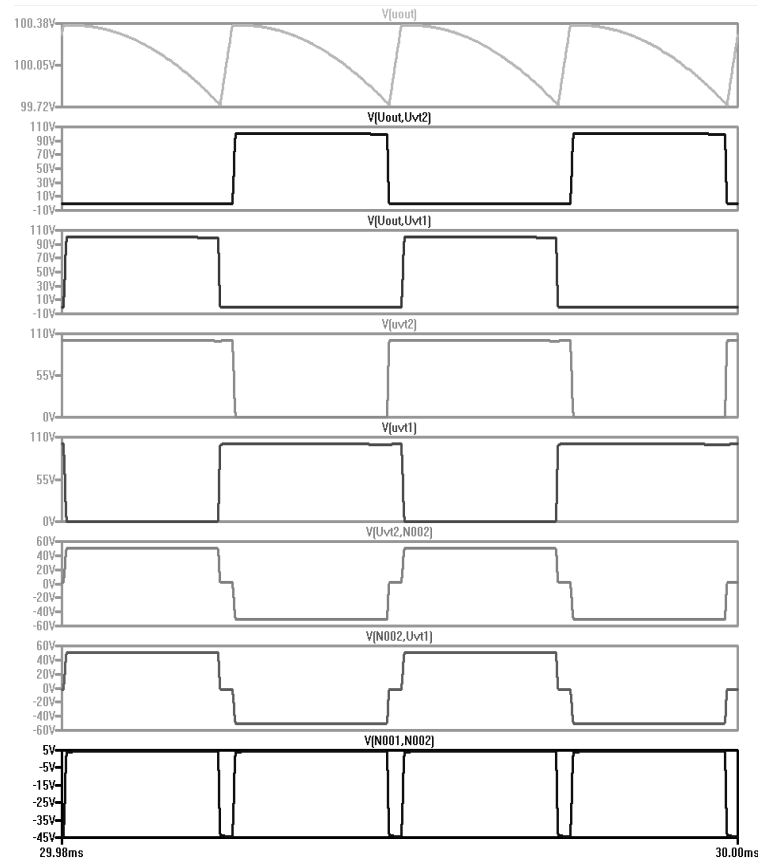


Fig. 6. Waveforms of CDR voltages in the AB discharge mode: V (out) – output voltage; V (out, Uvt2) and V (out, Uvt1) are the voltages on the diodes VD3 and VD2; V (Uvt2) and V (Uvt1) – voltage on transistors VT2 and VT1; V (Uvt2, N002) and V (N001, Uvt1) – voltage on the transformer windings TV1.2 and TV1.1; V (N001, N002) – voltage at the inductor L4

Рис. 6. Осциллограммы напряжений ЗРУ в режиме разряда АБ: V(out) – напряжение на выходной шине питания нагрузки; V(out, Uvt2) и V(out, Uvt1) – напряжения на диодах VD3 и VD2; V (Uvt2) и V (Uvt1) – напряжения на транзисторах VT2 и VT1; V(Uvt2, N002) и V(N002, Uvt1) – напряжение на обмотках трансформатора TV1.2 и TV1.1; V (N001, N002) – напряжение на дросселе L4

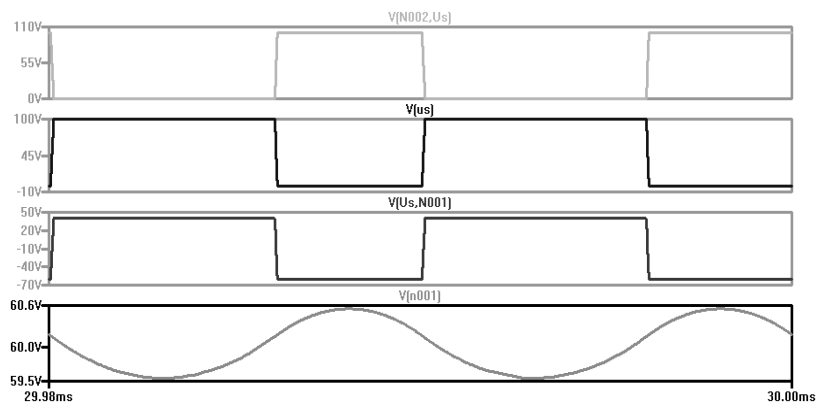


Fig. 7. Waveforms of CDR voltages in the AB charge mode: V (N002, Us) – voltage on the transistor VT3; V (Us) – voltage of diode VD0; V (Us, N001) – voltage at the inductor L4; V (n001) – AB charge voltage

Рис. 7. Осциллограммы напряжений ЗРУ в режиме заряда АБ: V (N002, Us) – напряжение на транзисторе VT3; V (Us) – напряжение на диоде VD0; V (Us, N001) – напряжение на дросселе L4; V (n001) – напряжение заряда АБ

Another promising option for implementing CDR model is its circuit design based on a Weinberg converter with a magnetically coupled inductor and an additional power diode [11–15].

In the LTspice IV environment, simulation models of the CDR based on the Weinberg converter with a magnetically coupled inductor for the charge and discharge modes of the AB were developed (fig. 8, 9).

The parameters of the elements of the simulation model of CDR: accumulator battery voltage in the discharge mode U_{AB_PA3} equal to 55 V, the voltage of the output power bus load U_H is 100 V, the inductance of

each winding of the transformer TV1.1 and TV1.2 is equal to 35 μ H, inductance of inductors L1.1 and L1.2 equal to 2.36 μ H, the frequency f is equal to 100 kHz for transistor model IRFP4668, diode model Mbr20200ct, the capacitor is 2 μ F and 32 μ F.

Converter capacity in the discharge mode is equal to 1500 W (when $U_H = 100$ V). Converter capacity in the in charge mode is 900 W (when the charge voltage of AB is 60 V).

Fig. 10, 11 show the waveforms of the voltages flowing in the converter in the discharge and charge mode of the AB.

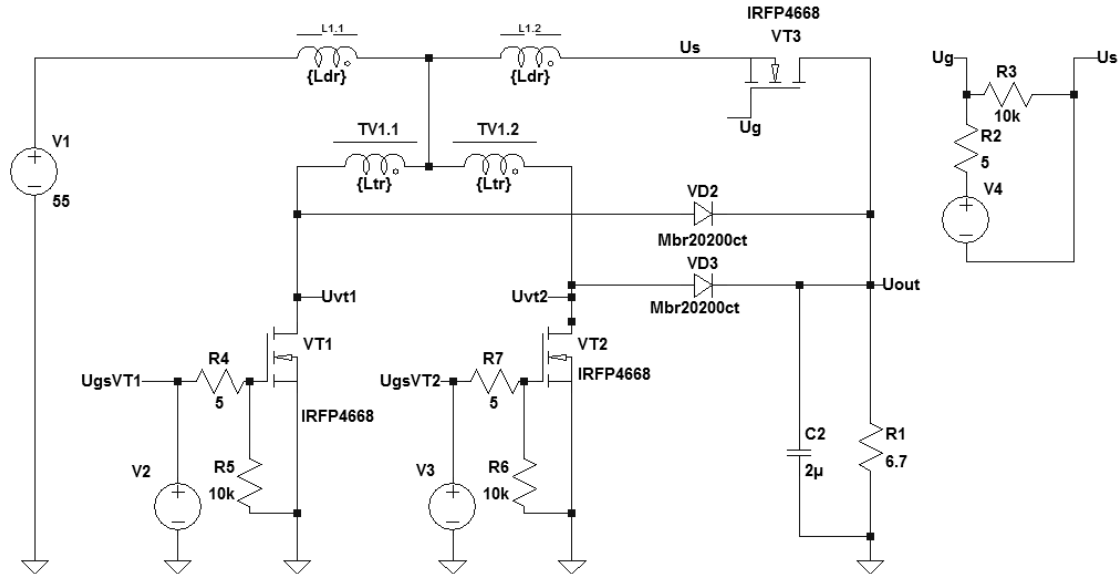


Fig. 8. Simulation model of CDR in AB discharge mode

Рис. 8. Имитационная модель ЗРУ в режиме разряда АБ

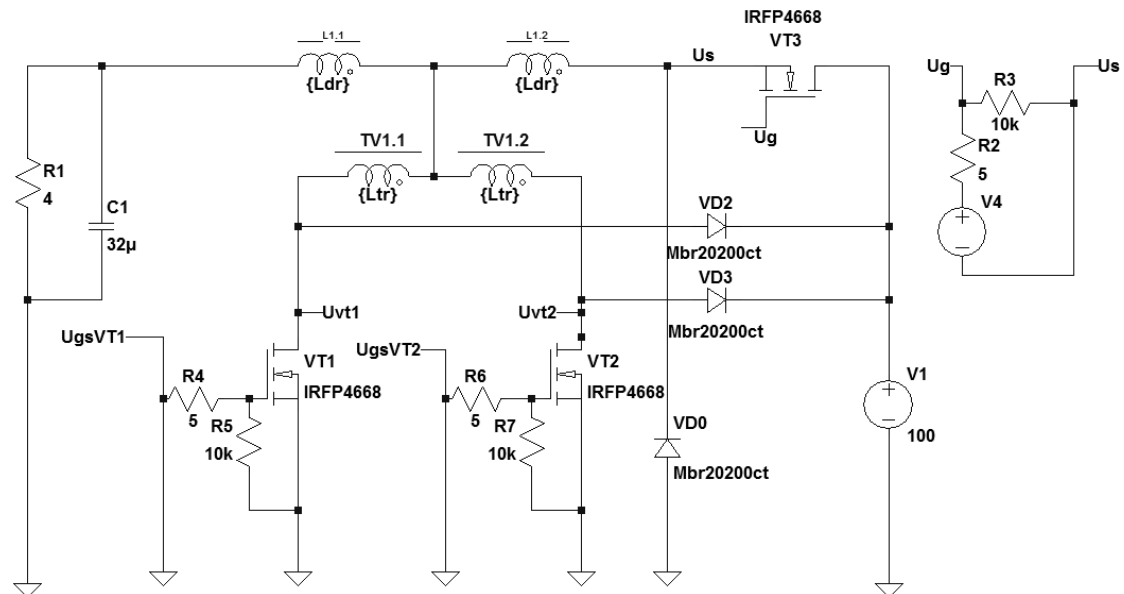


Fig. 9. Simulation model of CDR in AB charge mode

Рис. 9. Имитационная модель ЗРУ в режиме заряда АБ

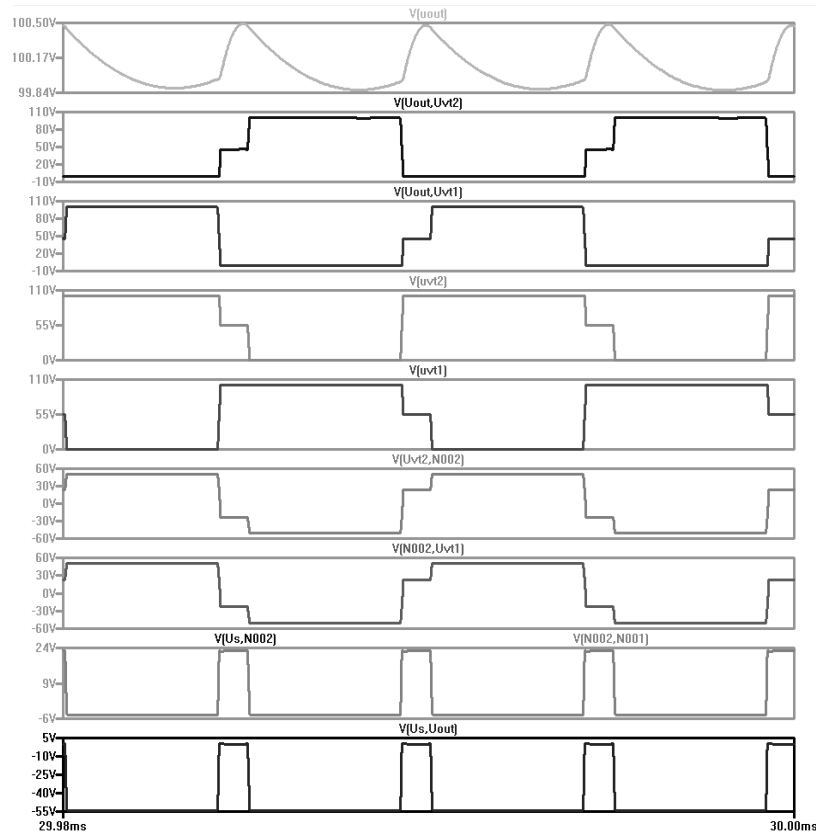


Fig. 10. Waveforms of CDR voltages in the AB discharge mode: V (out) – output voltage; V (out, Uvt2) and V (out, Uvt1) are the voltages on the diodes VD3 and VD2; V (Uvt2) and V (Uvt1) – voltage on transistors VT2 and VT1; V (Uvt2, N002) and V (N002, Uvt1) – voltage on the transformer windings TV1.2 and TV1.1; V (N001, N002) and V (Us, N002) – voltage at the magnetically coupled inductor; V (Us, Uout) – voltage of transistor VT3

Рис. 10. Осциллограммы напряжений ЗРУ в режиме разряда АБ: V (out) – напряжение на выходной шине питания нагрузки; V (out, Uvt2) и V (out, Uvt1) – напряжения на диодах VD3 и VD2; V (Uvt2) и V (Uvt1) – напряжения на транзисторах VT2 и VT1; V (Uvt2, N002) и V (N002, Uvt1) – напряжение на обмотках трансформатора TV1.2 и TV1.1; V (N002, N001) и V (Us, N002) – напряжения на магнитосвязанном дросселе; V (Us, Uout) – напряжение на транзисторе VT3

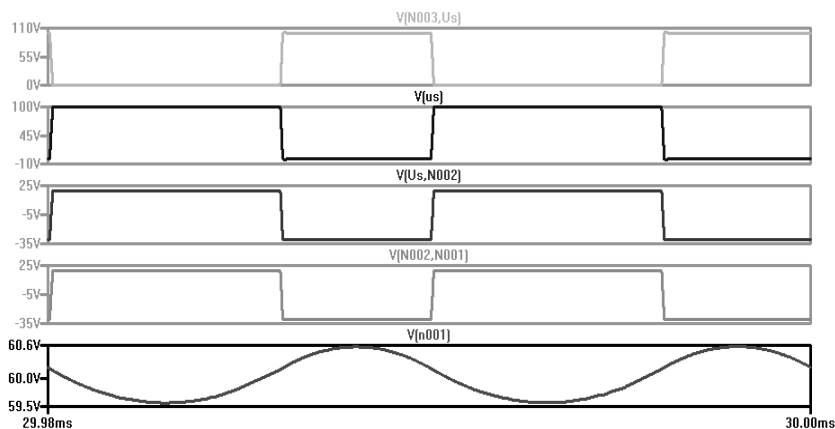


Fig. 11. Waveforms of CDR voltages in the AB charge mode: V (N002, Us) – voltage on the transistor VT3; V (Us) – voltage of diode VD0; V (Us, N002) and V (N002, N001) – voltage at the magnetically coupled inductor; V (n001) – AB charge voltage

Рис. 11. Осциллограммы напряжений ЗРУ в режиме заряда АБ: V (N002, Us) – напряжение на транзисторе VT3; V (Us) – напряжение на диоде VD0; V (Us, N002) и V (N002, N001) – напряжение на магнитосвязанном дросселе; V (n001) – напряжение заряда АБ

The implementation of the SRU module based on a Weinberg converter with a magnetically coupled choke and an additional diode makes it possible to reduce the nominal value of the choke inductance by 2 times and the output capacitor (in the AB discharge mode) by 3.7 times compared to a two-stroke Converter with a single choke, subject to the condition of ensuring an equal level of output voltage ripples (no more than 1 %) in the matched converters.

Conclusion. Nowadays, in the field of development and creation of high-voltage high-power SC PSS, a promising direction is the design based on combined modules of energy-generating equipment, in particular, taking into account the non-simultaneous processes of charging and discharging AB on the basis of combined CDR modules of accumulator batteries.

The study of the processes of energy flows in the PSS and of the comparative analysis found that both implementations of PSS can be optimal depending on the specified cyclogram of SC load and requirements for the specific energy and the weight dimension characteristics of PSS, as well as, for example, according to the requirements of restriction of currents of charge-discharge of AB, etc., which affects the redistribution of energy in PSS. In addition, the choice of the PSS structure should be made subject to taking into account the specific capacity of the energy-generating equipment used and the subsequent calculation of the weight dimension characteristics of PSS alternative options.

Based on the results of simulation of two variants of implementation of CDR module of AB, it was revealed that both studied variants can be used in the development and creation of the ECE of the high-voltage power supply system of the spacecraft. However, the development of a CDR based on the Weinberg converter allows reducing the ratings of the used inductors and output capacitors under the required levels of output voltage ripples.

References

1. Chernaya M. M. Method for calculating the energy characteristics and solar battery parameters of high-voltage power supply systems. *Siberian Journal of Science and Technology*. 2018, Vol. 19, No. 4, P. 651–657.
2. Soustin B. P., Ivanchura V. I., Chernyshev A. I., Islyayev Sh. N. *Sistemy elektropitaniya kosmicheskikh apparatov* [Power supply systems of space crafts]. Novosibirsk, Nauka Publ., 1994, 318 p.
3. Nesterishin M. V., Kozlov R. V., Zhuravlev A. V. [Comparative analysis of energy efficiency of energy converting equipment with parallel and serial solar battery power controller]. *Doklady TUSURa*. 2018, Vol. 21, No. 3, P. 98–102 (In Russ.).
4. Chebotaev V. E., Kosenko V. E. *Osnovy proektirovaniya kosmicheskikh apparatov informatsionnogo obespicheniya* [Basics of design of information space vehicles]. Krasnoyarsk, Sib. State Aerokos. Univ. Publ., 2011, 515 p.
5. Shinyakov Yu. A., Gurtov A. S., Gordeev K. G. et al. [The choice of the structure of power supply systems for low-orbit spacecraft]. *Vestnik Samarskogo gosudarstvennogo aerokosmicheskogo universiteta im.*

akademika S. P. Koroleva. 2010, No. 1(21), P. 103–113 (In Russ.).

6. Akishin A. I. [Impact of electrical discharges on solar panels]. *Nauchno-issledovatel'skii institut yadernoi fiziki imeni D. V. Skobel'tsyna MGU*. 2008, No. 4, P. 68–71 (In Russ.).

7. Lesnykh A. N., Sarychev V. A. [The research of high-voltage power supply systems for space crafts with boost converter]. *Vestnik SibGAU*. 2006, No. 6 (13), P. 63–66 (In Russ.).

8. Chernaya M. M., Shinyakov Yu. A. [Research and development of energy-converting equipment for high-voltage power supply systems for low-Earth orbit space remote sensing devices]. *Sbornik materialov VII Mezhdunarodnoi nauchnotekhnicheskoi konferentsii K. E. Tsiolkovskii – 160 let so dnya rozhdeniya. Kosmonavtika. Radioelektronika. Geoinformatika*. [Proc. of the VII International Scientific and Technical Conference named K. E. Tsiolkovsky]. Ryazan', 2017, P. 134–136 (In Russ.).

9. Chernaya M. M. [Spacecraft Power Systems with Charger-Discharge Module]. *Sbornik izbrannykh statey nauchnoy sessii TUSUR*. 2018, Vol. 1, No. 2, P. 163–166 (In Russ.).

10. Yan Li, Trillion Q. Zheng, Qian Chen. Research on High Efficiency Non-Isolated Push-Pull Converters with Continuous Current in Solar-Battery Systems. *Journal of Power Electronics*. 2014, Vol. 14, No. 3, P. 432–443.

11. Maset E., Ferreres A., Ejea J. B. et al. [High Efficiency Weinberg Converter for Battery Discharging in Aerospace Applications]. *IEEE PESC Conf*. 2006, P. 1510–1516.

12. Chen W., Rong P., Lu Z. Y. [Snubberless bidirectional DC-DC converter with new CLLC resonant tank featuring minimized switching loss]. *IEEE Trans. Ind. Electron*. 2010, Vol. 57, No. 9, P. 3075–3086.

13. Borodin D. B., Tyunin S. S., Kabirov V. A., Semenov V. D. [Weinberg Bidirectional Converter for spacecraft's charge-discharge device]. *XIII Mezhdunarodnaya nauchno-prakticheskaya konferentsiya, posvyashchennaya 55-letiyu TUSURa*. Tomsk, 2017, P. 204–207 (In Russ.).

14. Weinberg A. K., Rueda Boldo P. [A High Power, High Frequency, DC to DC Converter for Space Applications]. *Power Electronics Specialists Conference*. 1992, Vol. 2, P. 1140–1147.

15. Maset E., Ferreres A., Ejea J. B. et al. [5kW Weinberg Converter for Battery Discharging in High-Power Communications Satellites]. *IEEE PESC Conf*. 2005, P. 69–75.

Библиографические ссылки

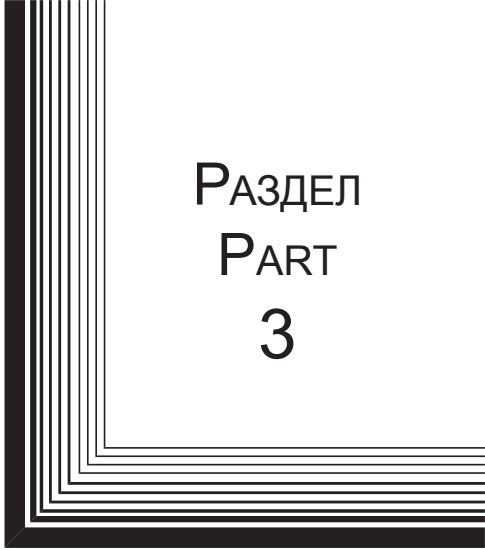
1. Chernaya M. M. Method for calculating the energy characteristics and solar battery parameters of high-voltage power supply systems // Сибирский журнал науки и технологий. 2018. Т. 19, № 4. С. 651–657.
2. Системы электропитания космических аппаратов / Б. П. Соустин, В. И. Иванчура, А. И. Чернышев, Ш. Н. Исляев. Новосибирск : ВО «Наука». Сибирская издательская фирма, 1994. 318 с.

3. Нестеришин М. В., Козлов Р. В., Журавлев А. В. Сравнительный анализ энергетической эффективности энергопреобразующей аппаратуры с параллельным и последовательным регулятором мощности солнечной батареи // Доклады ТУСУРа. 2018. Т. 21, № 3. С. 98–102.
4. Чеботаев В. Е., Косенко В. Е. Основы проектирования космических аппаратов информационного обеспечения. Красноярск, 2011. 515 с.
5. Выбор структуры систем электроснабжения низкоорбитальных космических аппаратов / Ю. А. Шиняков, А. С. Гуртов, К. Г. Гордеев и др. // Вестник Самарского гос. аэрокосмич. ун-та им. академика С. П. Королева. 2010. № 1(21). С. 103–113.
6. Акишин А. И. Воздействие электрических разрядов на солнечные батареи ИСЗ // Науч.-исслед. ин-т ядерной физики им. Д. В. Скобельцына МГУ. 2008. № 4. С. 68–71.
7. Лесных А. Н., Сарычев В. А. Исследование высоковольтных систем электропитания космических аппаратов со стабилизаторами напряжения вольтодобавочного типа // Вестник СибГАУ. 2006. № 6 (13). С. 63–66.
8. Черная М. М., Шиняков Ю. А. Исследование и разработка энергопреобразующей аппаратуры высоковольтных систем электропитания низкоорбитальных космических аппаратов дистанционного зондирования Земли // Сб. материалов VII Междунар. научно-техн. конф. К. Э. Циолковский – 160 лет со дня рождения. Космонавтика. Радиоэлектроника. Геоинформатика. Рязань, 2017. С. 134–136.
9. Черная М. М. Системы электропитания космических аппаратов с модулем зарядно-разрядного устройства // Сб. избр. ст. науч. сессии ТУСУР. 2018. Т. 1, № 2. С. 163–166.
10. Yan Li, Trillion Q. Zheng, Qian Chen. Research on High Efficiency Non-Isolated Push-Pull Converters with Continuous Current in Solar-Battery Systems // Journal of Power Electronics. 2014. Vol. 14, No. 3. P. 432–443.
11. High Efficiency Weinberg Converter for Battery Discharging in Aerospace Applications / E. Maset, A. Ferreres, J. B. Ejea et al. // IEEE PESC Conf. 2006. P. 1510–1516.
12. Chen W., Rong P., Lu Z. Y. Snubberless bidirectional DC-DC converter with new CLLC resonant tank featuring minimized switching loss // IEEE Trans. Ind. Electron. 2010. Vol. 57, No. 9. P. 3075–3086.
13. Двухнаправленный преобразователь Вейнберга для зарядно-разрядного устройства системы электропитания космических аппаратов / Д. Б. Бородин, С. С. Тюнин, В. А. Кабиров, В. Д. Семенов // XIII Междунар. науч.-практич. конф., посвященная 55-летию ТУСУРа. Томск, 2017. С. 204–207.
14. Weinberg A. K., Rueda Boldo P. A High Power, High Frequency, DC to DC Converter for Space Applications // Power Electronics Specialists Conference. 1992. Vol. 2. P. 1140–1147.
15. 5kW Weinberg Converter for Battery Discharging in High-Power Communications Satellites / E. Maset, A. Ferreres, J. B. Ejea et al. // IEEE PESC Conf. 2005. P. 69–75.


© Filonova M. M., 2020

Filonova Mariya Mikhailovna – Cand. Sc., senior Researcher; Tomsk State University of Control Systems and Radioelectronics, Department of Radio Engineering Systems. E-mail: cmm91@inbox.ru.

Филонова Мария Михайловна – кандидат технических наук, старший научный сотрудник; Томский государственный университет систем управления и радиоэлектроники, НИИ космических технологий. E-mail: cmm91@inbox.ru.



РАЗДЕЛ
PART
3



ТЕХНОЛОГИЧЕСКИЕ
ПРОЦЕССЫ
И МАТЕРИАЛЫ

TECHNOLOGICAL
PROCESSES
AND MATERIALS SCIENCE



UDC 539.21:537.86

Doi: 10.31772/2587-6066-2020-21-1-108-114

For citation: Konovalov S. O., Begisheva O. B., Hichem Abdelbaki, Rybina U. I., Yukhno M. Yu. Research on electrical properties of manganese sulphides doped by thulium and ytterbium ions. *Siberian Journal of Science and Technology*. 2020, Vol. 21, No. 1, P. 108–114. Doi: 10.31772/2587-6066-2020-21-1-108-114

Для цитирования: Коновалов С. О., Бегешева О. Б., Хишем Абдельбаки, Рыбина У. И., Юхно М. Ю. Исследование электрических свойств сульфидов марганца допированных ионами тулия и иттербия // Сибирский журнал науки и технологий. 2020. Т. 21, № 1. С. 108–114. Doi: 10.31772/2587-6066-2020-21-1-108-114

RESEARCH ON ELECTRICAL PROPERTIES OF MANGANESE SULPHIDES DOPED BY THULIUM AND YTTERBIUM IONS

S. O. Konovalov*, O. B. Begisheva, Abdelbaki Hichem, U. I. Rybina, M. Yu. Yukhno

Reshetnev Siberian State University of Science and Technology
31, Krasnoyarsky Rabochy Av., Krasnoyarsk, 660037, Russian Federation
*E-mail: kco.konovalov@yandex.ru

Materials exhibiting connection between electrical and magnetic properties are attractive for possible use as an element base in microelectronics, spintronics, and sensor devices. Compounds with mixed valence exhibit a number of metal-insulator phase transitions, magnetic phase transitions, including changes in magnetic properties without changing magnetic symmetry.

Promising materials for studying these effects are cation-substituted $Mn_{1-x}Re_xS$ compounds ($Re = 4f$ elements) synthesized on the basis of the antiferromagnetic semiconductor of manganese monosulfide. The latter is of practical importance in the development of new materials for temperature sensors, widely used in the metallurgical industry.

The structural and electrical properties of compounds with mixed valences $Tm_xMn_{1-x}S$ ($0 \leq x \leq 0.15$) and $Tm_xMn_{1-x}S$ ($0 \leq x \leq 0.25$) were studied in the temperature range 80–1100K. The regions of existence of solid solutions of $Tm_xMn_{1-x}S$ sulfides with an fcc (face-centered cubic) lattice of the NaCl type were determined. It was found that conductivity decreases upon the substitution of manganese cations with thulium ions and the lattice constant increases more sharply in comparison with Vegard's law. When ytterbium ions are substituted, the conductivity increases with increasing concentration and the temperature dependence has the form typical of semiconductors.

Key words: manganese sulfide, mixed valence, conductivity, X-ray diffraction analysis.

ИССЛЕДОВАНИЕ ЭЛЕКТРИЧЕСКИХ СВОЙСТВ СУЛЬФИДОВ МАРГАНЦА ДОПИРОВАННЫХ ИОНАМИ ТУЛИЯ И ИТТЕРБИЯ

С. О. Коновалов*, О. Б. Бегешева, Абдельбаки Хишем, У. И. Рыбина, М. Ю. Юхно

Сибирский государственный университет науки и технологий имени М. Ф. Решетнева
Российская Федерация, 660037, просп. им. газ. «Красноярский рабочий», 31
*E-mail kco.konovalov@yandex.ru

Материалы, обнаруживающие связь между электрическими и магнитными свойствами, являются привлекательными для возможного использования в качестве элементной базы в микроэлектронике, спинтронике, сенсорных устройствах. Соединения с переменной валентностью проявляют ряд фазовых переходов металл-диэлектрик, магнитные фазовые переходы, включая изменения магнитных свойств без изменения магнитной симметрии.

Перспективными материалами для изучения этих эффектов являются катион замещенные соединения $Mn_{1-x}Re_xS$ ($Re = 4f$ элементы), синтезированные на основе антиферромагнитного полупроводника моносulfида марганца. Последнее имеет практическую значимость в разработке новых материалов для датчиков температуры, широко используемых в металлургической отрасли.

Проведены исследования структурных и электрических свойств соединений с переменной валентностью $Tm_xMn_{1-x}S$ ($0 \leq x \leq 0.15$) и $Tm_xMn_{1-x}S$ ($0 \leq x \leq 0.25$) в области температур 80–1100K. Определены области существования твердых растворов сульфидов $Tm_xMn_{1-x}S$ с ГЦК решеткой типа NaCl. Установлено уменьшение проводимости при замещении катионов марганца ионами тулия и более резкое увеличение постоянной решетки по сравнению с законом Вегарда. При замещении ионами иттербия проводимость увеличивается с ростом концентрации и температурная зависимость имеет вид, типичный для полупроводников.

Ключевые слова: сульфид марганца, переменная валентность, проводимость, рентгеноструктурный анализ.

Introduction. Compounds containing rare-earth chemical elements with mixed valence such as Sm, Yb, Ce, Eu, Tm have a number of unique properties. Phase transitions of purely electronic nature and associated with change in the filling of 4f electronic levels [1] often occur in them when external conditions (temperature, pressure, composition) change. At the same time the magnetic properties also change [2–4] (localized magnetic moments disappear), i. e. the transitions are of the “magnetic – nonmagnetic” state type [5]. Change in the type of conductivity from semiconductor to metal type and a significant magnitude of magnetoresistance (of the order of 100 %) in the paramagnetic region at room temperatures and above [6–11] is observed in manganese sulfides substituted by samarium [6] and gadolinium [7] ions.

Thulium sulfide has a cubic crystalline structure with a lattice parameter of 5.412 Å. This compound is characterized by a metallic type of conductivity at $T > 100$ K with electron concentration of about 10^{22} cm⁻³ and resistivity of about 10^{-6} Ohm / cm at room temperature [2]. Thulium whose electronic configuration of the 4f – shell is unstable and close to a filled one, can enter the compounds with other elements, be in the state of $\text{Tm}^{2+} 4f^{13}$ term $^2F_{7/2}$ and $\text{Tm}^{3+} 4f^{12}$ term 3H_6 . In TmS a thulium ion is in the trivalent state with a 4f level filling of $n_f = 0.65$ and the energy difference between the divalent and trivalent states $E^{2+} - E^{3+} = 0.3$ eV [12]. The proximity of the energies of thulium aliovalent states leads to the fact that TmS exhibits a Condo effect in which band electrons group around thulium ions screening its magnetic moment [13]. Under the action of pressure “quasilocalized” states expand and pass into the conduction band, which will manifest itself in the form of transition to the usual metallic state. This is confirmed by the baric dependence of thulium thermopower, which decreases under pressure to 20 GPa, and ceases to change at higher pressures [14]. Pressure leads to changing magnetic characteristics and magnetic structure [15–18]

Ytterbium sulfide at normal pressure is a semiconductor with a direct gap in the spectrum of electronic excitations ~ 1.3 eV and an indirect gap ~ 1.0 eV between the fully occupied *f*-state and free *sd*-band states [19], which are 4 eV higher in energy than the 3 *p*-valence band of sulfur ions. Under pressure the gap monotonically decreases $dE_g / dp = -6 \pm 1$ eV / kbar [20], at 8 GPa the zones overlap and a metallic state arises [21]. At 10 GPa quantum resonance, that is, a superposition of f_{13} and f_{14} states and change in valence from 2 to 4 is observed. The density of current carriers per an ytterbium ion is 0.4 [22]

Materials and methods of research. The synthesis of $\text{Mn}_{1-x}\text{Re}_x\text{S}$ samples is described in detail in [8]. Solid solutions $\text{Mn}_{1-x}\text{Tm}_x\text{S}$ and $\text{Mn}_{1-x}\text{Yb}_x\text{S}$ were obtained by solid-phase synthesis, degrees of substitution 0.05; 0.10; 0.15 and 0.05; 0.10; 0.15; 0.2; 0.25 respectively.

X-ray diffraction analysis of $\text{Mn}_{1-x}\text{Tm}_x\text{S}$ ($x = 0.05; 0.15$) and $\text{Mn}_{1-x}\text{Yb}_x\text{S}$ ($x = 0.1; 0.2$) sulfides was carried out on a DRON-3 installation in $\text{CuK}\alpha$ -radiation at temperature of 300 K after they were obtained and their transport properties were measured. X-ray diffraction

patterns obtained after the measurements indicate that all the substances studied have a face-centered cubic (fcc) structure of the NaCl type typical of manganese monosulfide.

The conductivity was measured in the temperature range 80–1100 K using the four-probe method. The four-probe method for measuring electrical resistivity is the most common. The method is very convenient since there is no need to create ohmic contacts; it is possible to measure the resistivity of bulk samples of the most diverse shapes and sizes, as well as the resistivity of layers of semiconductor structures, for example, during ion implantation. In this case, one condition must be fulfilled as far as the shape is concerned, that is, the presence of a flat surface whose linear dimensions exceed the linear dimensions of the probe system (the distance between them).

Four metal probes with a small contact area (fig. 1) the distances between which are s_1, s_2, s_3 , are placed on the flat surface of the sample along a straight line. Electric current I_{14} is passed through two external probes 1 and 4, and the potential difference U_{23} is measured on two internal probes 2 and 3.

Results and discussion. X-ray diffraction patterns of the synthesized sulfides were obtained (fig. 2, 3). X-ray diffraction patterns obtained after measurements indicate that all the substances studied have a stable crystalline state up to temperatures of the order of 1100 K. X-ray diffraction analysis showed that the synthesized compounds are single-phase and have a face-centered cubic (fcc) structure of the NaCl type, typical of manganese monosulfide. With increase in the degree of cationic substitution (x), the unit cell parameter a increases linearly, which indicates the formation of $\text{Mn}_{1-x}\text{Tm}_x\text{S}$ and $\text{Mn}_{1-x}\text{Yb}_x\text{S}$ solid solutions (fig. 2, 3). Increase in the lattice constant, compared with linear growth according to Vegard's law, is possibly associated with the localization of electrons at the interface of manganese ions with substituted ones and with weak hybridization of 4f-3d orbitals, which is described by an exponential dependence on distance.

The temperature dependence on conductivity was measured for the synthesized samples $\text{Mn}_{1-x}\text{Tm}_x\text{S}$ ($0.01 \leq x \leq 0.15$) and $\text{Mn}_{1-x}\text{Yb}_x\text{S}$ ($0.05 \leq x \leq 0.25$) (fig. 4). The behavior of the $\ln \sigma$ ($10^3 / T$) dependences is characteristic of substances with semiconductor conductivity. Fig. 4, *a* shows the electrical conductivity of $\text{Tm}_x\text{Mn}_{1-x}\text{S}$ solid solutions. A sample with a thulium substitution degree of $x = 0.05$ has a conductivity plateau from 310 to 380 K. For $x = 0.1$ there is an anomaly in the conductivity behavior from 330 to 360 K. For $x = 0.15$ there is an anomaly in the conductivity behavior from 650 K to 690 K. All of the studied samples with thulium are characterized by a high resistance state even at room temperature in comparison with the electrical resistance observed in manganese monosulfide [8]. Fig. 4, *b* shows the electrical conductivity of $\text{Tm}_x\text{Yb}_{1-x}\text{S}$ solid solutions. When the temperature increases the conductivity grows significantly faster in the case of ytterbium than in the case of thulium.

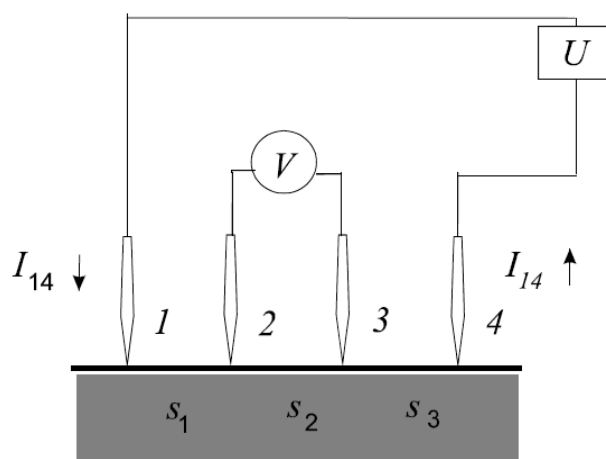


Fig. 1. A schematic diagram of measurements using the four-probe method

Рис. 1. Принципиальная схема измерений четырёхзондовым методом

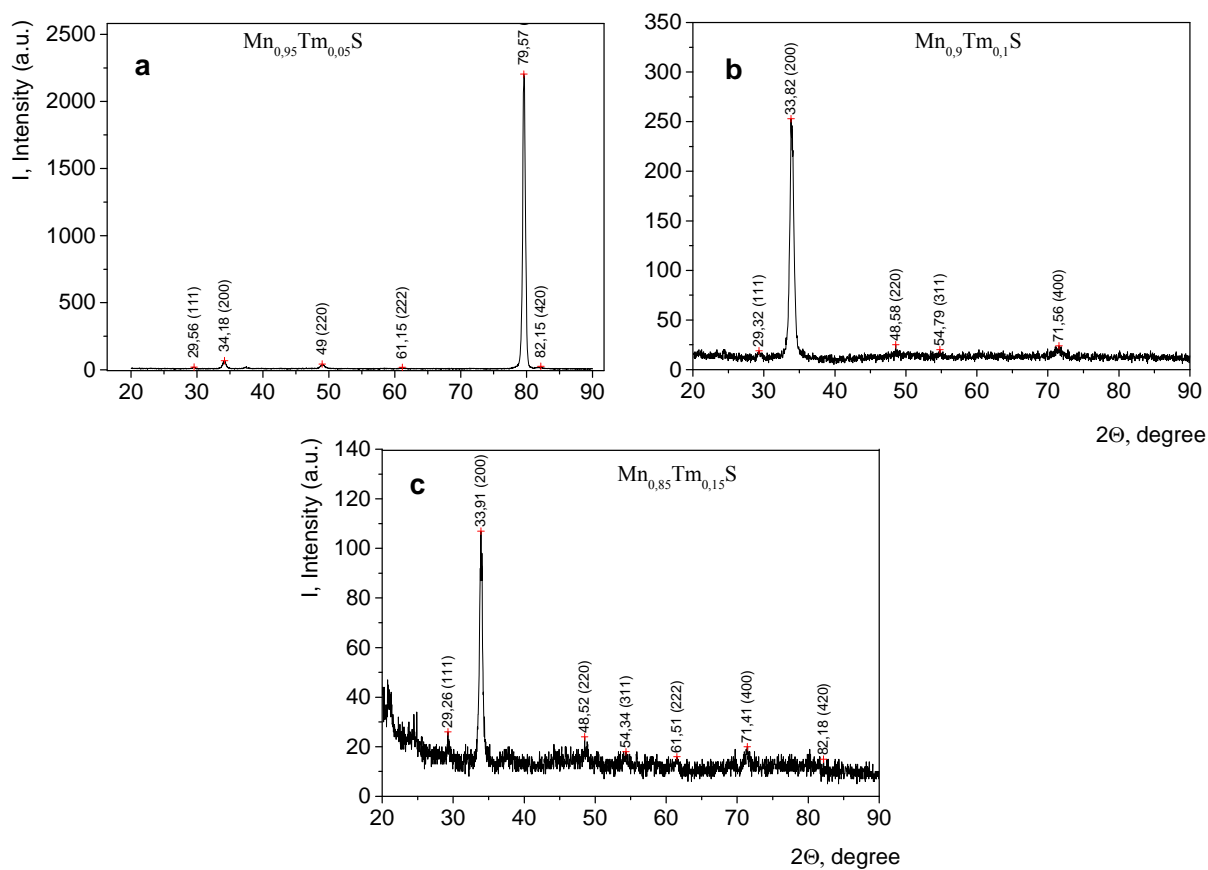


Fig. 2. X-ray diffraction patterns of $\text{Mn}_{1-x}\text{Tm}_x\text{S}$:
a – $x = 0.05$; b – $x = 0.1$; c – $x = 0.15$

Рис. 2. Рентгенограммы $\text{Mn}_{1-x}\text{Tm}_x\text{S}$:
a – $x = 0.05$; b – $x = 0.1$; c – $x = 0.15$

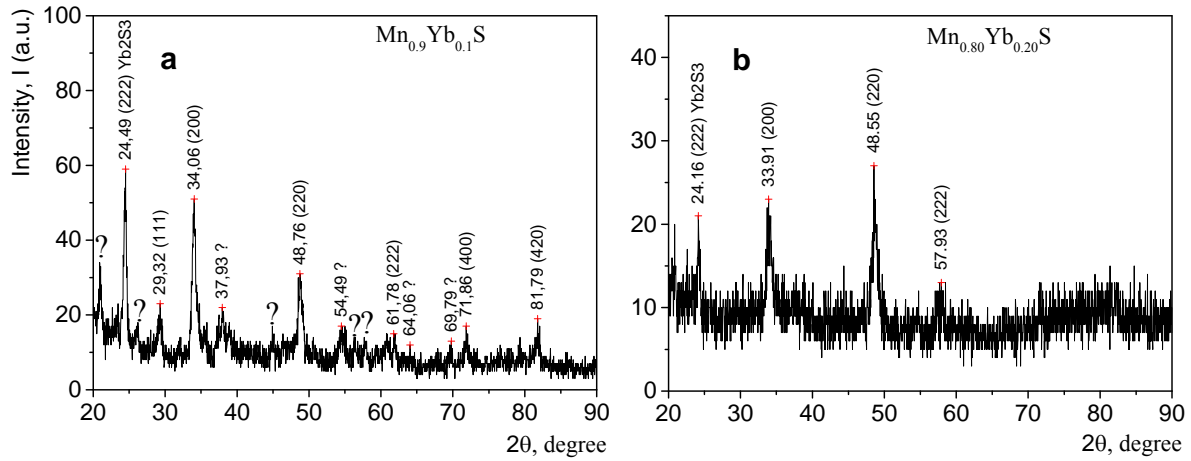


Fig. 3. X-ray diffraction patterns of $\text{Mn}_{1-x}\text{Yb}_x\text{S}$:
a – $X=0.1$; b – $X=0.2$

Рис. 3. Рентгенограммы $\text{Mn}_{1-x}\text{Yb}_x\text{S}$:
a – $X=0.1$; b – $X=0.2$

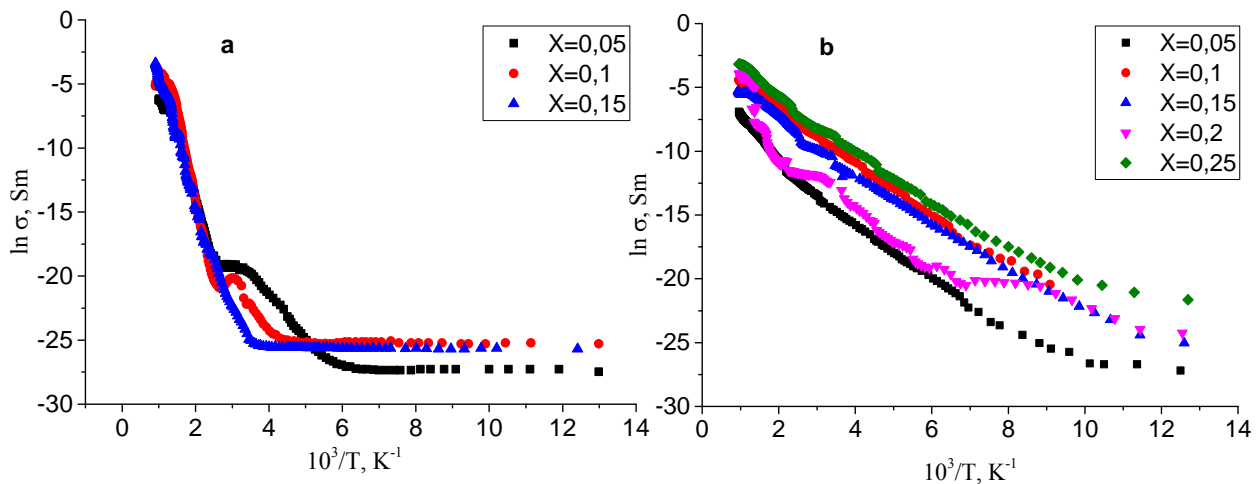


Fig. 4. Temperature dependence on conductivity:
a – $\text{Mn}_{1-x}\text{Tm}_x\text{S}$ ($0.05 \leq X \leq 0.15$); b – $\text{Mn}_{1-x}\text{Yb}_x\text{S}$ ($0.05 \leq X \leq 0.25$)

Рис. 4. Зависимость проводимости от температуры:
a – $\text{Mn}_{1-x}\text{Tm}_x\text{S}$ ($0.05 \leq X \leq 0.15$); b – $\text{Mn}_{1-x}\text{Yb}_x\text{S}$ ($0.05 \leq X \leq 0.25$)

The dependences of the conductivity on the substitution concentration of thulium and ytterbium ions at room temperature are shown in fig. 5. With increase in the degree of samples doping with thulium the conductivity decreases (fig. 5, a), and when doping with ytterbium a similar conductivity behavior occurs, but there is a section in the concentration range from $X = 0.1$ to $X = 0.2$ in which, on the contrary, growth is observed. In general, there is a nontrivial picture that is different from the behavior of impurity semiconductors, in which substitution with an alloying element increases the concentration of charge carriers and, as a result, the conductivity.

This behavior can be explained by the fact that an ytterbium ion is trivalent and, when a divalent manganese ion is substituted in a solid solution, both electrons and holes are formed by non-stoichiometry of the obtained samples. With increase in the substitution concentration, electrons and holes accumulate at intercrystalline boundaries and form a carrier-depleted layer similar to the p-n junction. Substitution with ytterbium ions leads to the formation of holes in the cationic subsystem; as a result, the conductivity decreases sharply compared to manganese sulfide. As the concentration of hole current carriers increases, the conductivity increases (fig. 5, b).

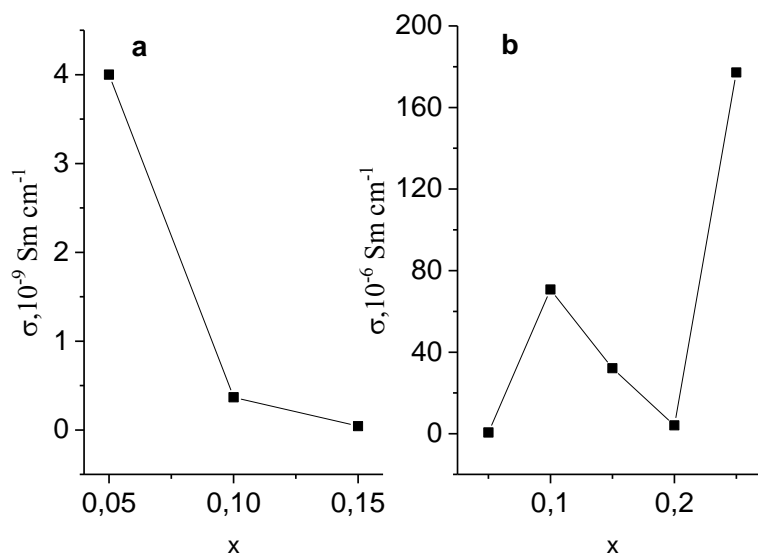


Fig. 5. Dependence of conductivity on the temperature of samples $\text{Mn}_{1-x}\text{Yb}_x\text{S}$ ($0.05 \leq X \leq 0.25$)

Рис. 5. Зависимость проводимости от температуры образцов $\text{Mn}_{1-x}\text{Yb}_x\text{S}$ ($0.05 \leq X \leq 0.25$)

Conclusion. X-ray diffraction analysis of solid solutions of manganese sulfides substituted by rare-earth ions of thulium and ytterbium was carried out. It was found that the synthesized compounds are single-phase ones and have a face-centered cubic (fcc) structure. There is increase in the unit cell when substituted by thulium and ytterbium.

Decrease in the conductivity upon substitution with thulium and increase in the conductivity of solid solutions upon substitution with ytterbium were found. The temperature dependence of substituted sulfides has a semiconductor form. The concentration dependence of the conductivity for $\text{Mn}_{1-x}\text{Tm}_x\text{S}$ is explained by the formation of a space charge at the boundaries of intercrystalline grains.

Acknowledgments. The research was financially supported by the RFPI No. 18-32-00079 mol_a and a grant from Siberian State University of Science and Technology.

Благодарности. Исследование выполнено при финансовой поддержке РФФИ № 18-32-00079 mol_a и гранта СибГУ.

References

1. Eerenstein W., Mathur N.D., Scott J. F. Dielectric and Magnetic Properties of Nano-Structure BiFeO_3 Doped with Different Concentrations of Co Ions Prepared by Sol-Gel Method. *Multiferroic and Magnetoelectric Materials. Nature Journal*. 2006, Vol. 442, P. 759–765.
2. Golubkov A. V., Goncharova E. V., Zhuze V. P., Loginov G. M., Sergeeva V. M., Smirnov I.A. *Fizicheskie svoystva khal'kogenidov redkozemel'nykh elementov* [Physical properties of chalcogenides of rare earth elements.]. Leningrad, Nauka Publ., 1973, 304 p.
3. Aplesnin S. S., Sitnikov M. N. Magnetotransport effects in paramagnetic $\text{Gd}_x\text{Mn}_{1-x}\text{S}$. *JETP letters*. 2014, Vol. 100, Iss. 1-2, P. 104–110.
4. Aplesnin S. S., Petrakovskii G. A., Ryabinkina L. I., Abramova G. M., Kiselev N. I., Romanova O. B. Influence of magnetic ordering on the resistivity anisotropy of α -MnS single crystal. *Solid State Communications*. 2004, Vol. 129, Iss. 3, P. 195–197.
5. Aplesnin S. S. Spin liquid and quantum effect in antiferromagnets. *Palmarium Academic Publ.*, 2012, 140 p.
6. Aplesnin S. S., Romanova O. B., Gorev M. V., Velikanov D. A., Gamzatov A. G., Aliev A. M. Magnetic and thermophysical properties of $\text{Gd}_x\text{Mn}_{1-x}\text{S}$ solid solutions. *J. Phys.: Cond. Matt.* 2013, Vol. 25, P. 025802.
7. Aplesnin S. S., Khar'kov A. M., Eremin E. V., Romanova O. B., Balaev D. A., Sokolov V. V., Pichugin A. Yu. Nonuniform Magnetic States and Electrical Properties of Solid Solutions. *IEEE Transactions on magnetics*. 2011, Vol. 47, P. 4413–4416.
8. Ryabinkina L. I., Romanova O. B., Aplesnin S. S. Sulfide compounds $\text{Me}_x\text{Mn}_{1-x}\text{S}$ (Me = Cr, Fe, V, Co): technology, transport properties, and magnetic ordering. *Bulletin of the Russian Academy of Science: Physics*. 2008, Vol. 72, Iss. 8, P. 1050–1052.
9. Ryabinkina L. I., Petrakovskii G. A., Loseva G. V., Aplesnin S. S. Metal-insulator transition and magnetic properties in disordered systems of solid solutions $\text{MEXMn}_{1-x}\text{S}$. *Journal of Magnetism and Magnetic Materials*. 1995, Vol. 140–144, Iss. 1, P. 147–148.
10. Aplesnin S. S., Ryabinkina L. I., Abramova G. M., Romanova O. B., Kiselev N. I., Bovina A. F. Spin-dependent transport in α -MnS single crystals. *Physics of the Solid State*. 2004, Vol. 46, Iss. 11, P. 2067–2072.
11. Aplesnin S. S., Romanova O. B., Khar'kov A. M., Balaev D. A., Gorev M. V., Vorotinov A. I., Sokolov V. V., Pichugin A. Yu. Metal-semiconductors transition in $\text{Sm}_x\text{Mn}_{1-x}\text{S}$ solid solutions. *Physica Status Solidi (B): Basic Solid State Physics*. 2012, Vol. 249, Iss. 4, P. 812–817.

12. Strange P., Svane A., Temmerman W. M., Szotek Z., Winter H. Understanding the valence of rare earths from first-principles theory. *Letters to nature*. 1999, Vol. 399, Iss. 6738, P. 756–758.
 13. Derr J., Kneel G., Sake B., M'easson M.-A., Flouquet J. J. Valence and magnetic ordering in intermediate valence compounds : TmSe versus SmB6. *J. Phys.: Condens. Matter*. 2006, Vol. 18, P. 2089–2106.
 14. Abdusalyamova M. N., Alekseev P. A., Klement'ev E. S., Nefedova E. V., Nizhankovskiy V. I. [Change of the tulium valence in TmSb $1 - x$ Te x compounds]. *Fizika Tverdogo Tela*. 1994, T. 36, Vol. 1, P. 145–151 (In Russ.).
 15. Aplesnin S. S. A study of anisotropic Heisenberg antiferromagnet with $S=1/2$ on a square lattice by Monte-Carlo method. *Physica Status Solidi (B): Basic Solid State Physics*. 1998, Vol. 207, Iss. 2, P. 491–498.
 16. Aplesnin S. S. Dimerization of antiferromagnetic chain with four-spin interactions. *Physics of the Solid State*. 1996, Vol. 38, Iss. 6, P. 1031–1036.
 17. Aplesnin S. S. Nonadiabatic interaction of acoustic phonons with spins $S = 1/2$ in the two-dimentional Heisenberg model. *Journal of Experimental and Theoretical Physics*. 2003, Vol. 97, Iss. 5, P. 969–977.
 18. Aplesnin S. S. Quantum Monte-Carlo analysis of the 2d Heisenberg antiferromagnet with $S = 1/2$: the influence of exchange anisotropy. *Journal of Physics: Condensed Matter*. 1998, Vol. 10, Iss. 44, P. 10061–10065.
 19. Syassen K., Winzen H., Zimmer H. G., Tups H., J. M. Leger. Optical response of YbS and YbO at high pressures and the pressure-volume relation of YbS. *Phys. Rev*. 1985, B. 32, P. 8246.
 20. Aplesnin S. S., Khar'kov A. M., Romanova O. B., Yanushkevich K. I., Galyas A. I., Sokolov V. V. Magnetic and electric properties of Yb $_x$ Mn $_{1-x}$ S alloys. *Bulletin of the Russian Academy of Sciences: Physics volume*. 2013, Vol. 77, No 10, P. 1252–1254.
 21. Matsunami M., Okamura H., Ochiai A., Nanba T. Pressure tuning of an ionic insulator into a heavy electron metal: an infrared study of YbS. *Physical review letters*. 2009, Vol. 103, Iss. 23, P. 237202.
 22. Aplesnin S. S., Ryabinkina L. I., Romanova O. B., Sokolov V. V., Pichugin A. Y., Galyas A. I., Demidenko O. F., Makovetski G. I., Yanushkevich K. I. Magnetic and electrical properties of cation-substituted sulfides Me $_x$ Mn $_{1-x}$ S (Me = Co, Gd). *Physics of the Solid State*. 2009, Vol. 51, Iss. 4, P. 698–701.
- Библиографические ссылки**
1. Eerenstein W., Mathur N.D., Scott J.F. Dielectric and Magnetic Properties of Nano-Structure BiFeO3 Doped with Different Concentrations of Co Ions Prepared by Sol-Gel Method // *Multiferroic and Magnetoelectric Materials* // Nature Journal. 2006. Vol. 442, No. 7104. P. 759–765.
 2. Физические свойства халькогенидов редкоземельных элементов / А. В. Голубков, Е. В. Гончарова, В. П. Жузе и др. Л. : Наука, 1973. С. 304.
 3. Аплеснин С. С., Ситников М. Н. Магнитотранспортные эффекты в парамагнитном состоянии в GD $_x$ MN $_{1-x}$ S. // Письма в ЖЭТФ. 2014. Т. 100, В. 1-2. С. 104–110.
 4. Influence of magnetic ordering on the resistivity anisotropy of α -MNS single crystal / S. S. Aplesnin, G. A. Petrakovskii, L. I. Ryabinkina et al. // *Solid State Communications*. 2004. Vol. 129, Iss. 3. P. 195–197.
 5. Aplesnin S. S. Spin liquid and quantum effect in antiferromagnets. *Palmarium Academic Publ*. 2012. P. 140.
 6. Magnetic and thermophysical properties of GdxMn1-xS solid solutions / S. S. Aplesnin, O. B. Romanova, M. V. Gorev et al. // *J. Phys.: Cond. Matt*. 2013. Vol. 25. P. 025802.
 7. Nonuniform Magnetic States and Electrical Properties of Solid Solutions / S. S. Aplesnin, A. M. Khar'kov, E. V. Eremin et al. // *IEEE Transactions on magnetics*. 2011. Vol. 47. P. 4413–4416.
 8. Рябинкина Л. И., Романова О. Б., Аплеснин С. С. Сульфидные соединения Me $_x$ Mn $_{1-x}$ S (Me = Cr, Fe, V, Co): технология, транспортные свойства и магнитное упорядочение // *Известия российской академии наук. Серия физическая*. 2008. Т. 72, В. 8. С. 1115–1117.
 9. Metal-insulator transition and magnetic properties in disordered systems of solid solutions ME $_x$ MN $_{1-x}$ S / L. I. Ryabinkina, G. A. Petrakovskii, G. V. Loseva, S. S. Aplesnin // *Journal of Magnetism and Magnetic Materials*. 1995. Vol. 140-144, Iss.1. P. 147–148.
 10. Спин-зависимый транспорт в монокристалле α -MNS / С. С. Аплеснин, Л. И. Рябинкина, Г. М. Абрамова и др. // *Физика твердого тела*. 2004. Т. 46, В. 11. С. 2000–2005.
 11. Metall-semiconductors transition in Sm $_x$ Mn $_{1-x}$ S solid solutions / S. S. Aplesnin, O. B. Romanova, A. M. Har'kov // *Physica Status Solidi (B): Basic Solid State Physics*. 2012. Vol. 249, Iss. 4. P. 812–817.
 12. Understanding the valence of rare earths from first-principles theory / P. Strange, A. Svane, W. M. Temmerman et al. // *Letters to nature*. 1999. Vol. 399, Iss. 6738. P. 756–758.
 13. Derr J., Kneel G., Sake B., M'easson M.-A., Flouquet J. J. Valence and magnetic ordering in intermediate valence compounds : TmSe versus SmB6 // *J. Phys.: Condens. Matter*. 2006. Vol. 18. P. 2089–2106.
 14. Изменение валентности тулия в соединениях TmSb $_{1-x}$ Te $_x$ / М. Н. Абдусалимова, П. А. Алексеев, Е. С. Клементьев и др. // *Физика твердого тела*. 1994. Т. 36, В. 1. С. 145–151.
 15. Aplesnin S.S. A study of anisotropic Heisenberg antiferromagnet with $S=1/2$ on a square lattice by monte-carlo method // *Physica Status Solidi (B): Basic Solid State Physics*. 1998. Vol. 207, Iss. 2. P. 491–498.
 16. Aplesnin S. S. Dimerization of antiferromagnetic chain with four-spin interactions // *Physics of the Solid State*. 1996. Vol. 38, Iss. 6. P. 1031–1036.
 17. Аплеснин С. С. Неадиабатическое взаимодействие акустических фононов со спинами $S = 1/2$ в двумерной модели Гейзенберга // *Журнал экспериментальной и теоретической физики*. 2003. Т. 124, В. 5. С. 1080–1089.
 18. Aplesnin S. S. Quantum Monte-Carlo analysis of the 2d Heisenberg antiferromagnet with $S=1/2$: the influence of exchange anisotropy // *Journal of Physics: Condensed Matter*. 1998. Vol. 10, Iss. 44. P. 10061–10065.

19. Optical response of YbS and YbO at high pressures and the pressure-volume relation of YbS / K. Syassen, H. Winzen, H. G. Zimmer et al. // Phys. Rev. 1985. B. 32. P. 8246.

20. Magnetic and electric properties of $\text{Yb}_x\text{Mn}_{1-x}\text{S}$ alloys / Aplesnin S. S., A. M. Khar'kov, O. B. Romanova et al. // Bulletin of the Russian Academy of Sciences: Physics volume. 2013. Vol. 77, No. 10. P. 1252–1254.

21. Matsunami M., Okamura H., Ochiai A., Nanba T. Pressure tuning of an ionic insulator into a heavy electron

metal: an infrared study of YbS // Physical review letters. 2009. Vol. 103, Iss. 23. P. 237202.

22. Магнитные и электрические свойства катион-замещенных сульфидов $\text{Me}_x\text{Mn}_{1-x}\text{S}$ (Me = Co, Gd) / С. С. Аплеснин, Л. И. Рябинкина, О. Б. Романова и др. // ФТТ. 2009, Т. 51, В. 4, С. 661-664.

© Konovalov S. O., Begisheva O. B.,
Abdelbaki Hichem, Rybina U. I.,
Yukhno M. Yu., 2020

Konovalov Stepan Olegovich – post-graduate student; Reshetnev Siberian State University of Science and Technology. E-mail: kco.konovalov@yandex.ru.

Begisheva Olga Borisovna – post-graduate student; Reshetnev Siberian State University of Science and Technology. E-mail: fisenko_o@mail.ru.

Abdelbaki Hicham – post-graduate student; Reshetnev Siberian State University of Science and Technology. E-mail: Abdel.hichem@outlook.fr.

Rybina Ulyana Ilinishna – student; Reshetnev Siberian State University of Science and Technology. E-mail: rybinau@mail.ru.

Yukhno Mikhail Yurievich – student; Reshetnev Siberian State University of Science and Technology. E-mail: 5993664@gmail.com.

Коновалов Степан Олегович – аспирант; Сибирский государственный университет науки и технологий имени академика М. Ф. Решетнева. E-mail: kco.konovalov@yandex.ru.

Бегешева Ольга Борисовна – аспирант; Сибирский государственный университет науки и технологий имени академика М. Ф. Решетнева. E-mail: fisenko_o@mail.ru.

Абдельбаки Хишем – аспирант; Сибирский государственный университет науки и технологий имени академика М. Ф. Решетнева. E-mail: Abdel.hichem@outlook.fr.

Рыбина Ульяна Ильинишна – студент; Сибирский государственный университет науки и технологий имени академика М. Ф. Решетнева. E-mail: rybinau@mail.ru.

Юхно Михаил Юрьевич – студент; Сибирский государственный университет науки и технологий имени академика М. Ф. Решетнева. E-mail: 5993664@gmail.com.

UDC 620.197.2

Doi: 10.31772/2587-6066-2020-21-1-115-124

For citation: Mikheev A. E., Girn A. V., Ravodina D. V., Elizar'eva I. G. The influence of prefinishing operations at titanium alloys on the characteristics of mao coatings. *Siberian Journal of Science and Technology*. 2020, Vol. 21, No. 1, P. 115–124. Doi: 10.31772/2587-6066-2020-21-1-115-124

Для цитирования: Влияние предварительной подготовки поверхности титановых сплавов на характеристики МДО покрытий / А. Е. Михеев, А. В. Гирн, Д. В. Раводина, И. Г. Елизарьева // Сибирский журнал науки и технологий. 2020. Т. 21, № 1. С. 115–124. Doi: 10.31772/2587-6066-2020-21-1-115-124

THE INFLUENCE OF PREFINISHING OPERATIONS AT TITANIUM ALLOYS ON THE CHARACTERISTICS OF MAO COATINGS

A. E. Mikheev, A. V. Girn, D. V. Ravodina, I. G. Elizar'eva

Reshetnev Siberian State University of Science and Technology
31, Krasnoyarsky Rabochy Av., Krasnoyarsk, 660037, Russian Federation
E-mail: michla@mail.ru

Improving the reliability, service life and operational safety of titanium alloy structures exposed to thermal, chemical and mechanical stresses can be achieved by applying various protective coatings.

One of the effective methods of protecting such alloys is the formation on their surface of oxide coatings that are resistant to external factors. Of great interest from this point of view is the method of micro-arc oxidation (MAO), which allows one to obtain multifunctional ceramic-like oxide coatings with unique properties. Such coatings can be used to create a durable heat and electrical insulating layer on parts, protect surfaces from erosion in high-speed gas flows, corrosion in aggressive environments and wear by friction, to increase the surface emissivity, etc.

This method is well established for the oxidation of aluminum alloys. Despite the fact that the mechanism of coating formation during MAO is the same for aluminum and titanium alloys, there are certain differences in the structure and characteristics of the resulting coating. For example, it is believed that during the MAO treatment of aluminum alloys, preliminary surface preparation is not required and the adhesive strength is comparable with the strength of the substrate material. However, when processing titanium alloys, we noted cases of a significant decrease in adhesive strength. One of the reasons may be the lack of preliminary surface preparation before coating.

Therefore, studies aimed at studying the influence of the method of surface preparation and the resulting roughness on the characteristics of the applied coatings are relevant.

Keywords: micro-arc oxidation, titanium alloys, surface preparation, thickness, adhesive strength, roughness.

ВЛИЯНИЕ ПРЕДВАРИТЕЛЬНОЙ ПОДГОТОВКИ ПОВЕРХНОСТИ ТИТАНОВЫХ СПЛАВОВ НА ХАРАКТЕРИСТИКИ МДО ПОКРЫТИЙ

А. Е. Михеев, А. В. Гирн, Д. В. Раводина, И. Г. Елизарьева

Сибирский государственный университет науки и технологий имени академика М.Ф. Решетнева
Российская Федерация, 660037, г. Красноярск, просп. им. газ. «Красноярский рабочий», 31
E-mail: michla@mail.ru

Повышение надежности, ресурса работы и безопасности эксплуатации конструкций из титановых сплавов, подвергающихся воздействию тепловых, химических и механических нагрузок, можно добиться нанесением различных защитных покрытий.

Одним из эффективных методов защиты таких сплавов является образование на их поверхности устойчивых против воздействия внешних факторов оксидных покрытий. Большой интерес с этой точки зрения представляет метод микродугового оксидирования (МДО), позволяющий получать многофункциональные керамикоподобные оксидные покрытия с уникальными свойствами. Такие покрытия могут применяться для создания на деталях прочного тепло- и электроизолирующего слоя, защиты поверхностей от эрозии в высокоскоростных газовых потоках, коррозии в агрессивных средах и износа трением, для повышения коэффициента излучения поверхности и т. п.

Этот метод хорошо отработан для оксидирования алюминиевых сплавов. Несмотря на то, что механизм образования покрытий при МДО для алюминиевых и титановых сплавов одинаков, существуют определенные различия в структуре и характеристиках полученного покрытия. Например, считается, что при обработке МДО алюминиевых сплавов не требуется предварительная подготовка поверхности и адгезионная прочность

сопоставима с прочностью материала подложки. Однако при обработке титановых сплавов нами были отмечены случаи значительного снижения адгезионной прочности. Одной из причин может быть отсутствие предварительной подготовки поверхности перед нанесением покрытий.

Поэтому исследования направленные на изучение влияния способа подготовки поверхности и полученной шероховатости на характеристики нанесенных покрытий являются актуальными.

Ключевые слова: микродуговое оксидирование, титановые сплавы, подготовка поверхности, толщина, адгезионная прочность, шероховатость.

Introduction. The composition, concentration of electrolyte components and the duration of MAO have a major effect on the characteristics of oxide layers. The essence of MAO is that under the influence of electric current applied between the part located in the electrolyte and the metal cathode (electrolytic cell body or electrode), migrating point micro-arc discharges (MAD) arise on its surface, from the effect of which a ceramic coating is formed on the surface [1–7]. The electrolyte composition for MAO is selected based on the chemical composition of the hardened valve alloy and the function of the coating.

In the MAO process, diffusion, thermal, plasmochemical and electrophysical processes play a significant role. Conventionally, these processes can be divided into several stages, which proceed sequentially or in parallel:

1) chemical interaction between the base material and the forming coating with the electrolyte;

2) electrochemical processes that occur both before ignition of an electric discharge and after its ignition in areas of the treated surface where there is currently no discharge (anodization in aqueous solutions of electrolytes and electrolysis);

3) in fact, micro-arc oxidation, which includes the short initial stages of luminescence and sparking and then the main stage of MAD combustion;

4) transition of a micro-arc discharge in an arc discharge after the formation of an MAO coating of a certain thickness.

The voltage at which sparking begins in the electrolyte depends on the composition of the material being processed and the electrolyte. At a small coating thickness, due to the large heat removal, a spark discharge is observed, which with an increase in the film thickness transforms into MAD, and at large thicknesses it transforms into an arc [8–10].

It is reputed that a necessary condition for the occurrence of an electric discharge in an electrolyte is the presence of a gas or vapor-gas layer between the electrolyte and the base metal. Apparently, the discharge during MAO is gas and arises as a result of electric breakdown of vapor-gas “plugs” formed in micro-pores of a porous oxide layer growing on the barrier layer. These plugs are formed during electrolysis processes of the discharge of H^+ or OH^- ions and boiling of electrolyte in pore channels [11].

It is generally thought that during MAO treatment of aluminum alloys, preliminary surface preparation is not required and the adhesive strength is comparable with the strength of the substrate material. However, when processing titanium alloys, we noted cases of a significant decrease in adhesive strength. One of the reasons may be the lack of preliminary surface preparation before coating.

Therefore, there is a need to study the effect of preliminary surface preparation on the characteristics of coatings.

Surface preparation can be carried out in many ways, such as: grinding, matting, polishing, tumbling, vibration processing, blast-abrasive treatment, degreasing, etching, activation.

MAO coatings are ceramics of complex composition [12–16]. The coating during micro-arc oxidation is formed due to the oxidation of the metal surface and oxide and hydroxide forms of this metal are formed. On the other hand, the coating grows due to the inclusion of electrolyte cells in its composition. Electrolyte elements enter the coating in the form of salts, oxides and hydroxides of complex composition. If necessary, the MAO technology allows you to enter into the coating any desired chemical element.

The main characteristics of the resulting coatings include the following parameters: adhesion, coating thickness, porosity, wear resistance, etc.

Experimental procedure. VT 6/BT 6 titanium alloy with a thickness of 3 mm, dimensions 50×40 mm was used for the manufacture of samples. The composition and characteristics of VT 6/BT 6 are presented in tab. 1. When choosing the material, it was assumed that this alloy is widely used for the manufacture of a significant range of parts in mechanical engineering, the manufacture of aircraft and spacecraft, fasteners and threaded parts, etc.

As already mentioned above, the speciation, the concentration of electrolyte components, and the duration of MAO have the greatest effect on the adhesion, thickness, structure and phase composition of oxide layers. The effect of surface pretreatment on the characteristics of the applied coatings is not well investigated.

Preliminary experimental studies were carried out to select the modes of MAO treatment. The samples were processed in an experimental MAO installation operating on a three-phase alternating current network of 380 V and a frequency of 50 Hz. The current source was the IAT-T2/IAT-T2 transformer (asymmetric current source).

As a result of a literature review and scientific patent search, several electrolyte compositions of interest to us were identified [17–19]. The formation of oxide coatings on products from titanium-based alloys was carried out in solutions of sodium hydrogen phosphate and sodium silicate with the addition of potassium hydroxide, which were prepared by dissolving the calculated amount of chemical reagents in distilled water (tab. 2).

During the experiment it was found that with an increase in the ratio of the cathodic and anodic components of the current strength, the thickness of the oxide layer decreases (fig. 1) and the adhesive strength of the coating increases (fig. 2).

Table 1

VT 6/BT 6 speciation and characteristics										
Grade					VT 6/BT 6					
Classification:					titanium wrought alloy					
Chemical composition in % for grade VT1-0/BT1-0 GOST 19807–91										
Fe	C	Si	V	N	Ti	Al	Zr	O	H	Impurities
to 0.6	to 0.1	to 0.1	3.5–5.3	to 0.05	86.45–90.9	5.3–6.8	to 0.3	to 0.2	to 0.015	others 0.3
VT 6/BT 6 hardness after quenching and aging					HB 10 ^{−1} = 293–361 MPa					
VT 6/BT 6 hardness after annealing					HB 10 ^{−1} = 255–341 MPa					

The speciation and concentration of electrolytes, processing modes

Table 2

Number of electrolyte	Speciation of electrolyte	Concentration, g/l	Alloy	The ratio of the cathode and anodic components of the current (I_k/I_a)	Current density, j A/dm ²
1					
2	Na ₂ HPO ₄	60	VT 6/BT 6	0,8; 1; 1,2	20, 30
	KOH	30			
	Na ₂ SiO ₃	50			

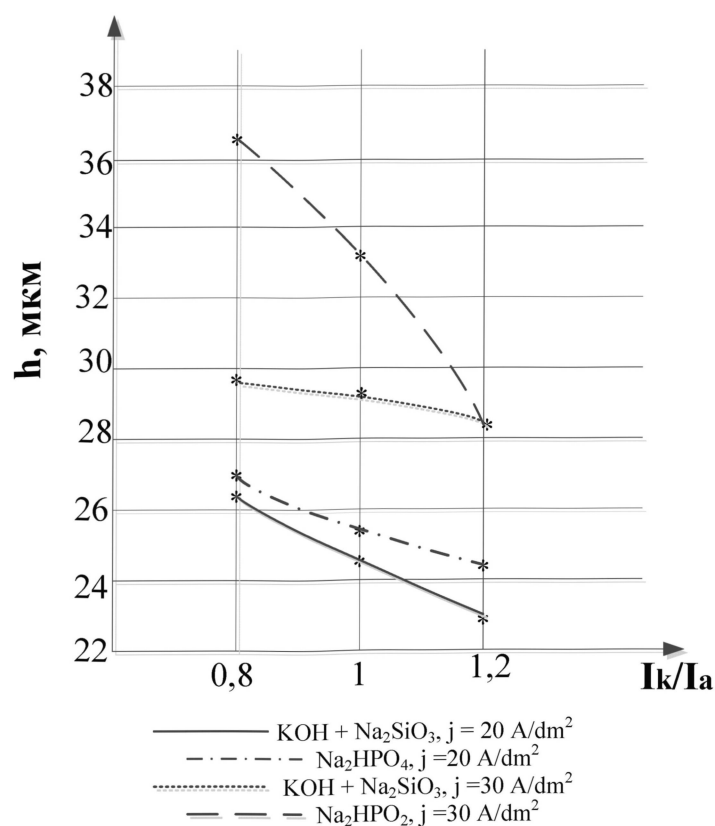


Fig. 1. Dependence of the coating thickness on the ratio of the cathode and anode component of the current

Рис. 1. Зависимость толщины покрытия от отношения катодной и анодной составляющей силы тока

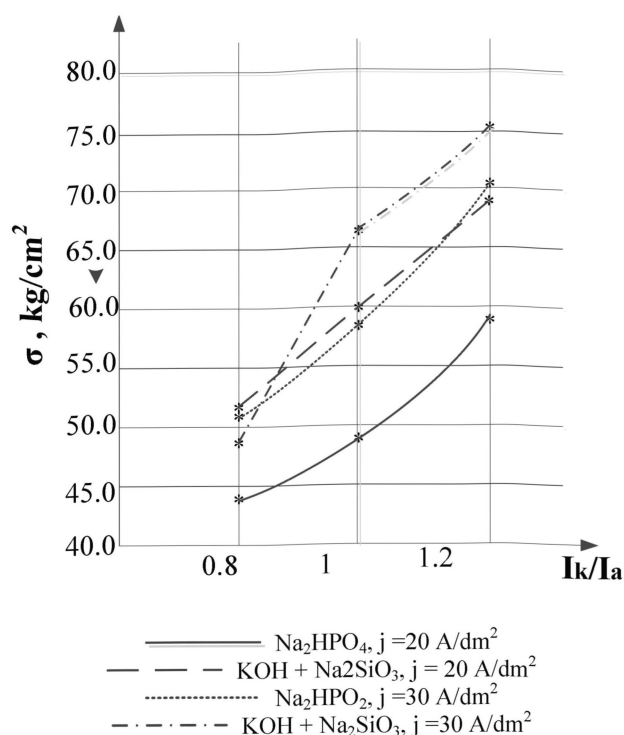


Fig. 2. Test results for adhesive strength of the coating

Рис. 2. Результаты испытаний на адгезионную прочность покрытия

Table 3

MAO processing mode

Parameter	Notation	Value
Run time	t	10 min
Current density	J	20 A/dm ²
The ratio of the cathode and anodic component of the current	I_k/I_a	1.2
Current	I_{k+}	5.2
	I_{a+}	4.4
Electrolyte compositions	№ 1	Na_2HPO_4
	№ 2	KOH
		Na_2SiO_3

It was also revealed that when processing with a current density of $J = 30 \text{ A/dm}^2$ in the aqueous Na_2HPO_4 solution, the samples burn up, and in the silicate-alkaline electrolyte ($\text{KOH} + \text{Na}_2\text{SiO}_3$) the solution boils. Based on this, a further mode of MAO processing was selected, which is presented in tab. 3.

A methodology for conducting experimental studies was developed to determine the dependence of coating properties on preliminary surface preparation.

As a method of surface preparation, the machining of samples on sanding paper of various grit sizes used on a Struers LaboPol-1 grinding and polishing machine and a sandblasting machine with corundum was chosen.

Acetone (GOST 2768–84) was used for degreasing.

As a result, the roughness data of the processed samples were obtained, presented in tab. 4 and in fig. 3 and 4. Roughness measurement was carried out with a TR110

profilometer, which meets the requirements of ISO and DIN standards.

The prepared samples were coated with MAO coatings. The thickness of the resulting coating was determined using a TT-260 thickness gauge according to GOST 9.302. Ten measurements were performed on one sample. The value of the coating thickness was determined as the arithmetic mean between ten measurements on a segment of 5 mm in one sample. The relative error of the method is $\pm 0.8 \mu\text{m}$ for coatings up to $25 \mu\text{m}$ and 10 % for coatings with a thickness exceeding $25 \mu\text{m}$ (tab. 5, fig. 5, 6). The results of measurements of the thickness of the coatings are presented in tab. 5 and fig. 5, 6.

The graphs show that in the overall picture, with a decrease in surface roughness, the coating thickness increases. This can be explained by the fact that with an increase in surface cleanliness, the time to reach the MAO treatment mode decreases.

Table 4

Surface preparation and sample roughness

Number of sample	Process	Grain size, microns	Ra, microns	Roughness grade
1.1	Degrease cleansing treatment	-	1.02	7
1.2	P80	200...250	0.8	7
1.3	P180	63...80	0.675	7
1.4	P320	40...50	0.505	8
1.5	P600	20...28	0.28	9
1.6	P1000	14...20	0.21	9
1.7	P1500	7...10	0.175	10
1.8	P2500	3...5	0.135	10
1.9	Sandblasting (corundum)	100...150	5.64	4

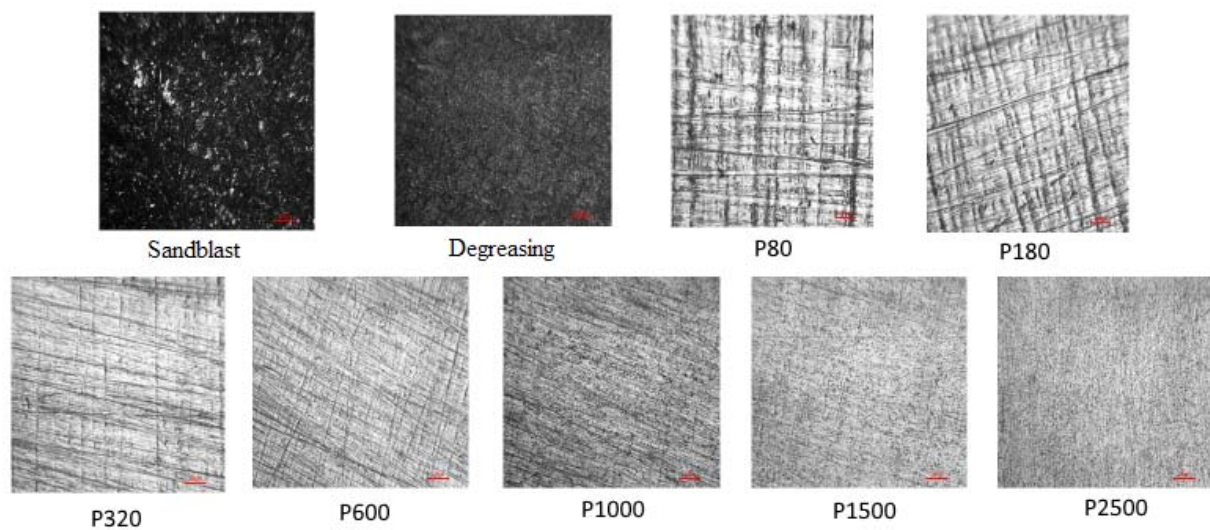


Fig. 3. Appearance of the surface of the processed samples

Рис. 3. Внешний вид поверхности обработанных образцов

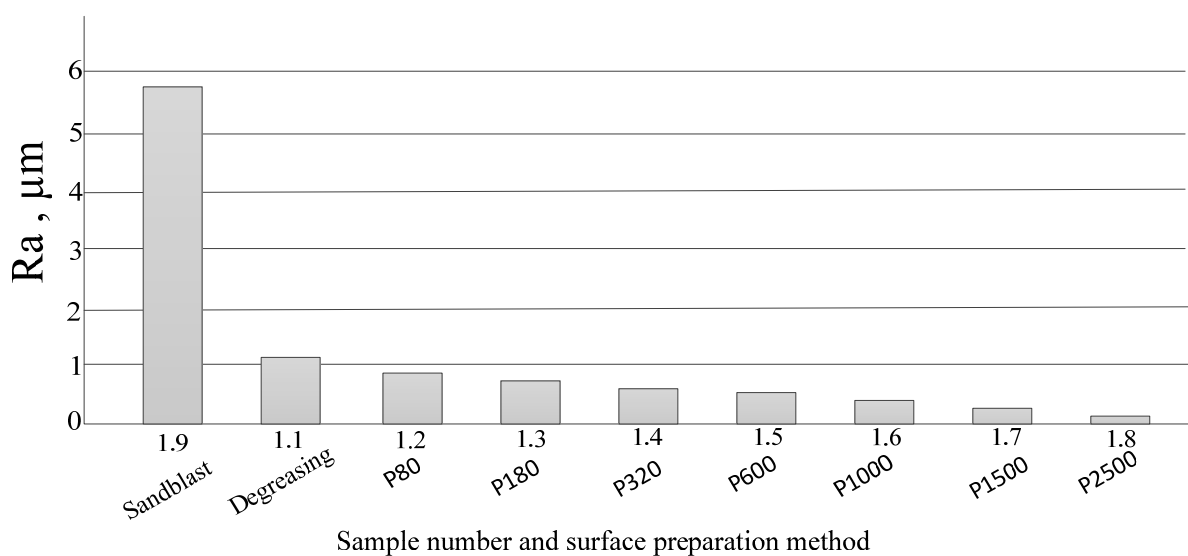
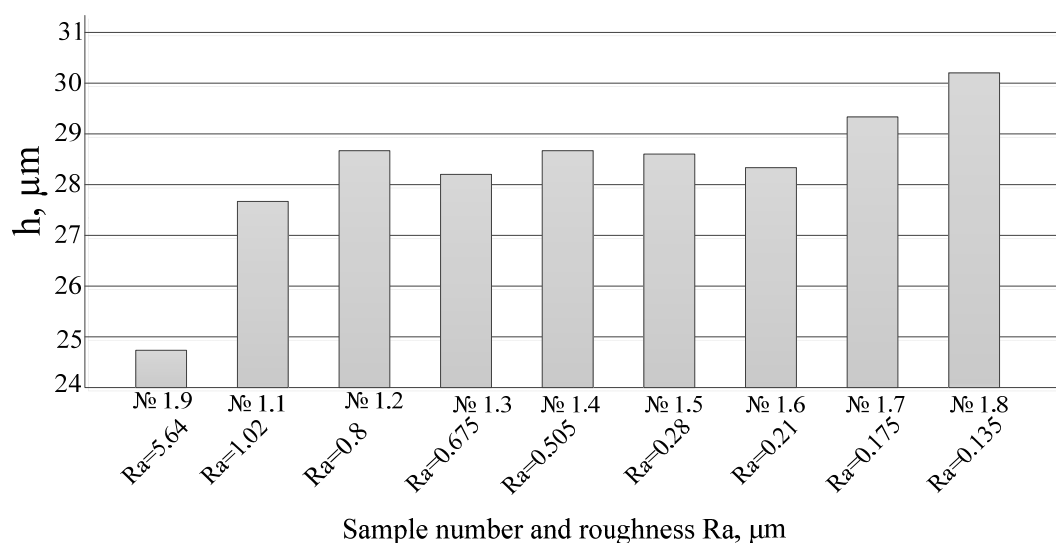
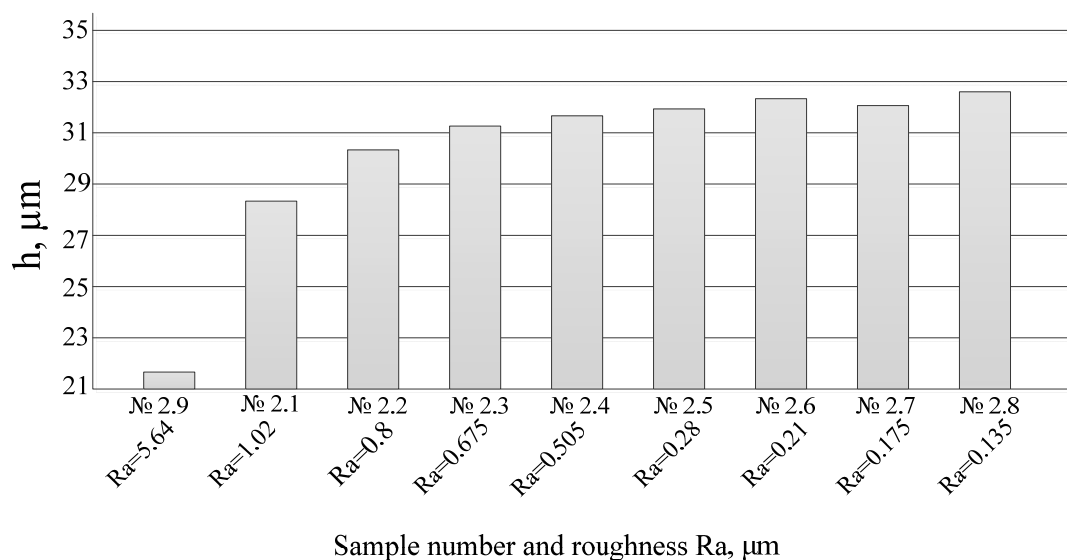


Fig. 4. Surface roughness of samples

Рис. 4. Шероховатость поверхности образцов

Table 5

Coating thickness									
Phosphate electrolyte (Na_2HPO_4)									
Number of sample and roughness (R_a , μm)	1.1 ($R_a = 1.02$)	1.2 ($R_a = 0.8$)	1.3 ($R_a = 0.675$)	1.4 ($R_a = 0.505$)	1.5 ($R_a = 0.28$)	1.6 ($R_a = 0.21$)	1.7 ($R_a = 0.175$)	1.8 ($R_a = 0.135$)	1.9 ($R_a = 5.64$)
h , μm	27.77	28.86	28.36	28.85	28.8	28.45	29.37	30.16	31.73
Silicate-alkaline electrolyte ($\text{KOH} + \text{Na}_2\text{SiO}_3$)									
Number of sample and roughness (R_a , μm)	2.1 ($R_a = 1.02$)	2.2 ($R_a = 0.8$)	2.3 ($R_a = 0.675$)	2.4 ($R_a = 0.505$)	2.5 ($R_a = 0.28$)	2.6 ($R_a = 0.21$)	2.7 ($R_a = 0.175$)	2.8 ($R_a = 0.135$)	2.9 ($R_a = 5.64$)
h , μm	20.01	30.45	31.45	31.78	32.1	32.32	32.24	32.47	21.38

Fig. 5. Roughness dependence of the thickness of coatings obtained in an aqueous solution of Na_2HPO_4 Рис. 5. Зависимость толщины покрытий, полученных в водном растворе Na_2HPO_4 , от шероховатостиFig. 6. Roughness dependence of the thickness of coatings obtained in an aqueous solution of $\text{KOH} + \text{Na}_2\text{SiO}_3$ Рис. 6. Зависимость толщины покрытий, полученных в водном растворе $\text{KOH} + \text{Na}_2\text{SiO}_3$, от шероховатости

Determination of adhesive strength. The adhesion strength was determined by the separation method according to GOST 209–75 [20] (adhesive method, VK-3/ BK-3 glue) as the ratio of the force (up to 10 kN) at which separation occurs from the counter sample glued with an oxide coating to the cross-sectional area (4.9 cm^2).

To measure the adhesion strength of the coating on a EUROTEST T-50 tensile testing machine (fig. 7) suspension equipment was developed and manufactured, as shown in fig. 8.

Fig. 9 shows the results of the dependence of the adhesion strength of coatings to the base obtained in the Na_2HPO_4 electrolyte with various pretreatment methods. The adhesion strength of the coating on the sample with $R_a = 5.64 \text{ }\mu\text{m}$ prepared by the sand blasting device turned

out to be maximum, but crack occurred in gluing area, i. e. true strength is not established. The remaining samples had a separation of the coating from the base. Coating adhesion decreases with a decrease in surface roughness.

Fig. 10 shows the results of the dependence of the adhesion strength of the coatings to the base obtained in the $\text{KOH} + \text{KOH} + \text{Na}_2\text{SiO}_3$ electrolyte with various pretreatment methods. In all samples, crack occurred in gluing area.

It is related to the fact that adhesive strength $\text{VK 3/BK 3} = 40 \text{ kg/cm}^2$, and the experimental sample area is $S = 2 \text{ cm}^2$, based on this, the adhesion of the coating to the sample does not exceed 80 kg/cm^2 , which corresponds to the adhesive strength.

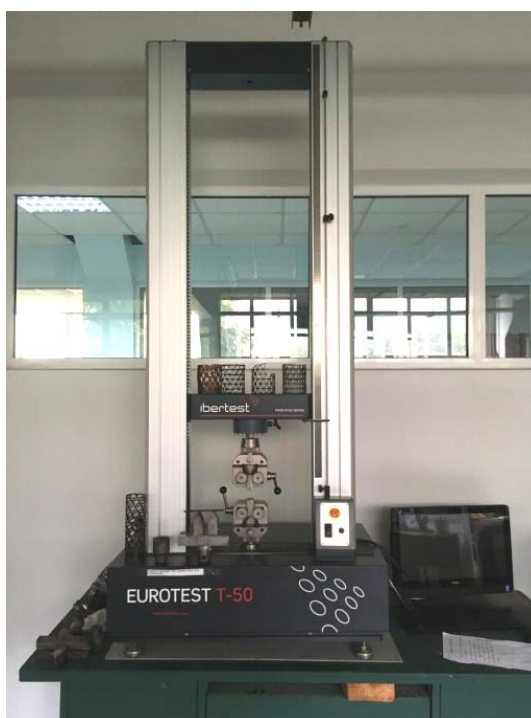


Fig. 7. Bursting machine EUROTEST T-50

Рис. 7. Разрывная машина EUROTEST T-50

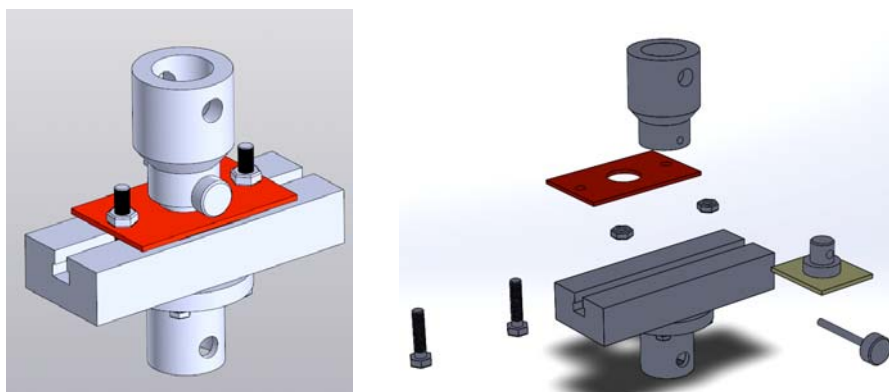


Fig. 8. 3D model of bolt clamp

Рис. 8. 3D модель зажима болтового

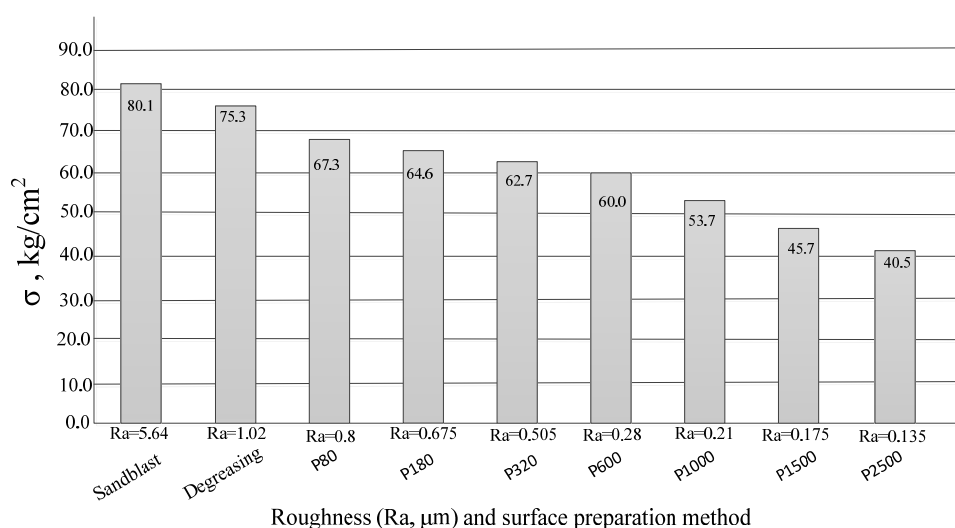


Fig. 9. Roughness dependence of the adhesion strength of coatings with a base obtained in Na_2HPO_4 electrolyte

Рис. 9. Зависимость адгезионной прочности покрытий с основой, полученных в электролите Na_2HPO_4 , от шероховатости

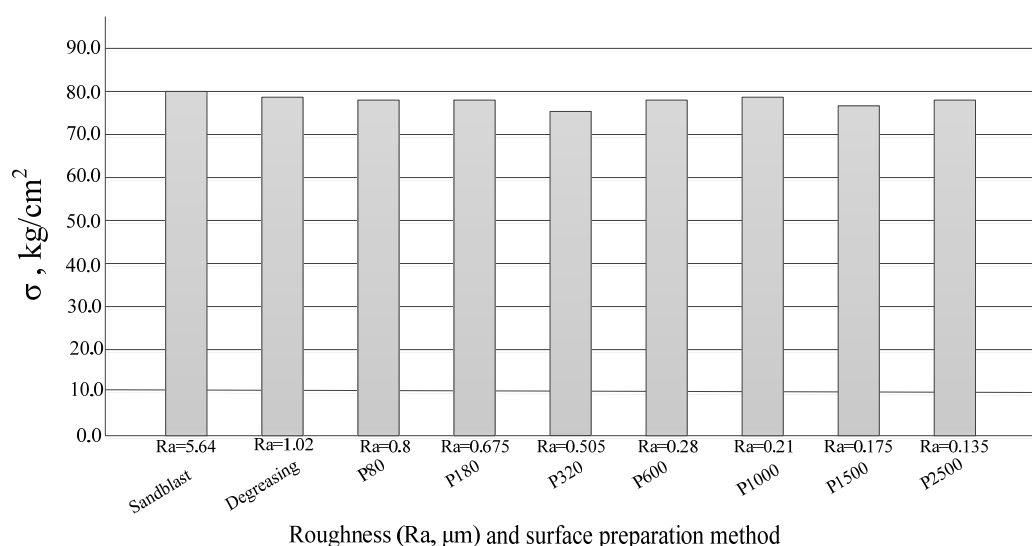


Fig. 10. Roughness dependence of the adhesion strength of coatings with a base obtained in $\text{KOH}+\text{Na}_2\text{SiO}_3$ electrolyte

Рис. 10. Зависимость адгезионной прочности покрытий с основой, полученных в электролите $\text{KOH}+\text{Na}_2\text{SiO}_3$, от шероховатости

The data obtained show that the adhesion strength of coatings to the base obtained in the $\text{KOH}+\text{Na}_2\text{SiO}_3$ electrolyte exceeds the strength of VK 3/BK 3 glue. Therefore, to determine the actual adhesion strength, it is necessary to conduct additional studies using a higher-strength adhesive or other methods of measuring adhesive strength.

Conclusion. By a process of the conducted work, it was found that preliminary surface preparation of titanium alloys affects the characteristics of MAO coatings.

Based on the results obtained, it was concluded that in order to achieve the highest adhesive strength of the coating, it is necessary to perform MAO treatment at a ratio of

$I_k / I_a = 1,2$ and at $I_k / I_a = 0,8$ to obtain the maximum coating thickness.

Preliminary surface preparation affects the thickness and adhesive strength of coatings. With increase in roughness the adhesive strength increases and the thickness of the coating decreases.

Furthermore, based on the results obtained when measuring the adhesion strength of coatings with a base obtained in $\text{KOH}+\text{Na}_2\text{SiO}_3$ electrolyte using VK 3/ BK 3 glue, the true strength has not been established. Therefore, it is necessary to conduct additional studies using a higher-strength adhesive or another method of measuring adhesive strength.

References

1. Kolomeychenko A. V. *Tekhnologii povysheniya dolgovечnosti detaley mashin vosstanovleniem i uprochneniem rabochikh poverkhnostey kombinirovannymi metodami s primeneniem mikrodrugovogo oksidirovaniya* [Technologies for increasing the durability of machine parts by restoration and hardening of working surfaces by combined methods using microarc oxidation]. Orel, Izd-vo Orel GAU Publ., 2013, 255 p.
2. Zhukov S. V. *Issledovanie protsessov i razrabotka tekhnologii formirovaniya mnogofunktsional'nykh pokrytiy MDO na titanovykh splavakh v priborostroenii. Kand. Diss.* [Investigation of the processes of formation and development of the technology of multifunctional coatings on titanium alloys MDO in instrument. Cand. Diss.]. Moscow, 2009.
3. Suminov I. V. et al. *Mikrodrugovoe oksidirovanie (teoriya, tekhnologiya, oborudovanie)* [Microarc oxidation (theory, technology, equipment)]. Moscow, EKO-MET Publ., 2005, 368 p.
4. Gordienko P. S., Gnedenkov S. V. *Mikrodrugovoe oksidirovanie titana i ego splavov* [Microarc oxidation of titanium and its alloys]. Vladivostok, Dal'nauka Publ., 1997, 185 p.
5. Girn A. V., Vakhteev E. V., Trushkina T. V., Orlova D. V. [The influence of technological parameters of micro-arc oxidation on the corrosion resistance of coatings]. *Miass. Mekhanika i protsessy upravleniya. Materialy XXXXI Vserossiyskogo simpoziuma*. Vol. 3. Moscow, RAN Publ., 2011, P. 168–173 (In Russ.).
6. Trushkina T. V., Girn A. V. [The corrosion resistance of MAO coatings in aggressive environments]. *Vestnik SibGAU*. 2014, Vol. 1(53), P. 179–184 (In Russ.).
7. Mamaev A. I., Dorofeeva T. I., Mamaeva V. A., Borikov V. N. [Adhesion and plasticity of coatings obtained by microplasma oxidation of titanium]. *Tekhnologiya materialov*. 2008, No. 3, P. 33–37 (In Russ.).
8. Mamaev, A.I., Mamaeva, V.A. *Sil'notokovye mikroplazmennye protsessy v rastvorakh elektrolitov* [High current microplasma processes in electrolyte solutions]. Novosibirsk, Izdatel'stvo SO RAN, 2005, 255 p.
9. Gordienko P. S., Vasilenko V. S. [Formation of coatings on valve metals and alloys in electrolytes with a capacitive energy regulation at microarc oxidation]. *Zashchita metallov*. 2006, Vol. 42, No. 5, P. 500–505 (In Russ.).
10. Mamaev A. I., Mamaeva V. A., Borikov V. N., Dorofeeva T. I. *Formirovanie nanostrukturnykh nemetallicheskih neorganicheskikh pokrytiy putem lokalizatsii vysokoenergeticheskikh potokov na granitse razdela faz* [Formation of nanostructured inorganic non-metallic coatings by the localization of high-energy fluxes at the interface]. Tomsk, Izd-vo Tom. un-ta Publ., 2010, 360 p.
11. Suminov I. V. *Plazmenno-elektroliticheskoe modifitsirovanie poverkhnosti metal-lov i splavov* [Plasma-electrolytic surface modification of metals and alloys]. Moscow, TEKhNOSFERA Publ., 2011, 512 p.
12. Terekhin N. A., Statsura V. V., Golenkova A. A., Ivasev S. S., Girn A. V. [Technological capabilities of micro-arc oxidation of aluminum alloys]. *Vestnik mashinostroeniya*. 2003, No. 2, P. 56–63 (In Russ.).
13. Andreev A. S. [The effect of the electrolyte composition on the structure with the properties of oxide coatings formed on titanium alloys by microarc oxidation]. *Reshetnevskie chteniya: materialy XIII Mezhdunar. nauch. konf., posvyashch. pamyati general. konstruktora ra-ket.-kosmich. sistem akademika M. F. Reshetneva* [Reshetnev readings. Materials of the XIII International scientific Conf. memory of the general. the designer of rockets. systems of academician M. F. Reshetnev]. Krasnoyarsk, 2009. Ch. 1. P. 307–308 (In Russ.).
14. Rudnev V. S. et al. *Sposob mikrodrugovogo oksidirovaniya ventil'nykh metallov i ikh splavov* [A method of micro-arc oxidation of valve metals and their alloys]. Patent RF, no 1783004, 1992.
15. Gordienko P. S. *Obrazovanie pokrytiy na anodno-polyarizovannykh elektrodakh v vodnykh elektrolitakh pri potentsialakh iskreniya i probuya* [Forming a coating on the anode-polarized electrodes in aqueous electrolytes at potentials sparking and breakdown]. Vladivostok, Dal'nauka Publ., 1996, 216 p.
16. Fedorov V. A. et al. [Formation of hardened surface layers by micro-arc oxidation in various electrolytes and when changing current modes]. *Fizika i khimiya obrabotki materialov*. 1991, No. 1, P. 87–93 (In Russ.).
17. Nechaev G. G. [Microarc oxidation of titanium alloys in alkaline electrolytes]. *Kondensirovannye sredy i mezhfaznye granitsy*. 2012, Vol. 14, No 4, P. 453–455 (In Russ.).
18. Kuznetsov Yu. A., Kulakov K. V., Goncharenko V. V. *Osobennosti vybora elektrolita dlya polucheniya tolstosloynnykh keramicheskikh pokrytiy* [Features choice of electrolyte to produce thick ceramic coatings] (In Russ.). Available at: http://science-bsea.narod.ru/2011/mashin_2011_14/kuznecov_texno.htm (accessed: 20.12.2019).
19. Gordienko P. S., Gnedenko S. V., Khisanfova O. A., Vostrikova N. G., Kovryakov A. N. *Elektrolit dlya formirovaniya pokrytiy na ventil'nykh metallakh* [The electrolyte for forming coatings on valve metals]. Patent RF, no. 2046156, 1995.
20. GOST 209-75. *Rezina i kley. Metody opredeleniya prochnosti svyazi s metallom pri otryve* [State Standard 209-75. Rubber and glue. Methods for determining the bond strength with metal upon separation]. Moscow, Publishing house of standards, 1993. 23 p.

Библиографические ссылки

1. Коломейченко А. В. Технологии повышения долговечности деталей машин восстановлением и упрочнением рабочих поверхностей комбинированными методами с применением микродугового оксидирования : монография. Орел : Орел ГАУ, 2013. 255 с.
2. Жуков С. В. Исследование процессов и разработка технологии формирования многофункциональных покрытий МДО на титановых сплавах в приборостроении : автореф. дис. ... канд. техн. наук. М. : МАТИ – Российский государственный технологический университет им. К. Э. Циолковского, 2009.
3. Микродуговое оксидирование (теория, технология, оборудование) / И. В. Суминов и др. М. : ЭКОМЕТ, 2005. 368 с.

4. Гордиенко П. С., Гнеденков С. В. Микродуговое оксидирование титана и его сплавов. Владивосток : Дальнаука, 1997. 185 с.
5. Влияние технологических параметров микродугового оксидирования на коррозионную стойкость покрытий / А. В. Гирн, Е. В. Вахтеев, Т. В. Трушкина, Д. В. Орлова // Миасс. Механика и процессы управления : материалы XXXXI Всеросс. симп. Т. 3. М. : РАН, 2011. С. 168–173.
6. Трушкина Т. В., Гирн А. В. Коррозионная стойкость МДО покрытий в агрессивных средах // Вестник СибГАУ. 2014. № 1(53). С. 179–184.
7. Адгезия и пластичность покрытий, полученных микроплазменным оксидированием титана / А. И. Мамаев, Т. И. Дорофеева, В. А. Мамаева, В. Н. Бороков // Технология материалов. 2008. № 3. С. 33–37.
8. Мамаев А. И., Мамаева В. А. Сильноточковые микроплазменные процессы в растворах электролитов. Новосибирск : Изд-во СО РАН, 2005. 255 с.
9. Формирование покрытий на вентильных металлах и сплавах в электролитах с емкостным регулированием энергии при микродуговом оксидировании / П. С. Гордиенко, В. С. Василенко и др. // Защита металлов. 2006. Т. 42, № 5. С. 500–505.
10. Формирование наноструктурных неметаллических неорганических покрытий путем локализации высокоэнергетических потоков на границе раздела фаз / А. И. Мамаев, В. А. Мамаева, В. Н. Бороков, Т. И. Дорофеева. Томск : Изд-во Том. ун-та, 2010. 360 с.
11. Суминов И. В. Плазменно-электролитическое модифицирование поверхности металлов и сплавов. М. : Техносфера, 2011. 512 с.
12. Технологические возможности микродугового оксидирования алюминиевых сплавов / Н. А. Терехин, В. В. Стацур, А. А. Голенкова и др. // Вестник машиностроения. 2003. № 2. С. 56–63.
13. Андреев А. С. Влияние состава электролита на структуру с свойства оксидных покрытий, сформированных на титановых сплавах микродуговым оксидированием // Решетневские чтения : материалы XIII Междуна. науч. конф., посвящ. памяти генерал. конструктора ракет.-космич. систем акад. М. Ф. Решетнева (10–12 ноября 2009, г. Красноярск) : в 2 ч. / под общ. ред. Ю. Ю. Логинова ; Сиб. гос. аэрокосмич. ун-т. Красноярск, 2009. Ч. 1. С. 307–308.
14. Патент России 1783004, МКИ5 C25D11/02. Способ микродугового оксидирования вентильных металлов и их сплавов / В. С. Руднев, П. С. Гордиенко, А. Г. Курносова, Т. И. Орлова ; заявл. 17.10.89 ; опубл. 23.12.92, Бюл. № 47.
15. Гордиенко П. С. Образование покрытий на анодно-поляризованных электродах в водных электролитах при потенциалах искрения и пробоя. Владивосток : Дальнаука, 1996. 216 с.
16. Федоров В. А., Белозеров В. В., Великосельская Н. Д. Формирование упрочненных поверхностных слоев методом микродугового оксидирования в различных электролитах и при изменении токовых режимов // Физика и химия обработки материалов. 1991. № 1. С. 87–93.
17. Нечаев Г. Г. Микродуговое оксидирование титановых сплавов в щелочных электролитах // Конденсированные среды и межфазные границы. 2012. Т. 14, № 4. С. 453–455.
18. Кузнецов Ю. А., Кулаков К. В., Гончаренко В. В. Особенности выбора электролита для получения толстослойных керамических покрытий [Электронный ресурс]. URL: http://science-bsea.narod.ru/2011/mashin_2011_14/kuznecov_texno.htm (дата обращения: 20.12.2019).
19. Патент РФ 2046156, МПК6 C25D11/04. Электролит для формирования покрытий на вентильных металлах / П. С. Гордиенко, С. В. Гнеденко, О. А. Хриسانфова, Н. Г. Вострикова, А. Н. Ковряков ; заявл. 21.05.92 ; опубл. 20.10.95 ; заявка № 5043332/26.
20. ГОСТ 209–75. Резина и клей. Методы определения прочности связи с металлом при отрыве. М. : Изд-во стандартов, 1993. 23 с.

© Mikheev A. E., Girn A. V.,
Ravodina D. V., Elizar'eva I. G., 2020

Miheev Anatolii Egorovich – Dr. Sc., Professor; Reshetnev Siberian State University of Science and Technology. E-mail: michla@mail.ru.

Girn Aleksei Vasilyevich – Cand. Sc., associate professor; Reshetnev Siberian State University of Science and Technology. E-mail: girn007@gmail.com.

Ravodin Daria Vladimirovna – engineer; Reshetnev Siberian State University of Science and Technology. E-mail: Dashaorlova12@yandex.ru.

Elizariyeva Irina Georgievna – undergraduate; Reshetnev Siberian State University of Science and Technology. E-mail: elirina777@mail.ru.

Михеев Анатолий Егорович – доктор технических наук, профессор, заведующий кафедрой летательных аппаратов, Сибирский государственный университет науки и технологий имени академика М. Ф. Решетнёва. E-mail: michla@mail.ru.

Гирн Алексей Васильевич – кандидат технических наук, доцент, доцент кафедры летательных аппаратов, Сибирский государственный университет науки и технологий имени академика М. Ф. Решетнёва. E-mail: girn007@gmail.com.

Раводина Дарья Владимировна – инженер, Сибирский государственный университет науки и технологий имени академика М. Ф. Решетнёва. E-mail: Dashaorlova12@yandex.ru.

Елизарьева Ирина Георгиевна – магистрант, Сибирский государственный университет науки и технологий имени академика М. Ф. Решетнёва. E-mail: elirina777@mail.ru.

UDC 629

Doi: 10.31772/2587-6066-2020-21-1-125-135

For citation: Titenkov S. V., Zhuravlev V. Yu. Peculiar properties of technological improvement and optimization of production costs of 3D-configuration pipes. *Siberian Journal of Science and Technology*. 2020, Vol. 21, No. 1, P. 125–135. Doi: 10.31772/2587-6066-2020-21-1-125-135

Для цитирования: Титенков С. В., Журавлев В. Ю. Особенности технологического совершенствования и оптимизации затрат производства 3D-конфигурации труб // Сибирский журнал науки и технологий. 2020. Т. 21, № 1. С. 125–135. Doi: 10.31772/2587-6066-2020-21-1-125-135

PECULIAR PROPERTIES OF TECHNOLOGICAL IMPROVEMENT AND OPTIMIZATION OF PRODUCTION COSTS OF 3D- CONFIGURATION PIPES

S. V. Titenkov¹, V. Yu. Zhuravlev^{2*}

¹JSC “Krasnoyarsk machine-building plant”

29, Krasnoyarsky Rabochy Av., Krasnoyarsk, 660123, Russian Federation

² Reshetnev Siberian State University of Science and Technology

31, Krasnoyarsky Rabochy Av., Krasnoyarsk, 660037, Russian Federation

*E-mail: VZ@sibsau.ru

The analyzes of the requirements to 3D configuration pipelines production at the rocket and space industry enterprises is done. A review of different approaches to pipe bending technology (with heat treatment and without heat treatment) is carried out. The object of the study is the bending process and a universal bending machine for pipelines' production of complex configuration. The article is divided into four sections, which consider the key factors, causing directly the effectiveness of the technological operation of pipeline bending of a complex 3D trajectory. An overview of no-temperature shaping of the pipeline is given in the first section. The requirements to the technology, excluding: corrugation, flattening, stretching and thinning of pipeline walls during their bending, are considered. The actual regulatory documents and industry aerospace standards, regulating production of pneumatic and hydraulic pipelines are given. An example of calculating the minimal allowable bend radius of the pipe, depending on the diameter and thickness of the pipe wall, is given. The requirements to unification of the pipe size production and gaps are listed. The dependence of the maximal allowable internal pressure in the pipeline is shown. The requirements to equipment, used in pipeline bending and to the design of the pipe bending machine are considered. In the second section, the possibilities of temperature influence on the pipe bending process are viewed. The analysis of patent and technical literature and six possible methods of effective thermal effects are presented: heating of the whole pipeline length, narrow zone heating of the bend pipe place, water cooling with nitrogen in the pipe, laser-cooling of atoms of the pipes, application of the petroleum products on the place of heating of the pipe and using of modern fillers inside the pipe to change its temperature. In the third section the tasks of the development of a universal bending machine are set; the system of the algorithm of the universal bending machine operation is considered; the system of algorithm of the bending machine operating with CNC is shown. The General functional scheme of the bending machine and the sequence diagram of the equipment operation is given.

Keywords: pipe bending, requirements to 3D configuration pipe bending, universal bending machine, technology of pipe bending, influence of temperature on the process of pipe bending.

ОСОБЕННОСТИ ТЕХНОЛОГИЧЕСКОГО СОВЕРШЕНСТВОВАНИЯ И ОПТИМИЗАЦИИ ЗАТРАТ ПРОИЗВОДСТВА 3D-КОНФИГУРАЦИИ ТРУБ

С. В. Титенков¹, В. Ю. Журавлев^{2*}

¹АО «Красноярский машиностроительный завод»

Российская Федерация, 660123, г. Красноярск, просп. им. газ. «Красноярский рабочий», 29

²Сибирский государственный университет науки и технологий имени академика М. Ф. Решетнева

Российская Федерация, 660037, г. Красноярск, просп. им. газ. «Красноярский рабочий», 31

*E-mail: VZ@sibsau.ru

В работе сделан анализ требований, предъявляемых к изготовлению трубопроводов 3D конфигурации на предприятии в ракетно-космической отрасли. Проведён обзор разных подходов к технологии гибки труб – с термообработкой и без термообработки. Объектом исследования является процесс гибки и универсальный гибочный агрегат изготовления трубопроводов сложной конфигурации. Статья разделена на четыре раздела, в которых рассмотрены ключевые факторы, непосредственно влияющие на успешность проведения технологической операции гибки трубопровода сложной 3D траектории. Приведён обзор безтемпературного формо-

образования трубопровода. Рассматриваются требования к технологии, исключаящей гофрообразование, сплющивание, растяжение и утонение стенок трубопроводов при их гйбе. Указаны действующие нормативные документы и отраслевые аэрокосмические стандарты, регламентирующие изготовление пневмогидравлических трубопроводов. Приведён пример расчёта минимально допускаемого радиуса гйбы трубы, зависящего от диаметра и толщины стенки трубы. Перечислены требования унификации размеров изготовления труб и требования к зазорам. Получена зависимость максимально допустимого внутреннего давления в трубопроводе. Рассмотрены требования к оснастке, применяемой в гйбе трубопроводов. Перечислены требования к проектированию агрегата гйбки труб. Во втором разделе рассмотрены возможности температурного воздействия на процесс гйбки трубы. Представлен анализ патентной и технической литературы и описаны шесть возможных методов эффективного температурного воздействия: нагрев всего трубопровода, узкозональный нагрев места гйбы на трубе, охлаждение азотом воды в трубе, лазерное охлаждение атомов трубы, нанесение смазок из нефтепродуктов на место нагрева на трубе и использование современных наполнителей внутри трубы изменяющих её температуру. В третьем разделе определены задачи, поставленные для разработки универсального гйбочного аппарата, сформулированы требования к управляющей программе и устройству шкафа автоматики универсального гйбочного аппарата, рассмотрена система алгоритма работы гйбочного станка с ЧПУ. Показана общая функциональная схема работы агрегата гйбы и циклограмма очередности работы оборудования.

Ключевые слова: гйбка трубы, требования к гйбке труб 3D конфигурации, универсальный гйбочный аппарат, технология гйбки труб, влияние температуры на процесс гйбки труб.

Introduction. The effectiveness of the process of technological development of production: large-size bench and frame structures, on which units are attached; elements of reinforcing structures – stiffeners and auxiliary fastening elements; pipes, intended for the transfer of any material resource (water, air, gas, fuel), and the production of electronic automation, high-tech mechanical aggregate elements and General Assembly depend on the created structure and model of functioning, as well as on the presence of a mechanism for self-regulating technological development.

New technological capabilities expand the space for implementing design innovations (in particular, manufacturing pipelines of a new, more complex configuration, etc.) and allow to solve economic problems – the production of more modern components of products with the required quality, reliability, service life and competitive cost.

Overview of the no-temperature pipeline forming method. The process of bending the pipeline can lead to corrugation on the part of the inner diameter of the bend, as well as to flattening, stretching and thinning of the outer wall of the pipe bend [1–5]. This factor is especially important if thin-walled pipelines with a thickness of 1–2 mm are subjected to bending. In this case determination of the minimal required wall thickness, which ensures transfer of the energy medium in the desired aggregate state and with the specified pressure, comes to the foreground during the pipe bending process.

In each industry, depending on the degree of significance and operating conditions of pipelines, the requirements for the minimal allowable bending radius are set, in case of violation of which critical deformation and rupture of the pipe wall may occur [6].

In the rocket and space industry, the production of pneumatic-hydraulic pipelines and assemblies is regulated by industry standards: OST 92-1600–84 ÷ OST 92-1604–84 [7–13].

OST 92-8536 should be followed when designing and manufacturing pipelines for stand equipment. The production of a particularly important product can be accompa-

nied by a specially developed normative document of technical requirements (TR).

The design documentation (DD) for both pipelines and bending unit must be developed in accordance with the requirements for ensuring manufacturability of the product design, taking into consideration the following factors:

1. Availability of the materials given in the specification.
2. Maximum possible application of standardized parts.
3. To minimize the number (to standardize) the bend radius of the pipe.
4. Make the most of all-stamped pipe fittings instead of welded ones.
5. Make the most of use of drop-off ends on the ends of pipelines instead of turned ones made of bar.
6. Maximum use of compensators according to OST 92-4903, bellows or other compensating elements in pipeline systems, which take into account the effect of temperature fluctuations on the product.
7. Availability of x-ray inspection of the bending area, welded and soldered joints.
8. It is recommended to set bends in the CD with a single radius and without double curvature within a single bend.
9. All dimensions, defining spatial configuration, geometric cross-section dimensions, bending radius, length of straight sections, bending and turning angles must be specified in the pipeline CD or in the drawing TT it is required to indicate manufacturing of the pipeline according to the reference sample (OST 92-0191 and OST 92-1600).
10. Location of pipelines on the products should allow access to them for installation and dismantling works.
11. Straight part of the pipe length (for drop – off ending- shaping of the tip) from the end of the pipeline to bending is not to be less than 60 mm (except the weld or solder lugs, for which a straight length is regulated by ability to install the weld head on OST 92-1602 or soldering device according to OST 92-1603).

12. Straight part of the pipe length (no winglets on the ends) from the end of the pipeline to bending: for pipes with nominal diameters up to 20mm – not less than 10mm; for tube with internal diameter more than 20 mm up to 50 mm – not less 50 mm; for pipes with internal diameter more than 50 mm – not less than 100 mm (paragraph 3.3.2 OST 92-8751–80).

13. Between the curves there should be straight runs not less than 2 x of the external diameter of the pipe, in this case there may be a straight section between bends in the pipe less than 2D, if it is ensured by the technical capabilities of pipe bending equipment at the plant (OST 92-1600–84).

14. Thinning of the walls in places, where pipes bend (fig. 1) and transitions of curved sections to straight sections should not exceed the initial wall thickness: for steel pipes – 20 %; for titanium and copper alloy pipes – 20%; for aluminum alloy pipes – 25 % (point 6.1.7 OST 92-1600–84).

For sections of pipes subjected to maximum load during frequent exploitation, this refinement index for all materials should not exceed 10 % (paragraph 3.3.3 of OST 92-8751–80).

15. The ovality of pipes in the places of bend is the amount, defined as the difference between the greatest and the least diameters divided in half, which is to be: for pipes of nominal sizes up to 10 mm – not more than 0.5 mm; for pipes with internal diameters from 10mm up to 30 mm – not more than 1 mm; for pipes with internal diameters from 30mm to 90 mm – not more than 2 mm; for pipes with internal diameters of more than 90 mm not more than 3mm.

16. During the development of Assembly drawings and layout, it is necessary to provide gaps of at least 5 mm between adjacent pipelines, as well as between pipelines and other structural elements. In places where, because of structural or technological need, it is necessary to reduce the gap between pipelines and structural elements, its minimal allowable value must be specified in the CD, TT or TU.

17. Minimal bending radius for pipes of different diameters and with different wall thicknesses along the middle line (fig. 1), both for cold bending and for bending with heating must be not less the values shown in fig. 2. At the request of operational decision-making of minimal bending radius, without calculation, it is allowed to use paragraph 3.3.1 OST 92-8751–80, according to which the minimum bending radius (at the average diameter of the pipe) for pipes with internal diameters of up to 20mm should be at least 2.5 Dy, and for pipes with internal diameters more than 20 mm – not less than 3.5 Dy, it is allowed to use pipe bends with a bending radius in the single internal diameter, if the radius is obtained by stamping, pulling, or by specially tested bending.

In fig. 1 and 2 the following notations are accepted: Rcp is the bend radius along the middle line; S – is wall thickness of the pipe; D – is the outside diameter of the pipeline.

The sequence of calculating the minimal allowable radius of cold bending along the middle line of three pipelines: Ø8 × 1; Ø34 × 1 and Ø75 × 1.5.

First, the S/D value on the vertical axis of the diagram in fig. 1 is defined.

For the first pipeline: $S/D = 1/8 = 0.125$.

For the second pipeline: $S/D = 1/34 = 0.029$.

For the third pipeline: $S/D = 1.5/75 = 0.020$.

Then, using the values obtained on the vertical axis of the diagram in fig. 1, through the line “a”, the value “x” is determined on the horizontal axis of the diagram, followed by calculating the minimal allowable radius of cold bending along the middle line:

for the first pipeline: $x = 2.5$;

$x = R_m/D \Rightarrow R_m = x \cdot D = 2,5 \cdot 8 \text{ mm} = 20 \text{ mm}$;

for the second pipeline: $x = 3.5$;

$x = R_m/D \Rightarrow R_m = x \cdot D = 3,5 \cdot 34 \text{ mm} = 119 \text{ mm}$;

for the first pipeline: $x = 4.7$;

$x = R_m/D \Rightarrow R_m = x \cdot D = 4,7 \cdot 75 \text{ mm} = 352 \text{ mm}$.

After bending a pipeline with a wall thickness of at least 1.5 mm, when burrs are formed inside the pipeline, their electrochemical removal is allowed with a simultaneous increase in the internal diameter of the pipe of not more than 0.2 mm above the maximal error of the internal diameter and at a length of not more than 4 mm in the cleaning zone, ensuring the required roughness value.

18. The height of the corrugations at the bend of the pipe (see fig. 1) must not exceed the values: for pipes with a conditional passage up to 30 mm – no more than 0.3 mm; for pipes with a conditional passage over 30 to 50 mm – not more than 0.5 mm; for pipes with a conditional passage over 50 mm – not more than 1mm. At the same time, corrugations and dents should have smooth transitions without breaks and tears, and the dimensions of the outer diameter in the places of corrugations should not exceed the permissible ovality (paragraph 6.1.10 OST 92-1600–84).

19. Pipe bending should be carried out from pre-formed pipes that have sufficient technological allowance along the length. The value of technological allowances, depending on the bending methods, must comply with the standards of OST 92–9346.

20. For steel pipe the gap between the flexible mandrel and the inner diameter of the pipe should be selected: for pipe with external diameter up to 20–0.2 to 0.4 mm; for pipes with outer diameter from 23 to 35 mm from 0.3 to 0.5 mm; for pipes with outer diameter from 36 mm to 40mm from 0.4 to 0.6 mm; for pipes with outer diameter from 41 to 100 mm from 0.6 to 1.0 mm. For aluminum pipes and pipes made of aluminum alloys: for pipes with an outer diameter of up to 40 from 0.5 mm to 0.6 mm; for pipes with an outer diameter of 40 to 100 mm – from 0.6 to 1.0 mm.

21. The radius of the pipe bending equipment (rollers, clamps, bending mandrel) must be less than the radius of the pipe bending by the amount of spring of the pipe material.

22. Flexible mandrels should be made of materials that can withstand high pressure, with a small friction

coefficient for the pipe material with high resistance to abrasion, eliminating the possibility of contamination of flexible pipe, preventing formation of scratches and «nadirov» on the inner surface of the pipe, eliminating the

thinning of pipe wall (e. g. steel, fiberglass plastics, textolite, nylon, etc.). There is an example of chrome plating and polishing of steel flexible mandrels with a surface layer hardness of $52 \div 58 \text{ HRC}_3$.

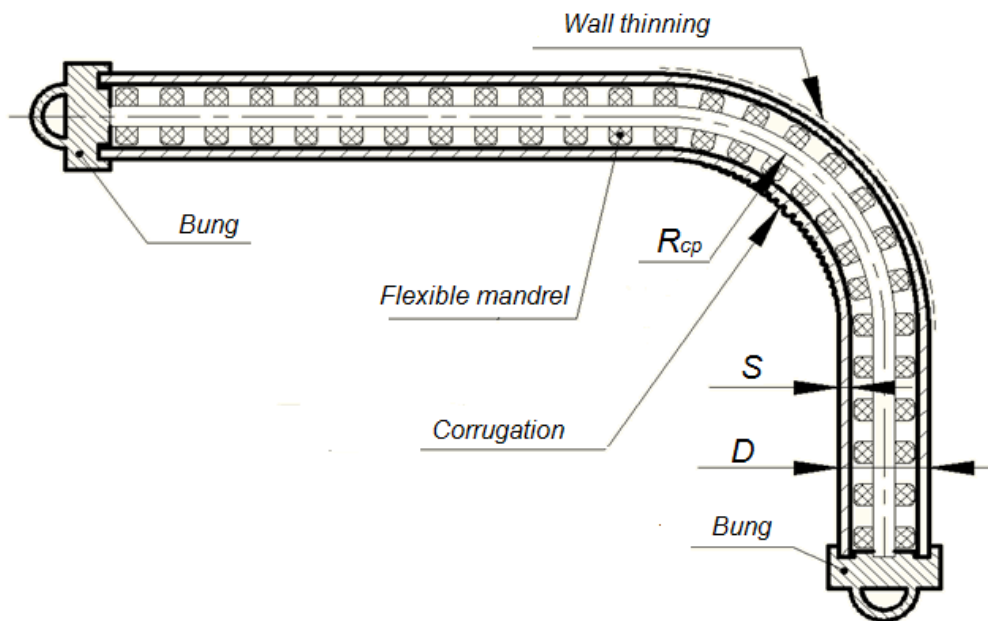


Fig. 1. Section of the projection of the bending in the mandrel

Рис. 1. Сечение проекциигиба трубопровода в дорне

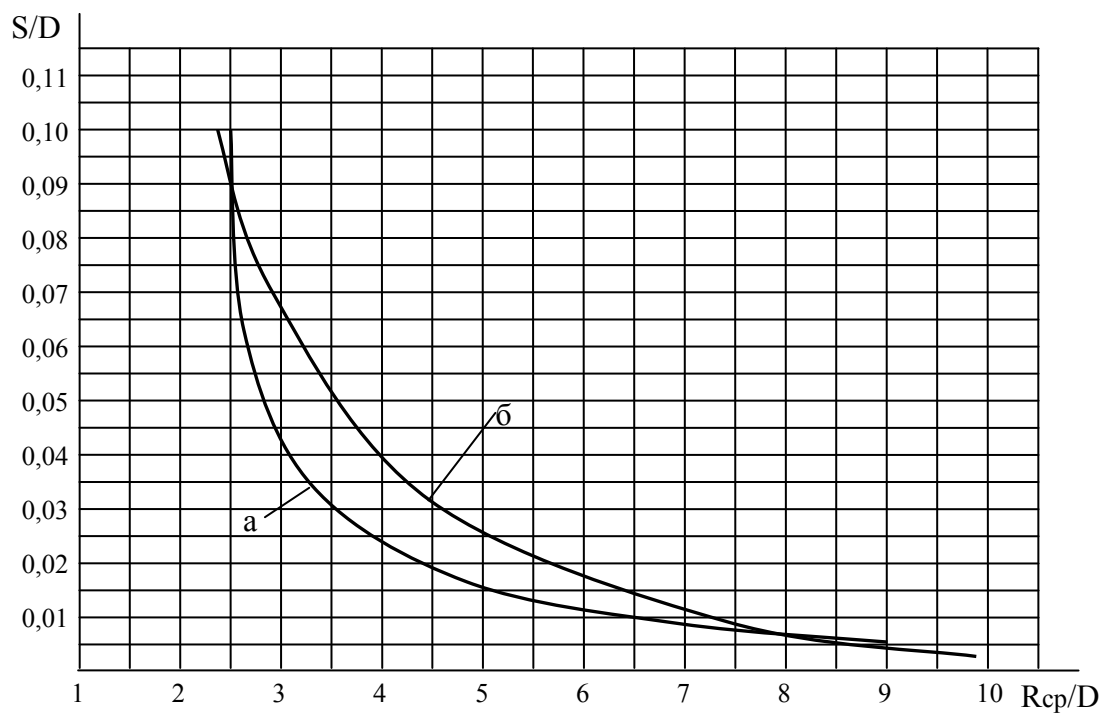


Fig. 2. Diagram of the minimal radiuses of a bend of pipelines:
a – for cold bending; b – for bending with heating

Рис. 2. Диаграмма минимальных радиусов изгиба трубопроводов:
a – для холодной гибки; b – для гибки с нагревом

Working pressure of the substance in steel pipe

Dy, mm	Pipe size, mm	Working pressure, MPa	Allowable internal pressure, MPa	Dy, mm	Pipe size, mm	Allowable internal pressure, MPa	Allowable internal pressure, MPa
4	6×1	0...39.2	47	50	56×3	0...9.8	13.5
6	9×1.5				60×5	9.8...19.6	22.3
10	14×2	0...39.2	39.6		65×8,5	19.6...39.2	39.2
20	24×2	0...19.6	19.8	80	85×3	0...2.5	8.8
	28×4	19.6...39.2	40.5		89×4.5	2.5...9.8	13.3
32	36×2	0...9.8	14		95×7.5	9.8...19.6	21.8
	38×3	9.8...19.6	20.5	100	110×5	2.5...9.8	11.8
	42×6	19.6...39.2	40.8		120×10	9.8...19.6	23

23. The allowable internal pressure in the pipe is determined by the formula:

$$P = \frac{2(\sigma_u / 2,6)\delta}{(D_o - \delta)} K,$$

where σ_u – is the ultimate tensile strength, N/m²; δ – is the (average) wall thickness of the pipe, m; D_o – is the outer diameter of the pipe, m; K – is a dimensionless correction factor:

$$K = \frac{\frac{5\delta_{\min}^2 + h^2}{\delta} + 2\sqrt{D_p\delta}}{\frac{5\delta_{\min}(D_o - \delta)}{(D_o - \delta)} + (D_o - \delta) + 2*\sqrt{D_p(\sigma_u / 2,6)}}$$

where δ_{\min} – is the minimal thickness of the pipe along the entire length of the pipeline, m; h – is the maximal pipe thickness over the entire length of the pipeline, m.

24. The working pressure of the medium, used in the steel pipeline, is determined according to OST 92-8751–80. Table shows some parameters that are allowed for the main sizes of steel pipelines/

25. In drawings, containing a complex configuration of 3D pipes, as well as in those, where there are bending forms of pipes, it is required to specify in the technical requirements, necessity to conduct hydraulic or pneumatic strength tests with a pressure exceeding the working pressure of the medium by 1.25÷1.5 times in accordance with paragraph 3.5.1 of OST 92-8751–80. This test must confirm absence of cracks, gas pores, and other non-metallic inclusions in the pipe wall and unacceptable wall thickness defects. In this case, the test equipment, technology for preparing and conducting tests must exclude contamination, grease, oil, gasoline and other liquids and their vapors from entering the internal cavities of the pipe. During the test, it is obligatory to perform pressure loading smoothly without sudden jumps to the set value for at least 30 seconds (deviation from the set pressure value by not more than ±5 % according to paragraph 3.5.11 of OST 82-8751–80). Measuring the pressure is to be held with pressure gauges of accuracy class not less than 2.5 in accordance with GOST 2405–88.

26. Requirements to the design of the bending unit are set out in section 2 of OST 92-8751–80. In particular, the following requirements are highlighted for the pipe bending unit: the unit must be protected from direct exposure to precipitation and the sun; the recoil and actuation forces must be firmly and reliably fixed in the unit (for example: it is necessary to specify the amount of tightening of threaded parts in the CD, provide locking – as a

means of protection against disconnection of parts during vibration); the diameter of the trunk is to be chosen, according to the desired pressure drop and allowable pressure drop; parameters of composite components of the bending unit and pipes (working environment, working pressure, nominal diameter, order of operation, etc.) should correspond to each other; releasable connection of the unit is to be placed in locations convenient for maintenance and repair; the height of the pipe bending table on the unit should also be convenient for the operator (not more than 1.5 m); protection of parts and the pneumatic hydraulic system from corrosion must be provided; the safety system of the device must be followed for the service personnel. The symbol and image of pipeline elements are regulated in GOST 2.784-96 and in OST 92-0039–74.

Opportunities of temperature influence on the pipe bending process. When defining method and technology of pipe bending, the first place is given to implementation of the specified parameters of pipe bending, optimizing the costs of the technological process simultaneously. If to use an unprepared pipe for bending (according to technical characteristics) and perform bending on a non-specialized (economical) manual pipe-bending apparatus, it is very difficult to provide a bending radius of less than 4D.

When determining whether a material is ready for the bending process, the following technical parameters are considered. The phenomena of elasticity and plasticity are well illustrated using the material tension diagram (fig. 3).

Diagrams of stretch and mechanical characteristics of materials depend on many factors. The most significant influence on them exert the rate of deformation, temperature, and technological factors.

Increasing the rate of deformation of the material v leads to a decrease in the plastic properties and strengthening of the fragile ones, reducing the relative deformation at break δ . Simultaneously, σ_t and σ_b increase. In this case, the elastic characteristics of the material - modulus of elasticity E and the coefficient of transverse deformation μ remain unchanged.

The influence of higher and lower temperatures on metals is more significant. When temperature E increases, σ_s , σ_u , in their turn, decrease, and the coefficient of transverse deformation μ and δ increase.

Calculations of structures, which operate beyond the elastic limits of the materia, are based on experimentally obtained tensile diagrams. To perform calculations,

the equation of the stretch diagram is given in the form: $\sigma = f(\varepsilon)$.

For an isotropic body within elastic deformations, when calculating the deformation process of a material, it is possible to write six equations, which link the stress components with components of deformation:

$$\begin{cases} \varepsilon_x = \frac{1}{E}(\sigma_x - \mu(\sigma_y + \sigma_z)) + \alpha T & \gamma_{xy} = \frac{\tau_{xy}}{G} \\ \varepsilon_y = \frac{1}{E}(\sigma_y - \mu(\sigma_x + \sigma_z)) + \alpha T & \gamma_{xz} = \frac{\tau_{xz}}{G}; \\ \varepsilon_z = \frac{1}{E}(\sigma_z - \mu(\sigma_x + \sigma_y)) + \alpha T & \gamma_{yz} = \frac{\tau_{yz}}{G} \end{cases}$$

Beyond the elastic limit, taking into account temperature deformations, Hooke's law has the following form:

$$\begin{aligned} \varepsilon_x &= \frac{\varepsilon_i}{\sigma_i} \left[\sigma_x - \frac{1}{2}(\sigma_y + \sigma_z) \right] + \alpha T \\ \varepsilon_y &= \frac{\varepsilon_i}{\sigma_i} \left[\sigma_y - \frac{1}{2}(\sigma_x + \sigma_z) \right] + \alpha T \\ \varepsilon_z &= \frac{\varepsilon_i}{\sigma_i} \left[\sigma_z - \frac{1}{2}(\sigma_y + \sigma_x) \right] + \alpha T \end{aligned}$$

The modulus of elasticity is replaced by the ratio of the deformation intensity ε_i to the stress intensity σ_i :

$$\begin{aligned} \sigma_i &= \frac{1}{\sqrt{2}} \sqrt{(\sigma_x - \sigma_y)^2 + (\sigma_y - \sigma_z)^2 + (\sigma_z - \sigma_x)^2 + 6(\tau_{xy}^2 + \tau_{yz}^2 + \tau_{zx}^2)} \\ \varepsilon_i &= \frac{\sqrt{2}}{3} \sqrt{(\varepsilon_x - \varepsilon_y)^2 + (\varepsilon_y - \varepsilon_z)^2 + (\varepsilon_z - \varepsilon_x)^2 + 3(\gamma_{xy}^2 + \gamma_{yz}^2 + \gamma_{zx}^2)} \end{aligned}$$

For an isotropic body, the main directions of deformation coincide with the main directions of displacement.

For aluminum, $E = 0.7 \cdot 10^5$ MPa; for copper, $E = 1.2 \cdot 10^5$ MPa; for steel, $E = 2 \cdot 10^5$ MPa.

It is also necessary to take into consideration such indicators as: the elastic limit, which is the maximum value of mechanical stress at which the deformation of this material remains elastic, and the limit of proportionality is the maximum amount of stress for a particular material, at which Hooke's law is still applied, namely, deformation of the body depends directly on the applied load.

A study of patent documentation and technical literature was conducted, in which the issues of force and temperature effects on the pipe bending process [14–16] were considered. On the basis of analysis and generalization of the information obtained, the following main parameters and regularities of technological processes are identified:

1. Performing bending of a heated pipeline: when heated to $800 \div 1000$ °C, the values of σ_b and σ_0 are reduced up to three times, what lowers index of the bending force and makes it possible to obtain complex curved trajectories of the pipe. However, this process is extremely energy-intensive and economic profitability of this method of blending is very uncompetitive. This method is

used only if there is no other way to manufacture a complex 3D pipeline.

2. Narrow-zone local heating of the place of bending on the pipe up to 1100 °C reduces the possibility of corrugation, and also the index of the impact force on the pipe by $6 \div 7$ times. When using modern energy-intensive technologies for narrow-zone heating of the place of bending on the pipe, good indicators of the diameter and radius dimensions of the pipe bend can be achieved through the heating elements of the flexible mandrel. Additional energy costs for heating the mandrel elements in this case can be compensated by means of reduced energy costs on the force of impact on the pipe during bending.

3. The pipeline (usually an aluminum alloy pipe) is cooled with nitrogen before being bend to the temperature of -200 °C, and water is used as a filler in the pipe (according to OST 92-1511). It is necessary to take into consideration possible structural changes in the pipe material, so if reliability and strength indicators are lowered, what results in prohibiting further application of the pipe, subsequent heat treatment of this pipe, according to OST 92-1311, will be required to restore the strength properties of it, what will reduce the financial profitability of this method.

Therefore, in order to make a decision about using this method, it is necessary to conduct testing of experiments (different temperature conditions, different bending forces used, different materials and pipe alloys used, etc.) and choose the optimal bending technology with cooling without [su4](#).

4. Laser cooling of atoms of the tube material (because of resonant light pressure) is laser irradiation of the tube material, and the average energy of the emitted photons must exceed the energy of the absorbed photons (in other words, when anti-Stokes emission occurs, at frequencies higher than the laser frequency, the Stokes emission dominates, frequencies of which have lower values, under a condition, that the speeds of non-radiative transitions from excited States are negligible in relation to the speeds of optical transitions), in this case, the internal degrees of freedom of the atoms of the pipe material, which are connected by heat exchange with the environment, are cooled. Cooling of atoms under resonant light pressure continues until the fluctuations of the atom's momentum, which are inevitable in the process of stochastic re-emission of a large number of atoms, enter the process. Types of laser cooling are as follows: anti-Stokes laser cooling (photoluminescence method); Doppler cooling (the method is based on the Doppler effect and spontaneous Raman scattering); fluorescent cooling (the frequency of laser radiation exceeds the frequency of ordinary light, absorbed by the tube material).

5. Application of greasing from petroleum products on the outer surface of the pipe material, such as mineral oils, fuel oil, paraffin, petrolatum, vegetable oils (castor), soap suspensions in oil (for example, an emulsion greasing for bending aluminum – a mixture of alkyl esters and an ox ethylated aliphatic mixture of surfactants), talc powders, graphite powders, molybdenum disulfide powders.

In the operation of cold bending of the pipe when applying one of the mixtures on the pipe in the material, near the surface in the stretch zone, stresses are reduced and plastic properties are improved. Slight heating of the bend area with this coating dramatically increases the coefficient of plasticity.

6. Application of modern fillers inside the bent pipe, which change its temperature and contain: over cooled ice, quartz sand, liquid mixtures, emulsions, oils, surface lubricants of the pipe and other fusible and loose fillers. It is necessary to conduct production experiments with different materials and temperature conditions: with registration of results; analysis of the results obtained and working out the most effective technology.

Mechatronic system of the CNC bending machine operation algorithm. The task of the 3D pipeline bending process is to create a universal bending machine (UBM), which has the following functions:

1. It is possible to use three types of bending technology: bending without heating and without cooling (including a flexible mandrel and without a flexible mandrel); bending only with narrow-zone heating; bending only with cooling.

2. It can operate in three operating modes: manual; automatic (with numerical control); universal variable mode (automatic reproduction of individual mechanical bending operations, using actuators or temperature control operations, which are started manually by the operator through control display).

3. The UBM is maintainable, has cheap, periodically replaced bending elements (bending rollers, gripping and rotating devices, oils, etc.) and does not have expensive imported parts and assemblies.

4. The UBM is designed as a constructor, allowing regulation and improvement of the machine, the possibility of using several bending technologies, and the possibility of experimenting with a bending head (consisting of lobes with bearings with an induction function), as well as allowing experiments with technologies.

5. The UBM allows the operator to produce a 3D pipeline according to the drawing without creating a special information program, that is, using only the interface and basic programs, recorded on the programmed logic microcontroller of the automation Cabinet.

The General functional schema of the UBM is shown in fig. 4.

A stand for entering a 3D pipeline bending task provides UBM with information for step-by-step operations [17; 18]. The device of the stand must be made in a universal mixed form: a touch-button panel [19].

The touch panel should perform the function of detailed input of bending information and allow further improvement of the UBM control software, and the keypad should reliably fulfill the function of performing a one-time mechanical bending operation. The pipe bending trajectory is set by pressing the keys on the sensor provided with designation of logical elements and numeric values for specifying the pipe size and the bending path. Also, the information input stand must have a USB socket for a Flash drive.

From the stand, information is sent to the programmable controller of the automation Cabinet (in which micro-electronic integrated circuits can be used as an element base). When developing the automation Cabinet of the UBM control system, it is necessary to take into account that in comparison with the controller, having relay-contact equipment, the microcontroller has contactless electronic blocks, which in turn have high reliability in operation and small size. A serious drawback of the microcontroller is the limited number of programmable operations, so the final choice of using the controller or microcontroller will depend on this parameter. The control program of the controller (a set of commands, written on the programming language, coinciding specified algorithm for the operation of bending machine) must contain both geometric and technological information, which should be able to be adjusted by the profile specialists.

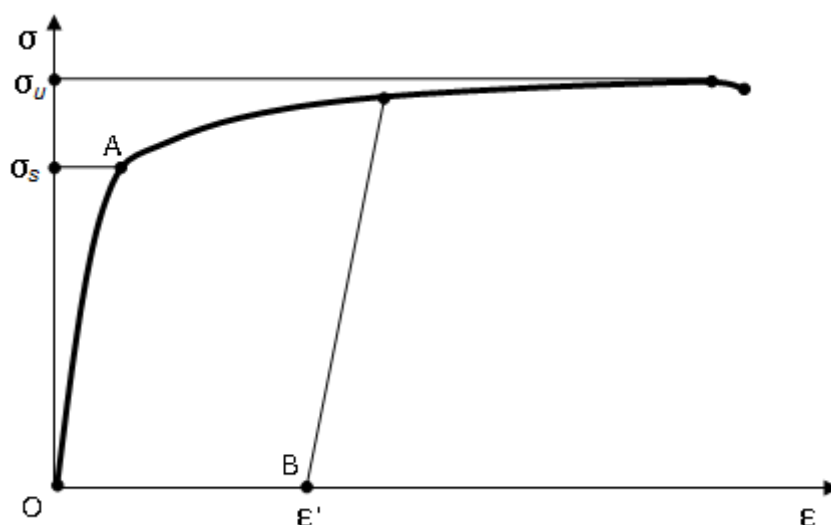


Fig. 3. The diagram of deformation of material under tension

Рис. 3. Диаграмма деформации материала при растяжении

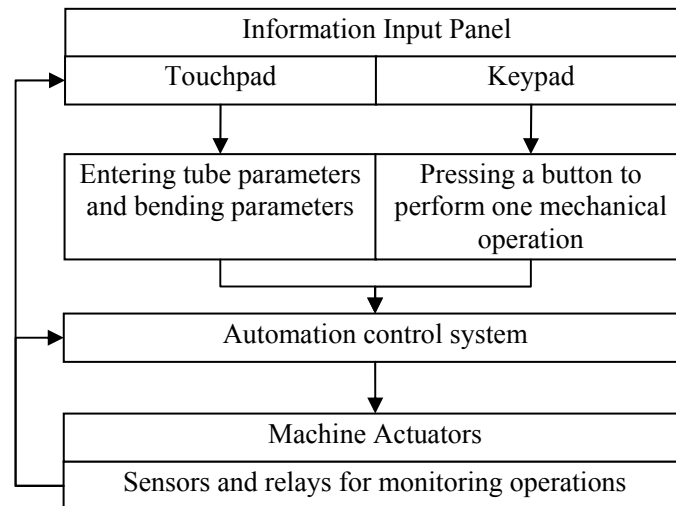


Fig. 4. Functional schema of the universal bending machine

Рис. 4. Функциональная схема работы универсального гибочного станка

The control program is to meet requirements of GOST 20999–83 (CMEA ST 3585–82), which will be clear to most systems, regardless of the manufacturer and operator.

Control of the UBM mechanisms' operation must be provided by sensors, located on the UBM bending table (light, magnetic, ray optical, etc.) and relays (pressure, time, etc.), the signal from which is sent to the controller of the automatic control system Cabinet. Connecting of the controller panel of automation system to the local network of the enterprise will allow to transmit information of the machine (presence of oil, air, pressure level in the system, etc.) and to perform maintenance in case of breakage or jamming of the operating mechanisms of the UBM. Operation of the actuators of the bending machine is determined by the drives (devices that convert electrical energy into mechanical energy through the electric motor and the actuators of the machine that control the parameters of the bending).

In the bending machine, it is possible to use the following types of drives: electric, electromechanical, pneumatic, hydraulic, and electro-hydraulic.

The movement parameters of the mechanism are controlled with the help of a control parameter Converter, a feedback sensor, a setting device, and a protection device. It is also necessary to use auxiliary drives, which implement movements, which have an auxiliary character: in clamping devices, loading devices, pumps, etc. With the help of an electric drive Converter, it is possible to smoothly adjust changes in current parameters – for example, with electric pitch splitting (which can allow changing the parameters of speed of bending rollers, as well as power of the roller pressure on the pipe, etc.) or voltage (for example, converting AC to DC).

Simultaneously, a mechanical transmission between the output link of the source of motion (the motor shaft) and the link consumption of mechanical energy (e. g. rod hydraulic cylinder) is to be used; in this process, a kine-

matic transformation of the change in the direction of force and speed of linear movement, or a transformation of the change in the plane of rotation during rotational movement takes place.

In the UBM mechanism it is necessary to determine the main motion drives, which are involved in the direct bending process and from which accuracy and quality of bending of pipelines depends. For this purpose, in these drives: increase of the range of regulation by the Converter, using zero position sensors (GOST 20523–80), ensuring shock-free start and braking (using a pulse sensor) are additionally used.

The cyclorama of the UBM executive mechanisms sequence is as follows:

1. Input pipe parameters on the touch panel (external diameter, wall thickness, total length of the pipe).
2. Installing the pipe in the UBM feed mechanism (in the delivery state).
3. Pipe capture by the “capture and movement Mechanism” of the UBM.
4. Input 3D bending path parameters sequentially on the touch panel:

LENGTH of straight section of pipe (mm)



BENDING TECHNOLOGY

- application of prepared pipe for bending (chilled);
- application of a spray grease on the surface of the pipe;
- application of a mandrel for bending (yes/no);



BEFORE BENDING WITH MANDREL

- application of a heating element of the mandrel (yes/no);
- input of the heating temperature of the heating elements;

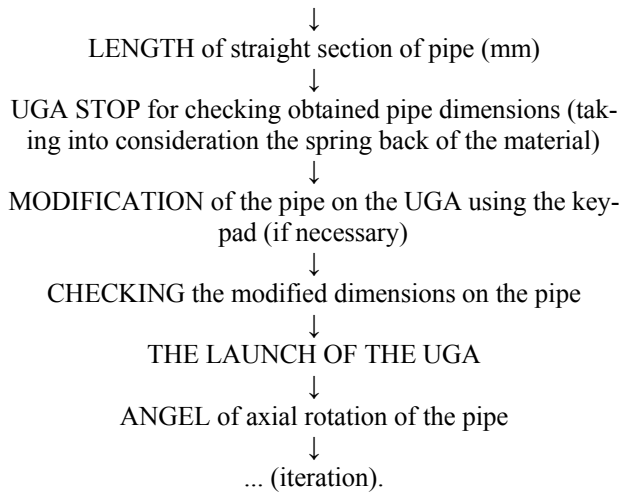


Horizontal turning RADIUS (mm)



The ANGLE at which the radius is turned (up to 360)





5. Execution of the UBM of the straight part of pipe, using capture and movement mechanism.

6. Location change of the bending rollers of the machine from the starting position to the position, taking into different bending radius of the pipe (see fig. 5, *b, c, g*).

7. Execution of bend of the pipe on the UBM in accordance with a predetermined trajectory of 3D model.

Several key factors, which affect the bending process and increase the efficiency of the UBM, should be taken into consideration:

- the possibility of general or local zone heating (for example, by high-frequency currents, etc.) application in case of some difficulties in the process of bending (thick pipe walls, pipe breaks, unacceptable pipe sinking, etc.);

- the possibility of using greasing oils of the pipe walls;
- the possibility of using a prepared cold billet (inside the pipe, water ice obtained with cooled nitrogen);
- the possibility to reduce goffer formation by installing an additional roller from the center of the bend;
- the ability to control the UBM manually, when modifying the pipe bend, if the material spring coefficient is not taken into consideration.

Conclusion. In the review of this article an attempt to consider all the factors, which affect the efficiency of the pipe bending process, is made. An overview of the normative documentation of industry aerospace standards, regulating pipeline bending, is presented, as well as requirements for a universal bending machine, which allow application a temperature-free and non-temperature technological process of bending pipelines of complex configuration. A cyclorama of the sequence of functioning of the UBM executive mechanisms is given and a schematic drawing of the process of bending by a universal machine is presented.

The main advantage of the technology, being developed, and universal bending equipment is the possibility of application of different bending technologies on this equipment, a large range of sizes of pipes being bended, simplicity of operation of the equipment, comparative cheapness of technologies and opportunity of improving them, low cost of repairing, simplicity of maintenance of the UBM. Additional advantage of the UBM is the possibility of working out and finding the most effective bending technology and the possibility of making improvements to the design of the UBM.

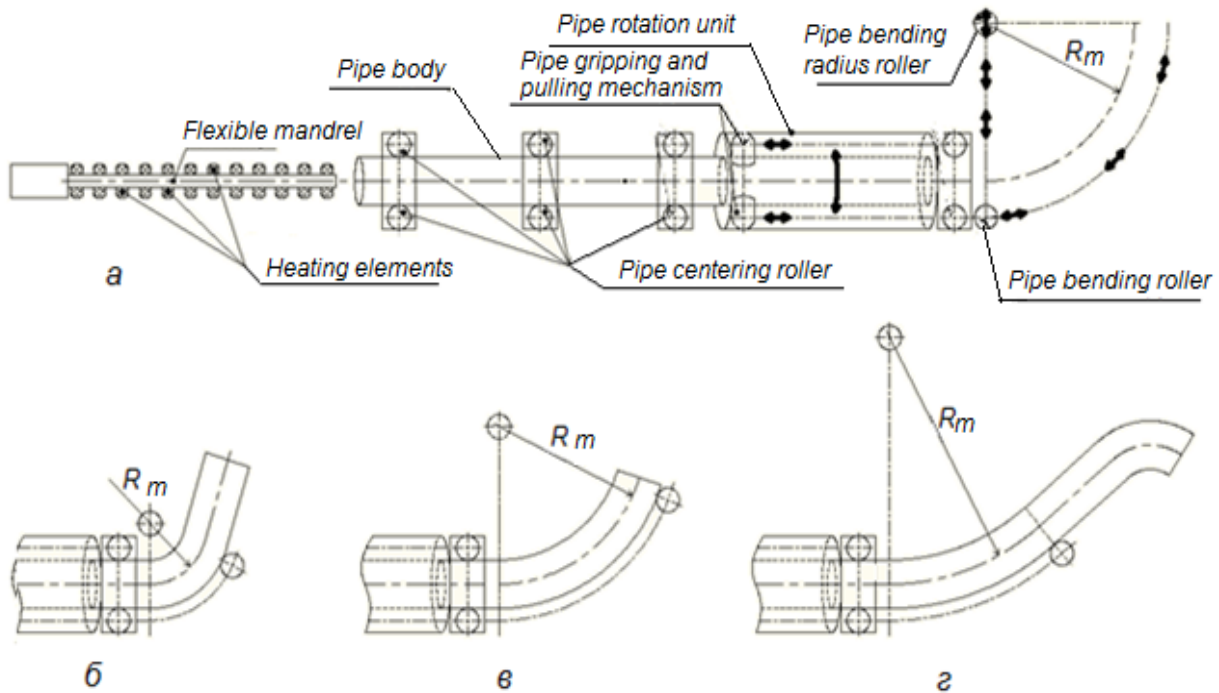


Fig. 5. Schematic drawing of the universal bending machine

Рис. 5. Схематический рисунок универсального гибочного агрегата

References

1. Glazkov A. S., Klimov V. P., Gumerov K. M. [Longitudinal-transverse bending of the pipeline in areas of soil changes]. *Problemy sbora, podgotovki i transporta nefi i nefteproduktov*. 2012. No. 1. P. 63–70 (In Russ.).
2. Glazkov A. V. [Technology of cold bending of pipes by longitudinal rolling. Scientific and technical statements of SPbSPU]. *Nauka i obrazovanie*. 2012, no. 2-2, P. 132–136 (In Russ.).
3. Gumerov A. G., Dudnikov Yu. V., Azmetov H. A. [Analysis of the stress-strain state of underground pipelines at turning angles in the horizontal plane]. *Problemy sbora, podgotovki i transporta nefi i nefteproduktov*. 2012, No. 1, P. 46–50 (In Russ.).
4. Sunagatov M. F., Gaysin A. Z. [Determination of the stress-strain state of the pipeline in the zone of landslide of soil]. *Neftegazovoe delo*. 2016, No. 2, P. 134–150 (In Russ.).
5. Haliulin E. V. [Measurement of curvatures and deformations of thin-walled pipes made of corrosion-resistant steels during their cold bending with rolling]. *Aktual'nye voprosy tekhnicheskikh nauk : V Mezhdunar. nauch. konf.* [Actual issues of technical sciences: V Intern. scientific conf.] St. Petersburg, Svoe izdatel'stvo Publ., 2019, P. 40–44 (In Russ.).
6. Ryzhkov E. V., Ryzhkov V. M. [On the effect of internal pressure on the bending of pipelines]. *Vestnik Volgogr. gos. arkhitekt.-stroit. un-ta. Ser.: Str-vo i arkhitekt.* 2012, Iss. 29 (48), P. 179–185 (In Russ.).
7. OST 92-1600–84. *Proizvodstvo truboprovodov. Obshchie tekhicheskie uslovia. Etalonirovanie truboprovodnih sistem, gibka trub i formoobrazovanie koncov truboprovodov* [State Standard 92-1600–1984. Production of pipelines. Standardization of pipeline systems, pipe bending and shaping of pipeline ends]. Moscow, Standartinform Publ., 1984. 47 p.
8. OST 92-1601–84. *Proizvodstvo truboprovodov. Obshchie tekhicheskie uslovia. Sbornka, okraska, markirovka, oshistka, kontrol i montaj truboprovodov* [State Standard 92-1601–84. Pipeline manufacturing. General technical conditions. Assembly, painting, marking, cleaning, monitoring and installation of pipelines]. Moscow, Standartinform Publ., 1984. 33 p.
9. OST 92-1602–84. *Proizvodstvo truboprovodov. Svarka. Obshchie tekhicheskie trebovaniya* [State Standard 92-1602–84. Pipeline manufacturing. Welding. General technical requirements]. Moscow, Standartinform Publ., 1984. 32 p.
10. OST 92-1603–84. *Proizvodstvo truboprovodov. Payka. Obshchie tekhicheskie trebovaniya* [State Standard 92-1603–84. Pipeline manufacturing. Soldering. General technical requirements]. Moscow, Standartinform Publ., 1984. 29 p.
11. OST 92-1604–84. *Proizvodstvo truboprovodov. Ispitaniya. Obshchie tekhicheskie trebovaniya* [State Standard 92-1603–84. Pipeline manufacturing. Tests. General technical requirements]. Moscow, Standartinform Publ., 1984. 60 p.
12. GOST 17365–71. *Truboprovodi dlya agresivnih sred* [State Standard 17365–71. Obshchie tekhicheskie trebovaniya]. Moscow, Standartinform Publ., 1971. 11 p.
13. ISO 6983–2009. *Avtomatizirovannye sistemi i integratsiya. Chislivoe programnoye upravlenie stankom. Format programmi i opredelenie adresnih slov* [State Standard 6983–2009. Automated systems and integration. Numerical control of the machine. The format of the program and the definition of address words]. Moscow, Standartinform Publ., 2009. 26 p.
14. Shinkin V. N. [Mathematical modeling of production processes of large diameter pipes for trunk pipelines]. *Vestnik SGTU*. 2011, No. 4 (62), Iss. 4, P. 89–74 (In Russ.).
15. Shotsky S. A., Malyushin N. A. [Stresses and displacements of a loaded underground pipeline at turning angles in a vertical plane]. *Izvestiya vysshikh uchebnykh zavedeniy. Ser.: Neft' i gaz*. 2009, No. 2, P. 83–85 (In Russ.).
16. Chudakov G. M., Ivanov M. G., Barambonne S., Degtyarenko N. A. [Improving the reliability of the linear part of main oil pipelines]. *Nauchnye trudy KubGTU*. 2016, No. 10, P. 70–85 (In Russ.).
17. About some tools and features of Lotsia PDM PLUS. Available at: <https://sapr.ru/article/25364> (accessed: 29.12.2019).
18. Creating opportunities for computer modeling of physical processes and engineering analysis. Available at: http://www.cadcamcae.lv/hot/CAE-WP_Part1_n53_n44.pdf (accessed: 29.12.2019).
19. Titenkov S. V., Zaporozhsky A. S., Nikishev A. A. *3D modelirovanie pri proektirovanii prostranstvennykh truboprovodnykh sistem* [3D-simulation at designing space pipeline systems]. Reshetnevsky readings. Materials of the XVII Intern. scientific. conf.]. Krasnoyarsk, 2013. Part 1.

Библиографические ссылки

1. Глазков А. С., Климов В. П., Гумеров К. М., Продольно-поперечный изгиб трубопровода на участках грунтовых изменений // Проблемы сбора, подготовки и транспорта нефти и нефтепродуктов. 2012. № 1. С. 63–70.
2. Глазков А. В. Технология холодной гибки труб методом продольного раскатывания. Научно-технические ведомости СПбГПУ // Наука и образование. 2012. № 2-2. С. 132–136.
3. Гумеров А. Г., Дудников Ю. В., Азметов Х. А. Анализ напряженно деформированного состояния подземных трубопроводов на углах поворота в горизонтальной плоскости // Проблемы сбора, подготовки и транспорта нефти и нефтепродуктов. 2012. № 1. С. 46–50.
4. Сунагатов М. Ф., Гайсин А. З. Определение напряженно-деформированного состояния трубопровода в зоне оползня грунта // Нефтегазовое дело. 2016. № 2. С. 134–150.
5. Халиулин Е. В. Измерение искривлений и деформаций тонкостенных труб из коррозионностойких сталей при их холодной гибке с раскатыванием // Актуальные вопросы технических наук : V Междунар. науч. конф. / под ред. И. Г. Ахметова и др. СПб. : Свое издательство, 2019. С. 40–44.

6. Рыжков Е. В., Рыжков В. М. О влиянии внутреннего давления на изгиб трубопроводов // Вестник Волгогр. гос. архит.-строит. ун-та. Сер.: Стр-во и архит. 2012. Вып. 29 (48). С. 179–185.
7. ОСТ 92-1600–84. Производство трубопроводов. Общие технические условия. Эталонирование трубопроводных систем, гибка труб и формообразование концов трубопроводов. М. : Стандартинформ, 1984. 47 с.
8. ОСТ 92-1601–84. Производство трубопроводов. Общие технические условия. Сборка, окраска, маркировка, очистка, контроль и монтаж трубопроводов. М. : Стандартинформ, 1984. 33 с.
9. ОСТ 92-1602–84. Производство трубопроводов. Сварка. Общие технические требования. М. : Стандартинформ, 1984. 32 с.
10. ОСТ 92-1603–84. Производство трубопроводов. Пайка. Общие технические требования. М. : Стандартинформ, 1984. 29 с.
11. ОСТ 92-1604–84. Производство трубопроводов. Испытания. Общие технические требования. М. : Стандартинформ, 1984. 60 с.
12. ГОСТ 17365–71. Трубопроводы для агрессивных сред. Общие технические требования. М. : Стандартинформ, 1971. 11 с.
13. ISO 6983–2009 Автоматизированные системы и интеграция. Числовое программное управление станком. Формат программы и определение адресных слов. М. : Стандартинформ, 2009. 26 с.
14. Шинкин В. Н. Математическое моделирование процессов производства труб большого диаметра для магистральных трубопроводов // Вестник СГТУ. 2011. № 4 (62), вып. 4. С. 89–74.
15. Шоцкий С. А., Малюшин Н. А. Напряжения и перемещения пригруженного подземного трубопровода на углах поворота в вертикальной плоскости // Известия высших учебных заведений. Сер.: Нефть и газ. 2009. № 2. С. 83–85.
16. Повышение надежности линейной части магистральных нефтепроводов / Г. М. Чудаков, М. Г. Иванов, С. Барамбонье, Н. А. Дегтяренко // Научные труды КубГТУ. 2016. № 10. С. 70–85.
17. О некоторых средствах и возможностях Lotsia PDM PLUS // «САПР и графика». 2017. № 1 [Электронный ресурс]. URL: <https://sapr.ru/article/25364> (дата обращения: 29.12.2019).
18. Создание возможностей для компьютерного моделирования физических процессов и инженерного анализа // «CAD/CAM/CAE observer». 2010. № 1(53) [Электронный ресурс]. URL: http://www.cadcamcae.lv/hot/CAE-WP_Part1_n53_n44.pdf (дата обращения: 29.12.2019).
19. Титенков С. В., Запорожский А. С., Никишев А. А. 3D-моделирование при проектировании пространственных трубопроводных систем // Решетневские чтения : материалы XVII Междунар. науч. конф., посвящ. памяти генер. конструктора ракет.-космич. систем акад. М. Ф. Решетнева : в 2 ч. ; под общ. ред. Ю. Ю. Логинова ; Сиб. гос. аэрокосмич. ун-т. Красноярск, 2013. Ч. 1.

© Titenkov S. V., Zhuravlev V. Yu., 2020

Titenkov Georgi Valerievich – leading design engineer; Krasnoyarsk machine-building plant. E-mail: Titenkov-sv@mail.ru.

Zhuravlev Victor Yurevich – Cand. Sc., docent, professor; Reshetnev Siberian State University of Science and Technology. E-mail: vz@sibsau.ru.

Титенков Сергей Валерьевич – ведущий инженер-конструктор; АО «Красноярский машиностроительный завод». E-mail: Titenkov-sv@mail.ru.

Журавлев Виктор Юрьевич – кандидат технических наук, доцент, профессор кафедры двигателей летательных аппаратов; Сибирский государственный университет науки и технологий имени академика М. Ф. Решетнева. E-mail: vz@mail.sibsau.ru.

UDC 621.628

Doi: 10.31772/2587-6066-2020-21-1-136-141

For citation: Shestakov I. Y., Khilyuk A. V. Influence of a constant electric field on the adsorption purification of water from iron ions. *Siberian Journal of Science and Technology*. 2020, Vol. 21, No. 1, P. 136–141. Doi: 10.31772/2587-6066-2020-21-1-136-141

Для цитирования: Шестаков И. Я., Хилук А. В. Влияние постоянного электрического поля на адсорбционную очистку воды от ионов железа // Сибирский журнал науки и технологий. 2020. Т. 21, № 1. С. 136–141. Doi: 10.31772/2587-6066-2020-21-1-136-141

INFLUENCE OF A CONSTANT ELECTRIC FIELD ON THE ADSORPTION PURIFICATION OF WATER FROM IRON IONS

I. Y. Shestakov, A. V. Khilyuk

Reshetnev Siberian State University of Science and Technology
31, Krasnoyarsky Rabochy Av., Krasnoyarsk, 660037, Russian Federation
E-mail: h-anna7@bk.ru

Using electrochemical action (ECA) to treat water was first proposed in UK in 1889. At present, many methods of ECA are known (electro flotation, electro coagulation, electro osmosis, electrophoresis, etc.).

In the production of rocket and space technology, galvanic technologies are used, as a result of which waste water is contaminated with metal ions. Known methods of wastewater treatment do not allow to ensure the maximum permissible concentration of metal ions in treated water, or are expensive or difficult to operate in industry. Iron ions are among the most polluting components of wastewater of most industries. So increased control and the development of effective methods of wastewater treatment are necessary. Iron affects the intensity of phytoplankton development and the qualitative composition of microflora in reservoirs. The toxicity of iron compounds in water depends on the hydrogen index of water. The alkaline environment dramatically increases the risk of fish poisoning, as in such conditions, iron hydroxides are formed, which are deposited on the gills, clog and corrode them. In addition, iron compounds bind oxygen dissolved in water, which leads to the mass death of fish and other hydrobionts.

The article presents the method of conducting experiments, the methods of sorption, electrochemical and combined water treatment, including electrochemical action and adsorption. The results of studies of these methods of water purification from iron ions are presented. The dependence of the degree of purification on the electric field strength, interelectrode distance and water treatment time is revealed. With an electric field strength of 5.16 V/mm, a temperature of 20–22 °C using quartz sand as an adsorbent and a processing time of 1 minute, the concentration of iron ions decreased from 2.5 to 0.25 mg/l (at MPC = 0.3 mg/l). The proposed combined cleaning method requires inexpensive and affordable materials and is easy to operate.

Keywords: *electrochemical method, iron, degree of purification, alternating current, direct current, sorbent.*

ВЛИЯНИЕ ПОСТОЯННОГО ЭЛЕКТРИЧЕСКОГО ПОЛЯ НА АДСОРБЦИОННУЮ ОЧИСТКУ ВОДЫ ОТ ИОНОВ ЖЕЛЕЗА

И. Я. Шестаков, А. В. Хилук

Сибирский государственный университет науки и технологий имени академика М. Ф. Решетнева,
Российская Федерация, 660037, г. Красноярск, просп. им. газ. «Красноярский рабочий», 31
E-mail: h-anna7@bk.ru

Использование электрохимического воздействия (ЭХВ) для обработки воды впервые было предложено в Великобритании в 1889 г. В настоящее время известно много методов ЭХВ (электрофлотация, электрокоагуляция, электроосмос, электрофорез и др.).

В производстве ракетно-космической техники применяются гальванические технологии, в результате которых происходит загрязнение сточных вод ионами металлов. Известные методы очистки сточных вод не позволяют обеспечить предельно-допустимую концентрацию ионов металлов в очищенной воде либо являются дорогостоящими или сложными в эксплуатации в промышленности. Одним из часто встречающихся загрязняющих компонентов является ионы железа, входящего в состав сточных вод большинства отраслей про-

мышленности, что требует повышенного контроля и разработки эффективных методов очистки сточных вод. Железо влияет на интенсивность развития фитопланктона и качественный состав микрофлоры в водоемах. Токсичность соединений железа в воде зависит от водородного показателя воды. Щелочная среда резко увеличивает опасность отравления рыб, так как в таких условиях образуются гидроксиды железа, которые осаждаются на жабрах, закупоривают и разъедают их. Кроме того, соединения железа связывают растворенный в воде кислород, что приводит к массовой гибели рыб и других гидробионтов.

В статье представлена методика проведения экспериментов, рассмотрены методы сорбционной, электрохимической и комбинированной очистки воды, включающие электрохимическое воздействие и адсорбцию. Представлены результаты исследований этих методов очистки воды от ионов железа. Выявлена зависимость степени очистки от напряженности электрического поля, межэлектродного расстояния и времени обработки воды. При напряженности электрического поля 5,16 В/мм, температуре 20–22 °С, использовании кварцевого песка в качестве адсорбента и времени обработки в течение 1 мин. концентрация ионов железа уменьшилась с 2,5 до 0,25 мг/л (при ПДК = 0,3 мг/л). Предлагаемый комбинированный метод очистки требует не дорогих и доступных материалов и прост в эксплуатации.

Ключевые слова: электрохимический метод, железо, степень очистки, переменный ток, постоянный ток, сорбенты.

Introduction. In the production of space rocket technology, galvanic technologies are used, as a result of which sewage is contaminated with metal ions. Known methods of wastewater treatment do not allow for the maximum permissible concentration of metal ions in treated water, or are expensive or difficult to operate in industry. Iron ions are among the most polluting components of wastewater of most industries. So increased control and the development of effective methods of wastewater treatment are necessary. The development of a method for cleaning industrial wastewater from metals is an actual area of research and assumes the presence of not only a high cleaning result, but also optimal parameters when introduced into the process [1; 2], which includes electricity costs, consumables and processing time.

The methodology of the experiment. The effect of a constant electric field on the adsorption treatment of water from iron ions was studied in a cell using pairs of plate electrodes (fig. 1). The cell is made of a dielectric material in the form of a cylindrical tube in which the anode and cathode are alternately mounted. The electrodes are made of stainless steel 12X18H10T (4 plates 1 mm thick each). The interelectrode distance is 12 and 25 mm. Sorbents (quartz sand or natural zeolites) were poured into the space between the electrodes. The electrodes were connected in parallel to a direct current source. The volume of treated water is 1 liter. A voltage was applied to the terminals of the electrodes and water was passed through in a non-pressure way for 1 minute with stabilization of the current strength of 0.025 A and a voltage at the terminals of the electrodes from 18 to 62 V. Fe (III) salts were dissolved in water at an average ion concentration of 2.5 mg/l. To record the process parameters, standard instruments were used – a voltmeter (accuracy class 0.4), ammeter (0.5).

The degree of purification was determined by the formula, %:

$$Y = \left(\frac{C_o - C_k}{C_o} \right) 100,$$

where C_o , C_k are the initial and final concentration of the removed metal ion, mg/L.

The specific energy consumption W for purifying a unit volume of water, (kW·h)/m³, was calculated by the expression:

$$W = \frac{IU t_{tr}}{V} 10^{-3}$$

where I is current, A; U is the voltage at the terminals of the electrodes, V; t_{tr} – flow interval passing through the treated water, h; V is the volume of filled water, m³; 10^{-3} is the conversion factor from W to kW.

Research results. Fig. 2 shows the results of purification of water from Fe ions with an initial concentration of 2.5 mg/l at a constant electric current of different tensions with sorbents

In the course of previous experiments at two plants for wastewater treatment [3–5] the main parameters that are most important in water treatment were analyzed: the distance between the electrodes (L , m), the voltage at the terminals of the electrodes (U , V) and processing time (T , s).

Fig. 3 shows the results of the analysis (obtained using the Statgraphics experimental data processing program) of the dependence of the degree of water purification from Fe ions when the time of the action of a constant electric current on quartz sand changes at different voltage on the electrodes.

The temperature of the treated water was in the range from 20 to 22 °C [6; 7] and the dispersion of quartz sand particles was from 0.5–1.2 mm [8–11].

When considering the response surface, it can be seen that the total iron indicators (fig. 3) in purified water are as close as possible to standard values with an increase in processing time [12].

An analysis of the obtained experimental data showed that the efficiency of the electrochemical method using direct electric current and alternating electric current of industrial frequency depends on the interelectrode distance, voltage at the terminals of the electrodes, and processing time. The degree of purification improves with increasing electric field strength [3–5; 13].

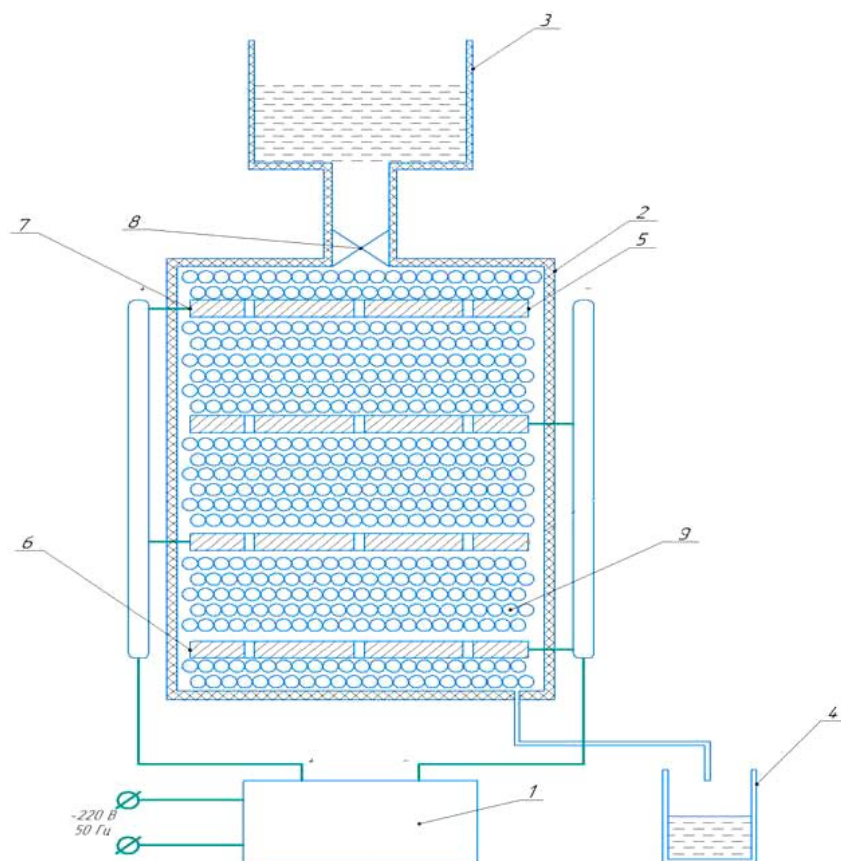


Fig. 1. Experimental setup diagram:
1 – DC power supply with output voltage regulation; 2 – casing cell; 3 – the upper container of water; 4 – purified water tank; 5 – steel electrodes-anodes; 6 – steel electrodes-cathodes; 7 – current leads; 8 – valve (clamp); 9 – adsorbent

Рис. 1. Схема экспериментальной установки:
1 – источник постоянного тока с регулированием выходного напряжения; 2 – корпус ячейки; 3 – верхняя ёмкость с водой; 4 – ёмкость для очищенной воды; 5 – стальные электроды-аноды; 6 – стальные электроды-катоды; 7 – токовводы; 8 – вентиль (зажим); 9 – адсорбент

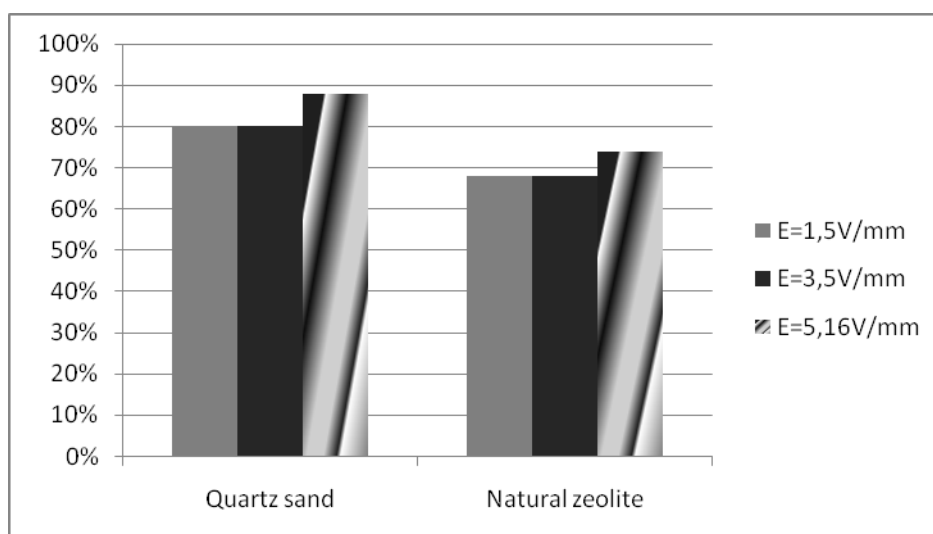


Fig. 2. Results of influence of input parameters of the process on the degree of purification in a plant with direct current and sorbents

Рис. 2. Результаты влияния входных параметров процесса на степень очистки в установке с постоянным током и сорбентами

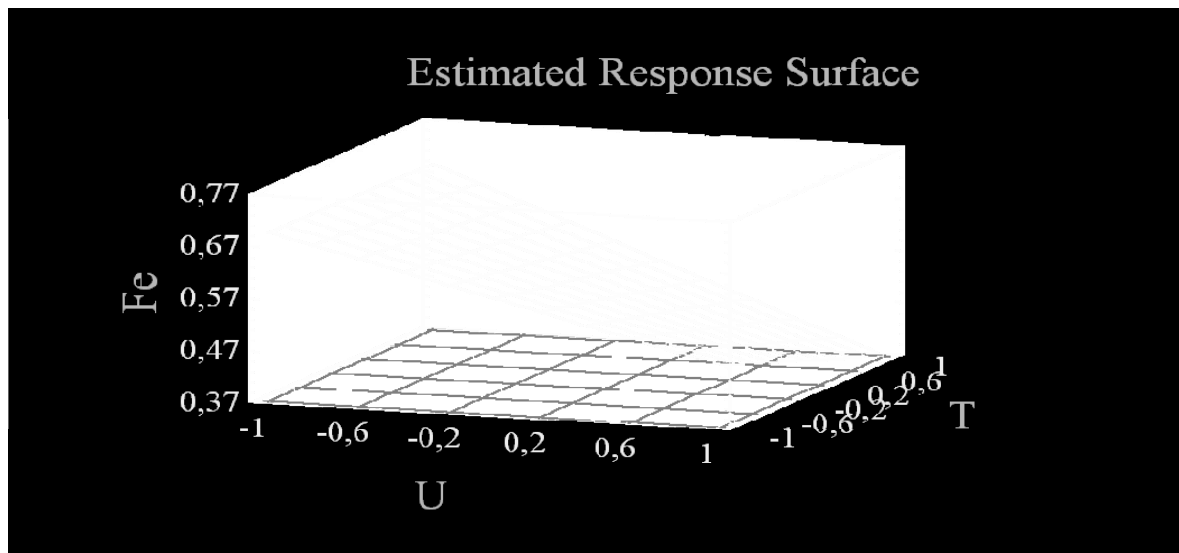


Fig. 3. Dependence of the degree of water purification from Fe ions when changing the time of exposure to direct electric current on quartz sand at different voltages on the electrodes

Рис. 3. Зависимость степени очистки воды от ионов Fe при изменении времени воздействия постоянного электрического тока на кварцевый песок при различном напряжении на электродах

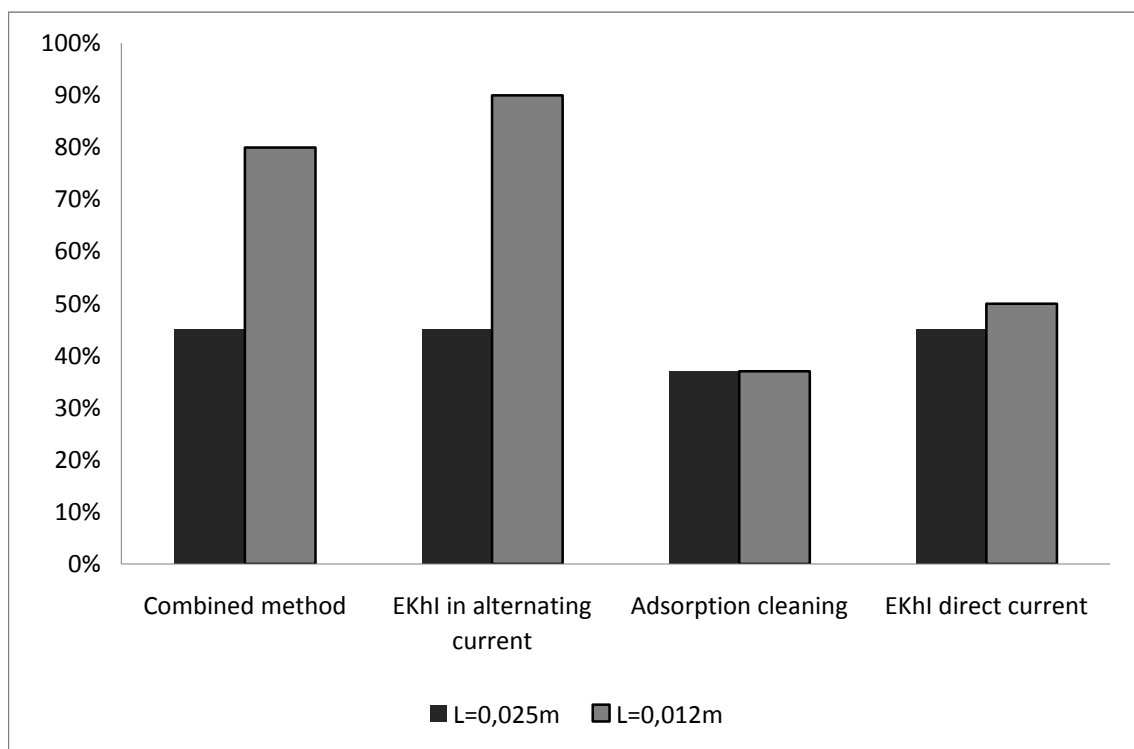


Fig. 4. Results of research on water treatment methods

Рис. 4. Результаты исследований методов очистки воды

At the same voltage ($U = 18 \text{ V}$) the cleaning technology with alternating electric current of industrial frequency turned out to be more effective.

The specific energy consumption and the degree of purification of the electrochemical method based on the use of direct electric current were:

$$W_E = \frac{1,5 \cdot 18 \cdot 0,0167}{0,001} 10^{-3} = 4,5 (\text{kW} \cdot \text{h}) / \text{m}^3$$

$$Y_1 = \left(\frac{2,5 - 0,5}{2,5} \right) 100 = 80 \% \text{ — at } U = 18 \text{ V}$$

The results of studies of water treatment methods at a voltage of $U = 18 \text{ V}$, processing time $t_{\text{proc.}} = 60 \text{ s}$, and the initial ion concentration $\text{Fe} = 2.5 \text{ mg/m}^3$ are presented in fig. 4.

Conclusion. The specific energy consumption and the degree of purification of the electrochemical method using alternating electric current of industrial frequency: $W = 1.8 (\text{kW} \cdot \text{h})/\text{m}^3$, $Y = 99 \%$ [4]. However, this method is based on the introduction of a coagulant after electrochemical exposure and settling of water for eight hours, which reduces productivity and requires additional settling tanks. In the electrochemical process, the formation of iron hydroxide occurred in the volume of water without sorbents, which led to an increase in the turbidity of the water. To extract iron hydroxide, water settling is necessary [4.14].

The combination of electrochemical action and the use of adsorbents made it possible to raise the degree of purification to 80 %, while the specific energy consumption is $4.5 (\text{kW} \cdot \text{h})/\text{m}^3$. An increase in the electric field strength to 5.16 V/mm will allow purifying water from iron ions to the MPC level (0.3 mg/l).

References

1. Strokach P. P., *Electrochem. Ind. Process. Bio.* 1975, Vol. 55, P. 375.
2. Micka K., Kimla A. Rousar. *Electrochemical engineering*. 1986. Part I. 337 p.
3. Shestakov I. Ya., Raeva O. V. Patent RF 2519383. *Sposob ochistki vody i vodnykh rastvorov ot anionov i kationov* [A method for purifying water and aqueous solutions from anions and cations]. 2014, 3 p.
4. Shestakov I. Ya., Raeva O. V., Nikiforova E. M., Eromasov R. G. *Issledovanie ochistki vody elektrokhimicheskim sposobom v nestatsionarnom elektricheskom pole s posleduyushchey koagulyatsiyey* [The study of water purification by the electrochemical method in an unsteady electric field with subsequent coagulation]. Available at: www.science-education.ru/107-8154 (accessed: 10.03.2014).
5. Khilyuk A. V., Rogov V. A., Prusakova V. A. [The effect of the electrostatic field on adsorption during the purification of natural water]. *Vestnik KrasGAU*. 2013, No. 12, P. 134–137 (In Russ.).
6. Kengerli A. D. [Influence of the temperature of the treated water on the process of flocculation]. *Tekhn. Tereggi ugrunda*. 1972, No. 4, P. 39–40 (In Russ.).
7. Kowal A. L., Mackiewicz J. The effect of water temperature on the course of alum coagulation of colloidal particles in water-Environ. *Prot. Eng. (PRL)*. 1975, Vol. 1, No. 1, P. 63–70.
8. GOST R 51641–2000 *Materialy fil'truyushchie zernisty. Obshchie tekhnicheskie usloviya* [State Standard R 51641–2000 Granular filtering materials.

General specifications]. Moscow, IVS URALTEST Publ., 2000.

9. Bratilova M. M., Grechushkin A. N. [Investigation of the properties of filter media for water purification from iron]. *Universum: Khimiya i biologiya: elektron. nauchn. Zhurn.* 2015, No. 6 (14). Available at: <http://7universum.com/ru/natur/archive/item/2185>.

10. Tagibaev D. D. [Filtering characteristics of granular filter materials]. *Innovatsionnaya nauka*. 2017, No. 1-2, P. 90–92 (In Russ.).

11. Kuznetsov L. K., Gabitov A. I. [Filtering technology in the physicochemical processes of water treatment]. *Bash. khim. zh.*, 2009, No. 2, P. 84–92.

12. GOST 4011–72 *Voda pit'evaya. Metody izmereniya massovoy kontsentratsii obshchego zheleza* [State Standard 4011–72 Drinking water. Methods for measuring the mass concentration of total iron.]. Moscow, IPK Izdatel'stvo standartov Publ., 1974.

13. Khilyuk A. V. [The study of the influence of pollutants and electroactivated water on aquatic organisms]. *Reshetnevskie chteniya: materialy XXII Mezhdunar. nauch.-prakt. Konf.* [Reshetnev readings: materials of the XXII Intern. scientific-practical Conf.]. Krasnoyarsk, 2018, Vol. 2, P. 66–69 (In Russ.).

Библиографические ссылки

1. Strokach P. P. *Electrochem // Ind. Process. Bio.* 1975. Vol. 55. P. 375.
2. Micka K., Kimla A. Rousar // *Electrochemical engineering*. 1986. Part I. 337 p.
3. Патент РФ 2519383. Способ очистки воды и водных растворов от анионов и катионов / Шестаков И. Я., Раева О. В. ; опубл.10.06.2014, Бюл. № 16. 3 с.
4. Исследование очистки воды электрохимическим способом в нестационарном электрическом поле с последующей коагуляцией / И. Я. Шестаков, О. В. Раева, Э. М. Никифорова, Р. Г. Еромасов [Электронный ресурс]. URL: www.science-education.ru/107-8154 (дата обращения: 10.03.2014).
5. Хилук А. В., Рогов В. А., Прусакова В. А. Воздействие электростатического поля на адсорбцию в процессе очистки природной воды // *Вестник КрасГАУ*. 2013. Вып. 12. С. 134–137.
6. Кенгерли А. Д. Влияние температуры обрабатываемой воды на процесс хлопьеобразования // *Техн. терегги угрунда*. 1972. № 4. С. 39–40.
7. Kowal A. L., Mackiewicz J. The effect of water temperature on the course of alum coagulation of colloidal particles in water-Environ // *Prot. Eng. (PRL)*. 1975. Vol. 1, No. 1. P. 63–70.
8. ГОСТ Р 51641–2000 *Материалы фильтрующие зернистые. Общие технические условия*. М. : ИВС «УРАЛТЕСТ», 2000.
9. Братилова М. М., Гречушкин А. Н. Исследование свойств фильтрующих загрузок для очистки воды от железа // *Universum: Химия и биология : электрон. научн. журн.* 2015. № 6 (14). URL: <http://7universum.com/ru/natur/archive/item/2185>.
10. Тагибаев Д. Д. Фильтровальные характеристики зернистых фильтрующих материалов // *Инновационная наука*. 2017. № 1-2. С. 90–92.

11. Кузнецов Л. К., Габитов А. И. Технология систем, академика М. Ф. Решетнева. Красноярск, 2018. Т. 2. С. 66–69.
12. ГОСТ 4011–72 Вода питьевая. Методы измерения массовой концентрации общего железа. М. : Изд-во стандартов, 1974.
13. Хилюк А. В. Исследование влияния загрязняющих веществ и электроактивированной воды на гидробионтов // Решетневские чтения : материалы XXII Междунар. науч.-практ. конф., посвящ. памяти генерального конструктора ракетно-космических

© Шестаков И. Я., Хилюк А. В., 2020

Shestakov Ivan Yakovlevich – doctor of technical Sciences, Professor, associate Professor, Reshetnev Siberian State University of Science and Technology, Department of electronic engineering and telecommunications. E-mail: yakovlevish@mail.ru.

Khilyuk Anna Viktorovna – senior lecturer, Reshetnev Siberian State University of Science and Technology, Department of life safety. E-mail: h-anna7@bk.ru.

Шестаков Иван Яковлевич – доктор технических наук, профессор, доцент, Сибирский государственный университет науки и технологий имени академика М. Ф. Решетнева, кафедра электронной техники и телекоммуникаций. E-mail: yakovlevish@mail.ru.

Хилюк Анна Викторовна – старший преподаватель, Сибирский государственный университет науки и технологий имени академика М. Ф. Решетнева, кафедра безопасности жизнедеятельности. E-mail: h-anna7@bk.ru.

